AD NUMBER

AD466691

NEW LIMITATION CHANGE

TO

Approved for public release, distribution unlimited

FROM

Distribution authorized to U.S. Gov't. agencies and their contractors; Administrative and Operational Use; May 1965. Other requests shall be referred to the Office of Civil Defense, Washington, DC 20301.

AUTHORITY

OCD, per ltr dtd, 29 Nov 1965

Final Technical Report

EVALUATION OF FALLOUT CONTAMINATION OF WATER SUPPLIES

By

WERNER N. GRUNE
Professor of Civil Engineering
and
HENRY S. ATLAS
Research Associate

GERARD J. HAMEL
Student Assistant

Covering the Period

1 October 1963 to 15 May 1965

CONTRACT NO. OCD-PS-64-62
OCD Subtask 3131B

Performed for

OFFICE OF CIVIL DEFENSE
DEPARTMENT OF DEFENSE
Washington, D.C. 20301

Division of Engineering
MERRIMACK COLLEGE
North Andover, Massachusetts

Errata Sheet for Final Technical Report
Contract OCD-PS-64-62

EVALUATION OF FALLOUT CONTAMINATION OF WATER SUPPLIES

By

Werner N. Grune, et al.
Division of Civil Engineering, Merrimack College
North Andover, Massachusetts

Page	Line	
i	19	3.7 should be 1.9
ii	11	0.49 should be .25
6	6 & 7	for Paterson, should be: 3 at 20 MT 3 at 5 MT, 4 at 10 MT
6	18	2.154 a. should be 2,154 a.
6	19	2.5 BG should be 25.0 BG
21		Case III for I-131; 1.37 should be 6.96 3.69 should be 1.88
26	11	"1 at 5 MT, 1 at 10 MT and 5 at 20 MT" should be: "3 at 5 MT, 4 at 10 MT and 5 at 20 MT"
28	23	"Wanaque River" should be "Wanaque Reservoir"
30	last	same as p. 26, line 11
31	last	same as p. 26, line 11
32	4 from last	same as p. 26, line 11
34		Springfield, including runoff: I-131 3.7 should be 1.9
35	13	same as p. 26, line 11
70	2 from bottom	same as p. 26, line 11
74	11	78.8 should be 116.
74	last	same as p. 26, line 11
127	22	(151), (153) and (154) should be: (149), (151) and (152)
127	23	$N_\alpha = Y_A^o r_o (A, t_1)$ should be: $N_\alpha = \frac{Y_A^o r_o (A, t_1)}{K_x}$
127	24	$N'_\alpha = Y_A^o r'_o (A, t_1)$ should be: $N'_\alpha = \frac{Y_A^o r'_o (A, t_1)}{K_x}$
186	24	3.7 should be 1.9
211	20	0.2635 should be 0.02635

Final Technical Report

EVALUATION OF FALLOUT CONTAMINATION OF WATER SUPPLIES

By

WERNER N. GRUNE
Professor of Civil Engineering
and
HENRY S. ATLAS
Research Associate

GERARD J. HAMEL
Student Assistant

Covering the Period

1 October 1963 to 15 May 1965

CONTRACT NO. OCD-PS-64-62
OCD Subtask 3131B

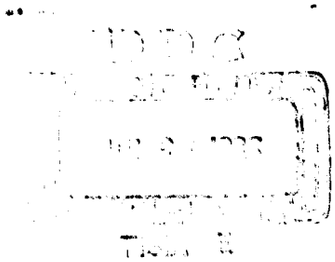

Performed for

OFFICE OF CIVIL DEFENSE
DEPARTMENT OF DEFENSE
Washington, D.C. 20301

ABSTRACT

A theoretical evaluation was conducted to determine the potential degree of water contamination from fallout and to assess the biological hazards associated with the ingestion of water following hypothetical nuclear attack. The appraisal was carried out by applying the assigned fallout model to various levels of nuclear war and by quantitative correlation of all phases of the flow of radioactive fallout in public water supplies.

The water supply systems of three cities were selected for the evaluation of water contamination to study the potential hazards and radiobiological effects from the ingestion of fallout contaminated water. The three selected target cities and the distribution of weapons to these were: San Francisco, California: 155 MT; Paterson, New Jersey: 115 MT; and Springfield, Massachusetts: 30 MT. Maximum levels of selected contaminants at the water intake for these cities under adverse wind conditions and including watershed runoff were calculated and reported in μc/ml as follows:

	Sr-89	Sr-90	Ru-106	I-131	Cs-137	Ba-140
San Francisco	2.7×10^{-2}	2.1×10^{-4}	2.7×10^{-3}	2.7×10^{-1}	1.7×10^{-4}	1.8×10^{-1}
Paterson	9.6×10^{-1}	8.9×10^{-3}	1.2×10^{-1}	1.2×10	5.9×10^{-3}	7.9
Springfield	1.4×10^{-3}	2.5×10^{-5}	4.3×10^{-4}	3.7×10^{-2}	7.4×10^{-6}	2.2×10^{-2}

These results indicate that water contamination for some cities may be at a substantial level of activity concentration, especially when watershed runoff is included. Direct surface contamination of these reservoirs, excluding any contribution from watershed runoff, resulted in activity concentrations which were lower by a factor from 10 to 100.

A detailed analysis of various criteria for biological uptake was completed. Results from four mathematical models of biological uptake have been summarized and were found to be in close agreement with each other. Absorbed dose for various organs computed according to the Miller-Brown model has been presented in two types of graphs designed for different kinds of use by civil

defense personnel. The possible internal hazard due to ingestion of contaminated water for the populations residing in the three selected cities was estimated. The values of the absorbed dose for total body for different starting times and ingestion periods have been summarized. Some typical short term hazard values (in rems) for ingestion starting at 7 days and for 30 days of consumption are:

	Sr-89	Sr-90	Ru-106	I-131	Cs-137	Ba-140
San Francisco	0.6	0.013	0.011	3.52	0.018	0.20
Paterson	22.	0.57	0.49	156.	0.62	8.9
Springfield	0.032	0.002	0.002	0.49	0.0008	0.025

These values include the effect due to watershed runoff contamination and are appreciably higher than the values obtained from direct surface contamination. Body burdens of individual radioisotopes may be determined from a consideration of the rate of ingestion, the effective decay rate, and the affinity for the isotope by the critical organ. It is believed that uptake of radioactive isotopes may be reduced or prevented by selective blocking of critical organs with stable isotopes.

A critical literature review of recent decontamination methods has been conducted. From an analysis of this study it appears that the desired level of water decontamination following nuclear attack will not be achieved by conventional treatment plants and that non-conventional or emergency treatment methods will be required.

Ten computer programs were established to assist the computations in various phases of this study. Six of these were written for different biological uptake models, including the Miller-Brown, Simplified Uptake, Greitz-Edverson and the Miller-Brown Periodic Intake models. Each program can be used to compute the absorbed dose due to ingestion for total body organs and GI tract. This report includes also a summary of the Miller fallout model; while a critical review of related studies to Miller's fallout model was presented in

interim report No. 2. The other completed computer programs were established to estimate sublimation pressures; to obtain ionization rate contours (fallout intensity at any location inside the fallout region for a given size nuclear detonation); to calculate the ionization rate at any location for multiple weapons; to evaluate fallout particle size distributions for any downwind location; and to obtain soluble nuclide contour ratios.

A study was also made to obtain a first approximation of the relationship between activity distribution and fallout particle size. The relationship is observed to be in close conformance to a log-normal distribution.

The assigned project outline has been adhered to closely during the performance of this research and each area of the scope was advanced. It was shown that the effect due to watershed runoff may be significant. Therefore, it is suggested that additional research be performed to study in detail the runoff contribution during the blast and thermal period from land areas to streams and from watersheds into reservoirs. Rainfall during the first 24 to 48 hours following nuclear attack will be critical as far as surface water contamination goes.

TABLE OF CONTENTS

TABLE OF CONTENTS (cont'd)

TABLE OF CONTENTS (cont'd)

LIST OF FIGURES

LIST OF FIGURES (cont'd)

LIST OF TABLES

LIST OF TABLES (cont'd)

ACKNOWLEDGEMENTS

This project, for the purpose of evaluating the contamination of water from fallout, was initiated on October 1, 1963. It was entirely supported by the Office of Civil Defense, Department of the Army. Throughout the project, Mr. William J. Lacy, Project Coordinator, Postattack Research Division, OCD, provided much valuable information and many suggestions which contributed directly to the conduct of this study. Mr. Lacy and other staff members of the Office of Civil Defense also aided materially with logistic support on several aspects of these investigations by making the necessary reports and documen's related to this work available, providing liason with co-workers in this field and acting as a clearing house on many detailed problems.

The research was conducted under the general guidance of Dr. Werner N. Grune, Professor of Sanitary Engineering and Chairman, Department of Civil Engineering, Merrimack College, North Andover, Massachusetts with Mr. Oliver S. K. Yu, Operations Analyst performing much of the Fallout Model analysis, Computer Programming and Biological Uptake Model modification during the first ten months of this project. After Mr. Oliver S. K. Yu joined the staff of the Stanford Research Institute, Mr. Henry S. Atlas, Instructor, Department of Physics, Merrimack College took over his duties and conducted further analyses of the Miller Fallout Model. Both men have contributed materially to the understanding and clarification of this theoretical model and the project has been fortunate indeed to have their support.

Full credit for the development of the basic fallout model goes to Dr. Carl F. Miller, Senior Scientist, Stanford Research Institute, who has always been ready to provide personal guidance and counsel. Without his valuable advice and interpretations the intelligent use of this model would have been incomplete.

Finally, the authors acknowledge the support, technical advice and recommendations obtained from staff members of the U. S. Naval Radiological Defense Laboratory, Hunter's Point, San Francisco, California. Among others, Mr. James Mackay and Dr. Paul Zigman have lent their support to these studies and made valuable criticisms and

suggestions to complete this final report for which the authors remain indebted. This work was done in part at the Computation Center of the Massachusetts Institute of Technology, Cambridge, Massachusetts, employing the IBM 7094 Electronic Computer. Programming was conducted by Mr. Richard T. Goller, Student Assistant (Mathematics), Merrimack College.

The task of obtaining the information necessary to evaluate the contamination of the individual water supply systems studied under this project was made much easier through the assistance provided by several waterworks officials. Their personal interest and cooperation is greatly appreciated and hereby gratefully acknowledged.

Harry W. Tracy, Manager, Water Purification Division, San Francisco Water Department, 1000 El Camino Real, Millbrae, California

Oral L. Moore, General Manager, Hetch Hetchy Water Supply Power and Utilities Engineering Bureau, 425 Mason Street, San Francisco 1, California

Harold L. Gunther, Chief Engineer, North Jersey District Water Supply Commission, Wanaque, New Jersey

Charles G. Bourgin, General Superintendent and Chief Engineer, Passaic Valley Water Commission, 1525 Main Avenue, Clifton, New Jersey, P.O. Box 230

John E. McCall, District Engineer, Water Resources Division, Branch of Surface Water, United States Department of the Interior, Geological Survey, 433 Federal Building, P.O. Box 967, Trenton, New Jersey, 08606

Peter C. Karalekas, Chief Water Engineer, Municipal Water Works, Springfield, Massachusetts

I. INTRODUCTION

The primary objective of this project has been to analyze the contamination of water supplies following hypothetical nuclear attack and to study the possible long and short term hazards and radiobiological effects from the ingestion of fallout contaminated water.

The general purpose of this study was to evaluate and summarize available information on the problem of water contamination by radioactive fallout in the event of nuclear war. The level of fallout that might result from a possible nuclear attack was obtained based on current theories of the formation and distribution of fallout.

The investigations included a detailed analysis of the radioactive contamination of public water supplies based on the Miller fallout model. The results are limited to the validity of this basic model. The attack model presented by Technical Operations, Inc. (1) was selected as most appropriate for this study. It was developed with due consideration to the relative importance of military, industrial, governmental, and power resource targets. This model assumes all detonations to be surface bursts, although a more realistic situation would include many air bursts, which would be more effective against an unhardened military or industrial target. As the type of burst exerts considerable influence on the distribution and level of fallout produced, it must be considered in a study of water contamination.

Following a thorough analysis of the fallout model, a number of important functions derived from it were utilized in this study. The analysis of the fallout model is discussed in detail in Chapter IV , "Summary Analysis of the Miller Fallout Model".

With information obtained from the fallout model of Miller (2), the degree of contamination for the public water supply systems of San Francisco, Cal., Springfield, Mass., and Paterson, N.J., from single and multiple surface bursts was established and the possible levels of contamination by selected isotopes determined. With due consideration of the assumptions, these results may be applied similarly to water supply systems of other municipalities.

A limited study of transport of fallout by surface water has been conducted. The contribution from each mode of contamination, i.e. that from direct contamination of reservoir and river surfaces and that from watershed runoff was determined. A further evaluation of the effects of watershed characteristics on the concentration of radioactivity in surface water would be valuable.

From the estimated levels of contamination, it was possible to calculate anticipated amounts of radioactivity intake for selected radionuclides for various periods of time following nuclear attack, taking into consideration the post-attack conditions of water supply systems as they affect the degree of contamination. The biological uptake and resultant body burdens for several short-term periods of ingestion of contaminated water have been studied. Analysis of several mathematical models of biological uptake shows that similar results are obtained from each. The results obtained from computer programs, according to the Miller-Brown model, are presented in graphical form to reflect the radiobiological hazard from specific radionuclides. The absorbed dose for total body for different starting times and ingestion periods to estimate the internal hazard was calculated for each of the water supplies and the results have been summarized. With this information reasonable estimates of the accumulation of body burden by the individual and the population at large can be made.

A study has been made to obtain a first approximation of the complex relationship between activity distribution and fallout particle size. The computer program for evaluating the nuclide solubility contour ratio has been improved, but due to the large amount of input data involved, has not been able to yield the expected results.

Based on a critical search of the literature, decontamination procedures and factors, for both standard and emergency treatment methods, have been presented. To obtain recent data on countermeasures, the search was confined to the literature since 1960, except to include important findings or articles of permanent value prior to 1960. Decontamination procedures are evaluated according to their efficacies for the

the removal of various radioisotopes and also according to the feasibility of their use after a nuclear attack. For the purpose of this study, it has been assumed that waterworks facilities have suffered only minimal damage and that personnel will be available for operation (3).

II. EVALUATION OF WATER CONTAMINATION

A. Levels of Nuclear War

The main purpose of this study was to estimate the degree of radiation hazard from nuclear fallout in water supplies. To accomplish this purpose, it was necessary to select representative communities and assume various patterns of nuclear attacks.

Following World War II, a threat of nuclear warfare has developed as the potentiality of nuclear weapons has increased. Therefore, a number of investigations of hypothetical levels of nuclear attacks were undertaken by various organizations. Among the more significant and comprehensive studies related to civil defense in recent years are: (a) the hypothetical nuclear war model presented during the 1959 Congressional J.C.A.E.C. hearings (4), (b) the special McGraw-Hill report of 1962 (5), (c) the Stanford Research Institute 20,000 MT attack model on the U.S. (6), and (d) the Technical Operations, Inc. model (1).

The 1959 Congressional J.C.A.E.C. hearings considered an attack consisting of a total of 263 nuclear weapons delivered on 224 military and "critical target" areas in the United States. The total attack level was assumed as 1,446 MT, comprised of weapon sizes ranging from 1 MT to 10 MT. The special McGraw-Hill report (5) distinguished between a 1,000 MT capacity of attack in 1962 and a future attack capability of 10,000 MT on military and civilian targets. The future attack was assumed to be comprised of one thousand 10 MT size bombs. The Stanford Research Institute study (6) defined a target system within the continental United States against which an attack of approximately 20,000 MT total yield would be delivered. Based upon unclassified sources, a total of 1,336 targets, including airfields, ballistic missile sites, naval bases, and industrial centers were selected. Three sizes of weapons were postulated: 5 MT, 10 MT, and 20 MT. The 20 MT weapons were assigned to the hard missle sites, the naval bases, and to seven of the major industrial centers. The 10 MT weapons were assigned to airfields, semi-hard Atlas sites, and to twenty of the industrial centers. The 5 MT weapons were assigned to the remaining targets.

The model developed by Technical Operations, Inc. (1) was established following a thorough analysis of the problem. The military attack was assumed to consist of 368 five MT weapons delivered on 159 targets, while the combined attack against approximately 310 military, government and industrial targets consisted of approximately 800 five MT weapons for a total, all-out attack of 4,080 MT. This nuclear war model takes into consideration the military, industrial, government, and power resource potential of each target and assigns priorities to each accordingly. A certain megatonnage is assigned to each target on the basis of the enemy's delivery capabilities, the size of individual nuclear weapons, their damage effects, and the number of weapons necessary to provide a 95 percent confidence level probability of target destruction.

B. Municipal Water Supply Systems Investigated

The contamination of public water supplies of three U.S. cities was studied. The cities of San Francisco, California; Paterson, New Jersey; and Springfield, Massachusetts, were selected on the basis that extensive information of their water supply systems could be made available, and because of their military, economic and political importance and strategic geographical locations. Furthermore, the water supply system of the city of Paterson, N.J. was included because information developed on water contamination will complement the results of other nuclear effects studies for this city.

The patterns of attack on these three cities emerge from a detailed study and careful consideration of the above four nuclear attack models. The distribution of weaponage to each city is generally in accordance with the Technical Operations, Inc. model. In addition to the 5 MT weapons, however, 10 MT and 20 MT weapons were also assigned. A summary of general information on population, wind directions, military and industrial values, a brief description of the water supply system, and specific assumptions on weaponage distribution for these three cities is presented in Table I .

Table I Summarized Information on Selected Cities

City and State	San Francisco, California			Paterson, New Jersey		Springfield, Mass.	
Total Population Served	1,500,000 (1960)			500,000 (1960)		225,000 (1962)	
Land Value Added by Manufacture	$5 million per square mile			$20 million/sq mi		$2 million/sq mi	
Total Attack	155 Megatons			115 Megatons(**)		30 Megatons	
Weapon Distribution Military Civilian	1 at 20 MT; 1 at 10 MT; 3 at 5 MT 2 at 20 MT; 4 at 10 MT; 6 at 5 MT			5 at 20 MT; 1 at 5 MT 1 at 10 MT		1 at 20 MT 1 at 10 MT	
Assumed Ground Zero(s)	City Hall San Francisoo			Vicinity Elmyra Bridge		Military: Westover Air Force Base Civilian: City	
Prevailing Wind Direction (Assumed Wind Direction) Spring Summer Autumn Winter	West - Northwest Northwest West - Northwest West - Northwest (West)			Northeast Southwest Southwest West (Southwest)		Northwest South West - Northwest North (East)	
Source of Water Supply	Hetch Hetchy	Calaveras	Cryst.Springs	Passaic	Wanaque	Little R.	Ludlow
Total Area of Watersheds	713 sq mi	135 sq mi	38 sq mi	485 sq mi	108 sq mi	49 sq mi	20 sq mi
Runoff Coefficient	0.50(*)			0.35		0.50(*)	
Surface Area of Reservoir	1,960 a.	1,435 a.	2.154 a.	475 a.	1,134 a.	213 a.	420 a.
Volume of Reservoir	115.0 BG	31.5 BG	29.8 BG	3.1 BG	22.5 BG	2.5 BG	2.0 BG
Average Plant Output	400 MGD(*)	33 MGD	26 MGD	75 MGD	41.5 MGD	36.5 MGD	2.2 MGD
Estimated Population Served	1,500,000			500,000		240,000	
Available Water Treatment Process	chlorine gas disinfection; sodium silicofluoride adjustment			chlorination; floccu-lation; sedimentation; rapid sand filtration		slow sand filtration	slow sand filtration; chlorinat.

(*) Estimated Value

(**) For the city of Philadelphia, Pennsylvania

C. General Method of Evaluation

1. Basic Assumptions

(a) It is assumed that the radionuclides from fallout mix homogeneously in water supplies (see also Appendix A). Therefore, the concentration of a radionuclide in water may be obtained from:

$$N = \frac{d \cdot S}{V} \tag{1}$$

where N = the atom concentration in water (atoms per unit volume)

d = the atom surface density when particles just reach the water surface (atoms per unit area)

S = the area of water surface (total area, i.e. watershed, including reservoir and feeder streams, open service reservoir(s) and stream or river to city intake)

V = the volume of water (total volume of reservoirs and river)

(b) It is assumed that for all long-lived radionuclides of interest, their parents have already decayed to a negligible amount at H + 1 hour. Therefore, the following relationship can be used to approximate the activity concentration from atom concentration in water:

$$A = \lambda_r N \tag{2}$$

where A = the activity concentration in water (curies per unit volume)

λ_r = the radioactive decay constant (time^{-1})

(c) An average value for the flow-rate of streams is assumed. The runoff from the watershed is assumed as a mean annual value with the coefficient of runoff equal to 0.50, unless a value has been determined from studies of the watershed characteristics.

2. Procedures for the Evaluation of Water Contamination

The contamination in water supplies may be derived from four sources:

(a) direct contamination of reservoir

(b) contamination from feeder streams (within watershed)

(c) contamination from watershed runoff

(d) contamination of streams (below reservoir)

The evaluation is performed in two stages. First, the effect from a single weapon is analyzed, then by the principle of super-position, the combined effect of several weapons is determined.

The general evaluation procedure may be outlined as follows:

(b) The fallout pattern for each assumed weaponage is superimposed over the city map with ground zero coinciding with the target point, and the down-wind axis parallel to the prevailing wind direction.

(b) The watershed map is divided into rectangular grids to evaluate the area of contamination. The size of the individual grid area depends on the required accuracy, the weapon size, and the area of the water supply reservoir. The fallout properties at the center of the grid area are assumed to represent the average fallout properties for the individual grid area.

(c) The soluble nuclide surface density is evaluated for any area of interest by multiplying the ionization rate for the area with the soluble nuclide contour ratio of that area.

(d) The surface density over the entire area of the water supply system is integrated and the result divided by the total volume of water to obtain the atom concentration in water. The activity concentration, A, is estimated from Equation (2) above.

Since all data on ionization contours and contour ratios(*) are determined at H + 1 hour, it should be noted that the activity concentration, A, is also obtained for time at H + 1 hour. For any other time, the activity concentration is decreased in accordance with the process of radioactive decay plus whatever natural coagulation and sedimentation may have occurred.

(*) For information on ionization contours and contour ratios, refer to Interim Technical Report No. 1 to the Office of Civil Defense, Contract No. OCD-PS-64-62 (October 1963 to December 31, 1963), January 1964

A detailed outline and summary of procedure for the three cases of reservoir, watershed and stream contamination, is presented in Appendix A.

3. Techniques for Evaluating Water Contamination from Multiple Weapons

When dealing with a multiple weapon attack, the problem of estimating nuclide atom surface density, d, and integrating this density over the entire area of the water supply system to obtain atom and activity concentrations increases rapidly and the volume of computations becomes very large and time-consuming. However, for this study, due primarily to the small number of assumed weapons, the method of evaluation was confined to manual computation and the development of computer programs.

As stated previously, three typical U.S. cities were selected for the evaluation of the degree of contamination of their water supply systems after a hypothetical nuclear attack and the possible radiobiological hazards from the ingestion of contaminated water. These cities are: San Francisco, California; Paterson, New Jersey; and Springfield, Massachusetts. Presented below are the summarized studies and results for each of these cities.

D. Evaluation of San Francisco Water Supply

The total weaponage assigned to the metropolitan area of San Francisco was 155 MT, consisting of three 20 MT, five 10 MT, and nine 5 MT weapons. Since the major water supply system of San Francisco, the Hetch Hetchy system is located in Yosemite National Park about 170 miles east of the center of the city, no appreciable difference in fallout effects on this watershed would be observed for any weapon detonations within metropolitan San Francisco. To simplify the calculations a single ground zero for all weapons was chosen near City Hall. The wind direction was chosen to be from the West, instead of the predominant West-Northwest direction, as the west wind will produce a maximum possible contamination to the water supply systems. The wind speed was assumed to be 15 mph.

San Francisco depends for its water on three main water supply systems: the Peninsula, Calaveras and Hetch Hetchy systems. Figure 1 is a reproduction of the Hetch Hetchy watershed. Figure 2 shows the Calaveras reservoir in proximity to

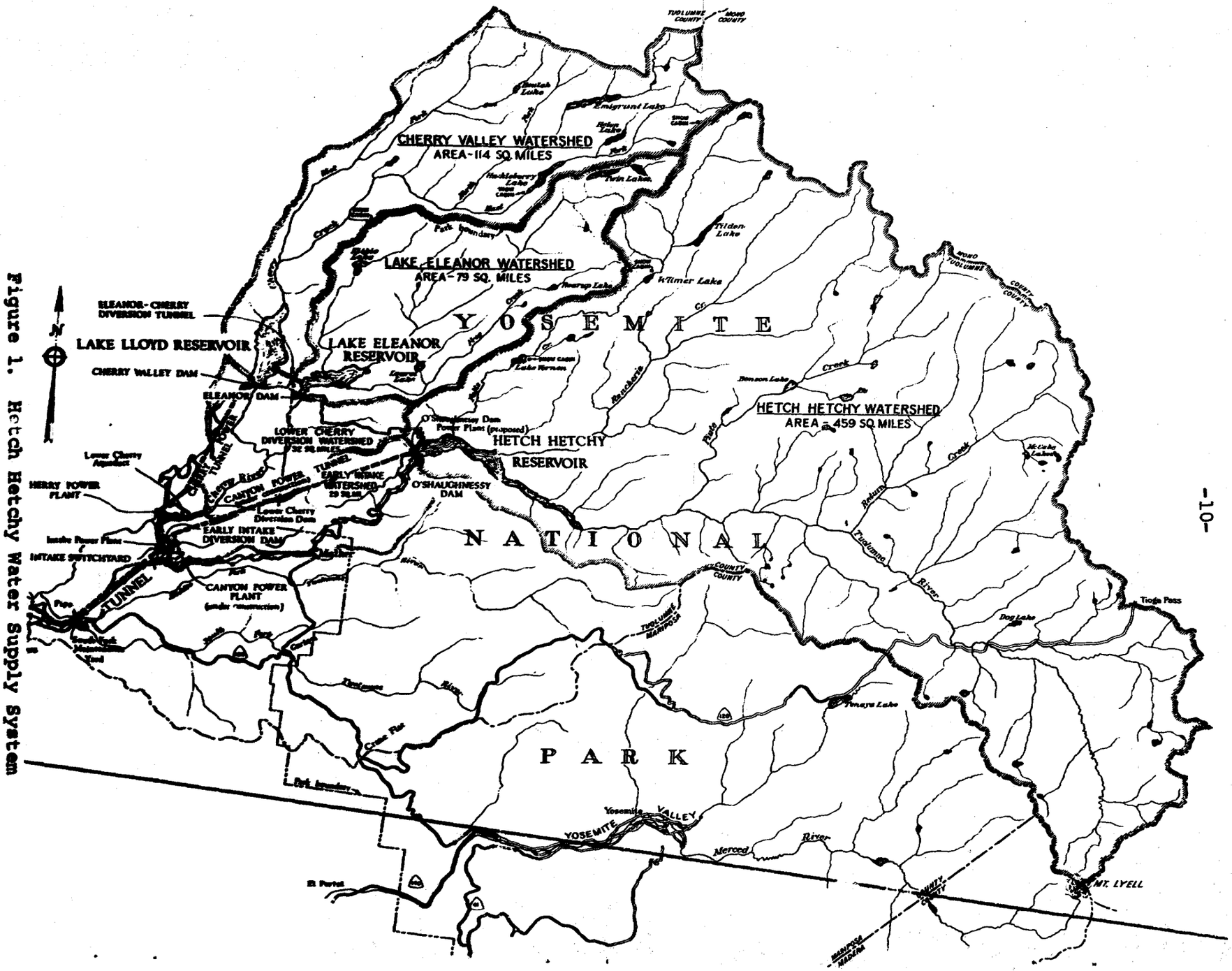

Figure 1. Hetch Hetchy Water Supply System

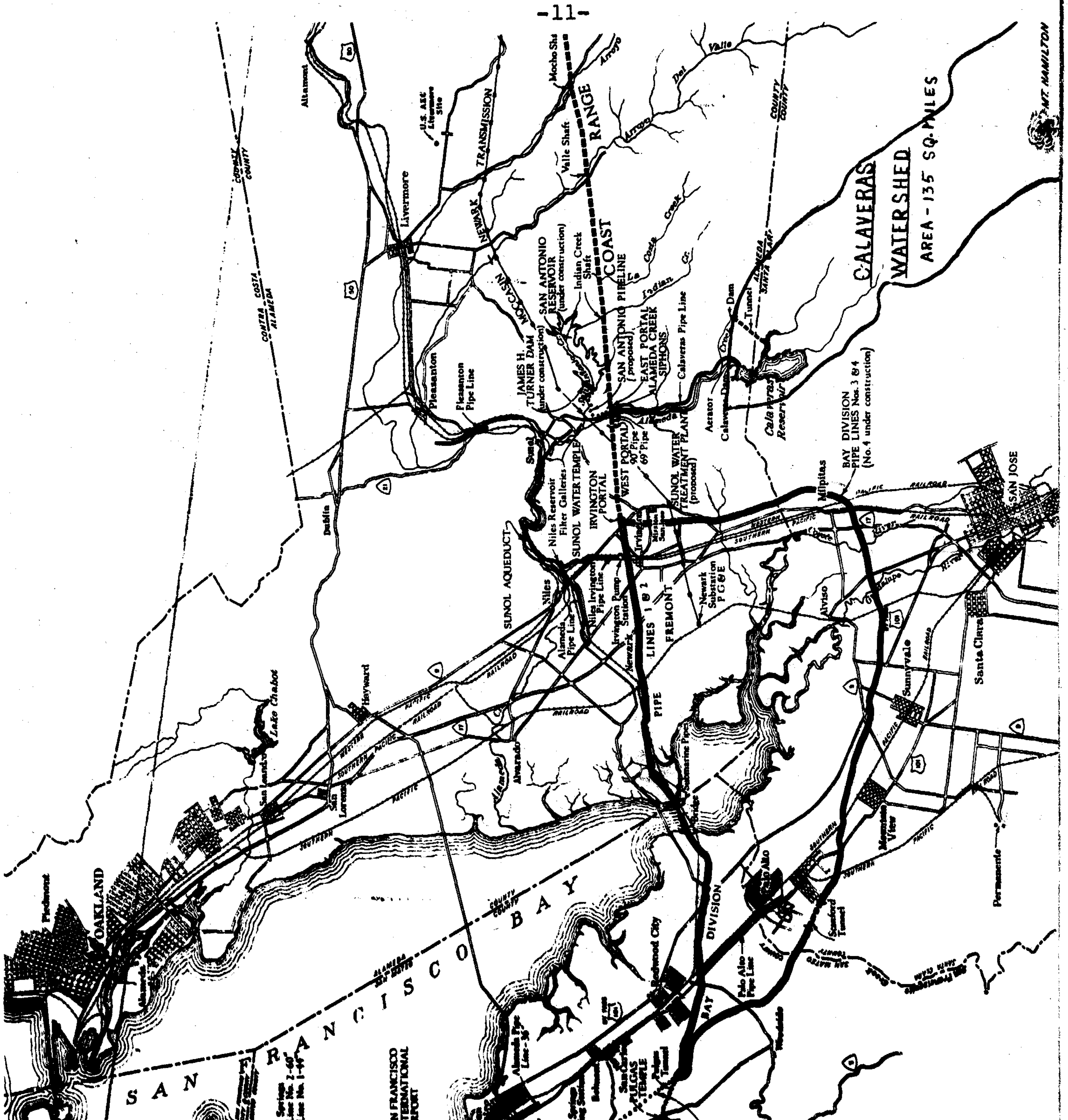

Figure 2. Proximity of Calaveras Reservoir to San Francisco.

San Francisco and the Peninsula water supply system (San Andreas and Crystal Springs Reservoirs). The Peninsula water supply system is situated about 20 miles south of the center of the city. It may be assumed that this system will receive only a relatively small amount of soluble fallout particles due to the presently chosen west wind. It is also reasonable to assume that this system will suffer severe damage from a hundred-megaton-level attack and will not render any service for a long period of time. Therefore, in these investigations, the contamination of the San Francisco water supply was confined to that contributed by the Calaveras and Hetch Hetchy systems.

1. Hetch Hetchy and Calaveras Water Supply Systems

The Hetch Hetchy system consists essentially of three streams in the Sierra Mountains which are being continuously developed to provide water and power for San Francisco, the Bay Area, and San Joaquin Valley. These streams are Eleanor Creek, the Cherry River, and the Tuolumne River and each flows into a reservoir. The Tuolumne River, contained by the O'Shaughnessy Dam, forms the largest reservoir with a capacity of 117.3 billion gallons. Hetch Hetchy Reservoir supplies the principal amount of water for domestic use from the 459 sq mi Hetch Hetchy watershed (7).

Tuolumne River water, including spill and releases at O'Shaughnessy Dam, and the runoff from 29 sq mi of Early Intake watershed are intercepted 12 miles downstream at the Early Intake Diversion Dam and turned into the main aqueduct. Water from 32 sq mi of watershed between the other two rivers is diverted into a canal at the Cherry River Diversion Dam and is delivered either to the Early Power Plant or to the Early Intake.

From the Early Intake, the diverted waters travel through a series of tunnels with over 400 m.g.d. capacity and are discharged into Priest Regulating Reservoir which has an impounding capacity of 77 m.g.d. The water then proceeds through the mile-long Power Tunnel to emerge in the Moccasin Reregulating Reservoir used to equalize the flow into Foothill Tunnel. Continuing through Foothill Tunnel the waters reach the Red Mountain Bar Pipeline, an inverted siphon under the Tuolumne River.

At the outlet end of this transmission line, water that is not to be transmitted to the service area, is released into the Don Pedro Reservoir where it is used in the Turlock and Modesto irrigation districts.

Water to be used by San Francisco continues on through a 10.6 mi. tunnel which ends in an overflow shaft located in the east San Joaquin Valley foothills at the Oakdale Portal. Two pipelines, varying from 56 in. to 72 in. in diameter, carry the water over the San Joaquin Division between the Oakdale and Tessla Portals where it enters the Coast Range Tunnel and travels 25.2 mi. until it reaches Alameda East Portal, the westerly end of the portion of the aqueduct operated and maintained by the Hetch Hetchy authority. It is also the beginning of the system under the San Francisco Water Department operation and maintenance.

The Alameda siphon consists of two pipelines between Alameda East and West Portals. It is between these two portals of the aqueduct that a second principal water supply is joined. Calaveras Reservoir has a capacity of 31.5 billion gallons and in addition to the water it releases into the aqueduct, it serves the Water Department's Sunol headquarters area and the town of Sunol.

From the siphon the water enters the second section of the Coast Range Tunnel and travels to the Irvington Portal where three pipelines, known as the Bay Division Pipelines No. 1, 2, and 3, carry water to Pulgas Tunnel. Pipelines No. 1 and 2 cross San Francisco Bay, while pipeline No. 3 circles the south end of the bay. All three pipelines convene again at Pulgas Tunnel.

One other source of water, when used, which enters the aqueduct before it reaches Pulgas Tunnel is the combined source from well fields(*) in Pleasanton and the Sunol filter galleries. This water flows through the 4.9 mi. Sunol-Niles Aqueduct (70 m.g.d. design capacity) to Niles Regulating Reservoir (5 m.g. storage capacity) and from there to the Irvington Portal where pumps lift the water into Bay Division Pipelines No. 1 and 2.

(*) About 100 wells have been developed in this field, varying in depth from 200 to 400 ft., but one is 734 ft. deep. Many of these wells are not usable and since 1949 no water from these wells has been provided to consumers outside the valley. Prior to 1949, the wells produced an average of about 10 m.g.d. for export.

Pulgas Tunnel is the last section of the Hetch Hetchy aqueduct and discharges its waters through the Pulgas Water Temple and into Upper Crystal Springs Reservoir. From the Peninsula system, of which Upper Crystal Springs is a part, the water is finally released to the City of San Francisco. Hetch Hetchy water traverses a distance of 150 miles from O'Shaughnessy Dam to Crystal Springs Reservoir; through river beds, tunnels and pipelines, entirely by gravity without any pumping of the water along the way necessary.

2. Method of Evaluation

The approach to the evaluation of reservoir and watershed contamination was essentially the method described previously. However, the few changes in the procedure are included in the brief outline below.

Both the Hetch Hetchy and Calaveras systems were located within the cloud fallout region and the ionization rate contours for these areas was found by interpolation between computer calculated contours for 5 MT, 10 MT and 20 MT weapons. These intensity contours were drawn over a grid system with each grid area equal to four square miles.

To facilitate evaluation, the area of each reservoir and its watershed were reproduced on the isointensity contour map, shown in Figure 3. The intensity at the centroid of each watershed grid area was estimated. The calculations for determining the soluble atom-concentration intensity ratio, $N'(A)/I(1)$, and the conversion from intensity over each grid area to the total activity in atoms per sq ft over the entire reservoir, were carried out in accordance with the procedure outlined previously.

Assuming complete mixing, the atom concentration (atoms/liter) of each nuclide in the water was obtained by dividing the total number of atoms by the volume of the reservoir. These values were then converted to $\mu c/ml$ by multiplication with the decay constant, λ, and appropriate dimensional conversion factor.

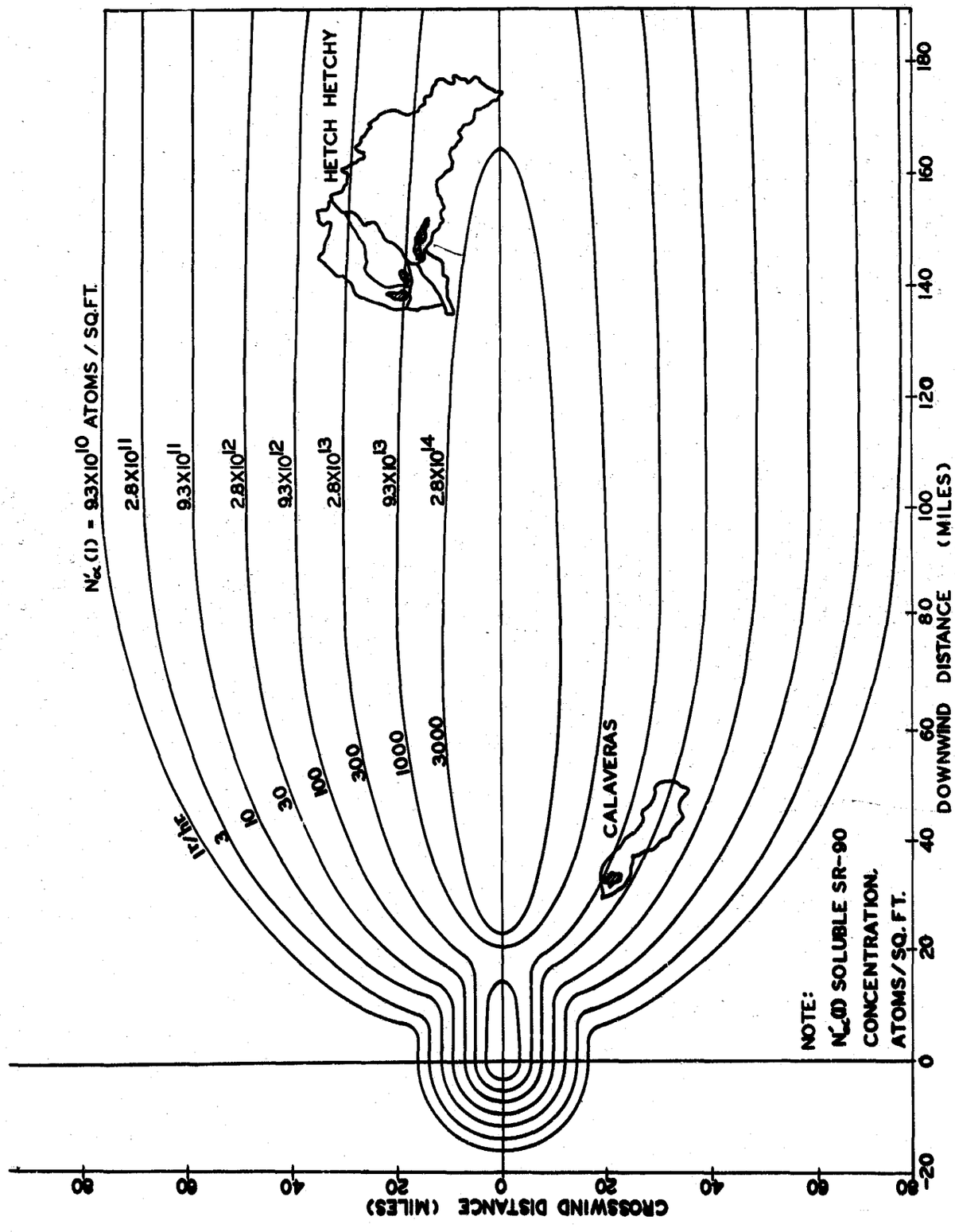

Figure 3. Hetch Hetchy and Calaveras Watersheds Superimposed on Soluble Nuclide Contour Ratio for Sr-90 for a 20 MT Weapon Yield and Wind Speed of 15 mph

To evaluate the degree of contamination when precipitation follows a nuclear attack, contamination of the reservoir due to watershed runoff was calculated in an identical manner, except for the introduction of a runoff coefficient of 0.5, to determine the number of atoms entering the reservoir from the watershed. These values of contamination due to watershed runoff are considered to be a maximum, and will vary considerably, depending on the instantaneous moisture content of the soil, the period of time between detonation and onset of rainfall, ion-exchange capacity and absorption in and on the soil, plant uptake, and other environmental factors.

3. Results

The final results of the computations for the concentrations of six biologically important radionuclides in the San Francisco water supply systems at H + 1 hour after a 155 MT nuclear attack have been summarized and are presented in Table II.

E. Evaluation of Springfield, Massachusetts Water Supply

1. Orientation of Fallout Model for Springfield

The total weaponage assigned to the city of Springfield is 30 MT; one 20 MT weapon for military targets and one 10 MT for civilian targets. Because of the close proximity between the water supply reservoirs and the target areas and the large difference in contamination effect which would result if both weapons were assumed to be detonated at the same ground zero, two separate areas were considered. Ground zero for the 20 MT weapon was located at Westover Air Force Base, while ground zero for the 10 MT weapon was assumed to be located in the center of the City of Springfield.

The annual northwest wind direction would cause a maximum fallout concentration in the Ludlow Reservoir, but it would also produce a minimum concentration in the Little River Supply system, the principal source of water supply for Springfield. Consequently, the wind direction was chosen to be from the east to maximize fallout effects on the city's water supply. Wind speed was again assumed to be 15 mph.

TABLE II

Contamination of San Francisco Water Supply System

System	Isotope	Direct Contamination of Reservoir		Contamination, including Runoff	
		(atom/liter)	(μc/ml)	(atom/liter)	(μc/ml)
	Sr-89	1.82×10^{11}	7.40×10^{-4}	7.07×10^{12}	2.88×10^{-2}
Hetch	Sr-90	2.93×10^{11}	6.23×10^{-6}	1.07×10^{13}	2.27×10^{-4}
Hetchy	Ru-106	1.22×10^{11}	7.24×10^{-5}	4.84×10^{12}	2.88×10^{-3}
System	I-131	2.84×10^{11}	7.64×10^{-3}	1.07×10^{13}	2.88×10^{-1}
	Cs-137	2.70×10^{11}	4.82×10^{-6}	1.04×10^{13}	1.86×10^{-4}
	Ba-140	3.01×10^{11}	5.09×10^{-3}	1.13×10^{13}	1.91×10^{-1}
	Sr-89	5.86×10^{10}	2.38×10^{-4}	1.08×10^{12}	4.38×10^{-3}
Cala-	Sr-90	1.29×10^{11}	2.74×10^{-6}	2.04×10^{12}	4.34×10^{-5}
veras	Ru-106	6.00×10^{10}	3.57×10^{-5}	9.36×10^{11}	5.56×10^{-4}
System	I-131	1.33×10^{11}	3.57×10^{-3}	2.09×10^{12}	5.63×10^{-2}
	Cs-137	7.96×10^{10}	1.42×10^{-6}	1.49×10^{12}	2.66×10^{-5}
	Ba-140	1.46×10^{11}	2.47×10^{-3}	2.28×10^{12}	3.87×10^{-2}
	Sr-89	1.70×10^{11}	6.91×10^{-4}	6.51×10^{12}	2.65×10^{-2}
	Sr-90	2.77×10^{11}	5.90×10^{-6}	9.90×10^{12}	2.11×10^{-4}
Entire	Ru-106	1.16×10^{11}	6.89×10^{-5}	4.48×10^{12}	2.66×10^{-3}
System(*)	I-131	2.70×10^{11}	7.26×10^{-3}	9.90×10^{12}	2.66×10^{-1}
	Cs-137	2.52×10^{11}	4.48×10^{-6}	9.58×10^{12}	1.71×10^{-4}
	Ba-140	2.86×10^{11}	4.77×10^{-3}	1.05×10^{13}	1.75×10^{-1}

(*) The entire system is computed according to the combination of the daily outputs of the two branch systems. Daily output of Hetch Hetchy system is 400 million gallons, and that of Calaveras is 40.5 million gallons.

2. Springfield Water Supply System

Springfield's water supply system is owned and operated by the City of Springfield, Board of Water Commissioners. The system consists of two surface supplies known as the Little River Supply system and the Ludlow Reservoir system. Until 1909 the Ludlow system was the only supply for the city of Springfield; has been retained since on a standby capacity. It continues to supply the town of Ludlow (pop. 15,135) and the Monsanto Chemical Company plant.

Two reservoirs, Borden Brook and Cobble Mountain, located about 18 miles west of metropolitan Springfield, form the major portion of the Little River Supply system and the principal water supply source for the total population of almost 225,000.

Water from Borden Brook Reservoir flows into the Cobble Mountain Reservoir and from there into the Little River. Some of the water is diverted directly from the reservoir by tunnel to the West Parish Filters. Water from the Little River flows through a power station, which is leased by the Commission to the Western Massachusetts Electric Company. After leaving the power station, the water flows into an intake reservoir where it is also diverted by tunnel to the West Parish Filters. At the West Parish Filters the water is settled in covered sedimentation basins and then treated by slow sand filtration. This is the only water treatment process employed by the Commission.

The treated water is carried from the West Parish filters, a distance of approximately 2.5 miles, to the completely covered Provin Mountain Reservoir, which consists of four reinforced concrete sections. The water is metered as it leaves Provin Mt. Reservoir, and from 25 to 55 m.g.d. (avg. 36.5 m.g.d.) enter the three transmissions mains which cross the Connecticut River into the City of Springfield.

The Little River watershed, Cobble Mountain and Borden Brook reservoirs, the West Parish Filters and transmission lines are shown in Figure 4.

3. Method of Evaluation for Contamination of Springfield Water Supply System

The evaluation of watershed and reservoir contamination was performed by the same method as was used for San Francisco. Since the computer programs for intensity

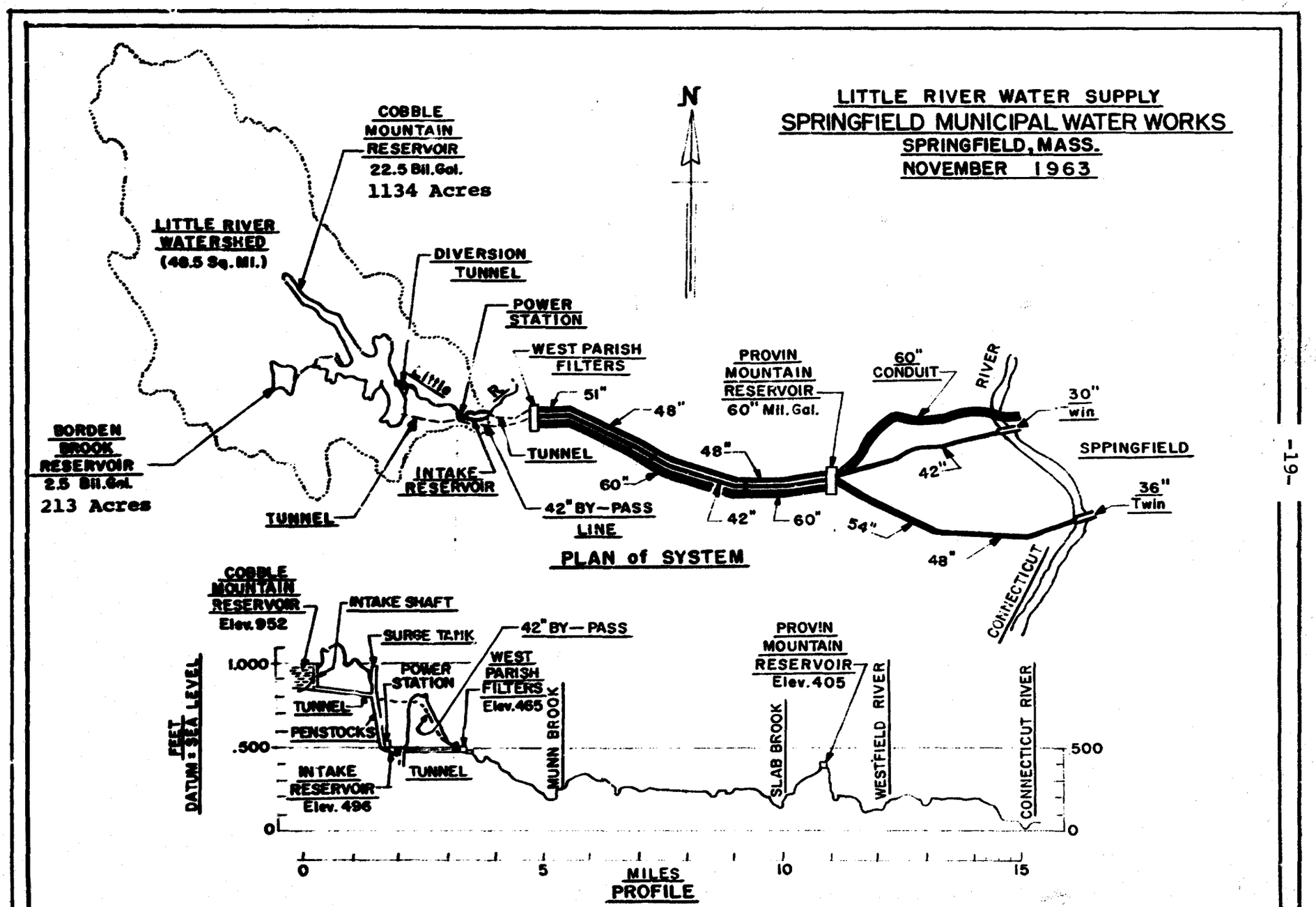

Figure 4. Springfield, Massachusetts Water Supply System

at any downwind location had not yet been verified, the area of each reservoir and its watershed were reproduced on the contour grids and the intensity determined by geometric interpolation as before. After the evaluation had been completed, the intensity values which had been estimated for the 10 MT weapon were compared with computer estimated values and were found to be in close agreement.

4. Results

The concentrations of six biologically important radionuclides in the Springfield, Massachusetts water supply system at H + 1 hour following a 30 MT nuclear attack have been summarized in Table III.

F. Evaluation of Paterson, New Jersey, Water Supply System

1. Orientation of Fallout Model for Paterson

The evaluation of contamination to Paterson's water supply began, as with the other selected target cities, with the orientation of the fallout model. Ground zero was assumed to be at Little Falls, New Jersey on the Passaic River, the location of the Paterson, New Jersey water supply intake. The wind direction was chosen as the predominant annual southwest wind. However, it became evident that this particular orientation, or any other orientation of the model which might be produced if Paterson were attacked with the assigned 60 MT, would yield inaccurate results of water contamination. Depending on the orientation of the model, one or both of the following situations would cause these inaccuracies:

(1) Most of the watersheds and reservoirs would not be affected by fallout, or if they were affected, contamination would consist principally of insoluble radionuclides

(2) The area being considered would be completely destroyed by the nuclear detonation (blast and thermal damage)

Consequently, it was decided to evaluate contamination of Paterson's water supply from an attack on some other city to approach a maximum degree of contamination for the Paterson supply, i.e. the Passaic River and Wanaque Reservoir. The

TABLE III

Contamination of Springfield Water Supply System

Location	Isotope	Direct Contamination of Reservoir		Contamination, including Runoff	
		(atom/liter)	(μc/ml)	(atom/liter)	(μc/ml)
Case I Ground Zero at Springfield 10 MT	Sr-89	6.96×10^{9}	2.83×10^{-5}	6.49×10^{10}	2.64×10^{-4}
	Sr-90	2.73×10^{10}	5.81×10^{-7}	2.71×10^{11}	5.76×10^{-6}
	Ru-106	1.99×10^{10}	1.18×10^{-5}	1.66×10^{11}	9.86×10^{-5}
	I-131	2.80×10^{8}	7.55×10^{-6}	7.50×10^{10}	2.02×10^{-3}
	Cs-137	4.14×10^{9}	7.38×10^{-8}	7.31×10^{10}	1.30×10^{-6}
	Ba-140	3.21×10^{10}	5.42×10^{-4}	3.19×10^{11}	5.39×10^{-3}
Case II Ground Zero at Westover 20 MT	Sr-89	1.60×10^{10}	6.40×10^{-5}	2.81×10^{11}	1.14×10^{-3}
	Sr-90	7.19×10^{10}	1.53×10^{-6}	8.93×10^{11}	1.90×10^{-5}
	Ru-106	4.88×10^{10}	2.90×10^{-5}	5.59×10^{11}	3.32×10^{-4}
	I-131	9.17×10^{9}	2.47×10^{-4}	6.21×10^{11}	1.68×10^{-2}
	Cs-137	1.69×10^{10}	3.01×10^{-7}	3.40×10^{11}	6.05×10^{-6}
	Ba-140	8.22×10^{10}	1.39×10^{-3}	9.98×10^{11}	1.69×10^{-2}
Case III 10 MT at Springfield and 20 MT at Westover	Sr-89	2.30×10^{10}	9.35×10^{-5}	3.46×10^{11}	1.41×10^{-3}
	Sr-90	9.92×10^{10}	2.11×10^{-6}	1.26×10^{12}	2.47×10^{-5}
	Ru-106	6.87×10^{10}	4.08×10^{-5}	7.25×10^{11}	4.31×10^{-4}
	I-131	9.45×10^{9}	2.55×10^{-4}	1.37×10^{12}	3.69×10^{-2}
	Cs-137	2.10×10^{10}	3.74×10^{-7}	4.13×10^{11}	7.36×10^{-6}
	Ba-140	1.14×10^{11}	1.92×10^{-3}	1.32×10^{12}	2.23×10^{-2}

new target was chosen to maintain a southwesterly wind direction. Consideration of the information presented in the Technical Operations, Inc., report (1) led to the selection of Philadelphia, Pennsylvania, as the target city. Ground zero was assumed in the vicinity of the Elmyra Bridge and the contamination of Paterson's water supply, due to a 115 MT weapon attack on Philadelphia, was evaluated.

2. Paterson Water Supply System

The Passaic Valley Water Commission was created by the three sister cities of Paterson, Passaic and Clifton. Its water source is a surface supply, most of which is diverted at Little Falls, New Jersey, where the commission has a 75 m.g.d. right to the waters of the Passaic River. However, the Passaic Valley Water Commission also has a 41.53 m.g.d. right as a partner in the North Jersey District Water Supply Commission's Wanaque Supply and receives water from this supply at Totowa, New Jersey, where there is an interconnection of the Passaic Valley Water Commission system with the Wanaque aqueduct. The supply system is further complicated because the North Jersey District Water Supply Commission has a 25 m.g.d. right to pump water from the Ramapo River at Pompton Lakes, New Jersey, into its Wanaque Reservoir. This water would normally flow past the Passaic Valley Water Commission plant at Little Falls by gravity. Figure 5 shows the watersheds of the Passaic River and tributaries and the intake at Little Falls, New Jersey.

The Passaic Valley Water Commission has three operating reservoirs floating on the system and an offstream flood flow storage reservoir, known as the Point View Reservoir, to augment low river flow, which was completed during the summer of 1964. The Point View Reservoir will receive flood water from the Pompton River and release it for future use during low river flow to guarantee the 75 m.g.d. Passaic River right throughout the year.

Water treatment at the Passaic Valley Water Commission's Little Falls Plant consists of "Precarbon slurry when necessary; prelime for alkalinity adjustment for flocculation when necessary; aluminum sulphate with flashmixing; super-prechlorination; flocculation; sedimentation; rapid sand filtration; postlime for pH adjustment,

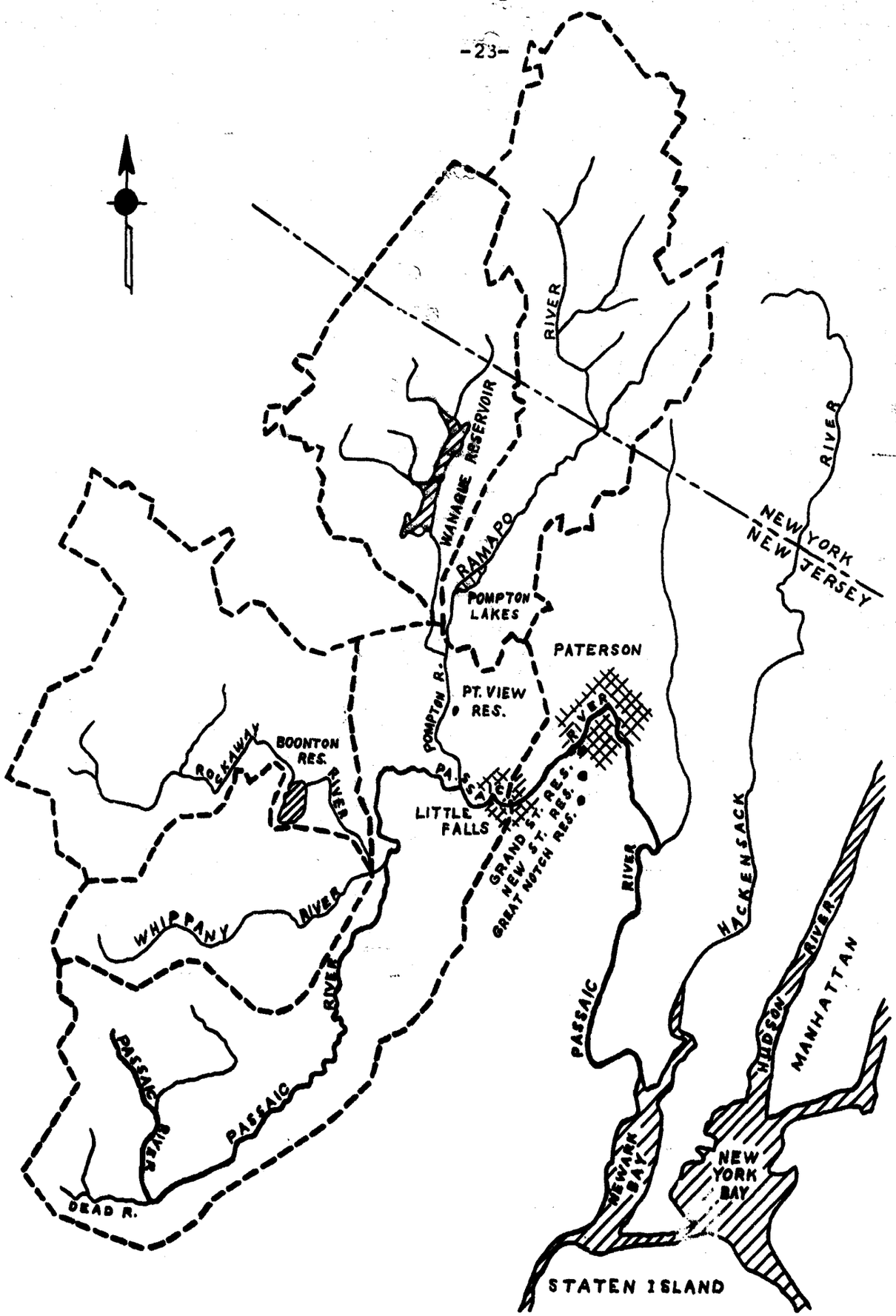

Figure 5. Watersheds of the Passaic River and Tributaries

followed by postchlorination and sodium dioxide for chlorine correction. The Wanaque supply is treated with prechlorination and pressure filtration through pulverized anthracite filter media" (8).

The Passaic Valley Water Commission serves also a number of smaller municipalities bordering on the three owner cities and supplies the water needs of approximately 500,000 people. The Paterson population according to the 1960 census was 43,633. The daily draft on the system for the city of Paterson averages about 80 million gallons.

3. Method of Estimating Contamination of Paterson Water Supply System

The method of evaluating reservoir and watershed contamination was carried out in much the same manner as for San Francisco. The major change in procedure was that geometric interpolation for intensity values was not necessary, because the computer program had been developed successfully to determine intensity values at any location for a particular weapon size. The primary concern with the Paterson supply was the type of system. The two previous target cities considered had large storage reservoirs for their water supplies, whereas Paterson's major source of water supply is diverted without storage from the Passaic River. Consequently, direct contamination to rivers had to be closely investigated. In the two previous cases, direct river contamination could be assumed to be negligible as compared to the contamination of the entire system.

The evaluation of river contamination is difficult without certain assumptions. As a basis for calculations to follow the same procedure, it was necessary to know the length of each river and also its exact location on a map grid system. Because of the meandering course of most rivers and their many tributaries, any attempt to define a river in this way was beyond the scope and precision of this project. Therefore, it was decided to consider only those portions of rivers that were downstream from reservoirs and upstream from the Little Falls intake plant. This decision was based on the assumption that due to the large volume of water in the reservoirs, the contamination in the river would be decreased due to releases from reservoirs. It

follows that a maximum degree of contamination at Little Falls could be estimated if the contamination effect from reservoirs and their feeder streams was eliminated.

The most effective generalization was that these selected portions of rivers could be treated as long rectangular reservoirs with their volume determined by the rate of stream flow. An outline of the procedure follows:

The surface area of a stream between its source and its point of confluence with another stream was evaluated by using the length and an average width. For the Passaic River the surface area was considered between the source and Little Falls. An average intensity value over the surface was obtained by taking an arithmetic mean of computer calculated intensities at various points along the stream. This average value was assumed to be characteristic of the entire surface area and the total number of soluble atoms, N'(A), on the stream surface was determined by the same procedure as that used previously for a single grid area over a reservoir. The average annual flow in cfs for each stream was converted to cu ft/day to obtain the approximate volume of water which flows through the stream in one day. With this data, the number of atoms per cubic foot, N, was calculated for each of the isotopes.

The estimate for N is based on (H + 1) hour. Therefore, the last calculation could be made because it has been generally accepted that the (H + 1) hour activity is essentially all the 24 hours deposition of fallout. This assumption allows cancellation of the time units in these calculations to obtain atoms per cubic foot, and with appropriate conversions - atoms/liter and micro-curie/ml concentrations.

Stream contamination due to watershed runoff was estimated by essentially the same procedure but with only 35% of the isotopes that fall on the watershed surfaces being considered in the calculations. As stated previously, the effects of contamination due to runoff will vary considerably, depending on the instantaneous moisture content of the soil, the period of time between detonation and onset of rainfall, ion-exchange capacity and absorption in and on the soil, plant uptake, etc. Runoff volume was calculated from the relation $Q = CiA$ where C is the runoff coefficient of the watershed, i is an estimated rainfall intensity in in/hr, and A is the

watershed surface area. Concentrations for runoff in atoms per cubic foot for the six isotopes were then calculated.

4. Results

The combined effect of stream and runoff contamination was obtained by computing a weighted average of the radioactive concentrations calculated separately for each case. Results of this evaluation, assuming a weapon distribution of 3 at 5 MT and 10 at 10 MT, appear in Table IV. After the computer program was able to determine intensity values at any location for any weapon size, it was used to obtain these values for a 20 MT attack. The contamination from a newly selected distribution of weapons, 1 at 5 MT, 1 at 10 MT and 5 at 20 MT, was calculated, as shown in Table IV and the results compared with the initially assumed distribution of weapons. Close agreement, with values in the same order of magnitude, was obtained.

TABLE IV

Contamination of Paterson Water Supply(*)

River or Reservoir	Isotope	Direct Contamination (atom/liter)	Direct Contamination (μc/ml)	Contamination, including Runoff (atom/liter)	Contamination, including Runoff (μc/ml)
Passaic River	Sr-89	1.33×10^{14}	5.40×10^{-1}	3.62×10^{14}	1.47
	Sr-90	2.42×10^{14}	5.15×10^{-3}	6.46×10^{14}	1.37×10^{-2}
	Ru-106	1.09×10^{14}	6.48×10^{-2}	3.04×10^{14}	1.81×10^{-1}
	I-131	2.43×10^{14}	6.55	6.78×10^{14}	1.83×10
	Cs-137	1.88×10^{14}	3.35×10^{-3}	5.12×10^{14}	9.13×10^{-3}
	Ba-140	2.63×10^{14}	4.44	7.25×10^{14}	1.22×10
Whippany River	Sr-89	2.56×10^{13}	1.04×10^{-1}	1.93×10^{14}	7.84×10^{-1}
	Sr-90	4.68×10^{13}	9.95×10^{-4}	3.47×10^{14}	7.38×10^{-3}
	Ru-106	2.11×10^{13}	1.25×10^{-2}	1.56×10^{14}	9.27×10^{-2}
	I-131	4.68×10^{13}	1.26	3.47×10^{14}	9.355
	Cs-137	3.64×10^{13}	6.49×10^{-4}	3.48×10^{14}	6.20×10^{-3}
	Ba-140	5.06×10^{13}	8.55×10^{-1}	3.75×10^{14}	6.33
Dead River	Sr-89	5.77×10^{12}	2.35×10^{-2}	2.97×10^{14}	1.21
	Sr-90	1.11×10^{13}	2.36×10^{-4}	5.71×10^{14}	1.21×10^{-2}
	Ru-106	5.00×10^{12}	2.79×10^{-3}	2.58×10^{14}	1.53×10^{-1}
	I-131	1.12×10^{13}	3.02×10^{-1}	5.72×10^{14}	1.54×10
	Cs-137	8.13×10^{12}	1.45×10^{-4}	4.12×10^{14}	7.34×10^{-3}
	Ba-140	1.20×10^{13}	2.03×10^{-1}	6.20×10^{14}	1.05×10
Pompton River	Sr-89	2.68×10^{12}	1.09×10^{-2}	1.07×10^{14}	4.35×10^{-1}
	Sr-90	4.72×10^{12}	1.00×10^{-4}	1.87×10^{14}	3.98×10^{-3}
	Ru-106	2.10×10^{12}	1.25×10^{-3}	8.47×10^{13}	5.03×10^{-2}
	I-131	4.70×10^{12}	1.27×10^{-1}	1.86×10^{14}	5.01
	Cs-137	3.84×10^{12}	6.85×10^{-5}	1.53×10^{14}	2.71×10^{-3}
	Ba-140	5.14×10^{12}	8.68×10^{-2}	2.03×10^{14}	3.43

(*) Employing 3 at 5 MT and 10 at 10 MT weapons = 115 MT attack

TABLE IV (cont'd)

Contamination of Paterson Water Supply(*)

River or Reservoir	Isotope	Direct Contamination (atom/liter)	Direct Contamination (μc/ml)	Contamination, including Runoff (atom/liter)	Contamination, including Runoff (μc/ml)
Wanaque River	Sr-89	1.27×10^{13}	5.16×10^{-2}	6.46×10^{13}	2.62×10^{-1}
	Sr-90	2.21×10^{13}	4.70×10^{-4}	1.12×10^{14}	2.38×10^{-3}
	Ru-106	1.05×10^{13}	1.18×10^{-2}	5.03×10^{13}	2.99×10^{-2}
	I-131	2.20×10^{13}	5.93×10^{-1}	1.11×10^{14}	2.99
	Cs-137	1.82×10^{13}	3.24×10^{-4}	9.24×10^{13}	1.65×10^{-3}
	Ba-140	2.38×10^{13}	4.02×10^{-1}	1.18×10^{14}	1.99
Rockaway River	Sr-89	8.16×10^{12}	3.32×10^{-2}	8.54×10^{13}	3.47×10^{-1}
	Sr-90	1.46×10^{13}	3.10×10^{-4}	1.52×10^{14}	3.23×10^{-3}
	Ru-106	6.56×10^{12}	3.90×10^{-3}	6.86×10^{13}	4.08×10^{-2}
	I-131	1.45×10^{13}	3.91×10^{-1}	1.52×10^{14}	4.50
	Cs-137	1.16×10^{13}	7.07×10^{-4}	1.27×10^{14}	2.26×10^{-3}
	Ba-140	1.56×10^{13}	2.63×10^{-1}	1.64×10^{14}	2.77
Wanaque River	Sr-89	2.27×10^{11}	9.23×10^{-4}	1.79×10^{12}	7.28×10^{-3}
	Sr-90	3.91×10^{11}	8.32×10^{-6}	3.20×10^{12}	6.80×10^{-5}
	Ru-106	1.75×10^{11}	1.04×10^{-4}	1.48×10^{12}	8.80×10^{-4}
	I-131	3.86×10^{11}	1.04×10^{-2}	3.08×10^{12}	8.30×10^{-2}
	Cs-137	3.24×10^{11}	5.78×10^{-6}	2.63×10^{12}	4.69×10^{-5}
	Ba-140	4.20×10^{11}	7.09×10^{-3}	3.33×10^{12}	5.62×10^{-2}
Grand Street Reservoir	Sr-89	3.63×10^{11}	1.48×10^{-3}	No increase in contamination from Surface Runoff	
	Sr-90	6.32×10^{11}	1.34×10^{-5}		
	Ru-106	2.83×10^{11}	1.68×10^{-4}		
	I-131	6.30×10^{11}	1.70×10^{-2}		
	Cs-137	5.20×10^{11}	9.27×10^{-6}		
	Ba-140	6.82×10^{11}	1.15×10^{-2}		

(*) Employing 3 at 5 MT and 10 at 10 MT weapons = 115 MT attack

TABLE IV (cont'd)

Contamination of Paterson Water Supply(*)

River or Reservoir	Isotope	Direct Contamination (atom/liter)	Direct Contamination (μc/ml)	Contamination, including Runoff (atom/liter)	Contamination, including Runoff (μc/ml)
New Street Reservoir	Sr-89	2.79×10^{12}	1.13×10^{-2}	in these City Reservoirs	
	Sr-90	4.88×10^{12}	1.04×10^{-4}	which float on the	
	Ru-106	2.18×10^{12}	1.30×10^{-3}	supply system and	
	I-131	4.86×10^{12}	1.31×10^{-1}	have no watersheds	
	Cs-137	3.99×10^{12}	7.11×10^{-5}		
	Ba-140	5.27×10^{12}	8.90×10^{-2}		
Great Notch Reservoir	Sr-89	2.71×10^{12}	1.10×10^{-2}	No increase in	
	Sr-90	4.76×10^{12}	1.01×10^{-4}	contamination	
	Ru-106	2.23×10^{12}	1.32×10^{-3}	from Surface Runoff	
	I-131	4.74×10^{12}	1.28×10^{-1}	in these City Reservoirs	
	Cs-137	3.88×10^{12}	6.92×10^{-5}	which float on the	
	Ba-140	5.15×10^{12}	8.70×10^{-2}	supply system and	
				have no watersheds	
(#) Entire System	Sr-89	8.61×10^{13}	3.50×10^{-1}	2.35×10^{14}	9.56×10^{-1}
	Sr-90	1.57×10^{14}	3.34×10^{-3}	4.19×10^{14}	8.91×10^{-3}
	Ru-106	7.05×10^{13}	4.19×10^{-2}	1.97×10^{14}	1.17×10^{-1}
	I-131	1.57×10^{14}	4.23	4.39×10^{14}	1.18x10
	Cs-137	1.22×10^{14}	2.18×10^{-3}	3.23×10^{14}	5.92×10^{-3}
	Ba-140	1.70×10^{14}	2.87	4.70×10^{14}	7.94

(*) Employing 3 at 5 MT and 10 at 10 MT weapons = 115 MT attack

(#) Contamination for the entire system is computed according to the combination of the Passaic Valley Water Commission's right to 41.53 MGD from Wanaque Reservoir and the commission's 75 MGD right to the waters of the Passaic River at Little Falls.

TABLE IV

Contamination of Paterson Water Supply(*)

River or Reservoir	Isotope	Direct Contamination (atom/liter)	Direct Contamination (μc/ml)	Contamination, including Runoff (atom/liter)	Contamination, including Runoff (μc/ml)
Passaic River	Sr-89	1.05×10^{14}	4.26×10^{-1}	2.83×10^{14}	1.15
	Sr-90	1.91×10^{14}	4.06×10^{-3}	5.93×10^{14}	1.26×10^{-2}
	Ru-106	8.81×10^{13}	5.23×10^{-2}	2.52×10^{14}	1.50×10^{-1}
	I-131	1.95×10^{14}	5.26	5.16×10^{14}	1.39×10^{1}
	Cs-137	1.48×10^{14}	2.64×10^{-3}	4.18×10^{14}	7.45×10^{-3}
	Ba-140	1.66×10^{14}	2.80	5.52×10^{14}	9.32
Whippany River	Sr-89	2.04×10^{13}	8.28×10^{-2}	1.62×10^{14}	6.58×10^{-1}
	Sr-90	3.70×10^{13}	7.87×10^{-4}	2.88×10^{14}	6.12×10^{-3}
	Ru-106	1.70×10^{13}	1.01×10^{-2}	1.34×10^{14}	7.96×10^{-2}
	I-131	3.78×10^{13}	1.02	2.95×10^{14}	7.95
	Cs-137	2.90×10^{13}	5.17×10^{-4}	2.22×10^{14}	3.96×10^{-3}
	Ba-140	3.97×10^{13}	6.71×10^{-1}	3.08×10^{14}	5.20
Dead River	Sr-89	3.65×10^{12}	1.48×10^{-2}	1.89×10^{14}	7.67×10^{-1}
	Sr-90	6.97×10^{12}	1.48×10^{-4}	3.60×10^{14}	7.65×10^{-3}
	Ru-106	1.87×10^{12}	1.11×10^{-3}	1.79×10^{14}	1.06×10^{-1}
	I-131	7.11×10^{12}	1.92×10^{-1}	3.64×10^{14}	9.81
	Cs-137	4.60×10^{12}	8.20×10^{-5}	2.58×10^{14}	4.60×10^{-3}
	Ba-140	7.63×10^{12}	1.29×10^{-1}	3.90×10^{14}	6.59
Pompton River	Sr-89	2.62×10^{12}	1.06×10^{-2}	9.82×10^{13}	3.99×10^{-1}
	Sr-90	4.54×10^{12}	9.65×10^{-5}	1.81×10^{14}	3.85×10^{-3}
	Ru-106	2.09×10^{12}	1.24×10^{-3}	8.44×10^{13}	5.01×10^{-2}
	I-131	4.67×10^{12}	1.26×10^{-1}	1.85×10^{14}	4.99
	Cs-137	3.76×10^{12}	6.70×10^{-5}	1.49×10^{14}	2.66×10^{-3}
	Ba-140	4.90×10^{12}	8.28×10^{-2}	1.92×10^{14}	3.24

(*) Employing 1 at 5 MT, 1 at 10 MT and 5 at 20 MT weapons = 115 MT attack

TABLE IV (cont'd)

Contamination of Paterson Water Supply(*)

River or Reservoir	Isotope	Direct Contamination (atom/liter)	Direct Contamination (μc/ml)	Contamination, including Runoff (atom/liter)	Contamination, including Runoff (μc/ml)
Wanaque River	Sr-89	1.26×10^{13}	5.12×10^{-2}	6.56×10^{13}	2.66×10^{-1}
	Sr-90	2.19×10^{13}	4.66×10^{-4}	1.13×10^{14}	2.40×10^{-3}
	Ru-106	1.00×10^{13}	5.94×10^{-3}	5.23×10^{13}	3.12×10^{-2}
	I-131	2.24×10^{13}	6.04×10^{-1}	1.16×10^{14}	3.13
	Cs-137	1.82×10^{13}	3.24×10^{-4}	9.42×10^{13}	1.68×10^{-3}
	Ba-140	2.32×10^{13}	3.92^{-1}	1.18×10^{14}	1.99
Rockaway River	Sr-89	6.03×10^{12}	2.45×10^{-2}	9.19×10^{13}	3.73×10^{-1}
	Sr-90	1.07×10^{13}	2.27×10^{-4}	1.63×10^{14}	3.46×10^{-3}
	Ru-106	4.98×10^{12}	2.96×10^{-3}	7.52×10^{13}	4.47×10^{-2}
	I-131	1.28×10^{13}	3.45×10^{-1}	1.70×10^{14}	4.58
	Cs-137	8.60×10^{12}	1.53×10^{-4}	1.36×10^{14}	2.42×10^{-3}
	Ba-140	1.11×10^{13}	1.87×10^{-1}	1.72×10^{14}	2.99
Wanaque Reservoir	Sr-89	2.34×10^{11}	9.50×10^{-4}	2.10×10^{12}	8.53×10^{-3}
	Sr-90	1.04×10^{11}	8.59×10^{-6}	3.50×10^{12}	7.44×10^{-5}
	Ru-106	1.87×10^{11}	1.11×10^{-4}	1.61×10^{12}	9.56×10^{-4}
	I-131	2.91×10^{11}	7.84×10^{-3}	3.43×10^{12}	9.25×10^{-2}
	Cs-137	3.38×10^{11}	6.02×10^{-6}	2.94×10^{12}	5.24×10^{-5}
	Ba-140	4.23×10^{11}	7.14×10^{-3}	3.60×10^{12}	6.08×10^{-2}
Grand Street Reservoir	Sr-89	3.52×10^{11}	1.43×10^{-3}	No increase in contamination from Surface Runoff	
	Sr-90	6.09×10^{11}	1.29×10^{-5}		
	Ru-106	2.83×10^{11}	1.68×10^{-4}		
	I-131	6.27×10^{11}	1.69×10^{-2}		
	Cs-137	5.08×10^{11}	9.05×10^{-6}		
	Ba-140	6.49×10^{11}	1.10×10^{-2}		

(*) Employing 1 at 5 MT, 1 at 10 MT and 5 at 20 MT weapons = 115 MT attack

TABLE IV (cont'd)

Contamination of Paterson Water Supply(*)

River or Reservoir	Isotope	Direct Contamination (atom/liter)	Direct Contamination (μc/ml)	Contamination, including Runoff (atom/liter)	Contamination, including Runoff (μc/ml)
New Street Reservoir	Sr-89	2.73×10^{12}	1.11×10^{-2}	in these City Reservoirs which float on the supply system and have no watersheds	
	Sr-90	4.71×10^{12}	1.00×10^{-4}		
	Ru-106	2.00×10^{12}	1.19×10^{-3}		
	I-131	4.84×10^{12}	1.30×10^{-1}		
	Cs-137	3.92×10^{12}	7.00×10^{-5}		
	Ba-140	5.00×10^{12}	8.44×10^{-2}		
Great Notch Reservoir	Sr-89	4.40×10^{12}	1.79×10^{-2}	No increase in contamination from Surface Runoff in these City Reservoirs which float on the supply system and have no watersheds	
	Sr-90	3.53×10^{12}	7.50×10^{-5}		
	Ru-106	1.62×10^{12}	9.62×10^{-4}		
	I-131	3.63×10^{12}	9.79×10^{-2}		
	Cs-137	2.89×10^{12}	5.15×10^{-5}		
	Ba-140	3.73×10^{12}	6.30×10^{-2}		
(#) Entire System	Sr-89	6.8×10^{13}	2.76×10^{-1}	1.84×10^{14}	7.47×10^{-1}
	Sr-90	1.24×10^{14}	2.64×10^{-3}	3.85×10^{14}	8.18×10^{-3}
	Ru-106	5.7×10^{13}	3.38×10^{-2}	1.64×10^{14}	9.74×10^{-2}
	I-131	1.26×10^{14}	3.40	3.35×10^{14}	9.03
	Cs-137	9.58×10^{13}	1.71×10^{-3}	2.71×10^{14}	4.83×10^{-3}
	Ba-140	1.07×10^{14}	1.81	3.58×10^{14}	6.05

(*) Employing 1 at 5 MT, 1 at 10 MT and 5 at 20 MT weapons = 115 MT attack

(#) Contamination for the entire system is computed according to the combination of the Passaic Valley Water Commission's right to 41.53 MGD from Wanaque Reservoir and the commission's 75 MGD right to the waters of the Passaic River at Little Falls.

G. Summary and Conclusions

The concentrations of six biologically important radionuclides in the San Francisco water supply system at H + 1 hour after a 155 MT nuclear attack were presented in Table II. These results show that the direct contamination of reservoirs will be of low level, with only I-131 and Ba-140 concentrations exceeding values of 10^{-3} μc/cc which may be considered as very safe concentrations of activity in water during the post-attack period. This conclusion is based on the fact that the peacetime continuous occupational exposure MPC (9) values for I-131 and Ba-140 in drinking water are 6×10^{-5} μc/cc and 8×10^{-4} μc/cc, respectively, and that a concentration below 3.5×10^{-3} μc/cc for beta-gamma activity has been considered "safe" during the initial 10-day period of consumption following a nuclear explosion based on unofficial estimates made in 1954 (10). The levels of contamination, including watershed runoff, for Sr-89, Sr-90, I-131 and Ba-140, as shown in Table V, exceed the peacetime MPC values by factors from 10 to 1,000 and the values of Sr-89, I-131 and Ba-140 exceed the "safe" 10- and 30-day consumption emergency levels by factors from 10 to 100. However, these concentrations of activity are not too high for the immediate post-attack period and for limited periods of consumption. Furthermore, a decontamination factor of 10^3 is quite feasible if water treatment processes can be implemented. An average runoff coefficient of 50% for the San Francisco Water Supply System watersheds was estimated from U.S. Department of Agriculture and U.S. Geological Survey data (11). This value also implies a 50% probability that the radionuclides in the watershed will mix into the reservoir. Therefore, except for an unusual long draught period, the effect due to runoff should be taken into consideration.

Contamination of the Springfield, Massachusetts water supply system from a 30 MT attack was generally lower than that observed for San Francisco. The results for the contamination of the Springfield supply were presented in Table III. Of the six biologically important radioisotopes investigated, the levels of I-131 and Ba-140 from direct contamination are the highest values; and when the effect of watershed runoff is included the contamination levels of I-131 and Ba-140 exceed 10^{-2} μc/cc as shown

TABLE V

Summary of Water Contamination Levels and Decontamination Requirements

(all values are given in μc/cc)

System	Sr-89	Sr-90	Ru-106	I-131	Cs-137	Ba-140
1. Entire San Francisco System						
a. Surface contamination	7×10^{-4} (SP)	6×10^{-6} (SP)	7×10^{-5} (SP)	7×10^{-3} (SE)	4.5×10^{-6} (SP)	4.8×10^{-3} (SE)
b. Contamination, including Runoff	2.7×10^{-2} (SE)	2×10^{-4} (SE)	2.7×10^{-3} (SE)	2.7×10^{-1} (DR)	1.7×10^{-4} (SP)	1.8×10^{-1} (DR)
2. Springfield Water Supply, Case III 10 MT Springfield 20 MT Westover AFB						
a. Surface contamination	9×10^{-5} (SP)	2×10^{-6} (SP)	4×10^{-5} (SP)	2.5×10^{-4} (SP)	3.7×10^{-7} (SP)	2×10^{-3} (SE)
b. Contamination, including Runoff	1.4×10^{-3} (SE)	2.5×10^{-5} (SE)	4.3×10^{-4} (SE)	3.7×10^{-2} (DR)	7.4×10^{-6} (SP)	2×10^{-2} (DR)
3. Entire Paterson Water Supply						
a. Surface contamination	3.5×10^{-1} (DR)	3.3×10^{-3} (SE)	4.2×10^{-2} (SE)	4.2 (DR)	2.2×10^{-3} (SE)	2.9 (DR)
b. Contamination, including Runoff.	9.6×10^{-1} (DR)	8.9×10^{-3} (SE)	1.2×10^{-1} (DR)	1.2x10 (DR)	6×10^{-3} (SE)	7.9 (DR)

Explanation of Symbols:

SP = Satisfactory without any additional treatment - meets peacetime standards
SE = Satisfactory without additional treatment for emergency conditions during immediate post-attack period
DR = Decontamination recommended - consumption during immediate post-attack period permissible but water treatment for decontamination should be implemented as soon as possible.

in Table V. These I-131 and Ba-140 concentrations in water call for the initiation of decontamination procedures at the earliest practical moment following nuclear attack.

In general, these concentrations are about one order of magnitude lower than similar values obtained for the San Francisco water supply system. The effect due to surface runoff from the watersheds appears to increase the level of contamination to a lesser degree than in the case of San Francisco which would be logical to expect because of the considerably smaller watershed to reservoir surface ratio.

Results of the radioactive concentrations from the combined effect of stream and runoff contamination for the various parts contributing to the Paterson, New Jersey water supply system were presented in Table IV. A 115 MT attack on Philadelphia, Pennsylvania, was assumed to maximize the effect on the Paterson water supply watershed. Two types of weapon distribution were assumed, in the first case, 3 at 5 MT and 10 at 10 MT and in the second case 1 at 5 MT, 1 at 10 MT and 5 at 20 MT weapons. Both weapon distributions produce the same magnitude of water contamination.

It is apparent that the maximum contamination has been obtained for the Passaic River and that Sr-89, Ru-106, I-131 and Ba-140 pose potential ingestion hazards. The situation is more serious when surface runoff is added due to precipitation following nuclear attack. The estimated values of contamination from direct surface contamination exceed the peacetime MPC values for all six nuclides by factors from 10 to 10^5, the latter for I-131. The contamination levels, including watershed runoff, are even greater, ranging up to 12 μc/cc for I-131, as may be seen in Table V. A decontamination factor of 10^2 to 10^4 for I-131 and Ba-140 appears necessary to produce a radiologically safe drinking water. It is possible to achieve this degree of decontamination with known water decontamination processes.

It is encouraging to note that in most cases the contamination levels can be reduced to even meet peacetime, continuous occupational exposure values by decontamination processes. The maximum decontamination required appears to be for the removal of I-131 for the Paterson, New Jersey, water supply system. The efficacies of available decontamination processes have been summarized in Table XXVI. Therefore, the

conclusions of this study do not materially differ from those obtained by Lee (12), especially if the contamination has been removed by passage through a water treatment plant. However, decontamination by water treatment or availability of uncontaminated water from ground water sources depend heavily on the continuous availability of electric power. A recent study (3) of the capability of waterworks systems to recover following nuclear attack does not assure recovery without serious interruption of service. During the post-attack period there is an urgent need for water supply but the recovery of the system, including treatment, may be slow and inadequate. Therefore, it is most important to estimate the absorbed dose in the human body from contaminated water over different periods of consumption.

During the process of estimation it was observed that the degree of contamination of an area is approximately a linear function of weapon size. Therefore, the contamination level from a 10 MT weapon will be about twice as much as that from a 5 MT weapon for a given water supply, while the blast, thermal, or initial radiation effect from a weapon is generally a power function of its size.

In the case of a 10 MT weapon with ground zero in the city of Springfield, the nuclide concentrations among the six isotopes varied significantly from those found in the cases of San Francisco and Paterson. A comparison of the results obtained from the 10 MT and 20 MT weapons at Springfield shows that the nuclide concentrations for Cs-137 and I-131 are approximately 10 and 100 times greater, respectively, from the larger weapon yield.

These effects result from the assumption that generally the fallout particles within the stem are of large size (small α) and that they fall out at a very early stage before the fireball has cooled down. Therefore, practically all the condensed radionuclides are fused inside the particles and become insoluble. Therefore, the solubility contour ratios are primarily derived from cloud fallout and as a result there is a limitation to the applicable downwind distance because of the dimensions

of the cloud. For α less than a certain value and consequently within a certain downwind distance, the soluble nuclide contour ratio of a given weapon yield approaches zero(*).

This assumption constituted a primary reason for eliminating from consideration the contamination effects to the Peninsula Water Supply when evaluating the contamination of the complete San Francisco Water Supply System. However, when examining the smaller water supply system of the City of Springfield with regard to a 10 MT weapon, it was necessary to assume a zero contamination to a large section of the water supply system. Although the limitation of the model increases with weapon yield, the effects of a 20 MT weapon on the Springfield Water Supply could be evaluated using the Miller model because its assumed ground zero was at Westover Air Force Base which is an additional 6 miles from ground zero at Springfield. To remedy this situation it was noted that the model's attempt to delineate zones in which there is or is no danger from soluble radioactivity is theoretical. Ordinarily this distinction is accepted on the basis that the range covered by insoluble nuclides is generally within the radius of blast and thermal damage and that any water supplies within this range would be destroyed. However, since part of the watershed area in question was in fringe areas, with regard to the cloud, grid areas within the downwind limits obtained from the model were assigned one half the value of the contamination effect that was calculated for the adjoining grid area outside the limits. It is believed that this method is more realistic than that represented by the model. However, concentrations calculated in this manner did not increase by half a magnitude over previous calculations.

Miller's fallout model will yield satisfactory soluble nuclide concentration results only for those water supply systems that are approximately twenty or more miles downwind from ground zero of a nuclear detonation.

(*) For the values of the limits of the applicable downwind distance see Appendix A.

III. BIOLOGICAL UPTAKE

A. Introduction

Following a nuclear attack against a city, the entire water supply system of the city is subject to severe damages and the contents exposed to fallout contamination. The soluble radionuclides become radily mixed with the feeder streams of a watershed and increase the radioactivity of the public water supply. When this water is consumed it constitutes a major source of the internal radiation hazard. The water with its contaminants may alsc enter the human body through indirect paths, such as the consumption of vegetables, meats, and other foods.

A recent study of the capability of waterworks systems to recover following nuclear attack (3), has revealed that the present state of preparedness of metropolitan water supply systems is not adequate to assure recovery without loss of life and serious interruption of industrial activity. Based on specific assumptions, some calculations and graphs were presented to indicate the time required for stored water in a reservoir to reach certain emergency levels of activity at stated depths for given radiation intensities at H + 1 hour. From these graphs an estimate of the amount of activity that may be ingested by the population can be obtained. The study indicated that the current preparedness will permit only 50 percent of the water supply systems to recover from the effects of a light to moderate attack, while only 16 percent of waterworks personnel are provided with adequate protection measures from fallout in metropolitan areas. During the post-attack period there is an urgent need for water supply but the recovery of the system, including treatment, may be slow and inadequate. Therefore, it is important to estimate the absorbed dose in the human body from contaminated water over different periods of consumption, as well as to evaluate the degree of destruction and contamination of water supply systems.

Information about the water supply systems for three selected cities and procedures for the evaluation of water contamination following surface weapon bursts were presented in Chapter II. Several mathematical models to estimate absorbed dose,

or biological uptake, have been studied and are presented in analytical form below. The scope of this research project is focused on the contamination of water supply systems from fallout. Therefore, the biological uptake investigations were confined to considerations of the intake of contaminated water.

B. The Miller-Brown Model of Biological Uptake

A very elaborate mathematical model for estimating the absorbed dose from the assimilation of radionuclides in body organs of humans has been presented by Miller and Brown (13). This model systematically evaluates the biological uptake of radionuclides from contaminated water or food as they pass through different sections of the gastrointestinal tract(*) and are absorbed by various body organs (**). This model has been modified to include the effects of daughter elements and the solubility of radionuclides. It has also been modified for such specific conditions as: (a) a food chain in which the ingestion consists initially of contaminated foliage, (b) short term, or periodic, ingestions of contaminated water or food, and (c) uptake in age-dependent, growing children.

1. Basic Assumptions.

(a) The contents of the digestive tract move continuously from one section to the next at rates determined by the intake rate functions. Therefore, the total quantity of intake of water or food is a continuous function of time.

(b) Only a fraction of some of the soluble radionuclides pass through the wall of the small intestine and enter the body organs. No radionuclide is absorbed by the body organs from any other section of the gastrointestinal tract.

(*) Gastrointestinal tract includes stomach, small intestine, upper large intestine and lower large intestine.

(**) Body organs are considered as thyroid gland, bone tissue and all other organs of human body according to the concept employed by Miller and Brown (13).

(c) The radiation dose absorbed by the gastrointestinal tract equals one half of the total dose, while that which reaches the body organs is fully absorbed.

(d) The biological elimination, or exchange rate, from human organs is of exponential form in its variation with time after assimilation. The relative biological effectiveness (RBE) is generally assigned the value of unity for all organs as gamma and high-energy beta radiations predominate.

2. Method of Estimation

The basic method of this model is to apply the following fundamental differential equation to different sets of conditions:

$$\frac{dN_{ik}}{dt} = f(t) - \lambda N_{ik} \qquad (1)$$

where N_{ik} is the amount of the i-th radionuclide in the k-th organ at time t, (atoms)

$f(t)$ is the intake rate function of a radionuclide into an organ (atoms per unit of time), and

λ is the effective decay constant which equals the sum of the radioactive decay constant, λ_i, and the biological elimination constant, λ_{ib}.

In the above equation, $f(t)$ and λ vary with different sections of the gastrointestinal tract and body organs. They also depend on the existence of daughter elements and the solubility of radionuclides. A summary of expressions for $f(t)$ and λ, depending on solubility, presence of daughter elements and stage of uptake, was presented in Table II of Interim Technical Report No. 2 (14).

The computations of absorbed dose start with an evaluation of the amount of nuclide, N_{ik}, at a given time, and the amount of disintegration, N_{ik}^{*}, over a period of time, in an organ. The evaluations are divided into two time-periods: The build-up and the steady-state flow-through. Since the contents of the digestive tract are assumed to move continuously, the steady state flow-through time-period for any section of the tract is reached at a time equal to the average time that water or food normally stays in that section. For the various body organs, this

time equals the average time that water or food normally stays in the smaller intestine. Taking into consideration the above assumptions, the absorbed dose from a radionuclide by an organ may be obtained from:

$$D_k = R \frac{\epsilon_k \lambda_i \int_{t_i}^{T} N_k dt}{m_k} \qquad (2)$$

where D_k is the absorbed dose from a radionuclide by organ k, (rems),

R is the dimensional conversion constant, equal to 16.02×10^{-9} rems per Mev per gram for body organs and one half this value for the gastrointestinal tract,

ϵ_k is the effective disintegration energy absorbed by organ k, (Mev per disintegration),

λ_i is the radioactive decay constant,

t_i is the initial time of a radionuclide entering organ k,

T is the end of the time-period for estimation,

N_k is the amount of a radionuclide in organ k at time t, (atoms),

m_k is the mass of organ k, (grams).

3. Modifications

For food chains in which the initial ingestion consists of contaminated foliage, e.g. milk, leafy vegetables, etc., it may be assumed that the level of contamination of the ingested foliage decreases with time at a rate which is proportional to the decontamination level of the foliage. The rate constant for this decrease is defined as α, the physical process decay constant (13). It is assumed to be the same for all radionuclides, and its value is determined from experimentally observed data. For this type of ingestion, the intake rate function, f(t), is accordingly modified by including the physical process decay constant as a part of the effective decay constant.

The Miller-Brown model can be adjusted also for brief periods of ingestion of radionuclides. Assuming that the ingestion period is from t_o to t_f, one can

obtain the amount of disintegration of a radionuclide in an organ during a period of time from t_o to any time, t, where $t > t_f + t_n - t_o$ by the following formula:

$$N^*_{ik}(t_1,t) = N^*_{ik}(t_o, t_f + t_n - t_o) + N^*_{ik}(t_f + t_n - t_o, t) \quad (3)$$

where

$N^*_{ik}(t_o,t)$ is the number of disintegrations of the i-th radionuclide in the k-th organ during a period of time from t_o to t,

$N^*_{ik}(t_o, t_f + t_n - t_o)$ is the number of disintegrations of the i-th radionuclide in the k-th organ during a period of time from t_o to $t_f + t_n - t_o$, (total time from ingestion until leaving section of G.I. tract),

t_o is the time of initial ingestion,

t_f is the time of last ingestion,

t_n is the time at which water or food leaves any of the n sections of the gastrointestinal tract after having been ingested at time t_o. It is equal to: $t_o + \sum_1^n T_n$, where T_n is the average time period that water or food stays in each of the n sections of the digestive tract,

$N^*_{ik}(t_f + t_n - t_o, t)$ is the number of disintegrations of the i-th radionuclide in the k-th organ for a period of time from $t_f + t_n - t_o$ to t. For computing the value of $N^*_{ik}(t_f + t_n - t_o, t)$ for parent or daughter nuclides refer to the previous report (14).

Since the contents in the digestive tract are assumed to move continuously, the radionuclides will completely move out of the n-th section of the gastrointestinal tract at time $t_f + t_n - t_o$ after ingestion. Therefore,

$$N^*_{ik}(t_f + t_n - t_o, t) = 0 \quad (4)$$

for all sections of the gastrointestinal tracts.

The absorbed dose for growing children is difficult to estimate since most parameters in Equations (1) and (2) vary with time. In this model, it is approximated by an incremental function related to adult absorbed dose:

$$D_{ik}(t, t_j) = \sum_{\ell=1}^{n} \Delta_{ik\ell}(t) \tag{5}$$

with $\Delta_{ik\ell}(t)$ being approximated as

$$\Delta_{ik\ell}(t) = \frac{U_i^o(t)}{U_i^o(A)} \; a_{ik\ell}(t) \; \Delta'_{ik\ell}(t) \tag{6}$$

where $D_{ik}(t,t_j)$ is the total absorbed dose of the i-th nuclide in the k-th organ of a growing child for a period t, starting at age t_i,

t is the time period over which the dose is estimated,

t_j is the age when ingestion commences,

n is the total number of time increments,

ℓ is the time increment number,

$\Delta_{ik\ell}(t)$ is the increment of dose at ℓth time increment for children (rems),

$\Delta'_{ik\ell}(t)$ is the increment of dose at ℓth time increment for adults (rems),

$U_i^o(t)$ is the initial intake rate at H + 1 hour for children (atoms per unit time),

$U_i^o(A)$ is the initial intake rate at H + 1 hour for adults (atoms per unit time),

and

$$a_{ik\ell}(t) = \frac{\epsilon_{ik}(t)}{\epsilon_{ik}(A)} \; \frac{m_k(A)}{m_k(t)} \; \frac{\lambda_{ik} \left[1/m_k(t)\right] \left[dm_k(t)/dt\right]}{\lambda_{ik}} \tag{7}$$

where $\epsilon_{ik}(t)$ is the effective energy absorbed by the child's organ (Mev/dis),

$\epsilon_{ik}(A)$ is the effective energy absorbed by the adult's organ (Mev/dis),

$m_k(t)$ is the mass of the child's organ (grams),

$m_k(A)$ is the mass of the adult's organ (grams), and

λ_{ik} is the biological elimination constant of the i-th radionuclide in the k-th organ of the adult.

The values of $\epsilon_{ik}(t)$, $m_k(t)$ and $\left[1/m_k(t)\right] \left[dm_k(t)/dt\right]$ have been summarized in

Tables V and VI by Miller and Brown, (13).

4. Results and Applications

A set of values of the absorbed dose, D_k, per unit initial intake rate at H + 1 hour, U_i^o, of total body for six biologically important radionuclides for various times of initiation of intake and periods of consumption are reproduced as Table VI from (13). Radionuclide concentrations in water are obtained from the ionization-rate and nuclide solubility contour ratios. From the tabulated data of absorbed dose per unit ingestion rate, these concentrations are applied directly to a post-attack situation to estimate the possible internal radiation hazards to the surviving population. This model is very elaborate and complete in its consideration of the absorbed dose problem; however, the calculations involved are very complex and tedious. The computations can be carried out with the assistance of an automatic desk calculator and mathematical tables but can be handled more efficiently by an electronic computer.

C. Simplified Uptake Model for Body Organs

In view of the large volume of computations introduced by the Miller-Brown model, the investigators proposed (14) a simplified uptake model for body organs and found it to serve as a rapid and close approximation to the solution of the uptake problem.

1. Basic Assumptions

(a) The model applies to a "standard" adult consuming a definite quantity of water within a short period each day. Therefore, the differences in age and overall metabolism of individuals are neglected, and the total quantity of intake of water is assumed as a step function of time, with the daily intake of water a constant impulse function.

(b) The model applies to the final stage of fallout contamination. This means that there will be no further significant increase in the degree of contamination in the water supplies. The reduction of contamination is simplified to include

TABLE VI **Absorbed Dose Per Unit Ingestion Rate for Total Body According to the Miller-Brown Model (13)**

(D_k/U_i^o in 10^{-14} rem/atoms per day)

t_o(days)	t(days)	Sr-89	Sr-90	Ru-106	I-131	Cs-137	Ba-140
	30	15.4	.201	.350	71.8	.290	3.40
	91	91.8	2.00	1.37	98.8	2.34	6.46
1	183	224.	8.52	2.72	99.2	9.28	6.69
	365	267.	32.9	4.78	99.2	20.1	6.69
	730	281.	128.	7.28	99.2	46.9	6.69
	30	13.2	.129	.248	35.6	.186	1.90
	91	77.5	1.71	1.26	58.6	2.07	4.63
7	183	173.	7.94	2.61	49.0	7.05	4.84
	365	246.	31.8	4.68	59.0	19.7	4.84
	730	259.	126.	7.19	59.0	46.5	4.84
	30	4.36	.0620	.140	12.2	.0921	.802
	91	62.8	1.44	1.13	30.9	1.77	3.12
14	183	153.	7.38	2.48	31.2	6.62	3.32
	365	222.	30.4	4.54	31.2	19.1	3.32
	730	237.	124.	7.06	31.2	45.9	3.32

only that caused by radioactive decay of radionuclides. This implies that water treatment for decontamination has not been practiced to any extent following the attack.

(c) The model applies to human body organs and, therefore, the biological elimination effect is considered. It is assumed that this effect reduces the amount of radionuclides in the same fashion as radioactive decay, following the Geiger-Nutall exponential law. Moreover, the radionuclides of interest are mostly the end-members or next-to-end-members of mass chains. For simplicity, the daughters of these radionuclides are neglected. It is also assumed in this model that the radiation dose is fully absorbed by body organs; while absorption by the gastro-intestinal tract is neglected.

2. Method of Estimation

(a) The initial concentration, C_o, of a radionuclide in water can be obtained by the method presented in Chapter II at time H + 1. Since most radionuclides of interest are long-lived end-members or next-to-end members of mass chains, their concentrations decrease exponentially according to their individual radioactive halflives. Therefore, the concentration of the radionuclide in water at time of initial consumption will be:

$$C_i = C_o e^{-\lambda_r t_i} \tag{8}$$

where C_i is the concentration at time of initial consumption(atoms per unit volume),

C_o is the concentration at H + 1 hour (atoms per unit volume),

λ is the radioactive decay constant, and

t_i is the time of initial consumption.

Since the daily intake of water by an adult has been assumed to be a constant impulse function, the amount of a radionuclide which enters the human body at time of initial consumption will be:

$$N_i = C_i d \tag{9}$$

where N_i is the initial body intake (atoms), and

d is the quantity of daily intake of water (units of volume).

(b) At time, $t_i + 1$ day, and thereafter, the biological elimination effect should be considered. The body intake at $t_i + 1$ day will then be:

$$N_1 = N_i e^{-(\lambda_r + \lambda_b)\cdot 1} + N_i e^{-\lambda_r \cdot 1} \tag{10}$$

where N_1 is the total body intake at the end of $t_i + 1$ day (atoms), and

λ_b is the biological elimination constant

(c) At the end of $t_i + n$ days, the expression for the total amount of body intake of a radionuclide can be deduced from Equation (10):

$$N_n = N_i \left[e^{-(\lambda_r + \lambda_b)n} + e^{-(\lambda_r + \lambda_b)(n-1)} e^{-\lambda_r \cdot 1} + \cdots\cdots \right.$$
$$\left. \cdots + e^{-(\lambda_r + \lambda_b)\cdot 1} e^{-\lambda_r (n-1)} + e^{-\lambda_r n} \right] \tag{11}$$

or

$$N_n = N_i \frac{r^{n+1} - b^{n+1}}{r - b} \tag{12}$$

with

$$r = e^{-\lambda_r \cdot 1} \tag{13}$$

$$b = e^{-(\lambda_r + \lambda_b)\cdot 1} \tag{14}$$

where N_n is the total body intake at the end of $t_i + n$ days (atoms)

(d) However, only a fraction of the amount of radionuclide being taken into the body will incorporate into the tissue of specific organs. Therefore, the uptake of an organ is

$$N_{nk} = f_{wk} N_n \tag{15}$$

where N_{nk} is the uptake of organ k at end of $t_i + n$ days, (atoms),

f_{wk} is the fraction of the ingested radionuclide in water that is retained by organ k

(e) The absorbed dose from a nuclide by an organ after n days of consumption of contaminated water will then be

$$D_k = R \frac{\epsilon_k \lambda_r \int_0^n N_{nk}\, dt}{m_k} \tag{16}$$

$$D_k = \frac{R\,\epsilon_k \lambda_r f_{wk} N_i}{m_k (r - b)} \left\{ \left[\frac{r}{\lambda_r} - \frac{b}{\lambda_r + \lambda_b} \right] - \left[\frac{r^{n+1}}{\lambda_r} - \frac{b^{n+1}}{\lambda_r + \lambda_b} \right] \right\} \qquad (17)$$

where D_k is the absorbed dose of a radionuclide by organ k, (rems),

R is the dimensional conversion constant which equals 16.02×10^{-9} rems per Mev per gram of body organ,

ϵ_k is the effective disintegration energy absorbed by organ k, (Mev per disintegration),

λ_r is the radioactive decay constant,

n is the number of days of consumption,

m_k is the mass of organ k, (grams).

The limits of integration are 0 and n instead of t_i and $t_i + n$. This choice is due to the fact that time t_i is the zero time of intake, and N_{nk} is strictly a function of n, a time that starts to count after t_i.

The initial intake rate, U_i^o, in accordance with the Miller-Brown model nomenclature, is equal to:

$$U_i^o = C_o d \qquad (18)$$

$$= N_i e^{\lambda_r t_i} \qquad (19)$$

where U_i^o is the initial intake rate of a radionuclide if the ingestion starts at H + 1 hour (atoms per day).

3. Results and Applications

Values for the absorbed dose of total body per unit initial intake rate at H + 1 hour for six biologically important radionuclides for various times of initiation of intake and periods of consumption are presented. The necessary parameters for calculation are listed in Table VII and the results are shown in Table VIII.

These results, due to the effect of neglecting gastrointestinal tract absorption as stated in the assumptions, are slightly greater than those shown in Table VI. Taking into consideration the simplified calculations and increased

TABLE VII

Summary of Parameter Values in Absorbed Dose Equation in Simplified Model

Parameter	Sr-89	Sr-90	Ru-106	I-131	Cs-137	Ba-140
λ_r (day^{-1})	1.3×10^{-2}	6.8×10^{-5}	1.9×10^{-3}	8.6×10^{-2}	5.7×10^{-5}	5.4×10^{-2}
λ_b (day^{-1})	5.3×10^{-5}	5.3×10^{-5}	9.5×10^{-2}	5.0×10^{-3}	1.0×10^{-2}	1.1×10^{-2}
ϵ_k (Mev/dis)	.55	1.1	1.4	.44	.59	.40
f_{wk}	.3	.3	.03	1.	1.	.05
m_k (gram)	70,000 grams for total body					

TABLE VIII **Absorbed Dose Per Unit Ingestion Rate for Total Body According to the Simplified Uptake Model**

(D_k/U_i^o in 10^{-14} rem/atoms per day)

t_o(days)	t(days)	Sr-89	Sr-90	Ru-106	I-131	Cs-137	Ba-140
	30	17.1	.244	.390	81.9	.315	3.73
	91	96.1	2.15	1.48	110.	2.41	7.07
1	183	199.	8.58	2.90	110.	7.61	7.07
	365	275.	33.6	5.10	110.	20.4	7.07
	730	289.	131.	7.75	110.	47.6	7.07
	30	10.6	.158	.281	41.2	.205	2.12
	91	81.2	1.88	1.36	65.4	2.14	5.11
7	183	179.	8.03	2.79	65.7	7.22	5.11
	365	253.	32.5	4.98	65.7	20.0	5.11
	730	267.	129.	7.63	65.7	47.2	5.11
	30	5.16	.0815	.164	15.9	.105	.929
	91	66.0	1.58	1.22	35.7	1.84	3.50
14	183	158.	7.41	2.65	36.0	6.78	3.50
	365	230.	31.2	4.84	36.0	19.5	3.50
	730	244.	126.	7.49	36.0	46.6	3.50

speed with which uptake values can be obtained by conventional computation means, the data shown in Table VIII are in very close agreement with those listed in Table VI. Within the limitations of the different assumptions employed by each model, the results of the simplified uptake model deviate from those of the Miller-Brown model on the average by only seven percent. Therefore, this model serves to estimate body uptake when high accuracy is not a critical requirement or computing facilities are limited.

Modifications can be added to this model. However, the more factors that are taken into consideration, the more complicated the model will be; the more lenghty and tedious its calculations will become; and hence the probability for errors increases. A compromise between input efforts and output accuracy has to be borne in mind when selecting a particular model.

D. Model of the I.C.R.P. Committee II on Permissible Dose

A mathematical model for a different purpose was established by K.Z. Morgan and the ICRP Committee (15). This model was designed to estimate the effects from peaceful uses of atomic energy and to evaluate occupational radiation hazards; while the Miller-Brown model was derived for the theoretical evaluation of absorbed dose in post-attack circumstances. However, the fundamental principles of both models are based on the same data, and the results from the ICRP-model can serve as a reference for comparison of biological uptake. Most of the basic premises of the simplified uptake model, including the concept of discrete intake rates, are drawn from the ICRP-model.

In this model, the rate of uptake of the radionuclide by body organs is assumed to be constant while the uptake rate decreases in the Miller-Brown model. Using the following differential equation, which is similar to Equation (1), the burden of the radionuclide in a particular body organ can be estimated from:

$$P = \frac{d(qf_2)}{dt} + \lambda(qf_2) \qquad (22)$$

P is the constant rate of uptake of the radionuclide by the organ in μc/day.

where q is the maximum permissible burden of an organ, (μc),

f_2 is the fraction of radionuclide in the organ to that in total body,

λ is the effective decay constant which equals the sum of the radioactive decay constant, λ_r, and the biological elimination constant λ_b, and

After the upper limit of burden in a body organ is established, the maximum permissible concentration of the radionuclide in water, food, or air can be determined.

During the course of these investigations, this model is used only as a reference to determine the degree of internal hazard created by the consumption of contaminated water. Based on the permissible internal radiation hazard one can evaluate the minimum degree of decontamination or the minimum period during which the water supply is not usable following nuclear attack.

E. The Greitz - Edvarson Model

A method for estimating internal doses from mixed fission products has been devised by Greitz and Edvarson (16). This method is based on essentially the same principle as the other models presented; i.e., the rate of change of the amount of radionuclide equals the input function minus the rate of decay. However, some of the other basic assumptions are different as listed below:

(a) A continuous daily intake of activity corresponding to one fission has been assumed.

(b) The transfers between different organs, including excretion, are treated as a first order process.

(c) The transport between different organs occurs with negligible time delay.

The method considers two different sets of conditions: (a) one is for the activity for a parent nuclide A in a specific organ, and (b) the other is for activity of a daughter nuclide B in a specific organ with appreciable parent activity A.

The definite differential equations are:

Case 1:

$$\frac{dN_A}{dt} = \frac{f_A}{\alpha} I_A - \alpha_e N_A \qquad (1)$$

$$N_A = 0 \qquad t = 0$$

$$I_A = I_A(0)e^{-\alpha t} \qquad 0 < t < t_1$$

$$I_A = 0 \qquad t > t_1$$

Case 2:

$$\frac{dN_B}{dt} = \frac{f_B}{\beta} I_B + f'_B \ \alpha N'_A - \beta_e N_B \qquad (2)$$

$$N_B = 0 \qquad t = 0$$

$$N'_A = \frac{f''_A A(0)}{\alpha(\alpha'_e - \alpha)} (e^{-\alpha t} - e^{-\alpha' t}) \qquad 0 < t < t < t_1$$

$$N'_A = N'_A(t_1)e^{-\alpha'_e(t-t_1)} \qquad t > t_1$$

$$I_B = I_B(0)e^{-\beta t} + \frac{BI_A(0)}{(\alpha-\beta)} (e^{-\beta t} - e^{-\alpha t}) \qquad 0 < t < t_1$$

$$I_B = 0 \qquad t > t_1$$

where I_A is the ingestion activity rate of nuclide A

I_B is the ingestion activity rate of nuclide B

N_A is the content of nuclide A in a specific organ

N'_A is the content of nuclide A in total body excluding GI tract

α, β are decay constants

α_e, β_e are effective decay constants in critical organ

α'_e is effective decay constant in total body

f_A is fraction of nuclide A reaching a specific organ from GI tract

f'_A is fraction of nuclide A reaching a specific organ from total body excluding GI tract

f''_A is fraction of nuclide A from GI tract to total body

$t = 0$ is start of intake

$t = t_1$ is end of intake

While the Miller-Brown models have separate formulae for the gastrointestinal tract and body organs, this model uses the same formulae for both parts. Therefore, the computations are simpler. A computer program for the first case of this model has been developed and was presented in the third interim report (17). The results obtained from this model, as well as those obtained from other models, will be summarized for comparison in a later section of this chapter.

F. Graphical Presentation of Absorbed Dose from Contaminated Water Intake (acc. to Miller-Brown)

1. Discussion of Established Criteria

To estimate the resultant body burden for various short term periods of ingestion, it is necessary to consider physical, chemical, biological and physiological factors in their relation to water consumption and their interrelationship within the human body. Therefore, it was necessary to establish certain basic criteria, including: (a) standard daily intake, (b) activity concentration in water, (c) selectivity, (d) critical organ, and (e) periods of consumption. These criteria were discussed in detail in the third interim report (17).

2. Presentation of Graphs

The results from calculations of the absorbed dose to the GI tract and body organs from the ingestion of contaminated water supplies, using the Miller-Brown models (13) are shown in Figures 6 through 13. These graphs were designed to provide a means for estimating the degree of internal hazard following ingestion of contaminated water after a nuclear blast and to provide a basis for the design of postattack radiological defense countermeasures.

The graphs present absorbed dose (rems) per unit original ingestion rate at (H + 1) hour versus period of ingestion for four selected isotopes: Sr-89, Sr-90, Ru-106 and I-131. Ingestion starting times, t_o, of one day and 14 days after detonation were considered. In the third interim report (17) similar graphs, with an ingestion starting time of 7 days, were shown. By comparison, it is observed that by

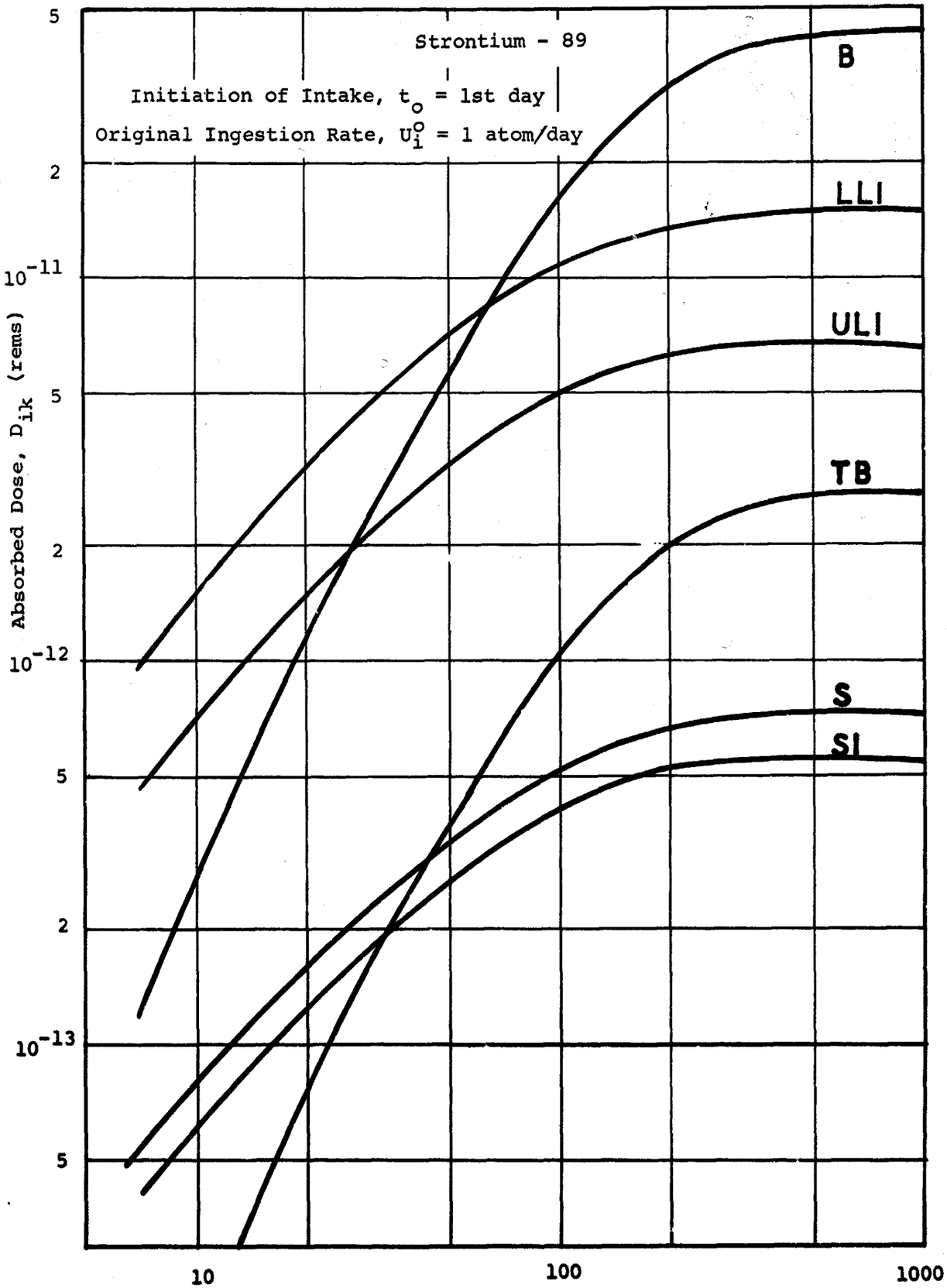

Figure 6. Build-up Curves of Absorbed Dose in Various Organs for Sr-89

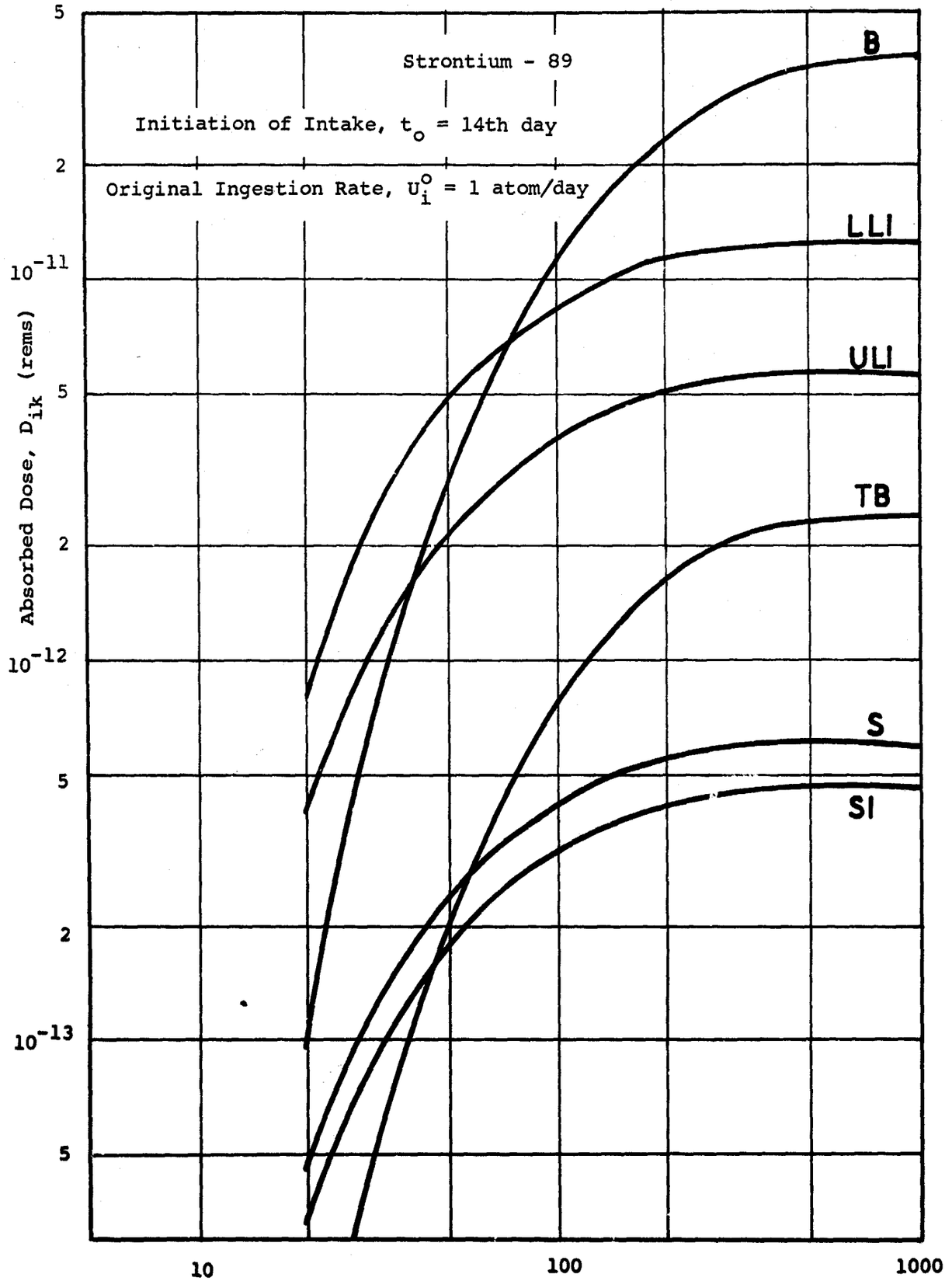

Figure 7. Build-up Curves of Absorbed Dose in Various Organs for Sr-89

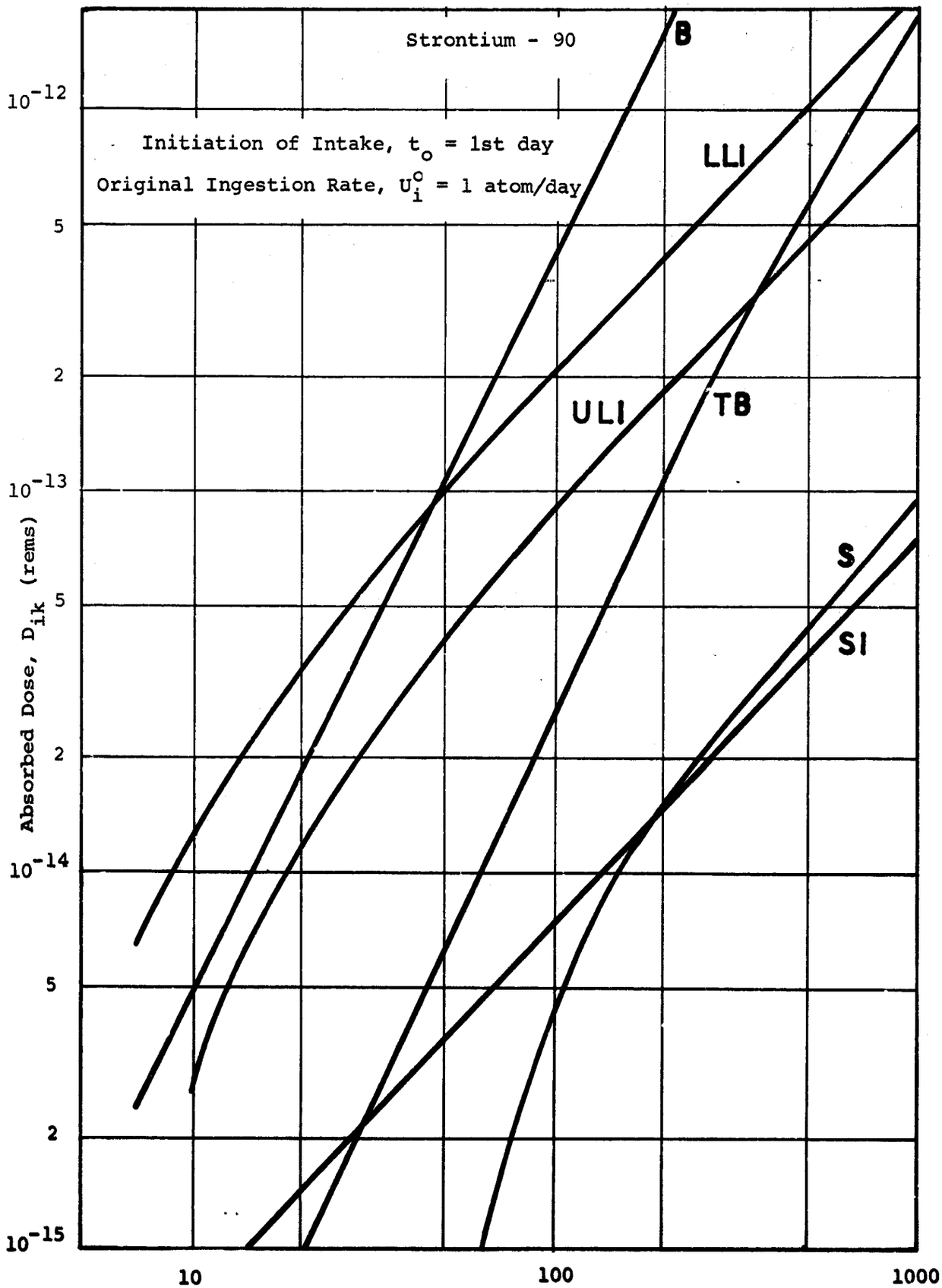

Figure 8. Build-up Curves of Absorbed Dose in Various Organs for Sr-90

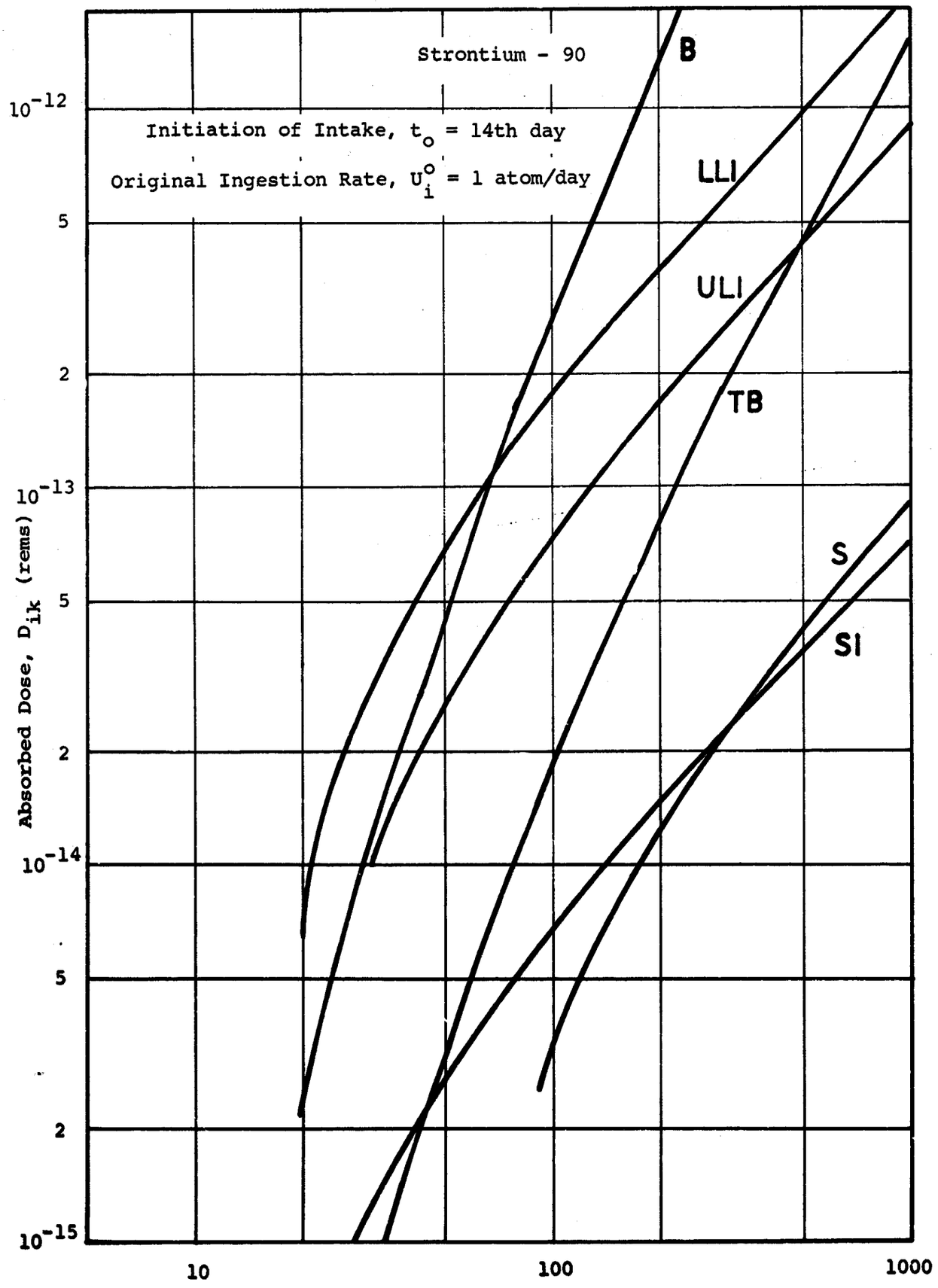

Figure 9. Build-up Curves of Absorbed Dose in Various Organs for Sr-90

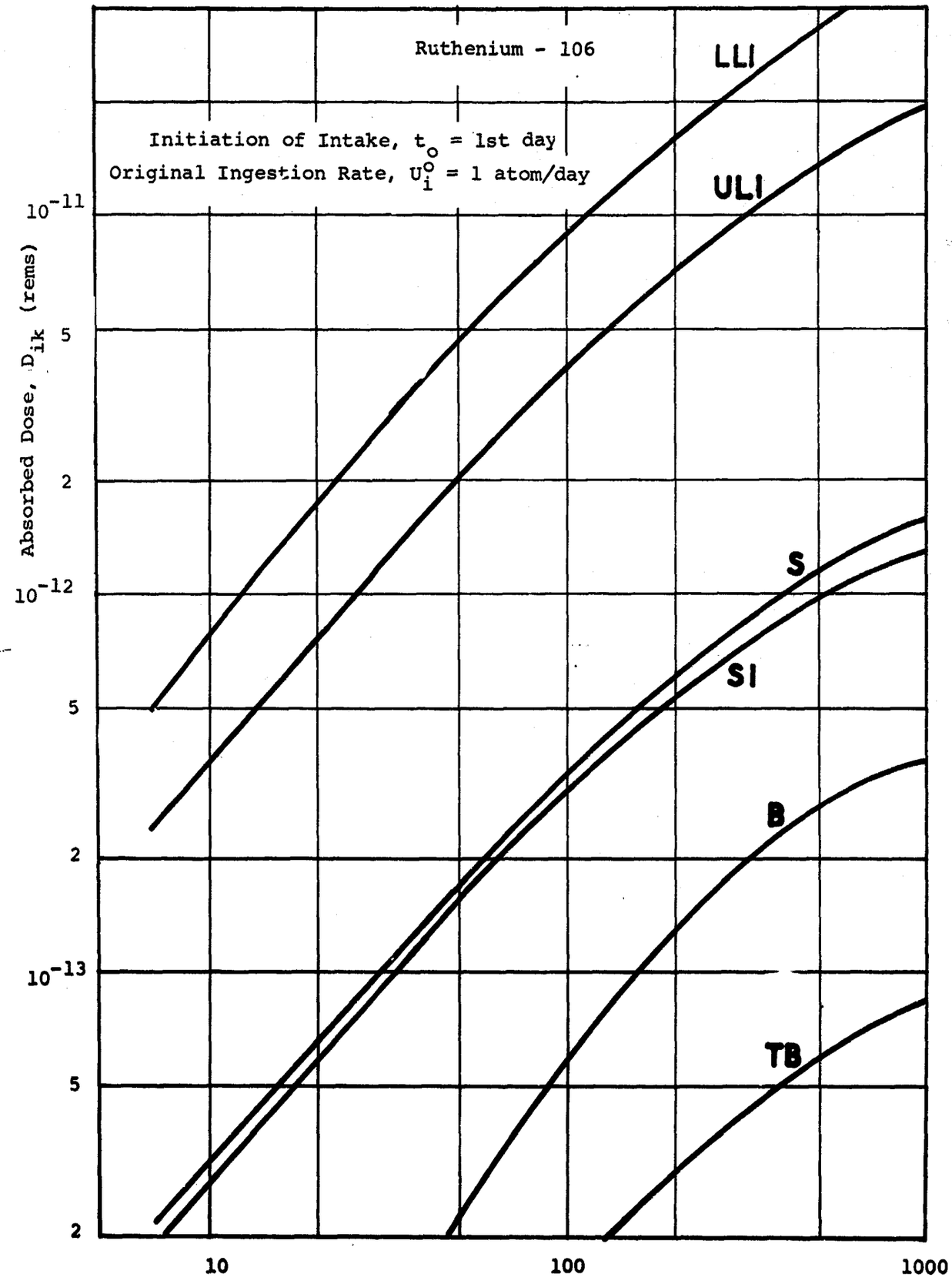

Figure 10. Build-up Curves of Absorbed Dose in Various Organs for Ru-106

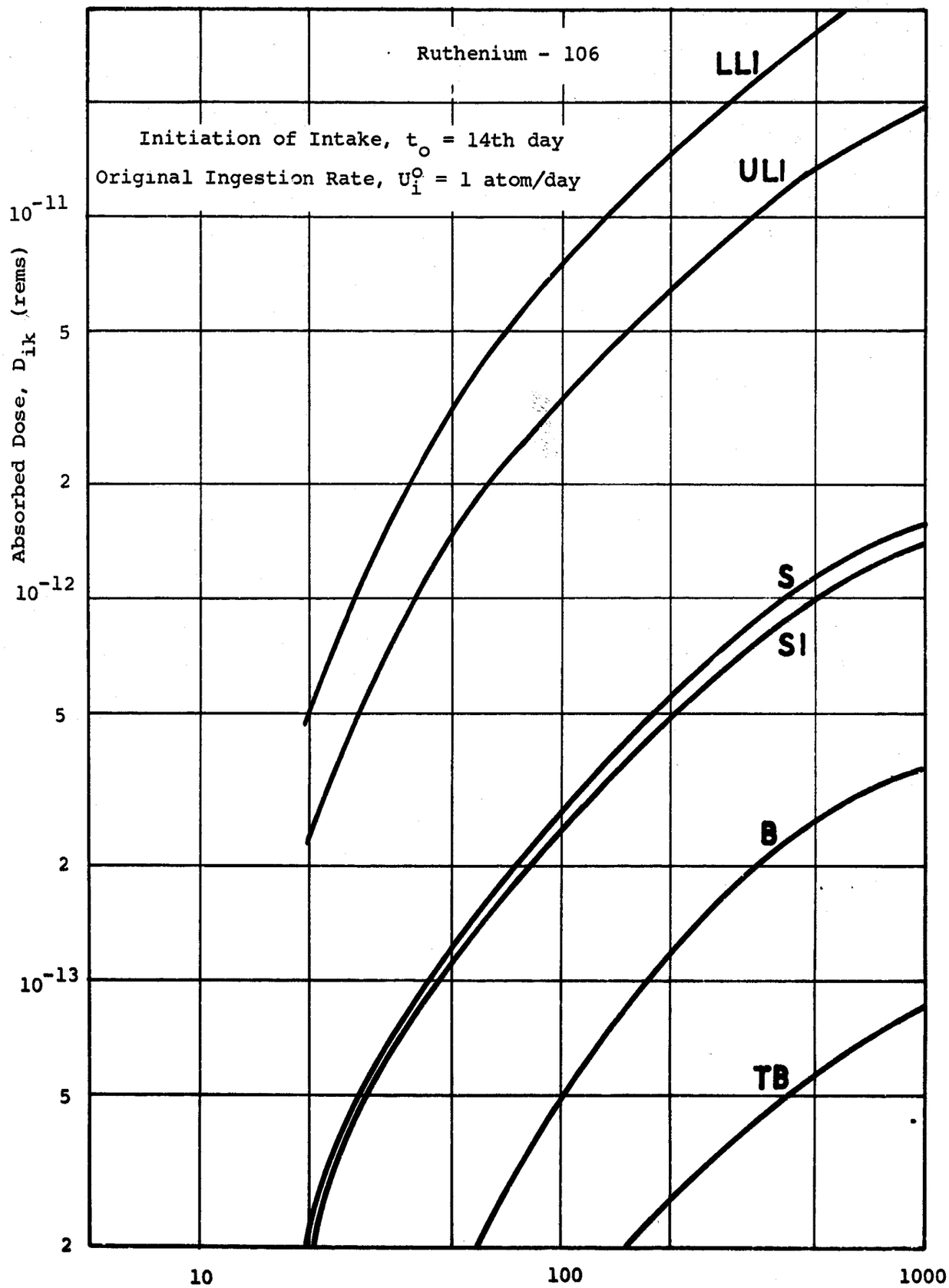

Figure 11. Build-up Curves of Absorbed Dose in Various Organs for Ru-106

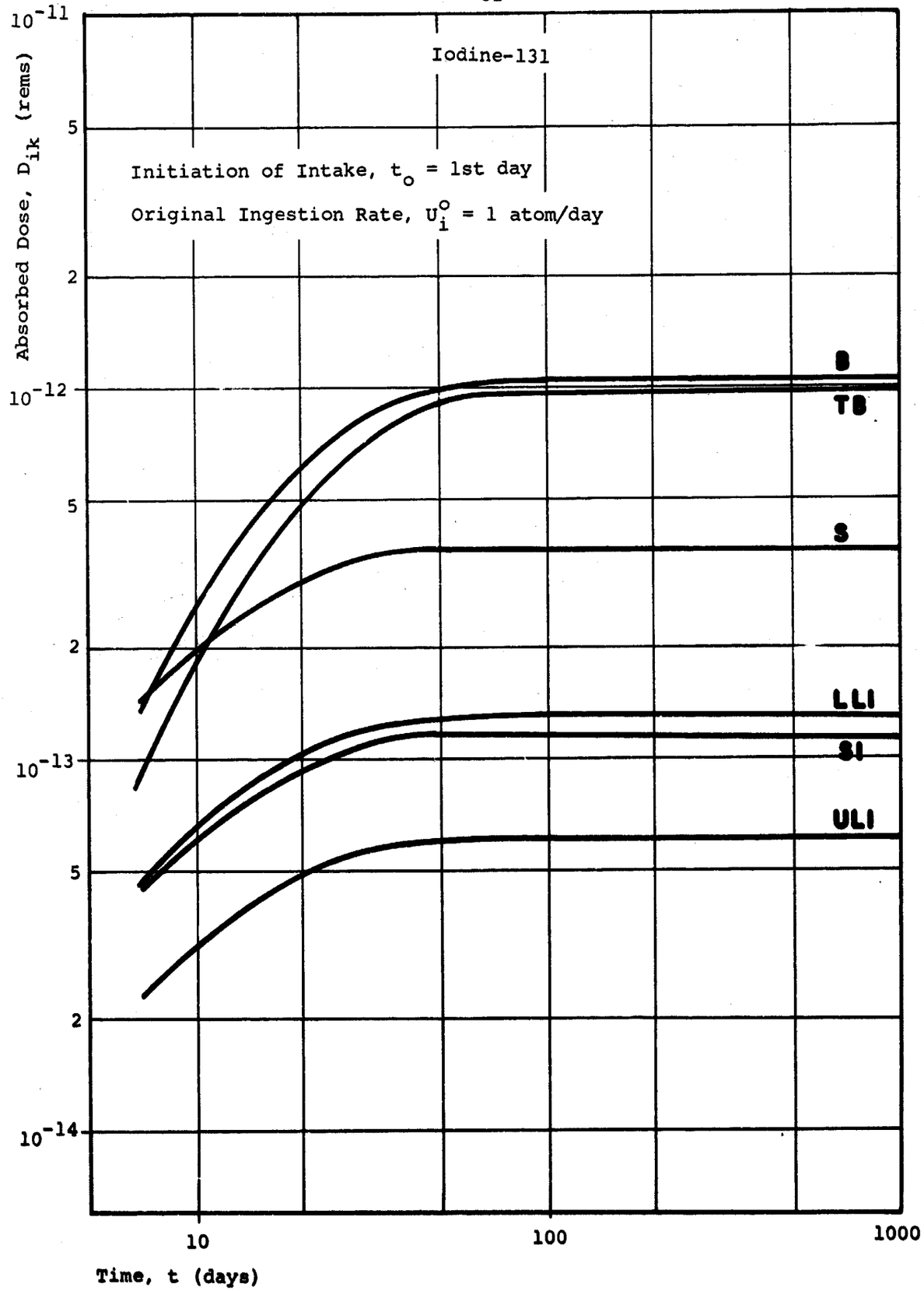

Figure 12. Build-up Curves of Absorbed Dose in Various Organs for I-131

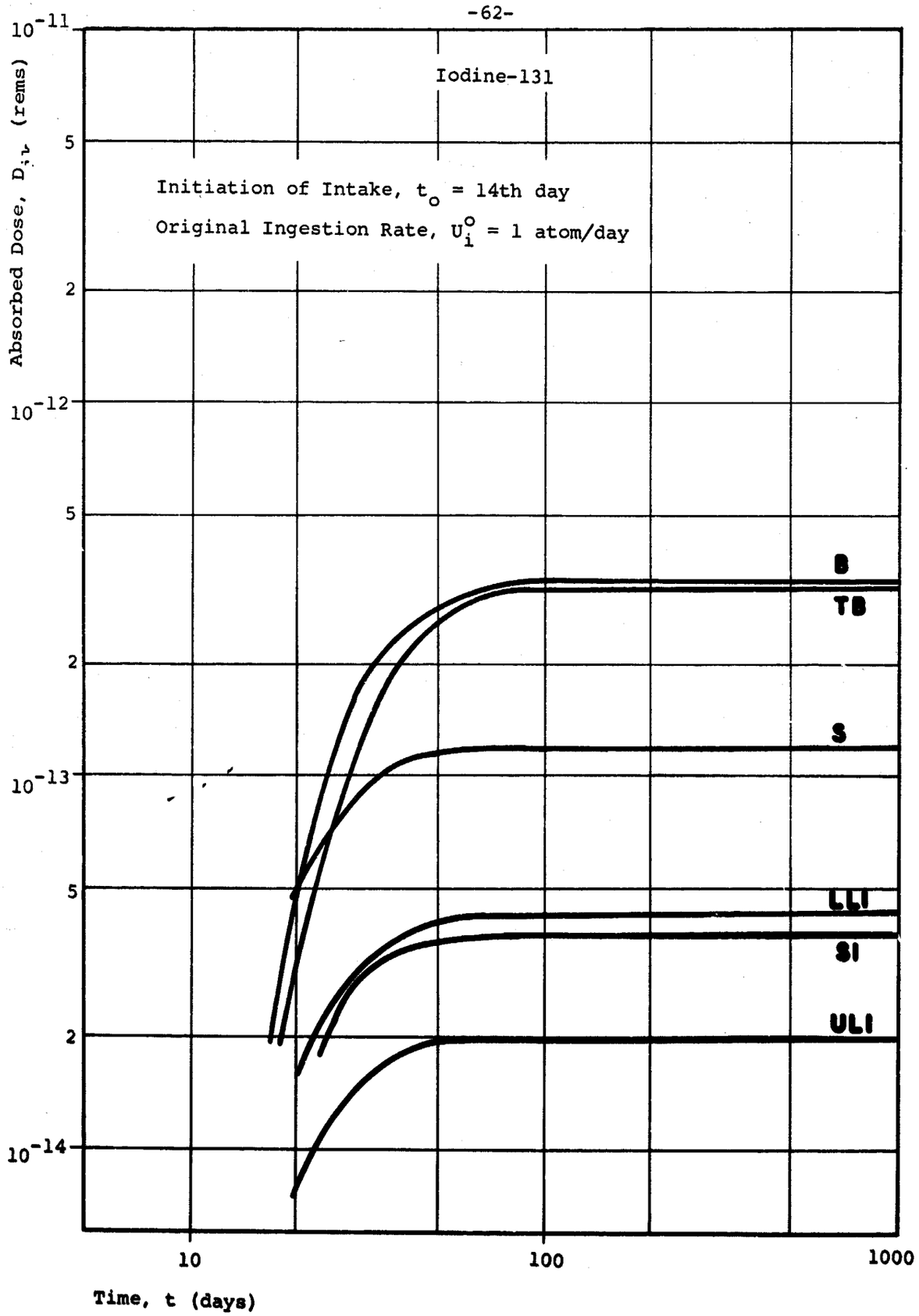

Figure 13. Build-up Curves of Absorbed Dose in Various Organs for I-131

advancing the initiation of intake following a nuclear blast, the absorbed dose is generally increased but that the amount of increase depends on the isotope and the specific section of the GI tract or part of body organs considered. The longer the half-life of the isotope the smaller is the effect. Similar graphs for ingestion starting times of 14 days for Cs - 137 and Ba-140 were also prepared and show the same trends but were not reproduced. The necessary data for the preparation of these graphs were obtained from the computer programs shown in Figures 11 and 12 of the third interim report (17).

3. Discussion of Graphs

Each of the graphs contains curves showing the build-up of dose from the radionuclide to the GI tract organs (stomach, small intestine, upper large intestine and lower large intestine), total body and bone.

The build-up of the dose from Sr-89 in the total body indicates that the "infinite dose", i.e. where the elapsed time exceeds five physical half-life values, is not reached for about 300 days. As may be seen from Figure 6, when the ingestion starting time is one day, this infinite dose is approximately 2.5×10^{-12} rem for a unit original (H + 1) ingestion rate of 1 atom/day[(a)]. Similarly, as shown in Figure 7, the "infinite dose" for Sr-89 in the total body is approximately 2.2×10^{-12} rem for a unit original (H + 1) ingestion rate of 1 atom/day when the ingestion starting time is 14 days.

In contrast to the relatively short-lived Sr-89, the absorbed dose from Sr-90 continues to build up at almost constant rate until the equilibrium dose[(b)] is reached. By comparison of these graphs, it may be seen that the absorbed dose by the total body would be 10^{-12} and 8×10^{-13} rem after 100 days of consumption for Sr-89 when t_o = 1 day and 14 days, respectively, while these values for Sr-90 would be 4×10^{-14}

(a) This refers to a constant rate of intake of water for 300 days which contained 1 atom for the first day. The number of atoms decreases according to their physical decay.

(b) The "equilibrium dose" is the absorbed dose at the time when the number of nuclides in an organ has reached its maximum value.

and 2×10^{-14} rem, when t_o = 1 day and 14 days, respectively, after 100 days of consumption. Similarly, the absorbed dose values after 100 days of consumption for the small intestine are about 10^{-13} and 10^{-14} rem, for Sr-89 and Sr-90, respectively. The absorbed dose for the small intestine from Ru-106 is about 3×10^{-13} rem (t_o = 1 day) and 2×10^{-13} rem (t_o = 14 days) after 100 days of consumption.

Another method of presenting these biological uptake data is shown in Figures 14 and 15 for Sr-89 and I-131. These graphs are obtained by assuming a standard intake of water of 2 liters per day and then by using the relationship

$$A = \lambda N$$

to obtain absorbed dose values from known initial activity concentration in water. This kind of graph has the advantage of stating activity concentration in terms that can be used directly, and may be especially beneficial to water works and civil defense personnel during and immediately following a nuclear attack.

It should be noted that with the availability of a relatively small number of graphs it is possible to make predictions of the absorbed dose by various parts of the human body for various isotopes and time periods of consuming radioactively contaminated drinking water. However, a similar set of curves for gross fission products would be of a more general interest and should be developed subsequently.

G. Status of Computer Techniques to Estimate Biological Uptake

The complexity of formulae and the difficulty to evaluate exponential values requires the use of computer methods to resolve the problem of estimating absorbed dose.

Computer programs were developed for the Miller-Brown models, the simplified uptake model, and the Greitz-Edvarson model. These programs, with typical results, were shown as Figures 11 through 15 in the third interim report (17). The computer programs for the simplified uptake model and the Greitz-Edvarson model are quite similar. The programs for the Miller-Brown models are rather intricate as they [illegible] various combinations of soluble and insoluble conditions of parent and

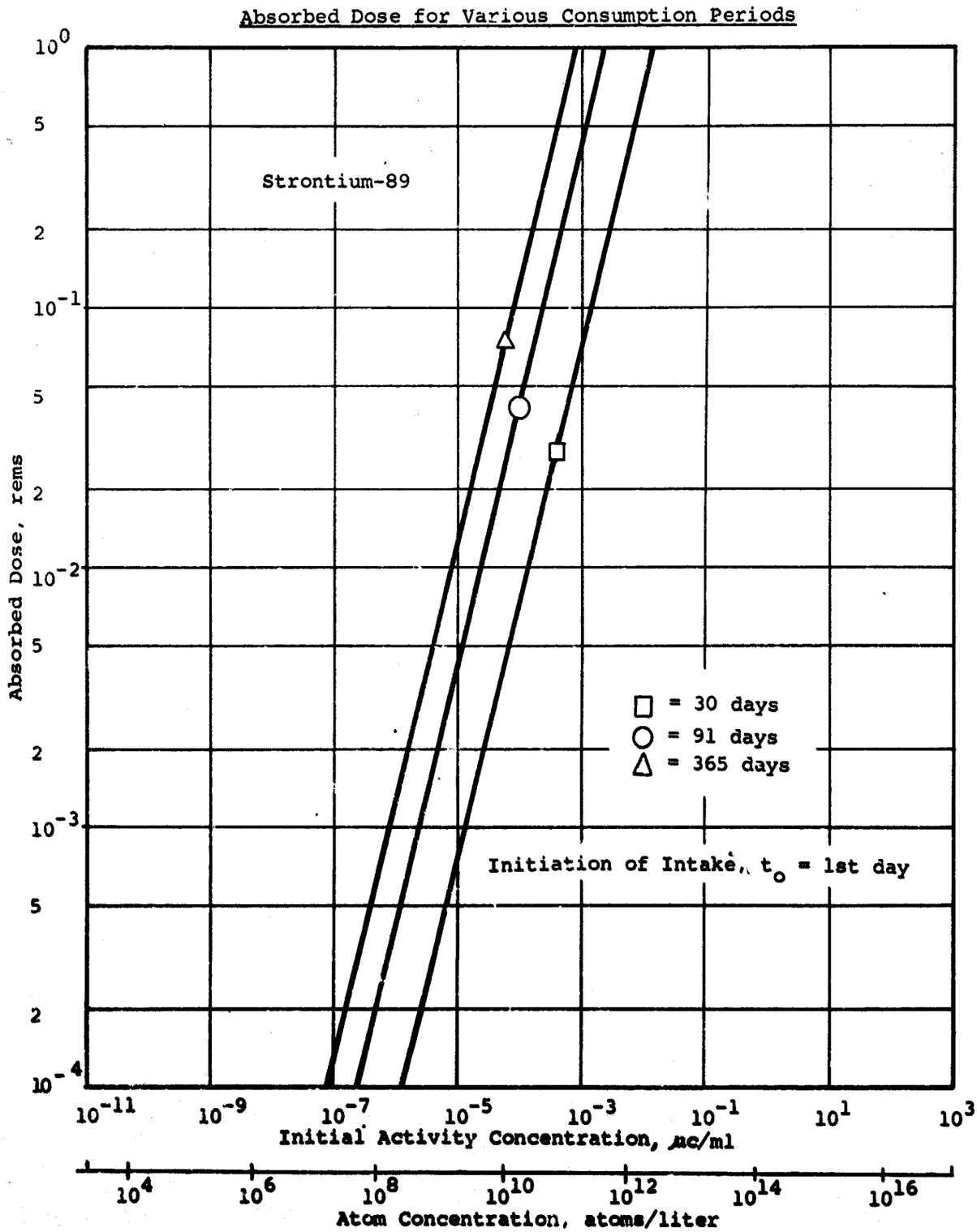

Figure 14. Absorbed Dose in Total Body for Various Consumption Periods for Sr-89

Absorbed Dose for Various Consumption Periods

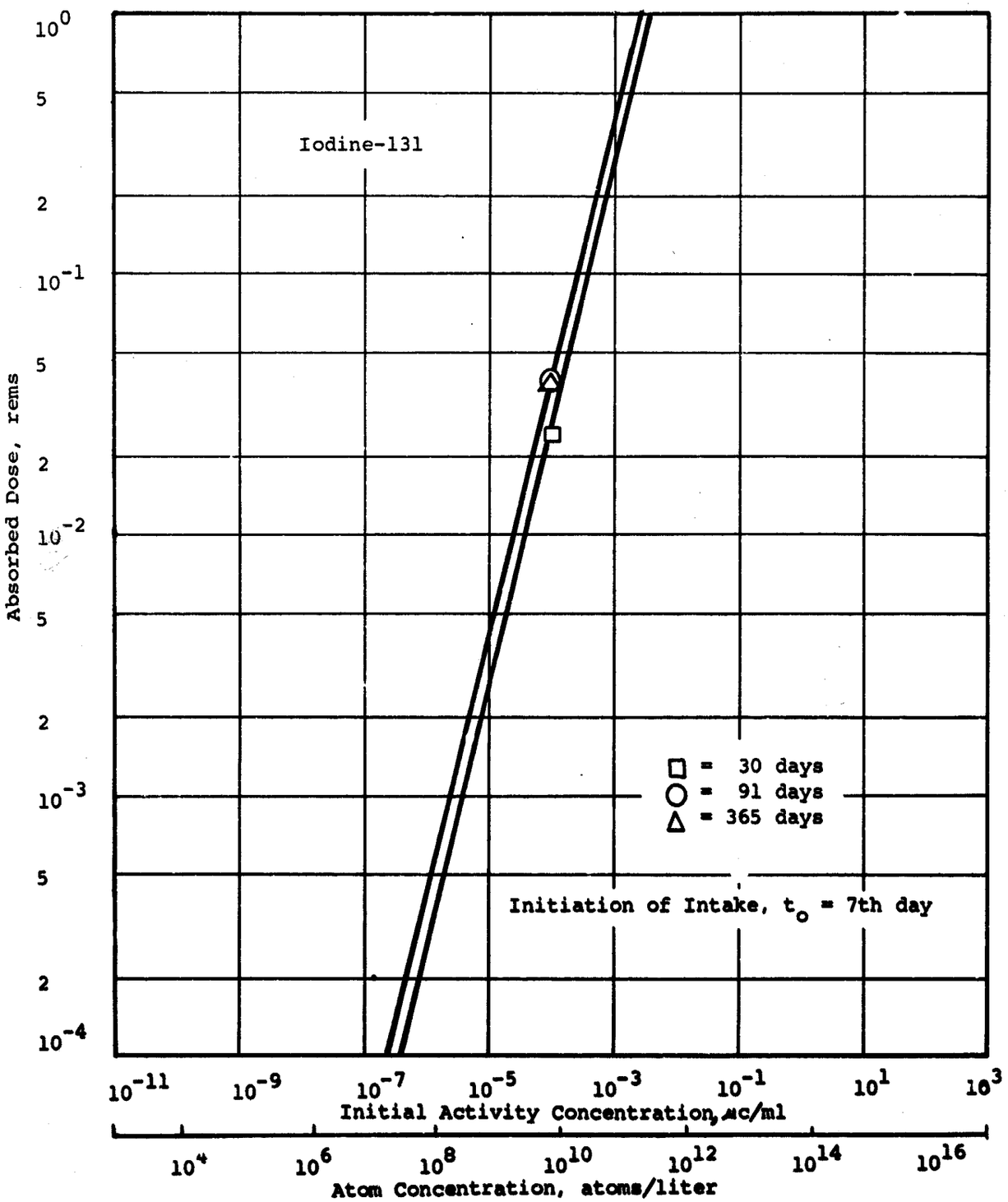

Figure 15. Absorbed Dose in Total Body for Various Consumption Periods for I-131

daughter. However, for the computation of a parent radionuclide only, the portion of the program concerning daughter products can be deleted. Programs for modifications of the Miller-Brown models on periodic intake have also been developed and were reproduced as Figures 14 and 15 in the previous report (17). For periodic intake, it was assumed that ingestion takes place three times a day with one hour period for each ingestion to simulate the general human ingestion pattern.

H. Discussion of Computer Program Outputs

The absorbed dose per unit ingestion rate for total body from six biologically important isotopes, estimated for different starting times and for various periods of ingestion according to the Miller-Brown model, the simplified uptake model, the Greitz-Edvarson model and the modified Miller-Brown models for periodic ingestion, are summarized in Table IX.

All the data are generally in close agreement. The generally higher values obtained from Greitz-Edvarson model and simplified uptake model can be mainly attributed to the effect of neglecting the separation between the gastrointestinal tract and other body organs. Due to the small decay constants (both physical and biological) for most of these isotopes and the short period of ingestion (1 hour period) assigned, the modified Miller-Brown model for periodic intake has made it difficult for the computer to distinguish between unity and the exponential values in the formulae. However, the values obtained from the modified Miller-Brown model were finally obtained and are shown in Table X.

It can be concluded from these results that the present biological uptake models are basically not only of the same principle but also yield values in close agreement. Moreover, the lack of basic data regarding human metabolism of fission products does not warrant the design of a more refined model at the present time.

I. Estimates of Internal Hazard from the Ingestion of Contaminated San Francisco, Springfield and Paterson Water Supplies

The internal hazard resulting from ingestion of contaminated San Francisco, Springfield and Paterson water after a nuclear attack can be readily computed

TABLE IX Summary of Absorbed Doses Per Unit Ingestion Rate for Total Body According to Various Biological Uptake Models (10^{-14} rem/atom/day)

Isotope	t_o	t	Miller-Brown Model	Simplified Uptake Model	Greitz-Edvarson Model	Miller-Brown Periodic Intake Model
89	1	30	15.5	17.1	16.9	12.7
		91	91.9	96.1	94.8	73.4
	7	30	9.49	10.6	10.5	7.81
		91	77.6	81.2	80.2	62.1
	14	30	4.43	5.16	5.12	3.72
		91	62.9	66.0	65.2	50.4
90	1	30	.215	.244	.245	.406
		91	2.04	2.15	2.15	2.34
	7	30	.135	.158	.158	.294
		91	1.77	1.88	1.88	2.09
	14	30	.0671	.0816	.0822	.183
		91	1.49	1.59	1.59	1.81
106	1	30	.350	.390	.372	.269
		91	1.37	1.48	1.41	1.05
	7	30	.248	.281	.268	.191
		91	1.26	1.36	1.29	.966
	14	30	.140	.164	.157	.108
		91	1.13	1.22	1.16	.868
131	1	30	71.9	81.9	75.3	75.2
		91	98.7	110.	101.	103.
	7	30	35.6	41.2	37.9	37.3
		91	58.7	65.4	60.1	61.3
	14	30	13.3	15.9	14.7	14.0
		91	32.0	35.7	32.8	33.4
137	1	30	.290	.315	.314	.306
		91	2.33	2.41	2.40	2.44
	7	30	.186	.205	.205	.196
		91	2.06	2.14	2.13	2.16
	14	30	.0916	.105	.105	.097
		91	1.77	1.84	1.83	1.86
140	1	30	3.40	3.73	3.53	2.67
		91	6.47	7.07	6.47	5.04
	7	30	1.89	2.12	2.00	1.49
		91	4.63	5.11	4.63	3.61
	14	30	.802	.929	.881	.635
		91	3.12	3.50	3.12	2.43

TABLE X

Absorbed Dose Per Unit Ingestion Rate for Total Body According to the Miller-Brown Model for Periodic Ingestion

(D_k/U_i^o in 10^{-14} rem/atoms per day)

t_o(days)	t(days)	Sr-89	Sr-90	Ru-106	I-131	Cs-137	Ba-140
	30	12.7	.406	.269	75.2	.306	2.67
	91	73.4	2.34	1.05	103.	2.44	5.04
1	183	153.	8.02	2.08	103.	7.79	5.20
	365	212.	28.8	3.66	103.	21.0	5.20
	730	223.	107.	5.57	103.	49.1	5.20
	30	7.81	.294	.191	37.3	.196	1.49
	91	62.1	2.09	.966	61.3	2.16	3.61
7	183	138.	7.55	1.99	61.6	7.39	3.76
	365	196.	27.9	3.57	61.6	20.6	3.76
	730	206.	105.	5.48	61.6	48.6	3.76
	30	3.72	.183	.108	14.0	.097	.635
	91	50.4	1.81	.868	33.4	1.86	2.43
14	183	122.	7.02	1.90	33.7	6.94	2.58
	365	178.	26.9	3.48	33.7	20.0	2.58
	730	189.	104.	5.39	33.7	48.0	2.58

fro[illegible]he information obtained in Tables II, III and IV and the absorbed dose data compiled in this chapter. Assuming a standard adult with 2 liters of water intake per day, the absorbed dose for total body for different starting times and ingestion periods have been summarized in Tables XI, XII, and XIII.

In the preparation of Table XI, it was assumed that the water supply outputs from both Hetch Hetchy and Calaveras Systems are mixed with each other in the main transmission line and are available to the population residing around the main line who have survived the attack. It can be observed from these data that ingestion of contaminated water for a short period of 1 to 3 months will give a substantial amount of dose to the total body; for mixed fission products the dose delivered to the thyroid, bones, liver and other specific organs will be much higher than these values obtained for total body from individual radionuclides. Similar conclusions may be deduced from Tables XII and XIII, for Springfield and Paterson(*) water supplies. Therefore, the water contamination problem assumes an important position in post-attack research, especially for a possible all-out thermonuclear war, after which most of the continental U.S. would be covered with fallout. Genetic effects to the entire population have to be considered as a vital problem and should be regarded as an integral phase of radiological countermeasure studies.

(*) Table XIII has been prepared for a 115 MT attack. As before in Table IV, the effect of two distributions of weaponage were calculated, one employing 3 at 5 MT and 10 at 10 MT weapons; the other 1 at 5 MT, 1 at 10 MT and 5 at 20 MT weapons for the total effect from 115 MT.

TABLE XI Internal Hazard of Total Body from Ingestion of Contaminated San Francisco Water Supply

Isotope	t_o	t	Dose due to Direct Contamination of Reservoir water (rems)	Dose including the Effect of Watershed Runoff(rems)
Sr-89	1	30	0.0263	1.01
		91	0.156	5.98
	7	30	0.0161	0.618
		91	0.132	5.05
	14	30	0.00753	0.288
		91	0.107	4.09
Sr-90	1	30	0.000595	0.0213
		91	0.00565	0.202
	7	30	0.000373	0.0134
		91	0.00490	0.175
	14	30	0.000186	0.00664
		91	0.00412	0.148
Ru-106	1	30	0.000406	0.0157
		91	0.00158	0.0613
	7	30	0.000287	0.0111
		91	0.00146	0.0564
	14	30	0.000164	0.00627
		91	0.00131	0.0506
I-131	1	30	0.194	7.12
		91	0.266	9.77
	7	30	0.0961	3.52
		91	0.158	5.81
	14	30	0.0359	1.32
		91	0.0864	3.17
Cs-137	1	30	0.000730	0.0278
		91	0.00587	0.223
	7	30	0.000468	0.0178
		91	0.00519	0.197
	14	30	0.000231	0.00878
		91	0.00446	0.170
Ba-140	1	30	0.00972	0.357
		91	0.0191	0.679
	7	30	0.00540	0.198
		91	0.0132	0.486
	14	30	0.00229	0.0842
		91	0.00892	0.327

TABLE XII Internal Hazard of Total Body from Ingestion of Contaminated Springfield Water Supply

Isotope	t_o	t	Dose due to Direct Contamination of Reservoir water (rems)	Dose including the Effect of Watershed Runoff (rems)
Sr-89	1	30	0.00356	0.0527
		91	0.0211	0.312
	7	30	0.00218	0.0323
		91	0.0178	0.264
	14	30	0.00102	0.0151
		91	0.0145	0.214
Sr-90	1	30	0.000213	0.00249
		91	0.00202	0.0237
	7	30	0.000124	0.00157
		91	0.00175	0.0205
	14	30	0.0000664	0.000778
		91	0.00148	0.0173
Ru-106	1	30	0.000240	0.00252
		91	0.000941	0.00986
	7	30	0.000169	0.00178
		91	0.000857	0.00907
	14	30	0.0000952	0.00101
		91	0.000768	0.00814
I-131	1	30	0.00679	0.985
		91	0.00928	1.352
	7	30	0.00335	0.488
		91	0.00552	0.804
	14	30	0.00126	0.182
		91	0.00301	0.438
Cs-137	1	30	0.0000609	0.00120
		91	0.000489	0.00955
	7	30	0.0000491	0.000763
		91	0.000433	0.00845
	14	30	0.0000192	0.000376
		91	0.000372	0.00726
Ba-140	1	30	0.000388	0.0449
		91	0.000712	0.0854
	7	30	0.000208	0.0249
		91	0.000509	0.0611
	14	30	0.0000882	0.0106
		91	0.000343	0.0412

TABLE XIII Internal Hazard of Total Body from Ingestion of Contaminated Paterson Water Supply(*)

Isotope	t_o	t	Dose due to Direct Contamination of Water Supply (rems)	Dose including the Effect of Watershed Runoff (rems)
Sr-89	1	30	13.3	36.4
		91	79.1	216.0
	7	30	8.17	22.3
		91	66.8	182.0
	14	30	3.81	10.4
		91	54.2	148.0
Sr-90	1	30	0.338	0.901
		91	3.20	8.55
	7	30	0.212	0.566
		91	2.78	7.42
	14	30	0.105	0.281
		91	2.34	6.24
Ru-106	1	30	0.247	0.690
		91	0.966	2.70
	7	30	0.175	0.488
		91	0.888	2.48
	14	30	0.0987	0.276
		91	0.797	2.23
I-131	1	30	112.0	316.0
		91	115.0	433.0
	7	30	55.9	156.0
		91	92.2	258.0
	14	30	20.9	58.4
		91	50.2	140.0
Cs-137	1	30	0.354	0.963
		91	2.84	7.74
	7	30	0.227	0.618
		91	2.51	6.84
	14	30	0.112	0.304
		91	2.16	5.88
Ba-140	1	30	5.78	16.0
		91	11.0	30.4
	7	30	3.21	8.88
		91	7.87	21.8
	14	30	1.36	3.77
		91	5.30	14.7

(*) Employing 3 at 5 MT and 10 at 10 MT weapons = 115 MT attack

TABLE XIII Internal Hazard of Total Body from Ingestion of Contaminated Paterson Water Supply(*)

Isotope	t_o	t	Dose due to Direct Contamination of Water Supply	Dose including the Effect of Watershed Runoff (rems)
Sr-89	1	30	10.5	28.5
		91	62.5	169.
	7	30	6.45	17.5
		91	52.8	142.8
	14	30	3.01	8.15
		91	42.8	78.8
Sr-90	1	30	.267	.828
		91	2.53	7.85
	7	30	.167	.520
		91	2.19	6.81
	14	30	.083	.258
		91	1.85	5.74
Ru-106	1	30	.200	.574
		91	.781	2.25
	7	30	.141	.407
		91	.718	2.07
	14	30	.080	.230
		91	.644	1.85
I-131	1	30	90.6	241.
		91	124.	331.
	7	30	44.9	119.
		91	74.0	197.
	14	30	16.8	44.6
		91	40.3	107.
Cs-137	1	30	.278	.786
		91	2.23	6.31
	7	30	.178	.504
		91	1.97	5.58
	14	30	.088	.248
		91	.170	4.80
Ba-140	1	30	3.64	12.2
		91	6.92	23.2
	7	30	2.02	6.77
		91	4.95	16.6
	14	30	.858	2.87
		91	3.34	11.2

(*) Employing 1 at 5 MT, 1 at 10 MT and 5 at 20 MT weapons = 115 MT attack

IV. SUMMARY ANALYSIS OF THE MILLER FALLOUT MODEL

A. Introduction

In any explosive detonated near the surface of the earth, large quantities of material are carried aloft by an updraft of rising gases. In a nuclear explosion, two important additional effects are present: (a) a large amount of non-radioactive material (silicate soil particles will be the only kind considered in this report) is liquified and vaporized and raised to an altitude of many thousands of feet and (b) radioactive elements are produced and vaporized in the fission process and condense on or into this non-radioactive soil. The resulting particles, which may be spread over a considerable area by the prevailing winds, are called fallout.

Generally, fallout is divided into two categories, the heavier particles which fall to earth within about 24 hours after detonation, i.e. "Close-in" or "Early" fallout, and smaller particles which are carried into the stratosphere and may not fall out for months or years, the so-called "world wide" fallout. Depending on the prevailing meteorological conditions, the latter type of particles may fall out almost anywhere on the earth's surface. In this report only the "Close-in" fallout is considered as it will be the major contribution to water supply contamination during the early postattack period.

The fission products consist of about 90 different atomic mass chains each of which contains, on the average, about five elements. Thus, in general there are about 450 radionuclides that have to be considered to evaluate the total post-attack contamination problem. In general each of these nuclides decays with a characteristic half-life to another member of the chain and in the process emits gamma and/or beta radiation, each of these radiations having characteristic energies for each radionuclide. As the decay rate of any nuclide is proportional to the number of atoms of that nuclide present in the fallout, to determine the radiation intensity, it is necessary to solve a set of simultaneous differential equations.

This has been done numerically and the results for the fission product spectrum of U-235 have been tabulated by Bolles and Ballou (18), based on the initial fission products yields derived from Glendenin (19) and Present (20).

Approximately 40 different elements are represented in the fission products mixture. Initially, all of these are in a vaporized state in the fireball. As the fireball cools, these fission products condense, but at varying rates. Some are volatile and do not condense even at room temperature, others condense at very high temperatures. Since there is such a large range of vaporization temperatures for the various fission products, it has been found that in the larger fallout particles (hence, those that fall out earlier) the relative abundances of the fission products is altered from that tabulated for U-235 by Bolles and Ballou (18). This alteration from the original fission yield abundances is called fractionation. Fission products from nuclear fallout are usually fractionated.

For the purpose of calculating all fallout phenomena and effects, radiation intensity levels are based on a standard intensity, I(1), which is defined as the air ionization rate, in r/hr, three feet above an infinite plane covered uniformly with fallout, decay-corrected to one hour after detonation. It should be noted that this ionization rate is not the actual air ionization rate at one hour (because all the fallout may not yet have arrived at one hour) but represents a number from which, by means of a standard decay correction, one may calculate the ionization rate at a time after all the fallout has arrived.

A typical means of plotting this standard intensity profile is by drawing lines of constant intensity, or isointensity contours. In the Miller model (2), which assumes a ground surface burst and silicate soil, these contours are functions of only two parameters, namely, the weapon yield and the wind velocity. The calculations to obtain these parameters are based on both a theoretical description of a nuclear burst (2) (21), necessary to obtain the functional form of the scaling functions, and experimental data (22) (23).

Selected isointensity contours for a 20 MT weapon yield are plotted in Figure 16 for a wind velocity of 15 mph (22 fps) in the direction indicated. The details of constructing these isointensity contours are discussed in Section D.7.

Many other fallout properties are of interest. For example, the number of soluble atoms of a particular isotope at a certain location plays an important role in assessing the degree of contamination and the biological hazard. The ratio of the value of the particular property of fallout (at H + 1 hour, i.e. at one hour after detonation) to the ionization rate at H + 1 hour, I(1), at the same point is called the contour ratio. If the number of soluble atoms is the property of interest the contour ratio is called the soluble nuclide contour ratio, $N'_{\alpha}(1)$. Figure 17 shows $N'_{\alpha}(1)$ for the radionuclide Sr-90 as a function of downwind distance, X, for a weapon yield of 20 MT and wind speed of 15 mph. Details of the derivations are found in Section E. below.

Given the soluble nuclide contour ratio, the ionization rate at H + 1 hour and ground zero, one can calculate the number of soluble atoms of a nuclide that will fall on any given area. Hence, one can calculate the number of soluble atoms that fall on a water supply reservoir and watershed of a particular city. This procedure has been followed for Paterson, New Jersey, Springfield, Massachusetts and San Francisco, California. A typical case was shown in Figure 3 for San Francisco, California. Details of derivation and other graphs are presented in Chapter II, and in Appendix A.

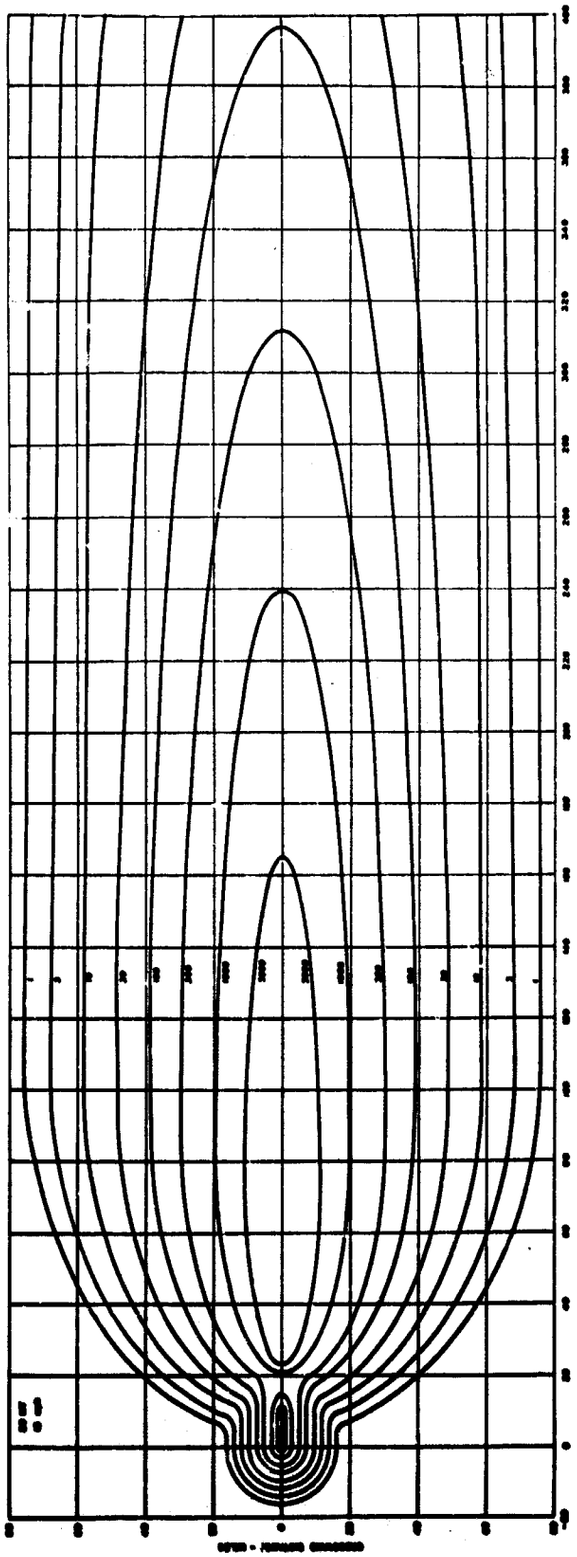

Figure 16. Selected Isointensity Contours for a 20 MT Weapon Yield and Wind Speed of 15 mph

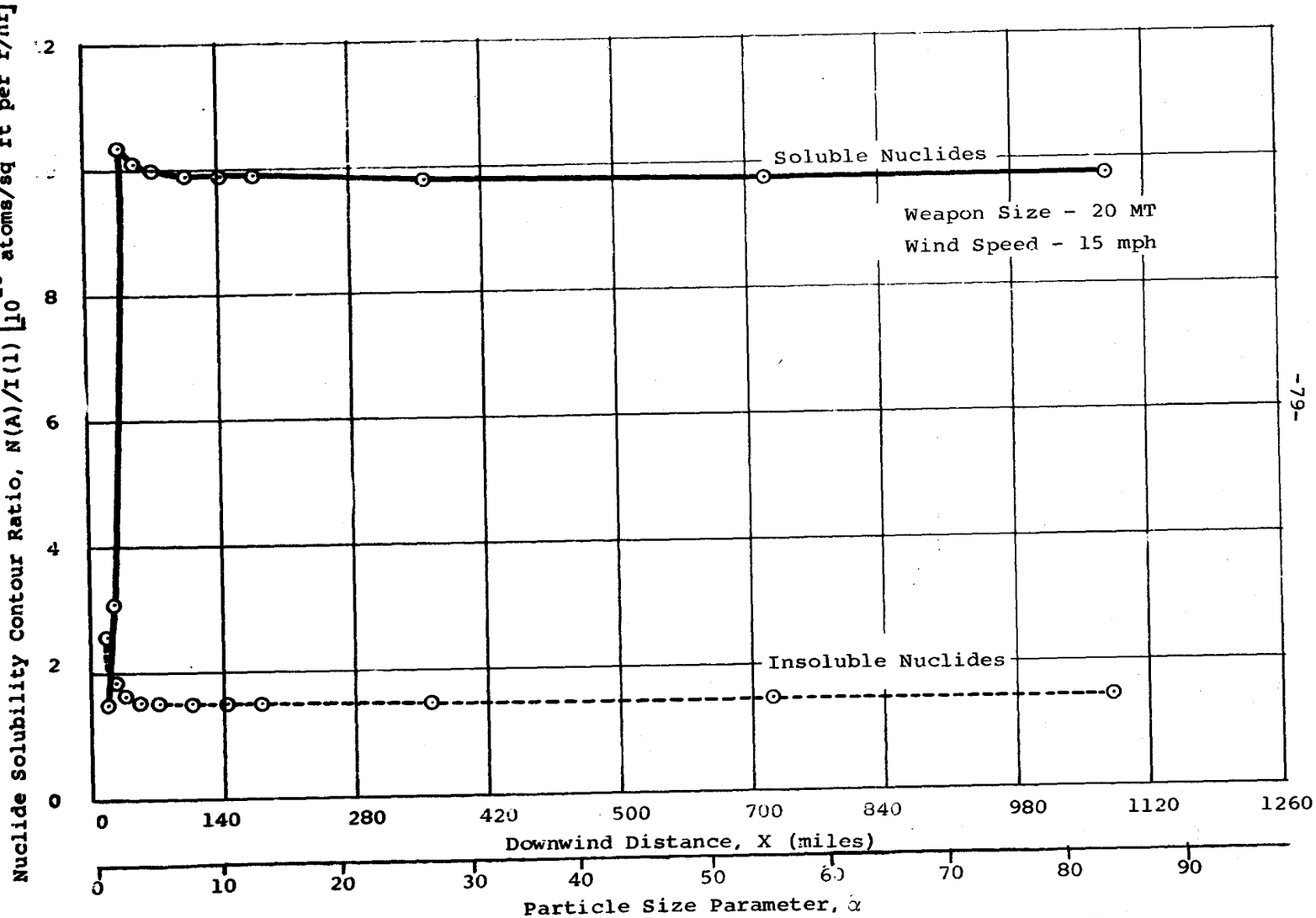

Figure 17. Nuclide Contour Ratio vs. Downwind Distance for Sr-90

From the volume of the reservoir one can calculate the concentration, assuming uniform mixing, of the nuclide in the water supply. Then, assuming a standard ingestion rate of water of 2 liters per day (17), one can obtain the input function for the biological uptake models presented in Chapter III. The contamination levels (atoms/liter) were shown in Tables II, III, IV for the six biologically most important nuclides.

B. General Description of Model Ground Surface Burst

To determine the correct values of the various parameters in the model ground surface burst, Miller (2) has first considered the basic description of an air burst (i.e. no air-ground interface, no addition of mass from the surface of the fireball) as summarized by Glasstone (22) and modified it to correlate better with more recent test data. This description implies a certain scaling with weapon yield.

1. Assumptions to extrapolate from Model Air Burst to Surface Burst

To obtain the model surface burst the presence of a ground-air interface is added. This modification is accomplished mainly by means of the following assumptions:

1. One half of the energy remaining in the fireball at the time of the second thermal maximum is used to heat the air in the fireball and the other half to heat the soil added to the fireball.
2. The vapor density of the fireball at the time of the second thermal maximum is the same in the air burst and in the ground burst.
3. In both types of burst, blast and shock carry away 28% of the released energy, 15% goes into nuclear radiation and the remainder of the energy is still in the fireball at the time of the second thermal maximum.
4. The fireball volume at the time of the second thermal maximum is the same in both cases; in the ground burst its shape is hemispherical rather than spherical.

The thermal properties for an ideal soil were specified by Miller (2) based on the data by Kelley (24) and Stull and Sinke(25). The soil is sucked into the fireball before the second thermal maximum and therefore affects the time at which the second thermal maximum occurs. Thus, the time for the second thermal maximum for a ground surface burst is:

$$t_2 = 0.061\ W^{0.373}\ \text{sec} \tag{1}$$

where W = weapon yield (KT)

At time t_2 the fireball of the model surface burst is a hemisphere centered at ground zero. It remains in this position until it reaches full expansion at time t_m. It then begins to rise and becomes spherical when it leaves the earth's surface at time t_s. During this period from t_m to t_s the volume is constant, i.e. essentially from 1.4 t_2 to 10 t_2. It should be observed that fallout particles enter the fireball some time after t_2 and presumably to a large extent after 10 t_2.

The corresponding radii for the above times are:

$$R_2 = 6.35 \times 10^3\ W^{0.333}\ \text{cm} \tag{2}$$

$$R_m = 7.88 \times 10^3\ W^{0.333}\ \text{cm} \tag{3}$$

$$R_s = 6.25 \times 10^3\ W^{0.333}\ \text{cm} \tag{4}$$

Estimates of t_m and t_s are given by:

$$t_m = 0.085\ W^{0.373}\ \text{sec} \tag{5}$$

$$t_s = 0.354\ W^{0.373}\ \text{sec} \tag{6}$$

The variation of temperature, T, is assumed to follow the same pattern of decrease with time as in the case of the air burst:

$$T \text{ varies as } (t/t_2)^{-n} \qquad \text{up to } t = 10\ t_2 \tag{7}$$

and

$$T \text{ varies as } \exp\left[-K\ (t/t_2)\right] \qquad \text{when } t > 10\ t_2 \tag{7a}$$

where n and K are yield independent parameters.

In more detail, the estimate of the fireball temperature for the surface burst is:

$$T = 7.2 \times 10^3 \, W^{-0.010} \, (t/t_2)^{-1/3} \, {}^{o}K \qquad t/t_2 = 1 \text{ to } 10 \qquad (8)$$

$$= 2.83 \times 10^3 \, W^{0.114} \, t^{-1/3} \, {}^{o}K \qquad t = t_2 \text{ to } 10 \, t_2$$

and

$$T = 4.66 \times 10^3 \, W^{-0.010} \exp(-0.033 \, t/t_2) \, {}^{o}K \qquad t/t_2 = 10 \text{ to } 50 \qquad (9)$$

$$= 4.66 \times 10^3 \, W^{-0.010} \exp(-0.546 \, W^{-0.373} t) \, {}^{o}K \qquad t = 10 \, t_2 \text{ to } 50 \, t_2$$

The radius of the fireball for a surface burst is given by:

$$R = 5.69 \times 10^3 \, W^{0.333} \exp(0.0104 \, t/t_2) \text{ cm} \qquad t/t_2 = 10 \text{ to } 50 \qquad (10)$$

$$= 5.69 \times 10^3 \, W^{0.333} \exp(0.170 \, W^{-0.373} t) \text{ cm} \qquad t = 10 \, t_2 \text{ to } 50 \, t_2$$

Some of the fireball temperatures and times for yields between 1 and 10^5 KT from the above equations are summarized in Table XIV below.

TABLE XIV

Summary of Some Fireball Parameter Values for Various Yields of the Model Surface Burst

Parameter	Weapon Yield (KT)					
	1	10	10^2	10^3	10^4	10^5
t_2 (sec)	0.061	0.14	0.34	0.80	1.89	4.47
T at $10t_2$ (^{o}K)	3340	3260	3190	3120	3050	2980
T at $20t_2$ (^{o}K)	2390	2340	2280	2230	2180	2130
T at $30t_2$ (^{o}K)	1720	1680	1640	1600	1570	1530
T at $40t_2$ (^{o}K)	1230	1200	1170	1150	1120	1100
T at $50t_2$ (^{o}K)	880	860	840	820	800	785
t/t_2 at 1673 ^{o}K	30.8	30.1	29.4	28.7	28.0	27.4
t at 1673 ^{o}K (sec)	1.88	4.34	10.0	23.1	53.1	122

For most yields the temperature range of interest occurs between 20 t_2 and 30 t_2. The time of the end of the first period of condensation (T = 1673 ^{o}K) varies from about 2 seconds for 1 KT to about 122 seconds for 10^5 KT. In scaled time, the change is only from 31 t_2 to 27 t_2 from 1 KT to 10^5 KT, respectively.

It is also necessary to determine the concentration of liquid soil in the fireball, $n(\ell)/V$,

where $n(\ell)$ = number of moles of liquid soil

V = volume of the fireball

The spherical fireball volume is:

$$V = 7.72 \times 10^{11} W \exp(0.510 W^{-0.373} t) \text{ cm}^3 \qquad t = 10\ t_2 \text{ to } 50\ t_2 \qquad (11)$$

while the amount of soil that could be liquified at the melting temperature plus that condensed from the vapor is:

$$n(\ell) = 4.38 \times 10^5 W \text{ moles} \qquad (12)$$

The only unclassified data directly applicable to the model surface burst are those of Operation Jangle, "S" shot. There is about a factor of two difference between the calculations based on the model and the data.

2. Formation and Geometry of Stem and Cloud

After a surface burst, the fireball assumes a spherical shape; as it rises, its horizontal and vertical radii expand at different rates (due to changing air density in the verticle direction) but both vary exponentially with altitude. Hence, the originally spherical fireball becomes an oblate spheroid (circular top-view and elliptical side-view). At its final stabilized height the fireball is generally known as the cloud. The stem has been formed by a continuously and exponentially expanding fireball and hence has the shape of an inverted, exponential horn.

The initial spherical radius of the fireball, R_s, the final horizontal semi-axis, a, the final vertical semi-axis, b, and the final height of the center, h, of the cloud are correlated to the weapon yield, W, through empirical data as shown in the following scaling functions:

$$R_s = 2.09 \times 10^2 \, W^{0.333} \text{ ft.} \qquad W = 1 \text{ to } 10^5 \text{ KT} \qquad (13)$$

$$a = 2.34 \times 10^3 \, W^{0.431} \text{ ft.} \qquad W = 1 \text{ to } 10^5 \text{ KT} \qquad (14)$$

$$b = 1.40 \times 10^3 \, W^{0.431} \text{ ft.} \qquad W = 1 \text{ to } 10^5 \text{ KT} \qquad (15)$$

$$h = 0.66 \times 10^4 \, W^{0.445} \text{ ft.} \qquad W = 1 \text{ to } 28 \text{ KT} \qquad (16)$$

$$h = 1.68 \times 10^4 \, W^{0.164} \text{ ft.} \qquad W = 28 \text{ to } 10^5 \text{ KT} \qquad (16a)$$

At a given altitude, Z, the horizontal and vertical semi-axes of the fireball are given by:

$$a_Z = a_o e^{k_a Z} \qquad (17)$$

$$b_Z = b_o e^{k_b Z} \qquad (18)$$

where a_o, b_o, k_a, k_b can be determined from the data on R_s, a, b, h.

The geometry of both stem and cloud is shown in Figure 18.

In the Miller model the fireball is assumed to behave like an ideal gas undergoing an adiabatic expansion, taking into account the variation of the change in free energy and external pressure with altitude.

The radioactive cloud, almost from the time it is formed, has the form of an oblate spheroid (pancake); hence, with constant wind velocity, the fallout patterns are generally cigar-shaped.

All dimensions and other properties of the fireball are scaled as functions of wind speed and weapon yield to correlate with test data.

NOTE: The particles with maximum a values and particles with minimum a values which fall on point X downwind from the cloud fall along paths described by r_{max} and r_{min} respectively.

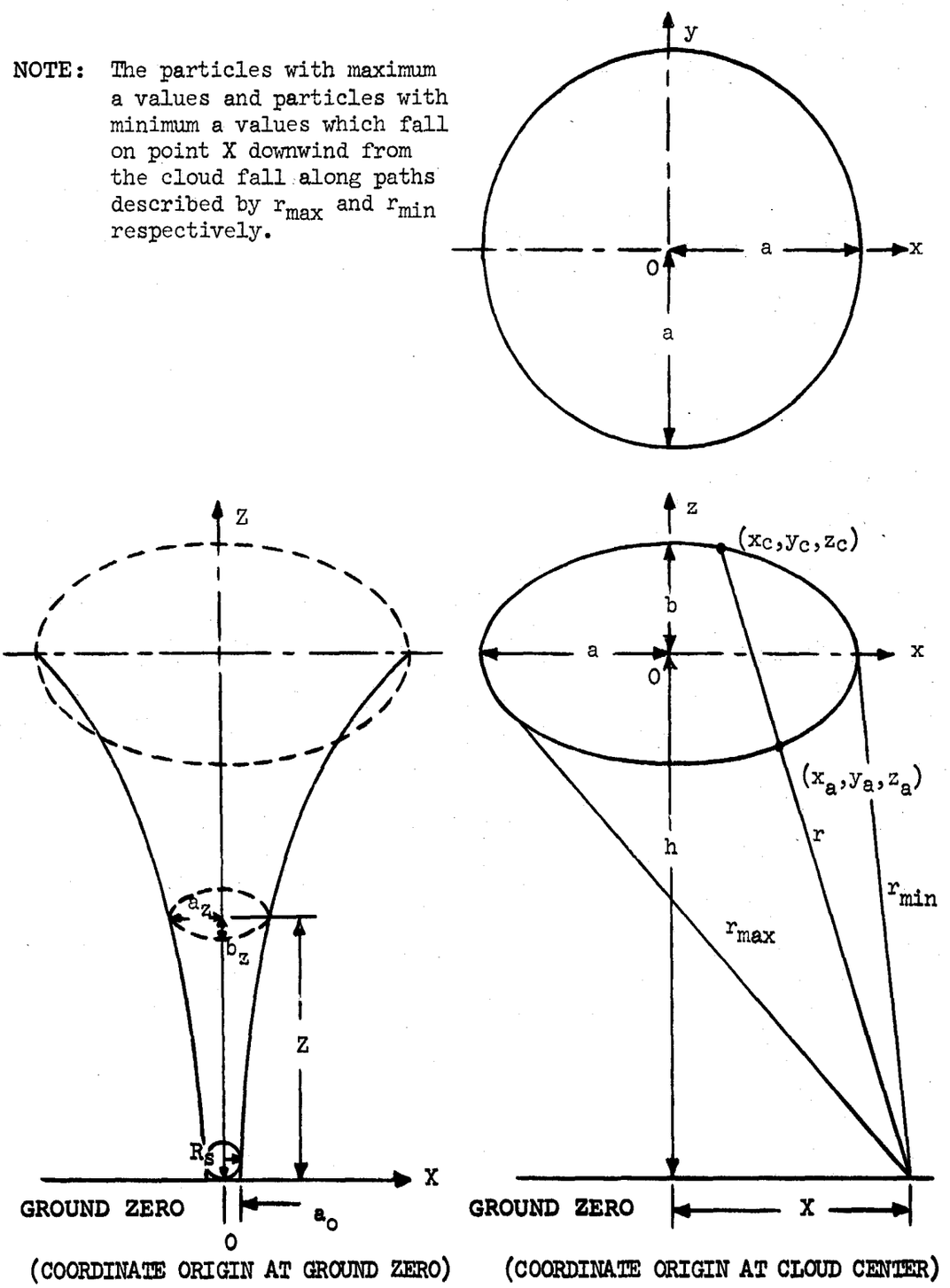

Figure 18. Geometry of Stem and Cloud

C. Formation of Fallout - Fractionation Theory

1. Physical Chemistry of the Fallout Formation Process

In the case of a ground surface burst, a great deal of soil is drawn up into the fireball. Initially this soil, which acts as the carrier for the fallout, is largely liquified or vaporized. Furthermore, all fission products are initially in a vaporized state. The Miller model for fallout considers the following idealized model: The silicate soil is initially in a completely liquified state at a uniform temperature and uniformly spread throughout the volume of the fireball. The fission products are vaporized and also uniformly spread throughout the volume of the fireball. The fireball cools by (a) radiation, (b) expansion and (c) heating up of more air drawn into its volume. The point at which the temperature drops to the solidification point of the silicate carrier material (1673°K) marks the end of the first period of condensation.

During the first period, the physico-chemical system is considered to be a very dilute solution, the solvent being the liquid silicate soil and the solutes the fission products, in equilibrium with the vaporized fission products and other gases present in the fireball. When the silicate carrier material solidifies the fission products that have been dissolved are trapped in the glassy solid.

During the second period of condensation there is a solid carrier in the presence of vaporized fission products. In this period the fission-product elements may condense by (a) sublimation on the surface of solid particles, or (b) they may react directly with the carrier substance. In either case the fission products end up on the outside of the carrier material. Hence, the fission-product elements are exposed and may be dissolved in water. In this surface effect, the solid carrier is coated and henceforth does not take part in the condensation process. Instead, the system is that of a number of solids (the condensed fission products) that sublime, in equilibrium with their vapor phases. Miller (2) has assumed that they act independently in the sense that for a given substance all the solid surface present is of that substance, i.e. there is no reduction in the surface area

at which molecules can evaporate due to the presence of other solidified fission products. It should be noted that the assumption of no reduced surface area was not made for the solution during the first period of condensation. The second period of condensation continues until the particular fallout particle under consideration leaves the fireball. The end of the second period of condensation is taken to be the time at which this particle enters into the toroidal circulation. Empirically, this time has been taken, for all cases, as 180 seconds before the particle has reached its maximum height, i.e., its "rise time" minus 180 seconds.

(a) Vapor-Liquid Equilibrium

(1) No Chemical Reactions

The vapor pressure of a pure liquid depends on the rate of escape of molecules from the surface of the liquid. If the liquid is mixed with another liquid, the concentration and hence the rate of escape of molecules from the surface is reduced. In an ideal solution, where the character of the liquid is unchanged, the partial vapor pressure of one component is directly proportional to the fraction of molecules of that component in the mixture. Therefore, for a mixture with two components:

$$p_A = \frac{n_A}{n_A + n_B} p_A^o = N_A p_A^o \qquad (19)$$

where p_A = partial pressure of component A

p_A^o = vapor pressure of pure A

n_A = number of moles of A

n_B = number of moles of B

N_A = mole fraction of A

and similarly,

$$p_B = N_B p_B^o \qquad (19a)$$

If there are several components in a mixture, each will have a partial vapor pressure equal to its vapor pressure in the pure state times its mole fraction in solution.

One case of equation (19), namely for very dilute solutions, is called Raoult's law:

$$p_{solvent} = p^{\circ}_{solvent} N_{solvent} \tag{20}$$

On the other hand, Henry's Law applies to the solute:

$$p_{solute} = K N_{solute}. \tag{21}$$

In general, the proportionality constant K is not the vapor pressure of the pure solute but an experimentally evaluated constant, for each solution. The difference between Eq (20) and (21) is that for the case of very dilute solutions the solute is so dilute that the properties of the solvent are little affected (Raoult's law, Eq (20)); on the other hand in Eq (21) the solute itself is diluted to such an extent that its properties may be greatly different from the pure state.

In the case of an ideal solution Both Henry's and Raoult's laws are exact. In addition, the proportionality constant K in equation (21) becomes identical with the vapor pressure of the pure solute,

$$p_{solute} = p^{\circ}_{solute} N_{solute} \tag{22}$$

In the present case we are concerned with nuclide (jA), i.e. element j of mass chain A, whose partial pressure is given by Henry's Law:

$$p_{jA} = p^{\circ}_{jA} N_{jA}, \text{ where } N_{jA} = \frac{n_{jA}}{n(\ell) + \sum_{jA} n_{jA}} \simeq \frac{n_{jA}}{n(\ell)} \tag{23}$$

and where $n(\ell)$ is the number of moles of solvent $\approx n(\ell) + \sum_{jA} n_{jA}$.

The vapor pressure of the nuclide will be very nearly equal to the vapor pressure of the element, or $p^{\circ}_{jA} = p^{\circ}_{j}$. Therefore,

$$p_{jA} = p^{\circ}_{j} N_{jA} \tag{24}$$

or

$$\frac{n_{jA}}{n(\ell)} = \frac{p_{jA}}{p^{\circ}_{j}} \tag{25}$$

12

But
$$\frac{p_{jA}}{P} = \frac{n^{o}_{jA}}{n} \tag{26}$$

where P = total gas or vapor pressure

n^{o}_{jA} = number of moles of element j of mass number A (j,A) vapor

n = total number of moles of gas and vapor.

Hence
$$\frac{n_{jA}}{n(\ell)} = \frac{n^{o}_{jA}\, P}{n\, p^{o}_{j}} \tag{27}$$

From the ideal gas law:
$$n = \frac{PV}{RT} \tag{28}$$

where V = total volume of gas (liters)

T = temperature of gas (^{o}K)

R = gas constant, 82.07, cm^3 atmos/mole ^{o}K

$$\frac{n_{jA}}{n(\ell)} = \frac{RT}{Vp^{o}_{j}}\ n^{o}_{jA} \tag{29}$$

or
$$n^{o}_{jA} = k^{o}_{j}\, n_{jA} \tag{30}$$

where
$$k^{o}_{j} = \frac{p^{o}_{j}}{(n(\ell)/V)\ RT} \tag{31}$$

p^{o}_{j} is obtained from:
$$\log p^{o}_{j} = \frac{A}{T} + B + C \tag{32}$$

where A, B and C are empirical constants tabulated in Table V (26).

(2) With Chemical Reactions

When the nuclides can form compounds with the carrier, either in the liquid or vapor state, the description of the processes involved becomes much more complex than in the simple case of dilute ideal solutions discussed above. There are two basic processes involved, the overall reaction in either case being summed up by:

$$A(g) + B(\ell) \text{ ----> } AB(\ell), \text{ dilute solution in } B(\ell) \tag{33}$$

where A = nuclide, or fission product element

B = carrier

g = gas or vapor

ℓ = liquid

One process is the formation of compounds with the carrier in the liquid state:

1. $A(g) \longrightarrow A(\ell)$
2. $A(\ell) + B(\ell) \longrightarrow AB(\ell)$
3. $AB(\ell) \longrightarrow AB(\ell)$, dilute solution in $B(\ell)$ (34)

and the other process is the formation of compounds with the carrier in the vapor state:

1. $B(\ell) \longrightarrow B(g)$
2. $A(g) + B(g) \longrightarrow AB(g)$
3. $AB(g) \longrightarrow AB(\ell)$
4. $AB(\ell) \longrightarrow AB(\ell)$, dilute solution in $B(\ell)$. (35)

The only difference in the two processes might be a difference in the reaction rates, but thermodynamic quantities like the change in the free energy are the same since the systems begin in the same state and end in the same state.

An additional complication is the possibility of reactions with the atmospheric oxygen where the degree of dissassociation of the oxide is different in the vapor and the liquid. The overall reaction in this case is:

$$A(g) + xO_2(g) + B(\ell) \longrightarrow AO_{2x}B(\ell), \text{ dilute solution in } B(\ell) \quad (36)$$

where x = the number of oxygen molecules that combine with each atom of element A.

For this to be a different reaction from the one above, the gases A and O_2 must be in equilibrium with the vapor of the oxide of A. Again the two processes are:

Carrier in the vapor state:

1. $A(g) + xO_2(g) \longrightarrow AO_{2x}(g)$
2. $AO_{2x}(g) \longrightarrow AO_{2x}(\ell)$
3. $)_{2x}(\ell) + B(\ell) \longrightarrow AO_{2x}B(\ell)$
4. $AO_{2x}B(\ell) \longrightarrow AO_{2x}B(\ell)$, dilute solution in the $B(\ell)$, (37)

and the other; with the carrier in the liquid state:

1. $A(g) + xO_2(g) \text{ ------> } AO_{2x}(g)$

2. $B(\ell) \text{ -------> } B(g)$

3. $AO_{2x}(g) + B(g) \text{ -------> } AO_{2x}B(g)$ (38)

4. $AO_{2x}B(g) \text{ ------> } AO_{2x}B(\ell)$

5. $AO_{2x}B(\ell) \text{ ------> } AO_{2x}B(\ell)$, dilute solution in $B(\ell)$ (39)

Although Henry's Law is used in the derivation of the material balance equations in the following sections, suitable modifications of the Henry's Law constants have been devised by Miller (2) to put the equations for the case of compound formation in the same form.

b. Vapor-Solid Phase Equilibrium

In the first analysis the process to be considered is that of equilibrium of vapor and solid phases of a pure substance. This is in fact somewhat fictitious since this equilibrium can exist only in a certain temperature range for a given substance. The equilibrium is expressed by:

$$p^{os}_j = P \tag{40}$$

that is the sublimation pressure of the solid of element j equals the total vapor pressure.

In the presence of other substances the situation is more complex. For example, if there are more than one gas present then

$$p^{os}_j = p_j \tag{41}$$

where p_j = the partial pressure of the vapor.

If more than one solid surface is present, so that only a fraction, equal to the mole fraction, of the surface is available from which the solid can sublime, we have:

$$p^s_j = p^{os}_j N_j = p^{os}_j \frac{n_j}{n_t} \tag{42}$$

where n_t is the total number of moles of solid surface,

and p_j^s = the partial sublimation pressure.

Miller (2), in fact, ignores this shielding effect and uses equation (41),

$$p_j^s = p_j^{os} = p_j \tag{43}$$

2. First Period of Condensation

Consider the radioactive cloud during the stage of formation in which the temperature is still above the solidification temperature of silicate soil.

Let $y_{jA}(t)$ = number of moles of nuclide (j,A) at time t where (j,A) means atomic number j and atomic mass A.

$n_{jA}(t)$ = number of moles of nuclide (j,A) dissolved in liquid carrier (fallout particles before solidification) at time t.

For $t = t_1$, the time of the end of the 1st period of condensation, this equals the number of moles of (j,A) that are in the interior of fallout particles and hence insoluble.

$n^o_{jA}(t)$ = number of moles of nuclide (j,A) in the vapor phase at time t for $t < t_1$.

Then, during the first period of condensation when the radionuclides can be in only the vapor phase, or dissolved in the carrier;

$$y_{jA}(t) = n_{jA}(t) + n^o_{jA}(t) \tag{44}$$

Let $n(\ell)$ = the total number of moles of liquid carrier at time t.

Then Henry's Law, equation (21), may be written:

$$p_{jA} = k_{jA} \frac{n_{jA}}{n(\ell)} \tag{45}$$

$$\text{since } n(\ell) \approx n(\ell) + n_{jA}$$

where k_{jA} is the Henry's Law proportionality constant. For a very dilute solution, k_{jA} becomes equal to p^o_{jA}, equation (22), the vapor pressure of (j,A) over the pure substance (j,A).

But:

$$\frac{p_{jA}}{P} = \frac{n^{o}_{jA}}{n} \tag{26}$$

where P = total pressure of gas and vapor

n^{o}_{jA} = number of moles of element j of mass number A (j,A) vapor

n = total number of moles of vapor and gas.

Assuming the perfect gas law:

$$PV = nRT, \tag{46}$$

$$n^{o}_{jA} = k^{o}_{jA}\, n_{jA} \tag{47}$$

where

$$k^{o}_{jA} = \frac{k_{jA}}{(\Sigma(\ell)/V)RT} \tag{48}$$

Substituting equation (47) into equation (44):

$$n_{jA}(t) = \frac{y_{jA}(t)}{1 + k^{o}_{jA}} \tag{49}$$

Consider, as a first approximation, a mass chain of atomic mass A, such that all the radioactive nuclides, except the last, have short half lives. Then, if all the atoms of this chain are in a container at time t = 0, at a time t greater than the short half lives, essentially all the nuclides will have decayed to the last of the series. Therefore, the total number of moles of (J,A) that end up in the interior of fallout particles (i.e. were in solution at the end of the first period of condensation), where (J,A) has a relatively long half-life, should be the sum of all the nuclides (j,A) in the chain up to (J,A):

$$n_{JA}(t_1) = \sum_{j}^{J} y_{jA}(t) = \sum_{j}^{J} \frac{n_{jA}(t_1)}{1 + k^{o}_{jA}(T_1)} \tag{50}$$

evaluated at the time of the end of the first period of condensation, t_1, when the fireball temperature is T_1. The fractionation number for the first period of condensation r_o (A,t), defined as the ratio of the number of moles of nuclide (J,A) in the interior of fallout particles to the total number of moles of that nuclide present (or total number of moles of that mass chain):

$$r_o(A,t_1) = \frac{1}{Y_A(t_1)} \sum_{j}^{J} \frac{y_{jA}(t_1)}{1 + k^{o}_{jA}\, T_1} \tag{51}$$

where

$$Y_A(t_1) = \sum_j^J y_{jA}(t_1) \tag{52}$$

3. Second Period of Condensation

The fractionation number for the second period of condensation, $r'_o(A,t)$, is derived similarly:

Let $n'_{jA}(t)$ = number of moles of nuclide (j,A) adsorbed on the surface of solid particles up to time t ($t \geq t_1$)

$n''_{jA}(t)$ = number of moles of nuclide (j,A) still in the vapor phase at time t

$n^o_{jA}(t_1)$ = number of moles of nuclide (j,A) not condensed from vapor during first period of condensation.

Then,

$$n^o_{jA}(t_1) = n'_{jA}(t) + n''_{jA}(t) \tag{53}$$

Assuming the perfect gas law, the number of moles of nuclide (j,A) still in the vapor phase during the second period of condensation is:

$$n''_{jA}(t) = \frac{p_{jA}V}{RT} \tag{54}$$

where p_{jA} the partial vapor pressure of (j,A) assumed equal (thermodynamic equilibrium) to, p^s_{jA}, the partial sublimation pressure of the solid (j,A) (atmos.)

V = volume of the fireball

R = gas constant = 82.07, cm^3 atmos/mole ^oK

The time dependent material balance equation for nuclide (j,A) becomes:

$$y_{jA}(t_1) = n_{jA}(t_1) + n'_{jA}(t) + n''_{jA}(t) \tag{55}$$

Using equations (47) and (54) we obtain:

$$n'_{jA}(t_2) = y_{jA}(t_1) - n''_{jA}(t_2) - n_{jA}(t_1)$$

$$= \frac{k^o_{jA}(T_1)}{1 + k^o_{jA}(T_1)} \; y_{jA}(t_1) - \frac{V}{RT} \; p^s_{jA}(t_2) \tag{56}$$

where t_2 = the time of the end of the second period of condensation.

The number of moles of (J,A) that will be soluble at some later time therefore will be:

$$\sum_j^J n'_{jA}(t_2) = \sum_j^J \frac{k^o_{jA}(T_1)}{1 + k^o_{jA}(T_1)} y_{jA}(t_1) - \frac{V}{RT} \sum_j^J p^s_{jA}(t_2) \quad (57)$$

where t_2 is a function of the particle size parameter α and is given by Miller (2) as:

$$t_2(\alpha) = \frac{1}{k_z} \ln \left[\frac{k_z \alpha / V_w + q}{p/Z_o + q} \right] - 180 \text{ sec} \quad (58)$$

where : k_z = an empirical constant describing the rise of the fireball = .011 sec^{-1}

α = particle size parameter, V_w/V_f

V_w = wind speed (fps)

V_f = particle falling speed (fps)

Z_o = fireball height limit (feet)

and

p,q = empirical parameters describing falling rate of particles. The values for p and q for 5,000 ft. $\leq Z_o <$ 50,000 ft., are:

$p = 0.95$; $q = 1.02 \times 10^{-5}$

180 sec = average delay time before particle starts to fall - this is the average time particles spend in the toroidal motion of the cloud.

The fractionation number for the second period of condensation, $r'_o(A,t_2)$, which is the fraction of the chain yield of mass chain A that ends up adsorbed on the surface of fallout particles and hence soluble at some later time is given by:

$$r'_o(A,t_2) = \sum_j^J \frac{n'_{jA}(t_2)}{Y_A}$$

$$= \frac{1}{Y_A} \sum_j^J \frac{k^o_{jA}(T_1)}{1 + k^o_{jA}(T_1)} y_{jA}(t_1) - \frac{V}{RT\,Y_A} \sum_j^J p^s_{jA}(t_2) \quad (59)$$

T(t) and V(t) have been given by equations (9) and (11) above. Since

$\frac{K}{1+K} = 1 - \frac{1}{1+K}$, the first term of equation (59) may be written:

$$1 - r_o(A,t_1) \quad (60)$$

Hence,

$$r'_o\,(A,t_2) = 1 - r_o\,(A,t_1) - \frac{V}{RTY_A} \sum_j^J p^s_{jA}\,(t_2) \qquad (61)$$

During this second period of condensation nuclides are adsorbed on the surface of solid fallout particles. The process of adsorption differs from that of solution in that the adsorbed material is "plated" onto the surface of the carrier rather than being mixed uniformly throughout the carrier as is the case during the first period of condensation. Therefore, the total rate of sublimation of a particular nuclide is reduced (from the case of the nuclide over the pure substance) by the fraction that it is of all the adsorbed materials, that is, by ratio:

$$\frac{n^o_{jA}\,(t)}{\sum_{jA}^J n^o_{jA}\,(t)}$$

The sublimation pressure is reduced by the same ratio (Henry's Law), to yield:

$$p^s_{jA} = \frac{n^o_{jA}(t_1)}{\sum_{jA} n^o_{jA}(t_1)}\; p^{os}_{jA} \qquad (62)$$

where

p^{os}_{jA} = the sublimation pressure over the pure substance (jA), and

$\sum_{jA} n^o_{jA}\,(t_1)$ = total number of moles of all mass chains condensed in first period of condensation, $= \sum_A \left[Y_A\,(t_1) - n_A\,(t_1)\right]$.

Therefore the last term of equation (61) may be written:

$$-\frac{V}{RT\,Y_A} \sum_j^J p^{os}_{jA}\; \frac{n^o_{jA}(t_1)}{\sum_{jA} n^o_{jA}\,(t_1)} \qquad (63)$$

If it is assumed that the sublimation pressure of the nuclide equals the sublimation pressure of the total element, then

$$p^{os}_j = p^{os}_{jA} \qquad (64)$$

This quantity is tabulated by Miller and in this report as:

$$\log p_j = \frac{A}{T} + B + C \tag{32}$$

Miller (2) makes a first approximation to equation (62) by assuming that

$$p^s_{jA} = p^s_j \frac{n^o_{jA}(t)}{n^o_j(t)} \tag{65}$$

that is, that the sublimation pressure is proportional to the abundance of the nuclide relative to the total element, where p^s_j is the partial pressure of the total element. Miller assumes that this partial pressure equals the total sublimation pressure over the pure substance, i.e.

$$p^s_j = p^{os}_j \tag{66}$$

We feel that, as above, the partial pressure is proportional to the relative abundance, i.e.:

$$p^s_j = \frac{n_j}{\sum_j n^o_j} p^{os}_j \tag{67}$$

Substituting (67) into (65) gives equation (62) above.

Miller's method (2) has been used as a first approximation. It should be kept in mind, however, that this correction should be one of the next ones made in the Miller fallout model.

Note also that the relative abundance means the ratio of the amounts not condensed in the first period of condensation. We have assumed, as a first approximation, that the relative amounts are not changed by selective condensation during the first period. This correction would involve long additional calculations and the term under consideration is usually not important anyway. How to use this correction is explained below. The data of Bolles and Ballou, even though they are tabulated in atoms per 10^4 fissions may be used here directly since (a) only ratios of fission yields are involved and (b) the number of moles is proportional to the number of moles is proportional to the number of atoms.

The term $\frac{n^o_{jA}}{n_j}$ as given in Bolles and Ballou (18) must be corrected in order to use it here, since some of the nuclides have been selectively removed in the first period of condensation, that is:

$$y'_{jA}(t_2) = \frac{y_{jA}(t_1) - n_{jA}(t_1)}{y_{jA}(t_1)} \; y^*_{jA}(t_2)$$

and

$$y'_{j}(t_2) = \frac{y_{j}(t_1) - n_{j}(t_1)}{y_{j}(t_1)} \; y^*_{j}(t_2) \qquad (68)$$

D. Distribution of Fallout

1. Dynamics of Fallout Deposition

In a ground surface burst a large quantity of soil is liquified or vaporized and drawn up into the fireball. Assuming that it is only liquified and at the melting temperature of 1673°K, the amount of liquified soil , $n(\ell)$, that could be in the fireball is:

$$n(\ell) = 4.38 \times 10^5 \; W \text{ moles} \qquad (12)$$

where W = weapon yield (KT).

Also present in the fireball are the radioactive fission products; at early times these are all vaporized. When the soil in the fireball is still in a liquid state, some fraction of these nuclides are dissolved in the liquid soil, forming very dilute solutions, assumed to be in equilibrium with the remaining vapors. When the fireball cools to about 1673°K, the liquid silicate soil solidifies and glassy particles of various sizes are formed. The portion of the radioactive fission product nuclides that has been dissolved in the liquid soil is now trapped inside the soil fallout particles. Hence, this portion of the nuclides will not be dissolved in the water, should the fallout particle enter the water supply. The remaining nuclide vapors can, however, still be adsorbed on the surface of the solid soil particles. Hence, these adsorbed nuclides can dissolve in water should the fallout particle enter the water supply.

The soil particles continue to rise with the fireball which eventually becomes the nuclear cloud. This cloud expands exponentially as it rises (the stem); at its highest point it has the shape of an oblate spheroid (pancake), the familiar mushroom cloud. Particles of a particular size are assumed to rise until their instantaneous

where y^*_{jA} and y^*_j are the unfractionated fission yields at time t_2 as reported by Bolles and Ballou (18)

falling rate, V_Z, equals the rate of rise of the surrounding air mass, $\frac{dZ}{dt}$:

$$V_Z = \frac{dZ}{dt} \tag{69}$$

where Z is the height of the cloud at time t (or fireball altitude).

If V_f is the average falling velocity of the particle,

$$V_f = Z/t \tag{70}$$

where Z = height from which particle falls

t = length of time to fall.

The following relations between V_Z and V_f were determined by Miller (2), using Anderson's data (27) on the falling rate of spherical particles:

$$V_Z/V_f = 0.95 + 1.02 \times 10^{-5} Z \tag{71}$$

for Z = 5,000 to 50,000 ft.

and d = 200 to 1,200 microns

where d = particle diameter (microns)

and:

$$V_Z/V_f = 0.58 + 1.74 \times 10^{-5} Z \tag{72}$$

for Z = 50,000 to 110,000 ft.

and d = 300 to 1,000 microns

Equation (71), applicable to most of the altitude range of stem fallout, fits Anderson's data quite well.

The rising cloud takes on toroidal circulation when the internal pressure and temperature approach ambient conditions and a large scale air circulation is established. Air rises and soil particles rush up into the cloud from directly below it and seem to flow out over the top and down the outside of the cloud.

A particle-altitude function which gives a good representation of the input data on particle arrival times and particle sizes according to Miller (2) is:

$$Z = Z_o(1 - e^{-k_Z t}) \qquad \text{for t = 20 to 480 seconds} \tag{73}$$

where $k_Z = 0.0111 \text{ sec}^{-1}$

and Z_o is a yield dependent multiplier. For values of Z_o see Figure 5, pp.45 and 54, in a previous report (28).

Equation (73) is a good approximation from about 20 seconds to 8 minutes after detonation.

The rate of rise of the air layer from which particles of size parameter α fall is:

$$\frac{dZ}{dt} = Z_o k_Z e^{-k_Z t} \tag{74}$$

$$= k_Z (Z_o - Z)$$

or

$$v_Z = \frac{dZ}{dt} \quad k_Z(Z_o - Z) \tag{75}$$

The particle size parameter, α, is defined as follows:

$$\alpha = \frac{V_w}{V_f} \tag{76}$$

where V_w = wind speed.

The parameter α is obtained from equations (71) or (72) and (74). The results are:

$$\alpha = \frac{V_w (p + qZ)}{k_Z (Z_o - Z)} \tag{77}$$

where p and q are the constants of equation (71) or (72).

In the functions for the simplified fallout scaling system, the standard conditions adopted are that:

$5000 < z < 50{,}000$ ft., hence use equation (71), and

V_w = 15 mph of 22 fps.

For these conditions,

$V_w\, p/k_Z = 1900$ ft. and $V_w\, q/k_Z = 0.020$.

Hence, equation (77) becomes:

$$\alpha = \frac{1900 + 0.020Z}{Z_o - Z} \tag{78}$$

When Z_o and Z are greater than 50,000 ft., these parameters are 1160 ft. and 0.035, respectively; where appropriate, they are substituted for the standard values in making computations.

From equations (78) and (73):

$$Z = \frac{Z_o\alpha - 1900}{\alpha + 0.020} = Z_o(1 - e^{-k_Z t}) \tag{79}$$

Solving for t gives us t_{rise}, the time it takes the particles of size parameter α to reach the height Z:

$$t_{rise} = \frac{1}{k_Z} \ln \left[\frac{\alpha + 0.020}{\frac{1900}{Z_o} + 0.020} \right] \tag{80}$$

This equation has been derived on the basis of the empirical fact that the second period of condensation, see equation (58), ends for almost all fallout particles while the fireball is still in the stem stage.

Within the accuracy of the available experimental data, the last 180 seconds of t_{rise} are spent on toroidal circulation in the cloud. Therefore, the time of the end of the second period of condensation $t_2(\alpha)$ is given by:

$$t_2(\alpha) = t_{rise} - 180 \tag{81}$$

Particles of a given size are usually assumed to be uniformly distributed throughout the cloud. For the purpose of some approximate calculations, however, all particles of a given size parameter may be assumed to start falling from the same altitude. In general, particles with the same size parameter will land at different downwind distances, because (a) they fall through different heights and (b) they start falling at different downwind distances. The average size parameter, α_o, for particles falling at a given downwind distance X is given by:

$$\alpha_o = \frac{X}{h} \tag{82}$$

where h is the fireball height limit.

2. <u>General Features of Fallout Patterns from Land Surface Bursts</u>

From relatively meager observed data, some important characteristics of the fallout pattern for a land surface burst are:

1. A very steep intensity gradient in the upwind and crosswind directions near ground zero exists

2. High intensities near ground zero appear as an intensity ridge along the downwind direction
3. The length of the high intensity ridge appears to be proportional to the lower stem width
4. The peak intensity of the ridge increases with yield in the 1 to 10 KT range and decreases in the 100 KT to 10 MT yield range.
5. The best empirical relationship for the variation of the intensity with upwind and crosswind distance from ground zero is $I = I_o e^{-kx}$, where I_o is the ridge peak intensity, x is the upwind and/or crosswind distance and k is a constant for a given yield.
6. Intensity contours downwind from ground zero appear to be parallel to the intensity ridge for its entire length.
7. Beyond the length of the ridge, the intensity contours directly downwind decrease with distance from ground zero.
8. There is another peak further downwind from ground zero.
9. The distance between these two peaks increases with yield.
10. The intensity of this second peak also increases with yield.
11. The maximum contour pattern width occurs further downwind than the peak intensity.
12. The full intensity from this peak also drops off as $I = I_o e^{-mx}$, where m is a yield dependent parameter.

3. Deposition of Activity on the Ground

The method outlined herein for estimating standard intensities and other radiological quantities is based on (a) corrected experimental data, (b) the geometry of the stem and cloud as sources of the fallout and (c) observed fallout intensity patterns. The mathematical derivations of the simplified fallout scaling system attempt to depict the fall of particles of different size-groups from a volume source in air; the boundaries of that source are assumed to depend only on weapon yield. The problem is to describe mathematically the dependence of the fallout pattern

features, in space and time, on (a) the cloud and stem geometry, (b) the particle fall velocities, (c) the wind velocity, (d) the radioactivity-particle size distributions, and (e) the weapon yield. The cloud is taken to be an oblate spheroid and the stem as an inverted exponential horn. The fall of particles from each of these source volumes is considered separately as may be seen from Figure 18 above.

a. Particles Falling from Cloud Altitudes

The equations for describing fallout from cloud altitudes are based on the following assumptions:

1. From about H + 6 minutes to H + 8 minutes the cloud has the shape of an oblate spheroid, with the major semi-axis a (parallel to the earth's surface) and the minor semi-axis b (perpendicular to the earth's surface).

2. Particles of a given size-parameter, α, fall with a constant terminal velocity, V_f, from their position in the cloud to the ground.

3. The wind velocity, V_w, is constant with time and space through all altitudes from the ground to the top of the cloud.

4. The initial distribution of the particles of each size-parameter is uniform throughout the cloud.

5. The fractional distribution of the total activity on each particle size group is a function of α (and can be determined from fallout pattern data as a function of that group's fall velocity parameter).

A detailed analysis based on these assumptions, is presented by Miller (2). The result is as follows:

Let A_α = the activity per unit volume of cloud carried by particles of size parameter α (concentration in fissions per cu.ft.)

y = crosswind distance from axis of the cloud

h = altitude at the center of the cloud

X = downwind distance from ground zero

Then

$A_x(\alpha)$, the activity per unit area on the ground from particles of size para-

meter, α, at downwind location (X,y) is given by:

$$A_x(\alpha) = \frac{2A_\alpha\, ab \sqrt{(a^2 + \alpha^2 b^2)(1 - y^2/a^2) - (X - \alpha h)^2}}{(a^2 + \alpha^2 b^2)} \tag{83}$$

Therefore, the isoactivity contours on the ground surface for a given value of α are ellipses with centers at $(\alpha h, 0)$.

The total activity per unit area deposited at (X,y)* is found by integrating equation (83) from α_{min} to α_{max}:

$$A_x = \int_{\alpha_{min}}^{\alpha_{max}} A_x(\alpha)\, d\alpha \tag{84}$$

where α_{max} and α_{min} are given by the two respective values of

$$\alpha_m = \frac{hX \pm \sqrt{X^2 b^2(1 - y^2/a^2) + (a^2 - y^2)\left[h^2 - b^2(1 - y^2/a^2)\right]}}{h^2 - b^2(1 - y^2/a^2)} \tag{85}$$

Equation (84) can be integrated numerically or graphically if the values of A_α and the other parameters are provided. From the data of Pugh and Galiano (29) and Schuert (30), the following empirical scaling functions were derived by Miller (2) for the yield-dependent parameters of the above equations:

$a = 2.34 \times 10^3\, W^{0.431}$ ft. W = 1 KT to 10^5 KT (86)

$b = 1.40 \times 10^3\, W^{0.300}$ ft. W = 1 KT to 10^5 KT (87)

$h = 0.66 \times 10^4\, W^{0.445}$ ft. W = 1 KT to 28 KT (88)

$h = 1.68 \times 10^4\, W^{0.164}$ ft. W = 28 KT to 10^5 KT (89)

An approximation method for estimating A_α can be derived from information on the final fallout pattern itself. From equations (86) and (87), the cloud volume for the ellipsoid of revolution about the minor axis can be obtained. Therefore, the cloud volume, V_c is:

$$V_c = 3.21 \times 10^{10}\, W^{1.162} \text{ cu.ft.} \qquad W = 1 \text{ KT to } 10^5 \text{ KT} \tag{90}$$

---

* y is taken as the same lateral dimension on the ground as it is in the cloud because the model assumes that the particles do not move crosswind.

If the fraction of the total activity that is on particles of size parameter α is f_α, and these particles are uniformly distributed throughout the volume, V_c, with the total activity A_c, then A_α is given by:

$$A_\alpha = \frac{f_\alpha A_c}{V_c} \tag{91}$$

where

$$A_c = 1.4 \times 10^{23}\, g_c \text{ BW fissions} \tag{92}$$

B = ratio of fission to total yield

g_c = fraction of the total activity produced that is contained in the cloud.

W = total yield in KT

Hence,

$$A_\alpha = 4.36 \times 10^{12}\, f_\alpha g_c\, BW^{0.162} \qquad W = 1 \text{ KT to } 10^5 \text{ KT} \tag{93}$$

where f_α and g_c are as yet unspecified functions of W.

From consideration of possible functional forms for A_α and $A_x(\alpha)$ and $\alpha_{max} - \alpha_{min}$ the following points are to be noted:

(a) the difference, $\alpha_{max} - \alpha_{min}$, generally is not large

(b) the maximum value of $A_x(\alpha)$ generally occurs near $\alpha = X/h = \alpha_o$

As a first approximation assume $A_x(\alpha)$ equals $A_x(\alpha_o)$ from α_{min} to α_{max}.

Hence: $A_x = A_x(\alpha_o)\,(\alpha_{max} - \alpha_{min})$ (94)

Substituting $\alpha = X/h$ in equations (83) and (85) above:

$$A_x(\alpha_o) = \frac{2\,abh\,A_\alpha}{\sqrt{a^2h^2 + b^2X^2}} \tag{95}$$

and

$$\alpha_{max} - \alpha_{min} \quad \frac{2\sqrt{b^2X^2 + a^2(h^2 - b^2)}}{(h^2 - b^2)} \tag{96}$$

Substituting in equation (94) and solving for A_α:

$$A_\alpha \simeq \frac{(h^2 - b^2)\,A_x}{4\,abh\sqrt{1 - \dfrac{1}{h^2/b^2 + X^2/a^2}}} \tag{97}$$

For all values of the constants, and for reasonable values of X, the radical has values between 0.95 and 1.00. Therefore, the value of A_α is within five percent:

$$A_\alpha \simeq \frac{(h^2 - b^2)\, A_x}{4\, abh} \tag{98}$$

b. Particles Falling from Stem Altitudes

The source volume for particles falling from the stem is the frustum of an inverted exponential horn, i.e. circular in the plane parallel to the ground but with radius increasing exponentially with altitude. The bottom radius equals that of the fireball when it leaves the ground, R_s. The stem radius at the height, h, is that of the cloud at full expansion, a. The volume and shape of the cloud as it rises are specified by the major radius, a, and the cloud half-thickness, b. Particles of a given value of α are assumed to fall from the same horizontal plane. The particles rise to the altitude at which their fall velocity (under gravity) equals the rate of rise of the air mass surrounding the particles. This altitude is assumed to be located in the region near or below the bottom of the rising cloud. Hence, particle groups with a given value of α fall only from the same altitude. Particles having the same value of α fall only from the same altitude. Particles having the same value of α fall in the downwind direction along the length of a high-intensity ridge near ground zero. The diameter of the stem at the altitude from which these particles fall therefore equals the length of this ridge.

In this stem-model approximation for the rising cloud, the shape of this exponential horn is derived from the empirical data, assuming only the exponential form. The volume of the stem, V_Z, is:

$$V_Z = V_o e^{k_v Z} \tag{99}$$

Since the stem volume must have the same shape as the cloud volume at full expansion, namely an elliptical spheroid of revolution about the z axis, the major semi-axis of the stem volume may be written as:

$$a_Z = a_o e^{k_a Z} \tag{100}$$

and its minor semi-axis as:

$$b_Z = b_o e^{k_b Z} \tag{101}$$

where all the constants are empirical, and

$$V_o = \frac{4}{3} \pi a_o^2 b_o \tag{102}$$

$$V = \pi a^2 b \tag{103}$$

$$k_v = 2 k_a k_b \tag{104}$$

The values of the constants a_o, b_o, k_a and k_b are determined from the following boundary conditions:

when $Z = h$, $a_Z = a$ and $b_Z = b$, and (105)

when $Z = R_s$, $a_Z = R_s$ and $b_Z = R_s$. (106)

The resulting expressions for the constants are:

$$k_a = \frac{1}{h - R_s} \ln \left(\frac{a}{R_s}\right) \tag{107}$$

$$k_b = \frac{1}{h - R_s} \ln \left(\frac{b}{R_s}\right) \tag{108}$$

$$\ln a_o = \ln a - \frac{h}{h - R_s} \ln \left(\frac{a}{R_s}\right) \tag{109}$$

$$\ln b_o = \ln b - \frac{h}{h - R_s} \ln \left(\frac{b}{R_s}\right) \tag{110}$$

It is next necessary to determine α_{min} and α_{max}, the minimum and maximum values of the particle size parameters of particles falling at a given downwind location X. These two values of α are for particles falling from the downwind and upwind edges of the stem, respectively. Then by integrating the activity over α from α_{min} to α_{max} the total activity at X may be found. The simplest case is along the y = 0 plane; the solution may be generalized to any value of y by replacing a_Z by $\sqrt{a_Z^2 - y^2}$

To determine α_{min} and α_{max}, three equations are required to eliminate a_Z and Z from the stem model equations with equation constants and yield-dependent parameters. Two of these equations are:

$$a_Z = \pm\ a_o e^{k_a Z} \qquad \text{where + sign is for } \alpha_{min} \text{ and - sign is for } \alpha_{max} \tag{111}$$

$$a_Z = X - \alpha Z \tag{112}$$

The third required equation must yield the α value of the particle group falling from a given altitude. From Anderson's particle falling-rate data for spherical particles (31), the following relation between V_Z and V_f was determined:

$$\frac{V_Z}{V_f} = p + q\,Z \tag{113}$$

where p and q are empirical constants.

Still another empirical equation used (from particle arrival times) is:

$$Z = Z_o\,(1-e^{-k_Z t}) \tag{73}$$

Hence

$$\alpha = \frac{V_w}{V_f} = \frac{V_w\,(p + q\,Z)}{k_Z\,(Z_o - Z)} \tag{77}$$

For the case discussed previously:

$$\alpha = \frac{1900 + 0.020Z}{Z_o - Z} \tag{78}$$

Using (78), (111) and (112) we find for α_{min} and α_{max}:

$$\frac{k_a(Z_o\alpha_m - 1900)}{\alpha_m + 0.020} = \ln\left\{\pm\left[X - \frac{\alpha_m(Z_o\alpha_m - 1900)}{\alpha_m + 0.020}\right]\right\} - \ln a_o \tag{114}$$

where $\alpha_m = \alpha_{min}$ takes the + sign, and $\alpha_m = \alpha_{max}$ takes the - sign.

Because equation (114) is not solved explicitly for α_{min} and α_{max} in terms of the equation constants and X, it is simpler to obtain α_{min} and α_{max} by graphically computing a_Z and α at selected values of Z, calculating X from Eq. (112), and then plotting the two values of α as a function of X.

Let A'_α = the number of fissions per unit cross-sectional area of the stem at an altitude Z corresponding to particle size parameter α. Then the total activity, $A_Z(\alpha)$, carried by each particle group is:

$$A_Z(\alpha) = \pi A'_\alpha \; a_Z^2 \tag{115}$$

The total activity per unit area, accumulated on the ground at the downwind distance X, is given by the sum of A_x from α_{min} to α_{max}, or:

$$A_x = \int_{\alpha_{min}}^{\alpha_{max}} A_x(\alpha) \; d\alpha \tag{116}$$

The procedure for estimating A_α for stem fallout is the same as that for estimating A_α for cloud fallout. The first approximation is obtained by calculating an average value of $A_x(\alpha)$, for the value of α at each of a series of selected values of X along the center of the pattern (y = 0), by use of:

$$A_x(\alpha) \simeq \frac{A_x}{\alpha_{max} - \alpha_{min}} \tag{117}$$

where for a first approximation $A_x(\alpha)$ equals $A_Z(\alpha)$ for $\frac{X}{Z} = \alpha$

4. Estimation of Ionization Rate from Activity Values

To estimate the air ionization rate from the gross activity, or number of radioactive atoms per unit area at H + 1 hour, $A_x(1)$, both a conversion from fissions per unit area to r/hr and a decay curve for the gross radioactive mixture are needed. The relationship between A_x and the standard (H + 1 hr.) intensity, $I_x(1)$, or the conversion factor from fissions/sq.ft. to r/hr is defined by:

$$I_x(1) = K_x(1) \; A_x \tag{118}$$

where A_x is in fissions per unit area, $I_x(1)$ in r/hr, and

$$K_x(1) = D_x(1) \; q_x \left[r_\alpha(1) \; i_{fp}(1) + i_i(1) \right] \tag{119}$$

where: $i_{fp}(1)$ = the air ionization rate per fission/sq.ft. at 3 ft. above an infinite plane for a uniform distribution of the normal fission product mixture

$i_i(1)$ = the same unit for neutron-induced activity

$r_\alpha(1)$ = the gross fission product fractionation number (defined subsequently)

q_x = the terrain shielding factor

$D_x(1)$ = an instrument response factor at H + 1 hour

t = the time after fission

The true air ionization rate, $I_x^o(1)$, is obtained when D is set equal to one.

Since most fallout data have been corrected to a standard reference time of H + 1 hour and reported in values as of this time (even though the fallout has not yet arrived at 1 hour), it is necessary to convert from the standard reference time to a time of interest by means of a decay correction factor, d(t,1) defined by:

$$I_x(t) = d(t,1)\ I_x(1) \tag{120}$$

where $I_x(t)$ is the air ionization rate at time, t.

Note that $I_x(t)$ will be the <u>actual</u> ionization rate at downwind distance X only at times after all the fallout has arrived at X.

Or:

$$I_x(t) = K_x(1)\ d(t,1)\ A_x \tag{121}$$

The decay correction factor, d(t,1) is the familiar $t^{-1.2}$ decay law factor for gross fission products. The relationship of $K_x(1)\ d(t,1)$ with time is plotted in Figure 19.

It is important to note that if the information of interest is the activity of a particular isotope rather than that of gross fission products, the use of the $t^{-1.2}$ decay law for gross fission products instead of the actual decay for the isotope of interest may introduce a serious error in the results. The magnitude of the error introduced by assuming the generalized decay law for gross fission products was not investigated.

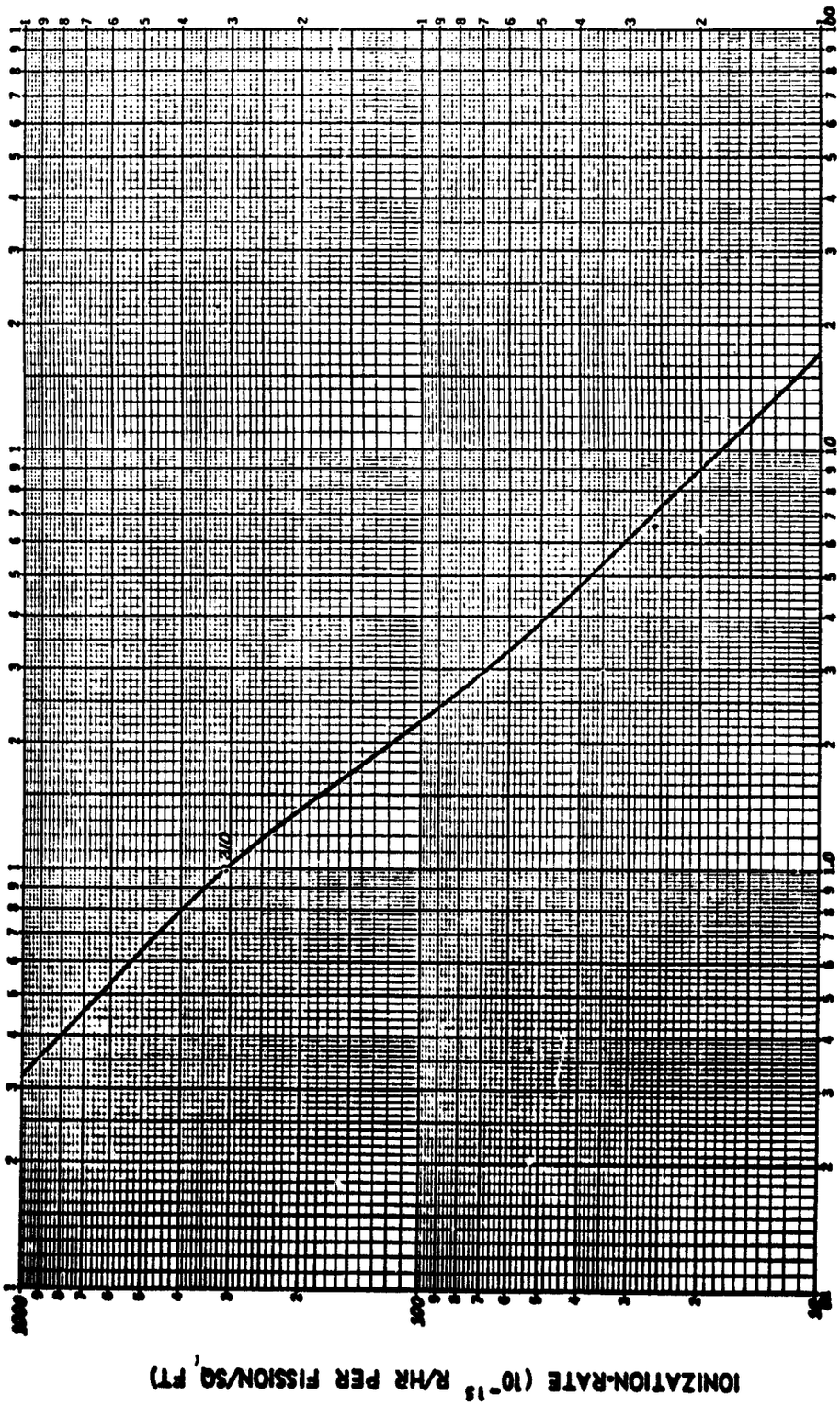

Figure 19. Ionization Rate from Gross Fission Products

The value of $i_{fp}(1)$ for U-238 fissions is 6.94×10^{-13} r/hr per fission/sq.ft. and the value for the indicated induced activity is $i_i(1) = 0.13 \times 10^{-13}$ r/hr per fission/sq.ft., when $i_i(1)/i_{fp}(1)$ is taken to be 0.019.

Then equation (119) becomes:

$$K_x(1) = 3.90 \times 10^{-13} \left[r_\alpha(1) + 0.019 \right] \frac{\text{r/hr}}{\text{fission/sq.ft.}} \tag{122}$$

5. Characteristic Points and Their Location

a. Fallout from Stem

The intensity ridge near ground zero results from stem fallout. The following points are defined for use in the derivation of isointensity contours:

X_1 = location of upwind 1 r/hr contour at 1 hr. intensity, derived directly from observed data

X_2 = distance to the upwind shoulder of the high intensity ridge

X_3 = distance to the downwind shoulder of the high intensity ridge

The length of the intensity ridge, $X_3 - X_2$, is assumed to be equal to the diameter of the stem, $2a_s$, for particles falling from an altitude Z_s. The particles that fall from the center of the stem must land near $(X_2 + X_3)/2$. Therefore the particle size parameter for these particles is:

$$\alpha_{2,3} = \frac{X_2 + X_3}{2 Z_s} \tag{123}$$

where Z_s is given by:

$$Z_s = \frac{1}{k_a} \ln \left[\frac{a_s}{a_o} \right] \tag{124}$$

Then

$$X_2 = \alpha_{2,3} Z_s - a_s \tag{125}$$

and

$$X_3 = \alpha_{2,3} Z_s + a_s \tag{126}$$

$\alpha_{2,3}$ is also used to determine the parameter, Z_o, that defines the rate-of-rise functions; which for 22 ft/sec wind speed, 5,000 to 50,000 ft. altitudes, and rise times of 20 to 500 sec, is given by:

$$Z_o = \frac{1900 + (\alpha_{2,3} + 0.020)\, Z_s}{\alpha_{2,3}} \tag{127}$$

The particle-size group designator, α_4, is for particles falling from the center of the stem. They land at X_4. X_4 is estimated from:

$$X_4 = \frac{\alpha_4(\alpha_4 Z_o - 1900)}{\alpha_4 + 0.020} \tag{128}$$

The half width of the stem fallout pattern, Y_s, is the lateral distance from the center-line of the stem-pattern, y = 0, to the 1 r/hr at 1 hr. contour.

Because of the geometry used for the stem, the ratio Y_s/a is assumed to vary uniformly with yield according to a function of the form:

$$\frac{Y_s}{a} = \text{const. } W^n \tag{129}$$

where the two constants are evaluated empirically.

b. Fallout From Cloud

The basic assumption is that the downwind locations are approximately proportional to the height from which the particles fall. The change from direct proportionality is described as a change in the average particle size parameter landing at a given location by the parameter α_o where

$$\alpha_o = \alpha_o^o W^n \tag{130}$$

where α_o^o and n are yield-independent parameters.

X_5 and X_9 are the upwind and downwind positions of the 1r/hr contour (along the y = 0 axis).

X_7 is the downwind distance to the peak intensity.

X_8 is the downwind distance to the point of maximum half-width, Y_8, of the cloud fallout pattern.

X_6 is an intermediate point between X_5 and X_7.

Y_8 is the maximum half-width to the 1r/hr contour.

In the central area of fallout from the cloud, the above assumptions result in a distance-scaling function given by:

$$X = 6.60 \times 10^3 \, W^{0.445} \, \alpha_o \qquad W = 1 \text{ to } 28 \text{ KT} \qquad (131)$$

or

$$X = 1.68 \times 10^4 \, W^{0.164} \, \alpha_o \qquad W = 28 \text{ KT to } 10^5 \text{ KT} \qquad (132)$$

The distances designated X_6, X_7, X_8, and X_9 are scaled by use of these functions.

For X_5 it is better to use α_{max} than α_o; the distance-scaling function for this location is:

$$X_5 = 6.60 \times 10^3 \, W^{0.445} \alpha_5 - 1.40 \times 10^3 \, W^{0.300} \sqrt{3.06 W^{0.262} + \alpha_5^2} \qquad (133)$$

with W = 1 to 28 KT

or

$$X_5 = 1.68 \times 10^4 \, W^{0.164} \alpha_5 - 1.40 \times 10^3 \, W^{0.300} \sqrt{3.06 W^{0.262} + \alpha_5^2} \qquad (134)$$

with W = 28 to 10^5 KT

where the scaling function for α_5 is assumed to be of the form $\alpha_5^o W^n$.

The maximum pattern half-width, Y_8, is at downwind location X_8 and the scaling function has been obtained from empirical data.

6. Intensity Levels at Characteristic Points of Fallout Pattern

a. Stem

The intensities I_1 and I_4 are set at 1 r/hr. In accordance with statement 5 on page 102, the peak intensity along the high intensity ridge near ground zero, $I_{2,3}$ is given by (exponential drop off in upwind direction):

$$I_{2,3} = \exp k_{1,2} (X_2 - X_1) \qquad (135)$$

where $k_{1,2}$ is a function of yield, evaluated from experimental data.

b. Cloud

Functions for estimating the variation of the standard ionization rate, or the radiation intensity, at the selected downwind locations are derived from the assumption that an average of A_α can be assigned to the particles centering at α_o. The average value of $A_x(\alpha)$ is then:

$$\overline{A_x(\alpha)} = \frac{2\,\bar{A}_\alpha\, ab}{\sqrt{a^2 + \alpha^2 b^2}} \tag{136}$$

The integral of eq. (138) is then:

$$A_x = \int_{\alpha_{min}}^{\alpha_{max}} \overline{A_x(\alpha)}\, d\alpha \tag{137}$$

$$= 2\,\bar{A}_\alpha\, a \ln \frac{\alpha_{max} + \sqrt{a^2/b^2 + \alpha^2_{max}}}{\alpha_{min} + \sqrt{a^2/b^2 + \alpha^2_{min}}}$$

where A_x is the total activity per unit area at downwind location (X,y).

In the logarithmic term, α_{max} and α_{min} are approximated as follows:

$$\alpha_{max} \simeq \frac{X + a}{h} \simeq \alpha_o + \frac{a}{h} \tag{138}$$

and

$$\alpha_{min} \simeq \frac{X - a}{h} \simeq \alpha_o - \frac{a}{h} \tag{139}$$

Since the lower limit of α from the stem model is $\alpha_{2,3}$, and the lower limits of α for the cloud model are not specified without complete evaluation of A_α, the value of α_{min} for locations at which $\alpha_o \leq ah$ is taken to be:

$$\alpha_{min} = \alpha_{2,3} \tag{140}$$

Although the scaling functions for the different characteristic standard intensities at locations underneath the cloud where $\alpha_o \leq ah$ ($X \leq a$) are evaluated in Eq. (123) by using $\alpha_{2,3}$ for α_{min}, better first estimates of A_α as a function of α are obtained when the quantity $X_i/(h-b)$ is substituted for α_{min}, provided X_i is less than X_7. The true values of α_{min} for different weapon yields have not yet been determined (2).

With the above limits on α_o, the scaling equations for the intensity levels at the selected locations become:

$$I_i = K_i(1)\ \bar{A}_\alpha\ a\ 4.606 \log \phi_i \qquad \alpha_i \geq a/h \tag{141}$$

and

$$I_i = K_i' (1) \overline{A_\alpha} \; a \; 4.606 \log \phi_i' \qquad \alpha_i \leq a/h \qquad (142)$$

where

$$\phi_i = \frac{(\alpha_i + a/h) + \sqrt{a^2/b^2 + (\alpha_i + a/h)^2}}{(\alpha_i + a/h) + \sqrt{a^2/b^2 + (\alpha_i + a/h)^2}} \qquad \alpha_i \geq a/h \qquad (143)$$

and

$$\phi_i = \frac{(\alpha_i + a/h) + a^2/b^2 + (\alpha_i + a/h)^2}{\alpha_{2,3} + \sqrt{a^2/b^2 + \alpha_{2,3}^2}} \qquad \alpha_i \leq a/h \qquad (144)$$

and

where α_i is the value α_o at the distance X_i.

For the value of X_5, however, α_5' is the same as α_{max}.

At X_9, ϕ_9 reduces to

$$\phi_9 = \frac{\alpha_9 + a/h}{\alpha_9 - a/h} \qquad (145)$$

The parameters $K_i (1) \overline{A}_\alpha$ and $K_i' (1) \overline{A}_\alpha$ are assumed to be functions of the yield only and of the form: const. W^n. The effect of wind speed on I_i is through the dependence of log ϕ_i on α_i by:

$$\alpha_i (V_w) = (V_w/15) \alpha_i(15) \qquad (146)$$

where V_w is in mph. The scaling functions of α_i with weapon yield were evaluated from data for a presumed effective wind speed of 15 mph.

7. Construction of Ionization Isointensity Contours

The characteristic intensity level points 1 through 9, listed in the previous section are used to construct the isointensity contours by the following procedure:

1. On semilog paper plot the intensity vs. downwind distance for the nine characteristic points (except point 8)

2. Connect points 1, 2, 3 and 4 by straight line segments; points 5, 6, 7 and 9 are similarly connected. This is the intensity profile of the fallout pattern along the y = 0 axis; it is plotted in Figure 20 for a weapon yield of 20 MT.

3. Connect the points (I_7, X_7) and $(1, X_8)$ by a straight line. This will be used in determining the lateral dimensions of the contours for cloud fallout.

4. Connect the points $(I_{2,3}, 0)$ to $(1, Y_s)$ by a straight line on semilog paper. This will be used to obtain the lateral dimensions of the contours for stem fallout.

5. It is next necessary to pick a set of values for the intensity levels on the contours to be plotted. Such a set might be the values 1, 10, 10^2, 10^3, 10^4 r/hr. Call any value of this set I_i'. Since the contours are closed curves, they will cross the x-axis at two points. For I_i' call the upwind point X_i' and the downwind point X_i''.

6. The procedure now consists of two parts, one for stem fallout and one for cloud fallout:

6a. For stem fallout:

(1) the upwind and downwind distances, X_i' and X_i'', to the selected intensities I_i' along the y = 0 axis are read off Figure 20. X_i' is found along the straight line segment joining points 1 and 2; X_i'', along the line joining points 3 and 4. (2) the lateral dimension of the I_i' intensity contour for the stem, Y_{si}', is read off the plot in Step 4 above. (3) the upwind portion of the contour for I_i' consists of an incomplete circle centered at X_2 with radius = $X_2 - X_i'$. (4) the downwind portion of the contour for I_i' for stem fallout is half an ellipse of semimajor axis =

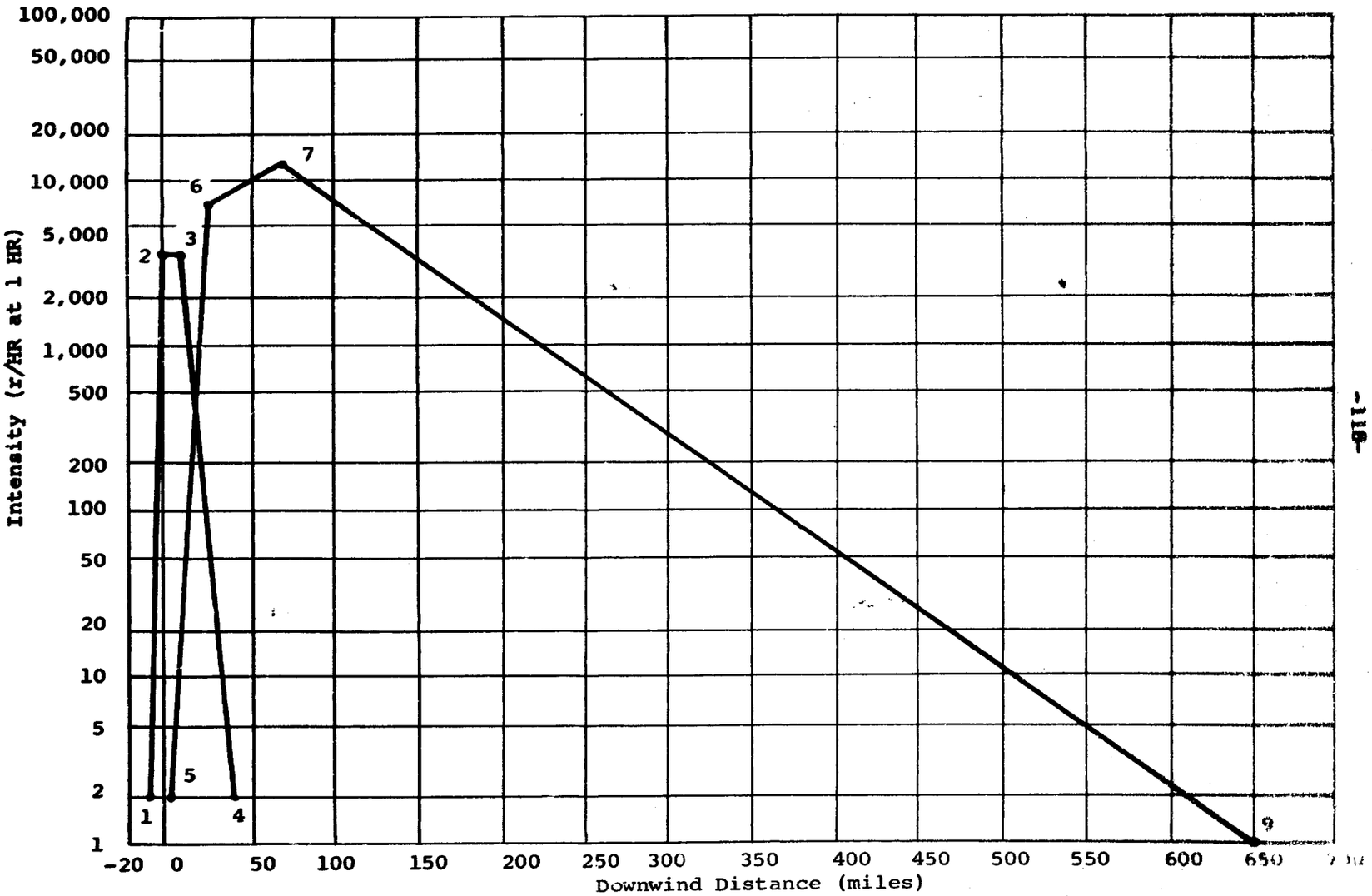

Figure 20. Intensity Profile for 20 MT Weapon

$X_i' - X_2$ and semi-minor axis = Y_{si}'. (5) the upwind incomplete circle is faired in smoothly to the downwind half-ellipse as indicated in the following sketch:

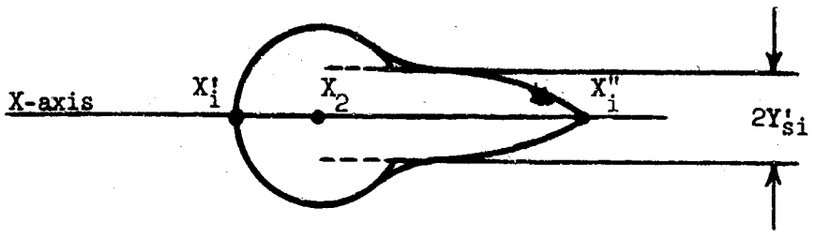

6b. For cloud fallout:

(1) the upwind and downwind distances, X_i' and X_i'', to the selected intensities along the y = 0 axis are read off Figure 7. X_i' is found on the portion of the plot between points 5 and 7: X_i'', on the portion of the plot between points 7 and 9. (2) the lateral dimension of the I_i' intensity contour for the cloud, Y_{8i}', is obtained from:

$$\frac{Y_{8i}'}{X_{8i}'} = \frac{Y_8}{X_8 - X_7}$$

where X_{8i}' is read off the straight line plotted in Step 3 above for the value I_i'. (3) the upwind portion of the I_i' contour is a half ellipse of semi-minor axis = Y_{8i}' and semi-major axis = $\left[X_{8i}' - X_i'\right]$. (4) the downwind portion of the I_i' contour is a half ellipse of semi-minor axis = Y_{8i}' and semi-major axis - $\left[X_i'' - X_{8i}'\right]$. (5) the two half ellipses are joined smoothly at X_{8i}'.

7. Where the contours for stem fallout overlap those for cloud fallout, they are joined together smoothly as was done in Figure 16 which shows a typical set of contours for a 20 MT weapon and a wind speed of 15 mph, and Figure 21 which shows a set of contours for a 1 MT weapon and a wind speed of 15 mph.

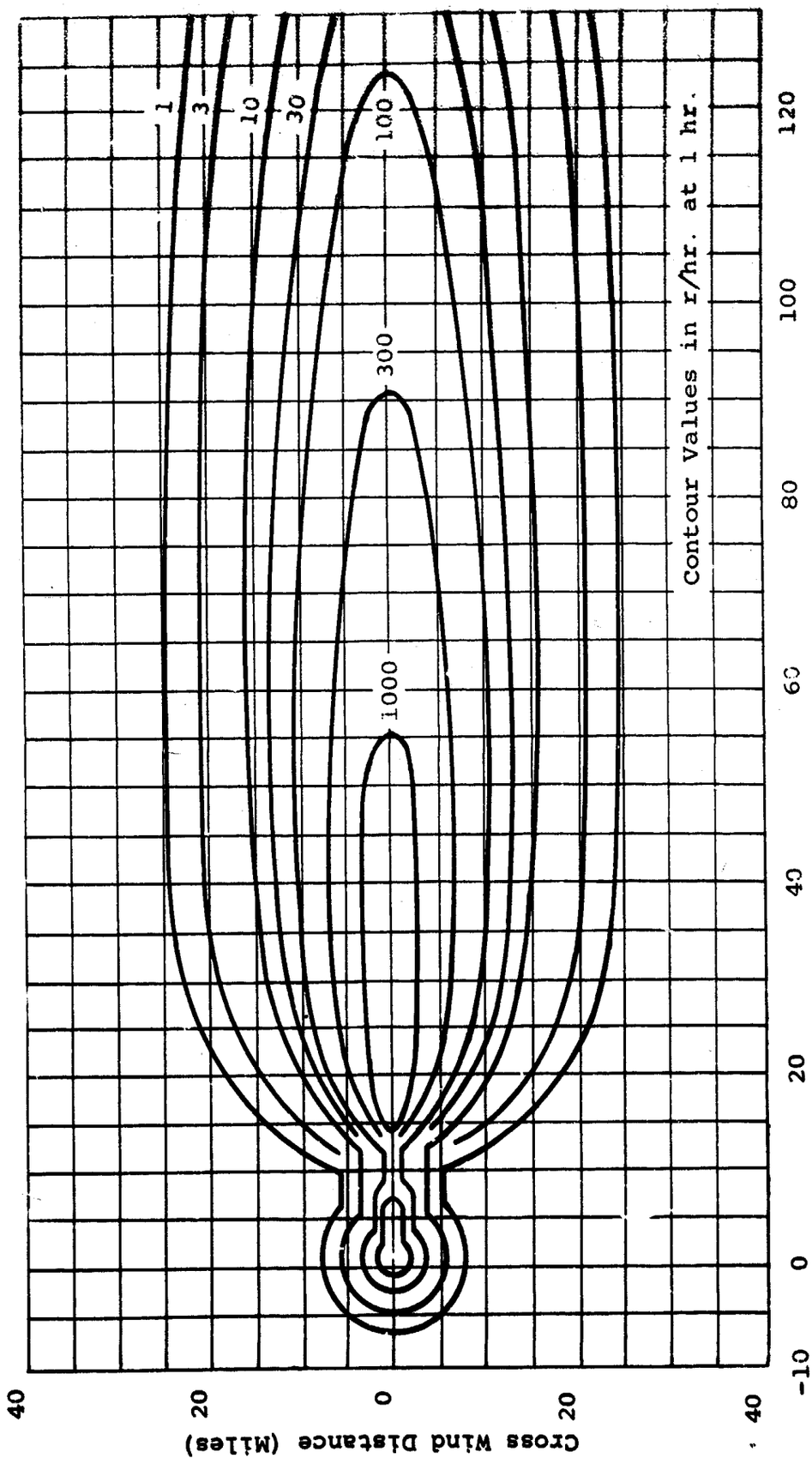

Figure 21. Selected Isointensity Contours for a 1 MT Weapon Yield Wind Speed of 15 mph

8. Summary of Derived Scaling Functions

The scaling functions for the values are:

$$\log \alpha_{2,3} = -0.509 + 0.076 \log W, \qquad W = 1 \text{ to } 10^5 \text{ KT}$$
$$\log \alpha_4 = 0.270 + 0.089 \log W, \qquad W = 1 \text{ to } 10^5 \text{ KT}$$
$$\log \alpha_5 = -0.176 + 0.022 \log W, \qquad W = 1 \text{ to } 10^5 \text{ KT}$$
$$\log \alpha_5' = -0.054 + 0.095 \log W, \qquad W = 1 \text{ to } 10^5 \text{ KT}$$
$$\log \alpha_6 = 0.030 + 0.036 \log W, \qquad W = 1 \text{ to } 10^5 \text{ KT}$$
$$\log \alpha_7 = 0.043 + 0.141 \log W, \qquad W = 1 \text{ to } 10^5 \text{ KT}$$
$$\log \alpha_8 = 0.185 + 0.151 \log W, \qquad W = 1 \text{ to } 10^5 \text{ KT}$$
$$\log \alpha_9 = 1.371 - 0.124 \log W, \qquad W = 1 \text{ to } 28 \text{ KT}$$
$$\log \alpha_9 = 0.980 + 0.146 \log W, \qquad W = 28 \text{ to } 10^5 \text{ KT}$$

The scaling functions for the distances are:

$$\log(-X_1) = 3.308 + 0.496 \log W, \qquad W = 1 \text{ to } 28 \text{ KT}$$
$$= 3.564 + 0.319 \log W, \qquad W = 28 \text{ to } 10^5 \text{ KT}$$
$$X_2 = \alpha_{2,3} Z_s - a_s$$
$$X_3 = \alpha_{2,3} Z_s + a_s$$
$$X_4 = \frac{\alpha_4(\alpha_4 Z_o - 1900)}{\alpha_4 + 0.020}$$

where

$$\log a_s = 2.880 + 0.348 \log W, \qquad W = 1 \text{ to } 10^5 \text{ KT}$$
$$Z_s = \frac{2.303 (\log a_s - \log a_o)}{k_a}$$
$$\log a_o = \log a - (h \log a/R_s)/(h - R_s)$$
$$\log a = 3.389 + 0.431 \log W, \qquad W = 1 \text{ to } 10^5 \text{ KT}$$
$$\log h = 3.820 + 0.445 \log W, \qquad W = 1 \text{ to } 28 \text{ KT}$$
$$\log h = 4.226 + 0.164 \log W, \qquad W = 28 \text{ to } 10^5 \text{ KT}$$
$$\log a/R_s = 1.070 + 0.098 \log W, \qquad W = 1 \text{ to } 10^5 \text{ KT}$$
$$\log R_s = 2.319 + 0.333 \log W, \qquad W = 1 \text{ to } 10^5 \text{ KT}$$
$$k_a = 2.303 \left[(\log a/R_s)/(h - R_s)\right]$$

and

$$Z_o = \frac{1900 + (\alpha_{2,3} + 0.020) z_s}{\alpha_{2,3}}, \qquad W \geq 9 \text{ KT}, \; v_w = 15 \text{ mph}$$

or

$$Z_c = (z - z) \qquad W \geq 9 \text{ KT}$$

For Z or Z_c greater than 50,000 feet, the constants 1900 and 0.020 are 1160 and 0.035, respectively. The parameters a_s, Z_s, and Z_o are assumed to be independent of the wind speed.

$$\log X_5 = 3.644 + 0.467 \log W, \qquad W = 1 \text{ to } 28 \text{ KT}, \ \alpha_5 \geq a/h$$
$$= 4.049 + 0.186 \log W, \qquad W = 28 \text{ to } 10^5 \text{ KT} \ \alpha_5 \geq a/h$$

$$X_5 = 5.83 \times 10^3 W^{0.540} - 1.24 \times 10^3 W^{0.395} \sqrt{1 + 3.93\, W^{0.072}}$$
$$W = 1 \text{ to } 28 \text{ KT}, \ \alpha_5 \geq a/h$$

$$X_5 = 1.48 \times 10^4 W^{0.259} - 1.24 \times 10^3 W^{0.395} \sqrt{1 + 3.93\, W^{0.072}}$$
$$W = 28 \text{ to } 10^5 \text{ KT}, \ \alpha_5 \geq a/h$$

$$\log X_6 = 3.850 + 0.481 \log W, \qquad W = 1 \text{ to } 28 \text{ KT}$$
$$= 4.255 + 0.200 \log W, \qquad W = 28 \text{ to } 10^5 \text{ KT}$$

$$\log X_7 = 3.862 + 0.586 \log W, \qquad W = 1 \text{ to } 28 \text{ KT}$$
$$= 4.268 + 0.305 \log W, \qquad W = 28 \text{ to } 10^5 \text{ KT}$$

$$\log X_8 = 4.005 + 0.596 \log W, \qquad W = 1 \text{ to } 28 \text{ KT}$$
$$= 4.410 + 0.315 \log W, \qquad W = 28 \text{ to } 10^5 \text{ KT}$$

$$\log X_9 = 5.190 + 0.319 \log W, \qquad W = 1 \text{ to } 28 \text{ KT}$$
$$= 5.202 + 0.311 \log W, \qquad W = 28 \text{ to } 10^5 \text{ KT}$$

$$\log Y_s = 3.223 + 0.400 \log W, \qquad W = 1 \text{ to } 10^5 \text{ KT}$$

Values of Y_8 for yields other than those given can be obtained from a plot of the listed values against yield.

TABLE XV

Variation of Y_8 with Weapon Yield

W	1 KT	10 KT	100 KT	1 MT	10 MT	100 MT
Y_8 (ft)	6,620	12,200	48,200	167,000	342,000	650,000

The scaling functions for the high intensity ridge near ground zero, the intensities at the shoulder in the cloud pattern, and the intensities of the downwind pattern features, are:

$$\log I_{2,3} = k_{1,2}(X_2 - X_1) / 2{,}303$$

where

$$\log k_{1,2} = 2.503 - 0.404 \log W, \qquad W = 1 \text{ to } 28 \text{ KT}$$
$$= -2.600 - 0.337 \log W, \qquad W = 28 \text{ to } 10^5 \text{ KT}$$

$$\log I_{2,3} = \log k_{2,3}(1)\, \bar{A}_f + \log \Delta Z_{2,3}$$

and

$$\log I_4 = \log k_4(1)\, \bar{A}_f + \log \Delta Z_4$$

where

$$\log \Delta Z_{2,3} = \log \Delta Z^o_{2,3} + n \log V_w \quad \text{(see Table XVI)}$$

TABLE XVI

Equation Parameter Values For The Variation of $\Delta Z_{2,3}$ With Wind Speed[a] And Derived Values of $K_{2,3}\, \bar{A}_f$

W (KT)	$\Delta Z^o_{2,3}$ (ft)	n	$K_{2,3}(1)\, \bar{A}_f$ (r/hr at 1 hr/ft)	$K_{2,3}(1)\, A_f\, \Delta Z^o_{2,3}$ (r/hr at 1 hr)
100	12,200	-0.78	23.9	292,000
200	12,700	-0.78	15.2	193,000
500	13,400	-0.77	8.39	112,000
1,000	13,800	-0.765	5.60	76,700
3,000	13,900	-0.76	3.94	54,800
5,000	14,000	-0.75	2.60	36,400
10,000	13,800	-0.74	1.92	26,500
20,000	13,100	-0.71	1.39	18,200
50,000	11,100	-0.63	0.923	10,200

[a] Wind speed in mph

and

$$\log \Delta Z_4 = 3.236 + 0.046 \log W - \log V_w, \qquad W = 10^2 \text{ to } 10^4 \text{ KT}$$

also

$$\log K_{2,3}\, \bar{A}_f = 2.088 - 0.452 \log W, \qquad W = 10^3 \text{ to } 10^5 \text{ KT}$$
$$\log K_4\, \bar{A}_f = 2.059 - 0.046 \log W, \qquad W = 10^2 \text{ to } 10^5 \text{ KT}$$

For i = 5 through 9:

$$I_i = 4.606a\, K_i\, \bar{A}_\alpha \log \phi_i, \qquad \alpha_i \geq a/h$$
$$= 4.606a\, K'_i\, \bar{A}_\alpha \log \phi'_i, \qquad \alpha_i < a/h$$

where

$$\log a/h = -0.431 - 0.014 \log W, \qquad W = 1 \text{ to } 28 \text{ KT}$$
$$= -0.837 + 0.267 \log W, \qquad W = 28 \text{ to } 10^5 \text{ KT}$$

$$\phi_i = \frac{(\alpha_i + a/h) + \sqrt{(a/b)^2 + (\alpha_i + a/h)^2}}{(\alpha_i - a/h) + \sqrt{(a/b)^2 + (\alpha_i - a/h)^2}} \qquad \alpha_i \geq a/h$$

and

$$\phi_i' = \frac{(\alpha_i + a/h) + \sqrt{(a/b)^2 + (\alpha_i + a/h)^2}}{\alpha_{2,3}\sqrt{(a/b)^2 + \alpha_{2,3}^2}} \qquad \alpha_i < a/h$$

where

$$\log (a/b)^2 = 0.486 + 0.262 \log W$$
$$\log a = 3.389 + 0.431 \log W$$

and where

$$\log K_5 \bar{A}_\alpha = -3.286 - 0.298 \log W, \qquad W = 1 \text{ to } 28 \text{ KT}, \ \alpha_5 \geq a/h$$
$$= -2.889 - 0.572 \log W, \qquad W = 28 \text{ to } 10^5 \text{ KT} \ \alpha_5 \geq a/h$$
$$\log K_5' \bar{A}_\alpha = -3.185 - 0.406 \log W, \qquad W = 28 \text{ to } 10^5 \text{ KT} \ \alpha_5' < a/h$$
$$\log K_6 \bar{A}_\alpha = -1.134 - 0.074 \log W, \qquad W = 1 \text{ to } 10^5 \text{ KT}, \ \alpha_6 \geq a/h$$
$$\log K_6' \bar{A}_\alpha = -1.225 - 0.022 \log W, \qquad W = 1 \text{ to } 10^5 \text{ KT} \ \alpha_6' < a/h$$
$$\log K_7 \bar{A}_\alpha = -0.989 - 0.037 \log W, \qquad W = 1 \text{ to } 10^5 \text{ KT}, \ \alpha_7 \geq a/h$$
$$\log K_7' \bar{A}_\alpha = -1.079 - 0.020 \log W, \qquad W = 1 \text{ to } 10^5 \text{ KT}, \ \alpha_7' < a/h$$
$$\log K_9 \bar{A}_\alpha = -2.166 - 0.552 \log W, \qquad W = 1 \text{ to } 10^5 \text{ KT}, \ \alpha_9 \geq a/h$$

The values of the fallout pattern features from the above scaling functions are given in Table XVII for several weapon yields.

E. Soluble Nuclide Contour Ratios

In general one may define a contour ratio as the ratio of the value of a particular property of fallout to the value of the standard ionization intensity at that point. The standard intensity was defined as the air ionization intensity (r/hr) corrected to H + 1 hour. Atoms of radionuclides may be divided as soluble or insoluble in water, depending on whether they are condensed outside or inside the carrier particles. The ratio of the soluble, or insoluble, atom concentration of a certain radionuclide to the standard ionization intensity at any point is called the fallout nuclide solubility contour ratio of that particular radionuclide. In the present instance, we are concerned with the number of atoms of particular isotopes that will be soluble in water supply.

TABLE XVII

Summary of Fallout Pattern Features and Fallout Scaling System Parameter Values for an Assumed Effective Wind Speed of 15 MPH[a]

Pattern Feature or Parameter	Weapon Yield					
	1 KT	10 KT	100 KT	1 MT	10 MT	100 MT
X_1	-2,030	-6,370	-15,900	-33,200	-69,200	-144,000
X_2	346	1,790	3,790	4,350	3.360	3,820
X_3	1,860	5,120	11,300	21,200	40,200	79,600
X_4	7,710	32,000	60,200	97,000	162,000	282,000
X_5	4,400	13,600	26,400	37,000	23,200	- 76,100
X_6	7,080	21,400	45,200	71,600	114,000	180,000
X_7	7,280	28,000	75,500	152,000	308,000	621,000
X_8	10,100	39,900	110,000	226,000	468,000	966,000
X_9	155,000	323,000	667,000	1,360,000	2,790,000	5,710,000
Y_s	1,670	4,200	10,500	26,500	66,700	167,000
Y_8	6,620	12,200	48,200	167,000	342,000	650,000
$I_{2,3}$	1,730	22,900	35,300	9,800	3,550	1,440
I_6	130	222	540	1,720	5,260	15,500
I_7	180	317	803	2,712	9,070	30,510
Z_o	5,200	14,900	22,300	28,900	39,000	54,900

[a] Distances are in feet; intensities are in r/hr at 1 hr (observed)

The insoluble fallout nuclide contour ratio, $N_\alpha(1)$, and the soluble fallout nuclide contour ratio, $N'_\alpha(1)$, have been defined as follows:

$$N_\alpha(1) = \frac{N(A)}{I(1)} \tag{147}$$

$$N'_\alpha(1) = \frac{N'(A)}{I(1)} \tag{148}$$

where N(A) = number of atoms per unit area of nuclide J at the end of mass chain A that is in the interior of fallout particles and hence insoluble in water

N'(A) = number of atoms per unit area of the nuclide J at the end of mass chain A that is on the exterior of the fallout particles and hence soluble in water

I(1) = the measured ionization intensity corrected to H + 1 hour (r/hr)

The subscript α indicates that N_α is a function of the particle size parameter. This functional dependence on α is mainly through the fractionation number as discussed previously. Now,

$$I(1) = K_x(1)\ F(1) \tag{149}$$

where F(1) = one half the number of fission products per unit area (fissions/sq ft) assuming 2 fission products per fission - corrected to H + 1 hour;

$K_x(1)$ = is an overall conversion factor relating the ionization intensity (fissions per unit area) to the density of radionuclides (fission products)(r/hr per fission/sq ft)

Further,

$$K_X(1) = D_X(1)\ q_x\ i_{fp}(1)\ \left[r_\alpha(1) + i_i(1)/i_{fp} \right] \tag{150}$$

where

$D_X(1)$ is the instrument response factor at H + 1 hour, usually assigned the value of 0.75.

q_X is the shielding factor for gamma rays, usually assigned the value of 0.75.

$i_{fp}(1)$ is the ionization rate generated by unfractionated fission products at 3 feet above an ideal plane in (r/hr at 1 hr)/(fission/sq ft)

$i_i(1)$ is the ionization rate generated by induced activity at 3 feet above an ideal plane in (r/hr at 1 hr)/(fission/sq ft). It is usually assumed to be 0.02 of $i_{fp}(1)$ as most of the relevant information is classified.

$r_\alpha(1)$ is the gross fractionation number at H + 1 hour (the ratio of the ionization rate of unfractionated fission products to the ionization rate of unfractionated fission products)

Furthermore,

$$N(A) = Y_A^o \, r_o(A, t_1) \, F(1) \tag{151}$$

where

Y_A^o = chain yield of mass A per fission (atoms/fission);

$r_o(A, t_1)$ = fractionation number for first period of condensation

t_1 = the time at end of first period of condensation (sec)

Similarly,

$$N'(A) = Y_A^o \, r_o'(A, t_2) \, F(1) \tag{152}$$

where

$r_o'(A, t_2)$ = fractionation number for the second period of condensation

t_2 = time at the end of the second period of condensation; t_2 is a function of α.

From equations (151), (153) and (154):

$$N_\alpha(1) = Y_A^o \, r_o(A, t_1) \tag{153}$$

$$N_\alpha'(1) = Y_A^o \, r_o'(A, t_2) \tag{154}$$

The values of Y_A^o may be obtained from the data of Bolles and Ballou (18) as was discussed in an earlier section. The expressions for $r_o(A, t_1)$ and $r_o'(A, t_2)$ were also derived previously. It is necessary to further specify $r_\alpha(1)$ and $i_{fp}(1)$.

The activities and abundances of various kinds of fission products have been studied extensively in recent years. Formal and complete tabulation of these properties exist only for U-235 fission product mixtures. They have been presented by

Bolles and Ballou (18). Other scientists have studied and published comparisons of fission yields among U-235, U-238, Pu-239, etc. (32)(33). In the present model, a correlation among the three types of fission products has been established and the relative fission yield shown as Table 2.3 by Miller (2) or Table I by Grune, et al (34). The yield of a mass chain in atoms per fission can therefore be obtained conveniently by taking values proportional to the value of U-235 thermal neutron fission products. Since U-238 with 8-Mev broadband neutron spectrum fission products are more applicable to nuclear detonation, all the calculations in this report are based on this standard. This is the proportionality constant b.

In the study by Miller and Loeb (35), the activity data from Bolles and Ballou have been translated into ionization rates by means of disintegration multipliers, which are the average values of conversion between radioactivity and radiation intensity for each radionuclide. The values of these disintegration multipliers, m, have been presented in Table 3.16 (2) or Table II (34). Therefore, the ideal ionization rate per 10^4 fissions per sq ft of normal fission products may be computed according to the following expression:

$$i_{fp}(t) = \Sigma\, mbA_t \qquad (155)$$

where m is the disintegration multiplier (from Table 3.16 (2) or Table II (34) in (r/hr per disintegration/sec per sq ft)

b is the proportionality constant parameter obtained from Table 2.3 (2) or Table I (34).

and A_t is the activity per 10^4 fissions at time t of the nuclide, computed by Bolles and Ballou from the Glendenin Theory.

The variations of normal fission products from U-235, U-238 and Pu-239 are shown in Table V, p. 21 (36).

The gross fractionation number, $r_\alpha(1)$, is defined as the ratio of the ionization rates at H + 1 hour from fractionated fission products to the intesity from unfractionated fission products (or the ratio of the ionization rates of condensed and normal fission products). It may be expressed as:

$$r_{\alpha}(1) = \frac{i_{fp}^{*}(1)}{i_{fp}(1)} \tag{156}$$

where

$$i_{fp}^{*}(t) = \Sigma\, mbA_t\, r_o(A,t_1,t) + r_o'(A,t_2,t) \tag{157}$$

and

$r_o(A,t_1,t)$ is the fractionation number for the first period of condensation, extrapolated by radioactive decay to the time t.

and

$r_o'(A,t_2,t)$ is the fractionation number for the second period of condensation, extrapolated by radioactive decay to the time t.

F. Summary and Conclusions

Following a thorough analysis of the Miller Fallout Model, a number of important functions derived from it were utilized in this study of water contamination. However, the analytical validity of the results can be no greater than the validity of the Miller Model. As noted earlier in this Chapter the range of accuracy of the model has been estimated by Miller to yield values that agree with the available unclassified data only within a factor of two. This fact is important in determining the amount of effort and detail with which the analysis of water contamination should be conducted. In general, the analysis and calculations have gone into considerable detail in view of this limitation. However, this great detail is warranted since better data on fallout may at some time in the future be made available (through declassification) in which case the overall accuracy may be improved. The solubility nuclide contour ratio computer program will still be valid.

The use of the sublimation pressure to compute fractionation appears somewhat arbitrary at first because certain of the reactions have not been used in the calculations. The choice of the proper chemical reactions for estimating the sublimation pressures has presented a problem. The pressure data used was selected to agree with Miller's calculations for 1673 ^{o}K. However, as the pressure decreases very rapidly with temperature, it will not exert a significant effect when computing the fractionation numbers for the second period of condensation.

The analysis of the second period of condensation as outlined by Miller (2) and as followed in this report appears to have some unwarranted assumptions as noted in this chapter. To compute the fractionation number for the second period of condensation, it has been assumed that each vapor is in equilibrium with its own pure solid phase. It would appear that the sublimation pressure of a particular nuclide would be reduced due to the presence of other nuclides in the solid phase.

In the present study attention has been centered on six specific radionuclides that are considered to be biologically important. The method of calculation finds the amount of a specific nuclide by considering gross fission products and their decay. Thus, the present analysis assumes that the specific nuclide has the same half-life as do the gross fission products. This simplifying assumption may lead to considerable error.

V. DECONTAMINATION OF WATER SUPPLIES

A. Objective

The purpose of this study was to collate recent data on available methods for the decontamination of water. An evaluation and analysis of these methods provides a measure of their applicability to reduce hazards from the ingestion of contaminated waters.

Therefore, decontamination methods and their efficiencies were examined with special attention directed to:

(a) conventional purification methods as are employed by municipal and industrial treatment plants; individual unit processes and overall purification method efficiencies,

(b) non-conventional purification methods as are employed to meet special municipal or industrial requirements, or specifically developed for the removal of trace elements and radionuclides from water, and

(c) emergency treatment methods developed to serve municipal, industrial and military needs, often lightweight and portable; generally to achieve a high degree of water decontamination.

B. Removal by Conventional Water Treatment Processes

Conventional municipal water purification processes include aeration, chemical coagulation and flocculation, sedimentation, rapid sand filtration and chlorination. Special processes, such as lime-soda ash softening, slow sand filtration and others may also be employed but are generally encountered to a lesser extent. Except for aeration, these processes are capable of removing a certain degree of radioactive contamination, either singularly or in combination. The decontamination capability of each type of process is discussed separately below, with special reference to the six biologically significant elements: barium, cesium, iodine, lanthanum, ruthenium and strontium.

Municipal water supplies employing filtration, sedimentation, and coagulation may remove 90% of the total radioactivity. Sedimentation can remove 50% to 60% of the insoluble radioactivity. Coagulation can remove 75% of soluble and suspended solids. Combined with filtration, coagulation can effect as high as 90% removal, according to Saule (37). Ion exchange resin used as a slurry in a pretreatment has been shown to be effective in removing over 98% of the dissolved radioactive contamination. Home water softeners have been found to be very effective devices, yielding about 98% removal of radioactive material according to Lacy and Stangler (38).

In a report by Straub, Lacy and Morton (39), the authors examined 18 isotopes for efficiency of removal by conventional water treatment processes. Results are summarized in Table XVIII.

TABLE XVIII

Removal of Radioactive Materials By Conventional Water Treatment Processes

	Removal Range in Per Cent of Initial Activity		
Isotope	Chemical Coagulation and Settling	Sand Filtration	Soda-Ash Softening
Cs-137/Ba-137 (Cl)	0-37	10-70	< 50
Sr-89 (Cl)	0-15	1-13	50-95
Ba-140/La-140 (Cl)	1-84	39-99	50-95
Cd-115 (NO_3)	-	60-99	50-99
Y-91 (Cl)	1-99 +	84-89	50-95
Zr-95/Nb-95 (oxalate complex)	2-99	91-96	50-99 +
I-131 (iodide)	0-96	-	-
Ru-103 (Cl)	43-96	-	-
Ce-144/Pr-144 (Cl)	28-99 +	-	-

A number of water treatment processes were investigated at Oak Ridge by Cowser and Morton (40) to determine their efficiencies for Sr-90, Cs-137 and the rare earths from tap water. The characteristic efficiencies of five treatment processes are shown in Table XIX.

TABLE XIX

Removal of Radionuclides From Water By Conventional Water Treatment Processes

Radio-isotope	Process Waste Stream Composition (% gross beta)	Percent Removal by Treatment Process				
		Chemical Coagulation(a)	Chem. coag. + 100ppm Clay	Sand Filtration	Lime-Soda Softening	Phosphate Coagulation
Sr	19.6	3	0-51	4	97.3	97.8
Ce	15.2	91	85-96	-	-	99.9
Trivalent Rare Earths (+Y)	30.4	91	-	87	90.0	-
Cs	29.9	0.5	35-65	50	not effective	-
Ru	1.9	77	-	-	-	-

(a) Coagulant includes alum, ferrous sulfate or ferric chloride, lime, soda ash or sodium hydroxide, and sodium silicate.

1. Chemical Coagulation

The most common coagulants in water treatment are aluminum and iron salts. When introduced into water, they form aluminum and ferric hydroxides which precipitate as chemical floc. This floc acts as an efficient scavenger by adsorbing, entrapping or otherwise bringing together suspended matter, particularly that which is colloidal in nature. The artificial increase of the alkalinity in water may also form the hydroxides of heavy metals which co-precipitate with the aluminum or ferric hydroxide.

Cowser and Morton (40), investigating a number of water treatment processes at Oak Ridge to determine the removal efficiencies for Sr-90, Cs-137 and the rare

earths from tap water, obtained a decontamination factor of 11 for rare earths using chemical coagulation, as shown in Table XIX.

According to Voznesenskii and coworkers (41), decontaminations of 64% for ruthenium-106, 93.5% for strontium-89, and 99% for zirconium-95 and rare earth cations were obtained by means of ferric hydroxide coagulation preceded by flocculation.

Matsumura, Ishiyama, and Mamuro (42) conducted tests on low-level radioactive waste water. Optimum results of Sr-89 removal were obtained in the pH range 9.5 to 10.5 using 100 ppm ferric hydroxide. After two minutes of stirring the flocculation became slight, and after two hours of flocculation did not further influence the effectiveness of decontamination. They also used flocculation to remove radionuclides from tap water spiked with Sr-89, Zr-Nb-95, Ru-Rh-106 and Ce-Pr-144. Addition of ferric sulfate and hydrous ferric chloride coagulants in 0.1N hydrochloric acid at a pH from 9.5 to 10.5 resulted in a Sr-89 decontamination factor of 2.5×10^2, a Zr-Nb-95 DF of 2.5×10^2, a Ce-Pr-144 DF of 91, and for Ru-Rh-106 a DF of 8.7.

The principles of response surface methodology were employed by Gardiner and Cowser (43) in an attempt to discover those combinations of: (a) dose of Grundite clay, (b) particle size of clay, (c) excess soda ash and (d) proportion of stoichiometric requirement for lime, which will remove the greatest amounts of Cs-137 and Sr-90 from ORNL process wastes.

The method of steepest ascent is a relatively new statistical technique which is applicable to experimentation in which the variables are measurable on a continuous scale. The variables in the experimental program were accordingly: (a) lime added, as a proportion of the stoichiometric requirement; (b) excess soda ash (in ppm); (c) ppm of clay per dose; (d) particle size of clay added.

Laboratory experiments performed led to combinations of the treatment variables which remove up to 95 percent of the Cs-137 and 96 percent of the Sr-90. The largest removal of Cs-137 occurred at 600 ppm clay of 200-mesh, 470 ppm of excess soda ash

and 1.4 times the stoichiometric amount of lime. The removal of Sr-90 was largest at 360 ppm clay of 200-mesh, 520 ppm excess soda ash and 2.5 times the stoichiometric amount of lime.

Graham, Beard, and Kvam (44) outlined the chemical treatment in use at the Lawrence Radiation Laboratory, Livermore, and gave information on drum filtration as a slurry dewatering technique. Decontamination factors of 10^4 were obtained routinely from the laboratory waste in batch sizes ranging from 500 to 30,000 gallons. Similarly, reductions in beryllium content from 10,000 µg/l to less than 2 µg/l were achieved by this technique.

Fernandez (45) reported the following decontamination factors obtained from chemical treatment of radioactive effluents at Marcoule, France, as shown in Table XX below:

TABLE XX

	Low Activity	High Activity		
Radionuclide	D.F. after $CaCO_3$	Cumulative D.F. after treatment with:		
	treatment	$Fe(OH)_3$	Nickel Ferrocyanide	$CaCO_3$
Total β emitters	12	40	65	150
Cerium-141, 144	500	750	5000	7000
Zirconium-95	250	750	4000	4000
Cesium-137	1.2	18	200	500
Strontium-89,90	75	3.0	3.5	160
Ruthenium-106	1.8	4.0	5.0	6.0

2. Rapid Sand Filtration

Except for removal by simple straining, rapid sand filters have not proven to be effective for the removal of most radiocontaminants. The amount of radioactivity removed by filtration will vary depending on the nature of the material. Removals of up to 93% by sand filtration alone for Y and Zr, probably present in the colloidal state, were reported by ORNL (46), while other materials in true solution, such as Sr and Cs, were not greatly reduced (4% and 50% reductions) by passage

through sand filters. The report shows that Ba and La can be removed up to 95% and 74%, respectively, while no data could be found on the removal of I or Ru by rapid sand filtration.

3. Slow Sand Filtration

Slow sand filters for removing activity have been studied by Gemmell (47) at Brookhaven and by Eden, et al., (48) in Great Britain. Their action is due to simple sorption by biological life on the top of the filter. Gemmell obtained 92% removal of P-32, 88% removal of I-131, and 99% removal of Sr-90. Working with mixed fission products (age 6 months), Gemmell reported a 98% removal of the activity by means of slow sand filtration.

Qualitatively similar results on slow sand filters were obtained by Eden, et al., (48) and although the reported removals of strontium and iodine were less efficient, they obtained 93% removal of ruthenium-106.

4. Chlorination

Hannah, et al. (49) studied various methods for the removal of I-131 from water and found small dosages of chlorine (0.05 to 0.1 ppm) in the presence of 100 ppm activated carbon produced up to 80% removal. The authors concluded that the only effective method found for removing I-131 with materials normally available in water treatment plants involves chlorination followed by adsorption of liberated iodine on activated carbon. Removal of I-131 decreases to less than 20% when the chlorine dosage increases to 1 ppm. Therefore, normal prechlorination employed by the water treatment plant could not be used for iodine removal because the chlorine residuals would generally exceed the required dosage for activity removal. Stable iodine, in dosages greater than 0.01 ppm, inhibited removal of I-131 with chlorine and Aqua Nuchar A (activated charcoal). Variation of pH, achieved by adding sulfuric acid and sodium hydroxide, was found to have little effect on the removal of iodine by chlorine and activated charcoal.

5. Lime-Soda Ash Softening

McCauley, Lauderdale, and Eliassen (50) investigated the efficacy of the lime-soda ash process on the removal of mixed fission products. These studies were carried out by adding 2,000 ppm of C.P. calcium carbonate to test solutions containing 250 ppm of $CaCl_2$ (as $CaCO_3$), stirring for 20 minutes and then assaying the solutions for activity. Following this, 330 ppm of Na_2CO_3 was added, stirring was continued for another 20 minutes and a second activity assay was made. About 85% of mixed fission products activity was removed with the C.P. calcium carbonate and this value was increased to about 94% removal after softening with sodium carbonate.

To examine the efficiency of a hot softening process for removing radioactive strontium, a number of qualitative tests were made. These tests were made by heating samples containing Sr-89 and various concentrations of $CaCl_2$ to boiling and then adding varying amounts of soda ash. The test results were obtained by adding about 50 mg. per liter of excess Na_2CO_3 (as $CaCO_3$) and then adding an equivalent amount of $CaCl_2$ in about ten equal increments of 5 mg. each. Temperatures of 85° to 95° C. were the effective boiling temperature range. Removals in excess of 99.9 percent of strontium were easily demonstrated by this hot softening process.

McCauley and Eliassen (51) showed that strontianite ($SrCO_3$) forms mixed crystals with both forms of $CaCO_3$, viz. calcite in the cold softening process and aragonite in the hot softening process. For a given removal of calcium, more strontianite is incorporated into aragonite than into calcite, and hence hot softening gives better decontamination, although this might be offset in large-scale practice by higher capital and operating costs. The process may be improved by adding freshly precipitated $CaCO_3$ to act as seeds for further precipitation. With the aid of seed material, large well-developed crystals were obtained, giving a sludge with good settling properties. McCauley and Eliassen claim that a single pass through a conventional softening plant working at a maximum efficiency will effect greater than 50% removal of strontium, and that over 99% removal can be obtained by modifying the conventional treatment into a multi-stage process.

Cowser and Morton (40) investigated a number of water treatment processes at Oak Ridge to determine the removal efficiencies for Sr-90, Cs-137 and the rare earths from tap water. They obtained a decontamination factor of 10 for rare earths using lime-soda softening.

C. Removal by Non-Conventional Treatment Methods

Below are listed several methods of water decontamination not commonly employed in municipal treatment plants. Economic considerations may limit the use of many of these methods, except under emergency conditions.

1. Ion Exchange

Relatively few large water treatment plants use ion exchange as a softening measure. This method of softening is more prevalent among the smaller plants. Ion exchange resins have been found to provide one of the most effective methods for the removal of individual radionuclides and gross fission product mixtures.

Moeller, Leddicotte, and Reynolds (52) conducted a study of an ion-exchange decontamination system for the recirculating cooling water of a low-intensity test reactor. They found that in the cation, anion, and mixed-bed columns, the concentration of radionuclides on the resin decreased with increasing bed depth. At the same time, the overall half-life of the retained materials simultaneously increased. Considerable variation with depth was observed in relative radionuclide composition with bed depth, the shorter-lived materials predominating near the surface, the longer-lived near the bottom of each column. The authors claimed that as a general rule the removal efficiency of an ion exchange column will be least for those radionuclides whose half-lives are long in comparison to their retention time.

Although the ion exchange process offers one of the most efficient methods for the removal of radiocontaminants, the cost may preclude widespread application unless cheaper and more suitable regeneration techniques are developed.

The possibility of using home water softeninrs of the ion exchange type post-attack has been discussed in the literature (38) (53).

(a) Natural Exchangers

Burns and Glueckauf (54) using a vermiculite exchange column have reported a Sr-90 decontamination factor range of 2.5 to 10 x 10^3 representing up to 99.99% removal. Column studies of lignite (17), a variety of brown coal, have demonstrated decontamination factors of (a) 55 for percolation; (b) 143 for filtration; and (c) 20 for centrifugation.

Thomas, et al. (55) studied vermiculite, variscite, Tennessee rock phosphate, and Florida pebble phosphate to determine the feasibility of their use in columns for the sorption of strontium from high pH, intermediate-level wastes produced at ORNL. Excepting vermiculite, all materials were effective for strontium removal.

The addition of soluble phosphate to the waste solution remarkably improved the strontium-sorption characteristics of vermiculite, 100 ppm of PO_4^{3-} being a satisfactory concentration. A reduction of pH of the solution adversely affected strontium-removal properties of all the materials. The following results, interpolated from graphs which Thomas and others reported, are summarized below:

Exchange Material	Maximum Sr sorbed (%)
Natural vermiculite	22%
Phosphate + lunstone-treated vermiculite	99%
Variscite	96%
Florida pebble phosphate	99.5%
Tennessee rock phosphate	99.9% or more

Klein, Harten, and Kaufman (56) did experimental work to provide a basis for the design of an ion exchange system for small scale decontamination of drinking water following a nuclear attack. Their experimental work was limited to the isotopes, Y-91, Ba-140, and La-140.

Greensand proved superior to strongly acidic sulfonated polystyrene resin for the removal of Y-91, Ba-140, and La-140, but according to Klein, Harten, and Kaufman, its capacity is much smaller. The greensand glauconite removed 99.4% Y-91, 99.6% Ba-140, 98.6% La-140, and > 99.999% of Ba-La-140. With the cation resin Duolite C-20; 98.5% of Y-91, 98.4% of Ba-140, 98.6% of La-140, and 99.4% of Ba-La-140 were

removed. The authors concluded that an ion exchange unit, using both cation and anion exchangers in non-equivalent proportions and natural alumino-silicate exchangers would produce optimum removal.

(b) Synthetic Exchangers

In one of the earliest studies to decontaminate water with synthetic resins, Ayres (57) using a mixed bed, has obtained a mixed fission product decontamination factor of up to 10^6.

Sammon and Watts (58) have obtained a decontamination factor for Sr-90 of 5×10^4 using a mixed resin bed.

Hickok (59) obtained a decontamination factor of 10^4 for cesium using an ion-exchange process with ammonium phosphomolybdate (APM). The procedure consisted of a flow of 5 to 8 gal/ft^{-2} hr^{-1} of process waste through a column of APM-silica gel in which APM was 20% by weight. One percent breakthrough came at about 27 column volumes, 50% breakthrough at 36 column volumes.

Roberts and Holcomb (60) developed a laboratory scale process involving (a) pH adjustment to slightly under 12; (b) clarification; and (c) passage of the waste through a bed of phenolic cation exchange resion (Duolite Cs-100 or C-3). The process obtained a decontamination factor range for Ru-106 of from 2 to 6 using low-level waste water.

According to Caron (61), thallous phosphotungstanate (TPT) is a highly specific cation exchanger for cesium. The heteropoly salt is converted into a form suitable for column use by mixing with paper pulp. A major advantage over other methods using synthetic inorganic exchangers is that the final cesium fraction is obtained free of ammonium ion, a frequently used eluent which is troublesome to remove. The column retention capacity of TPT is 0.5, 0.3, and 0.1 meq. per gram for cesium, rubidium, and potassium, respectively. Decontamination factors for cesium removal were found to be in excess of 10^3.

In 1962 Culler, et al. (62) evaluated the available, effective decontamination processes. In their investigation of overall removal of activity from ORNL waste they summarized their results which appear below, abbreviated from Culler's original tabulation.

Run No.	Bed Volumes	Sr-90 DF	Sr-90 % removed	Cs-137 DF	Cs-137 % removed
HR-1	2000	2,956	> 99.99	288	99.7
HR-2	2086	2,047	> 99.9	246	99.6
HR-3	1959	4,982	> 99.9	429	99.8
HR-4	1789	5,588	> 99.9	2,520	> 99.9
HR-5	2046	2,316	99.96	543	99.82
HR-7	2086	12,160	99.99	451	99.78
HR-8	2000	4,200	99.98	3,444	99.90
HR-9	2131	> 8,196	99.99	~ 77	98.70

Skarpelos (63) reported an investigation to evaluate the decontamination ability of a commercial grade mixed bed resin (Illco) TM-1) for Purex tank farm condensate was conducted at Hanford. The steamstripper bottoms had a pH of about 7.3 and contained 20 ppm NH_3, 5 ppm. Na^+, 25 ppm NO_3^-, and 32 ppm NO_2^-. The following decontamination factors are claimed: > 1000 for Cs, when over 500 column volumes were treated; 100 for Ru; and 350 for Sr. The initial high efficiency removal experienced with strong-base anion resins was not obtained with weak-base anion resins.

Brooksbank, et al., (64), obtained decontamination factors for Sr-90 ranging from 2.9 to 12 x 10^3 representing 99.99% removal in up to 2,086 bed volumes. This pilot plant demonstration process involved (a) scavenging precipitation with hydrous ferrous oxide and alkaline earth carbonates followed by solution clarification and filtration, and (b) sorption of the Sr-90 and other isotopes on a carboxylicphenolic ion-exchange resin.

A method for the routine radiochemical determination of rare earths from fission of uranium is described by Wolfsberg (65). Separation of individual rare earths is achieved by eluting with alpha-hydroxyisobutyrate solutions through cation-

exchange resin columns operated at room temperature. The procedure was developed for the routine determination of Y, Eu, Sm, Pm, Nd, Pr, Ce, and La activities from thermal neutron fission of uranium. Titration with EDTA was used as a method of obtaining chemical yield. Decontamination factors of 3.3×10^4 for Y-91, 5×10^5 for Nd-147 and Pr-143, and 2.5×10^5 for Pm-149, 151 were reported.

An anion exchange process for the recovery of americium, curium, and rare earths contained in the effluent from plutonium processing has been developed and tested on a laboratory scale by Lloyd (66). The waste, a solution of americium, curium, aluminum, and fission products, in concentrated nitric acid, was concentrated by evaporation until a temperature of 140°C was reached. This removed excess acid, and the proper feed concentration of 2.34M $Al(NO_3)_3$ was obtained by dilution. The radionuclides were sorbed on Dowex 1-10X resin, and were eluted with 0.65M HNO_3. The following DF values were observed: one for Ce, 500 for Cs, 20 for Ru, and 100 for Zr.

(c) Ion Exchange and Absorption Materials

Skarpelos (67) conducted a comprehensive investigation of a number of ion exchange and absorption materials on a laboratory scale. The organic, nonradioactive impurities in the feed were successfully removed by steam stripping and filtering. Excellent decontamination of all significant isotopes, except ruthenium, was achieved by ion-exchange. This result was expected in view of the complex chemistry of ruthenium. When the waste was passed through a series of beds of strong acid cation and strong base anion exchange resins, or together in mixed beds, > 99% of the ruthenium was removed although the capacity of the two bed system for ruthenium was relatively low.

Research was undertaken to examine the zeolite mineral clinoptilolite for the removal of radiocesium because it has properties which adsorb cesium from solutions containing much higher concentrations of other cations. Significant quantities of NH_4^+ reduce efficiency of cesium removal because of the similarity between Cs^+ and NH_4^+. Activated charcoal successfully removed both soluble and emulsified organics. A summary of the experimental results achieved by Skarpelos (67) was presented in

Table II of the third interim report (17).

Using a H-based clinoptilolite column with a feed at a constant pH of 3.0, Mathers (68) obtained the following decontamination efficiencies: greater than 98% for Ce-144; greater than 92% for Sr-90; and in excess of 92% for Cs-137. Decontamination factors of 98% for Sr-90 and 97% for Cs-137 were obtained in experiments using Li-based clinoptilolite at a pH of 7.0.

Experiments using citric acid to chelate corrosion products from a Purex type waste at BNL (69) have shown that decontamination factors for strontium of the order of 10^5 can be achieved.

A 1-ft. column of clinoptilolite passing 4 liters of a Purex type waste containing corrosion products and added Sr-90 gave a decontamination factor of 2.0×10^6. To investigate the possibility of further decontamination in such a system, the effluent (pH = 3.0) with Sr-90 was passed through a second 1-ft. column. An additional decontamination factor of 3.2×10^3 was obtained for a cumulative DF of 6.4×10^9.

Tuthill, Weth, and Abriss (70) investigated the adsorption of strontium on columns of clinoptilolite at 65°C. Three runs were made using citric acid chelation and one run with the hydrogen form of clinoptilolite. With one foot columns of the exchanger, the decontamination factors were 10^5 for the chelated system, and 10^6 for the hydrogen clinoptilolite with a throughput in each case of 57 column volumes.

Honstead and coworkers (71), working with clinoptilolite and other minerals for fixation-decontamination, have reported decontamination factors from 2 to 8×10^7 from radioactive wastes. The column capacity for this waste was about 43 column volumes before dilution.

A form of treatment that is commonly used at research establishments such as AERE at Harwell (72), is chemical precipitation followed by filtration of the sludges thus produced. If this process is then followed by ion exchange on a natural inorganic material such as vermiculite, a decontamination factor of 10^3 to 10^4 is obtained. In the case of cesium treatment with copper ferrocyanide yields 99% removal which reduces subsequent loading on ion exchange columns. Treatment with an evaporator

followed by a separator packed with knitted wire mesh yields an anticipated decontamination factor of 10^5.

Nelson (73) reported on the use of inorganic ion exchange work at Hanford on acid high-level waste (FTW), a formaldehyde treated waste (about 0.5M acid). Operating a clinoptilolite column at a one column volume/hour rate up to about 80 column volume/hour rate, up to 99.5% of cesium-137 was removed. From experimentation the following D.F.'s from Cs are claimed: $> 9.0 \times 10^4$ for Ce-144, 2.1×10^3 for Sr-90, $> 1.4 \times 10^5$, for Ru-106, and 7.0 for Nb-95.

Coleman, et al (74) investigated the efficiency of a 3-bed demineralizer (clinoptilolite, Dowex-I anion resin in the OH-form, and Dowex 50-W cation resin in the H-form) for removing radionuclides from steam stripped alkaline Purex tank farm condensate. Overall DF's of > 250, > 500, and 23 were obtained for Cs, Sr and Ru, respectively, on a total of 7400 gal. of feed processed.

2. Sorption

A Belgian patent for the removal of radioactive elements by adsorption on a column of cellulosic material was reported (75). The most suitable cellulosic material is sawdust prepared from poplar wood. Up to 99% decontamination is claimed. Before passage through the column, waste waters were treated to remove organic materials and any other interfering elements. Addition of $FeCl_3$ to the waste water before passage through the column increased the fixation on the adsorbent of certain radioactive elements, such as ruthenium.

The degree of recovery of Cs-134 from solution, using gelatine foam formation, was estimated radiometrically by Pushkarev, et al (76) by comparison of the activity of the original solution with that after foam formation. Recovery of cesium 134 from a solution by sorption with mixed ferro-and ferri-cyanides of the heavy metals and separation of the solid phase by a gelatine foam yielded 99.4% and 99.1% removals with nickel ferro-and ferricyanides.

In characterizing the reactions of strontium with sorbent materials, four possible mechanisms were suggested by Tamura, et al (77): (1) ion exchange as an absorption process exemplified by the resins, clinoptilolite, and the clay minerals; (2) ion exchange as an absorption process characterized by the reaction of alumina; (3) metasomatic replacement as characterized by the $CaCO_3^-$ phosphate reactions; and (4) precipitation reactions as evidenced by natural vermiculites and clinoptilolite in contact with phosphate waste.

The following maximum percentage removals of Sr were claimed: 98.2% using 50-100 mesh Dowex 50W-X12; 90.5% using 35-70 mesh Duolite C-3; and 90.8% using 35-70 mesh clinoptilolite. All of these removals were obtained over a 72-hr contact period. Alumina was shown to remove a maximum of 98% strontium from a solution at pH 8.0 during a 24 hr contact period. A maximum of 99.8% removal of Sr at a 5,000 ppm phosphate concentration is claimed to have occurred by a metasomatic replacement reaction with $CaCO_3$ over a 72 hour contact period.

According to Tamura and co-workers a maximum of 98.1% Sr is removed by natural clinoptilolite in the presence of limestone. Also, over a contact period of 312 hours 98.6% of Ru-106 was removed from solution by reduction and sorption in the presence of 0.1M $Na_2S_2O_4$.

Jacobs (78) investigated the cesium-exchange properties of various grades of commercially available vermiculite and compared them with other natural ion-exchange materials. Studies of the kinetics and the thermodynamics of the exchange reaction permit extrapolation of the data for consideration of the extended use of vermiculite columns for decontaminating other waste streams.

Data obtained from bench-scale and field-scale (10-ft.long, 2-in.I.D.) column studies compared closely with those obtained by slurry studies. K-treated vermiculite removed a maximum of 99% of Cs-137 by sorption from solution containing 0.1M NaCl.

The use of a mineral-filled column is regarded as an inexpensive, yet efficient alternative method for decontamination, if ground disposal cannot be controlled.

Struxness, et al. (79) explored the ruthenium sorptive properties of sulfide minerals. Sorption of ruthenium from synthetic waste solution tagged with Ru-106 Cl_3 was reported as > 95% using stibnite[(a)] and > 90% using chalcopyrite[(b)]. Use of $Na_2S_2O_4$ as a reducing reagent in alkaline media increased sorption of ruthenium. Optimum removal of ruthenium from solution occurred in the pH range, y to 10, where polymeric species of ruthenium would be at a maximum.

Pushkarev et al. (80) studied the sorption of microamounts of cerium-144, Yttrium-91, and zinc-65 from aquaeous solutions by active manganese dioxide and also obtained additional information on the sorption of Zr-Nb-95, Cs-134, Ru-106 and Zn-65.

The following percents express the degree of sorption of the radioisotopes obtained by active manganese dioxide: Ru-106 92%, Zr-Nb-95 99.5%, Y-91 99% and Ce-144 99%. Cesium-134 was not sorbed under the experimental conditions.

Kokotov, et al. (81) investigated the sorption of Ce-144 by two soils differing considerably in properties, namely, southern black earth and Devonian strongly podzolic soil (podzolic level). The effect of various macrocomponents and complex formers on the sorption of Ce-144 were also studied. Values of 91 and "100" percent sorption were reported.

Tamura et al. (82) investigated several heat-treated hydrous oxide minerals of iron and aluminum to test properties favorable for the sorption of strontium: diaspore ($HAlO_2$), geothite ($HFeO_2$), and limonite ($Fe_2O_3 \cdot xH_2O$) were used.

For Diaspore the maximum removal from solution was 86.1% after 48 hours contact time; for geothite the maximum sorbed from solution was 98.1% after 24 hours contact and limonite sorbed 99.8% from solution after 48 hours contact time.

Mercet (83) made an investigation of high-level waste treatment by sorption on a clinoptilolite column. The cesium from a simulated FTW (acid waste) solution,

---

(a) stibnite has the chemical formula Sb_2S_3

(b) chalcopyrite has the chemical formula $CuFeS_2$

containing 14% actual Purex 1WW, was loaded on and eluted from a 14 ml column of clinoptilolite. Analytical results yielded decontamination factors of 700 and 70 for Zr-95 and Nb-95, respectively.

Katy and Rothbart (84) developed a flow sheet, using Linde AW 400 molecular sieves, which provides effective decontamination of cesium and probably of strontium from highly alkaline waste supernates containing potassium and aluminum. The authors claim a maximum percent decontamination of Purex waste of 99.5%.

Kolarik and Kritil (85) conducted an interesting sorption study of these radionuclides: Cs-137, Sr-90, Y-90, Ce-144, Eu-152, 154, Ru-106 (NO), and Zr-95. Approximately 99% elution of the sorbed radionuclides (Cs-137, Sr-90) and rare earths is claimed. However, only 90% elution of Ce-144, Ru-106, and Zr-95 was reported for these isotopes.

3. Mineral Reactions

Rimshaw and Winkley (86) tested a series of minerals as to their efficiency in removing Ru-106 from dilute alkaline wastes prior to ground disposal. The kinetics and adsorption of Ru-106 are known to be complex and slow due to the presence of many chemical forms of ruthenium. Rimshaw and Winkley report that copper in conglomerate, various sulfide minerals containing copper, cuprite (copper-I-oxide), and descloizite (basic zinc lead vandate) removed 90% Ru under reducing conditions at a pH of 7 when heated to 60°C for 16 hours. At lower temperatures ruthenium removal took days or even weeks.

A synthetic Purex neutralized waste supernatant solution containing a small amount of actual waste was diluted 1:20 with water and cesium decontamination factor of $> 10^7$ was obtained (87) for 420 column volumes of diluted waste. Breakthrough of Sr-90 took place after Cs-137 breakthrough. This result is attributed to a reaction between calcite impurity in the mineral and phosphate in the waste. A decontamination factor of at least 10^3 was indicated for rare-earth nuclides. Clinoptilolite was used to obtain these DF's at Hanford's Micro Pilot Plant for the decontamination of various types of Purex wastes.

Experiments were conducted by Honstead, Ames, and Nelson (88) at Hanford to determine the value of mineral reactions for the removal of radioactivity. Calcite was used to remove Sr-90 from 3M $NaNO_3$ solution containing 0.05M PO_4^{3-} and 10^{-2} $\mu c/cm^3$ of Sr-90. A [illegible]on factor in excess of 10^6 was maintained for 3000 bed volumes at a flow rate of 10 to 20 ml hr^{-1} cm^{-3}.

4. Clays

Lacy (89) investigated the removal properties of a montmorillonite type clay on Ru-Rh-106, Zr-Nb-95, Sr-Y-90, I-131, Ce-Pr-144, Ba-La-140 and MFP which resulted in decontamination values rangi[illegible] 99.9%, as shown in Table III, interim report No. 3 (17). Lacy also found that a moderate concentration of activity yielded the highest percent r[illegible]al, while the highest concentration gave the lowest percent removal.

Glueckauf (90) has shown that clays give a small overall removal, but do enhance the removal of activity on hydroxide and phosphate flocs. Clays improve the removal because of their ability to take up alkali metals and alkaline earths by ion-exchange. Kaolinite was found to be as efficient as montmorillonite because its rate of exchange is greater.

Slurrying with clays has proven uneconomic on a larger scale because of the cost of disposing of the large volumes of sludge, though it could be useful on a laboratory scale.

Tamura (91) in a 1962 report on mineral exchange work at ORNL claims that 90% removal of cesium can be effected using 200 ppm of Illite added to low level waste. A table summarizing effective strontium removals up to 91%, employing Kaolinite, Nontronite, Vermiculite, Montmorillonite and Clinoptilolite is presented.

Brockett and Placak (92) have been successful in absorbing radioisotopes onto Conasauga shale using a jar-stirring method. They have obtained a Ba-140 decontamination factor of 50 and an I-131 decontamination factor of 2.4.

Jacobs and Tamura (94) conducted a study to determine the effect of clay mineral structure on the sorption of cesium. The following results are claimed: (1) using the mineral Kaolinite, a maximum of 75% of the cesium-137 present was removed, (2) Arizona Bentonite removed 74% of cesium-137 contamination; (3) Wyoming Bentonite removed a maximum of 40% of the cesium-137; and (4) Illite removed a maximum of 98% of the cesium-137 contaminant.

Cesium sorption data obtained for a number of clay minerals indicate that cesium exchange is influenced markedly by the structure of the clay mineral. A collapsed C-spacing is requisite for cesium fixation, though the fixation process differs depending on whether the clay mineral lattice is previously collapsed or whether it collapses during the fixation process.

Sorathesn et al. (95) investigated decontamination techniques based upon mineral and sediment affinity for radionuclides. The experimental results they obtained are summarized in Table XXI.

5. Metal Dusts

Lauderdale and Emmons (96) conducted experiments using two columns, each 3/4 in. in diameter and 24 in. long. The first was packed with steel wool, calcinated clay and activated carbon. The second column was packed with a mixture of quarternary amine-polystyrene (strong base) type anion exchange resin and nuclear-sulfonic polystyrene (strong acid) type cation exchange resin. The results, ranging from 96% removal of Ru-106 to 60% removal of Cs-137, were shown in detail in Table IV in the third interim report (17).

Lacy (97) investigated the absorptive capacity of iron, aluminum, copper and zinc. The procedure and the results of this investigation were discussed previously (17). Removals up to 99.6% for Ru-Rh-106 and up to 99.9% for Ce-Pr-144 were reported.

6. Phosphate Coagulation

Ruthenium removal depends upon the composition of the waste solutions which determines the chemical state of ruthenium. Prior treatment with an oxidizing agent

TABLE XXI

Maximum Sorption of Radionuclides by Clays

Radionuclide	Standard Clays	Contact Time	% Activity Sorbed pH 6	pH 9
Cs-137	Illite	7 days	98.4	98.6
	Kaolinite	1 hour	74.2	93.2
	Montmorillonite	1 hour	61.2	58.3
	Vermiculite	8 days	99.6	99.8
	River Sediment	7 days	97.8	97.6
Sr-85	Illite	7 days	26.9	43.1
	Kaolinite	3 days	67.5	71.2
	Montmorillonite	1 hour	70.9	71.9
	Vermiculite	8 days	97.3	98.7
	River Sediment	7 days	41.8	66.8
Zr-95-Nb-95	Illite	7 days	94.1	89.1
	Kaolinite	7 days	94.9	85.8
	Montmorillonite	7 days	35.2	42.1
	River Sediment	7 days	86.6	79.9

destroys ruthenium complexes. Following this passage of the waste solution over calcium phosphate-ferrous floc in the presence of $NaHSO_3$ improves removal. 99 percent removal of ruthenium was obtained by this method by Dejonghe (98).

Cerrai, Scaroni, and Triulzi (99) studied the decontamination of liquid waste containing radiostrontium. Preliminary experiments were carried out on a bench scale to select best pH conditions, stirring, and settling (30 min and 3 hrs). Different amounts of flocculants (PO_4/Fe = 2 in W.) were used to check the minimum quantity required for a good decontamination in respect to divalent elements present. A single stage strontium decontamination of 95% was claimed. Before final discharge of processed liquids, the low residual activity is completely removed by absorption on a cation exchange resin.

Zlobin (100) conducted investigations of the adsorption of yttrium and zirconium phosphates under a different solution condition. A maximum percent adsorption of 95% for yttrium from 0.3N HCl is claimed. For zirconium-95 a maximum sorption of 99.3% from solution in the presence of 0.3N HCl and Na_2HPO_4 was reported.

Cowser and Tamura (101) reported on the results of process waste treatment of ORNL low-level waste, essentially tap water contaminated with small quantities of radionuclides. Both supplemental phosphate addition to lime-soda softening and aluminum phosphate coagulation yielded 98 percent removal for strontium. Coagulant acids reduced the turbidity in treated waste and resulted in improved efficiency. Vermiculite (grade BO-4), one of the most promising of the minerals investigated, exhibited distribution coefficients for strontium and calcium in excess of 5000 for a solution typical of the effluent from the waste treatment plant.

Seedhouse, et al., (104) reported 97.8 percent removal of Sr-89 with calcium phosphate floc in the presence of excess trisodium phosphate.

7. Flotation

On the basis of laboratory experience, Lacy (103) deemed it possible that a flotation process, using as surface-active agent a quaternary ammonium compound, may be effective in the removal of suspended or colloidal radioactive contamination in

water due to fallout. The specific compound was a cyclic amine; cetylpyridinium chloride, USP grade.

The following maximum percent removals for specific radiocontaminants were reported: for Ba-La-140 chloride in 1N HCl-78% removal; for Ce-Pr-144 chloride in 1NHCl-81% removal; for Cs-Ba-137 chloride in 1N HCl-85% removal; for Ru-Rh-106 chloride in 3N HCl-91% removal; and for Zr-Nb-95 oxalate complex in 5N $H_2C_2O_4$ 77% removal. 62% removal of mixed fission product nitrates in 3N HNO_3 was the maximum claimed by Lacy.

Pushkarev, et al. (76) found that the best recovery of Cs-134 from a solution was obtained using ferro-and ferricyanides of nickel and cobalt as the sorbent. A further increase of the recovery of Cs-134 could be achieved by repeated treatment of the solution with the addition of gelatine and the introduction of air. Following triple aeration with a purified solution, the total recovery of cesium amounted to 99.99 percent.

According to a report from the literature (104), foam separation with a liquid feed throughput of 30 gal/(sq ft) (hr) and with a gas-to-liquid feed ratio of 12.4 produced a strontium DF > 1000. The DF increased as the gas-to-liquid ratio and the height of the foam column below the feed distributor were increased. In the preliminary steps of the one-step process, strontium decontamination factors of 200 to 300 were achieved.

Cardozo using a synthetic effluent has obtained a decontamination factor of greater than 25 for cesium. The synthetic effluent, from which Cardozo (105) obtained DF's > 25 for Cs-134, > 200 for Eu-152, and approximately 1.5 for Sr-89, was made up from tap or distilled water. Cardozo also reported a DF of 7 for mixed fission products. The tracers were added as follows: 10^{-2} μc/ml for europium and mixed fission products; and, 10^{-2} μc/ml of strontium-89.

Blanco and Parker (106), using sodium dodecylbenzenesulfonate (NaDBS) as the foaming agent and ORNL tap water with a Sr-85 tracer as feed in a two-step process,

obtained a decontamination factor for strontium in excess of 1.5×10^4. The process consists of removal of most of the calcium and magnesium in a sludge column, followed by a foam separation process for the removal of strontium.

8. Solvent Extraction

Effective methods for removing long-lived hazardous fission products from a simulated acid aluminum nitrate fuel processing waste were presented by Krieger, Goldin, and Straub (107). By combining cocrystallization, coprecipitation, and liquid-liquid extraction, the cesium and strontium activities can be segregated from the other fission products on potassium alum and barium sulfate, respectively, while the rare earths, zirconium, yttrium, niobium, and ruthenium can be removed into undiluted tributyl phosphate. Exploratory results of serial treatment combinations on decontamination of one or more tracers from the acid $Al(NO_3)_3$ solution are summarized in Table XXII.

A solvent extraction process was developed by Butler and Ketchen (108) for the specific purpose of separating Y-91 and Ce-144 from the gross rare earth fission products fraction. It involves the extraction of these two elements into di(2-ethylhexyl)-phosphoric acid (D2EHPA) in Amsco. The process has been incorporated in the ORNL Fission Products Pilot Plant chemical flow sheet to provide a pure Ce-144 fraction and a Pm-147 rare earth fraction for subsequent separation and purification.

Experimentation with a short-cooled rare earth fission products feed yielded a 92% extraction of Y-91 and 99.3% removal of Ce-144. Work with Long-Cooled Rare Earth Fission Products was reported to have yielded 98% removal of Ce-144.

In a method developed by Marsh, et al. (109), radiochemical cerium in fission product mixtures is oxidized to the quadrivalent state with bivalent silver and extracted as the tetra-n-propylammonium nitratocerate ion-associated complex into nitroethane. Cerium is then stripped from the organic phase with hydrogen peroxide-hydrochloric acid and precipitated as cerous oxalate. This method is rapid, safe, and requires a minimum of laboratory technique. Depending on the anions present, various extraction percentages ranging in excess of 99% can be expected from this extraction.

TABLE XXII

Percent Activity Removed by Solvent Extraction and Coprecipitation

Serial Treatment Combinations	Cs-137	Sr-89	Ru-106	Ce-144	Ce-137 Sr-89 Ru-106 (*)	All Activities Fresh	All Activities Aged
Solvent Extraction +	-	97.1	-	-	98.0	96.0	98.3
Cocrystallization +	99.1	99.3	97.9	99.94	99.4	97.0	98.0
Coprecipitation	-	99.3	-	-	98.1	-	-
Cocrystallization +	-	-	-	-	-	99.6	99.3
Coprecipitation +	99.9	99.8 (*)	97.9	99.98	98.3	99.8	99.1
Solvent Extraction	99.9	99.7	-	-	99.8	99.9	-
Coprecipitation +	-	-	-	-	-	98.9	98.8
Cocrystallization +	-	99.3	-	-	-	99.7	98.6
Solvent Extraction	99.0	-	-	-	-	99.8	-
Solvent Extraction +	-	-	-	-	-	98.2	98.2
Coprecipitation +	98.8	98.9	97.5	99.95	-	98.8	98.0
Cocrystallization	-	-	-	-	-	-	-
Cocrystallization +	-	-	-	-	-	-	99.2
Solvent Extraction +	98.8	99.1	-	-	-	99.6	99.1
Coprecipitation	-	-	-	-	-	-	-

(*) These values represent replicate determinations.

Cesium solvent extraction methods were investigated by Bray and Roberts (110) for possible use at Hanford. Dipicrylamine, dissolved in a high-dielectric - constant solvent such as nitrobenzene, was found to be a very effective and highly selective extractant for cesium.

Three successive, equal-volume, ambient temperature batch extractions, of both Alkaline Supernate and Purex Acidic Waste (1WW), removed over 98% of the third initial cesium. Purification for other fission products was excellent for DF's from Ce-144, Ru-106, and Zr-Nb-95 ranging from several hundred to several thousand.

A new, quick and efficient solvent extraction method of separating various constituents from irradiated fuel samples has been evolved by Healy (111) at Harwell. In this method the following groups are isolated, using diethyl hexyl phosphoric acid, (HDEHP), as solvent: (1) Ru, Cs, Sr, Ba, (2) Ce, (3) Y plus rare earths, (4) Zr and Nb. Further solvent extraction methods are used for separation of individual elements.

In addition, a rapid method is described for the extraction and estimation of zirconium-95 from fission product solution utilizing HDEHP. The method using HDEHP usually takes half an hour and an accuracy of ± 1% is obtained. The effective extraction results for Ru, Cs, Sr, Ba, I_2, La, Ce, Y and Zr-Nb are summarized.

An efficient radiochemical method for the determination of cerium-144 was developed by Awwal (112). This method is based on the principle of the synergic effect in solvent extraction with 2-thenoyltrifluoracetone and tri-n-butyl phosphate. The mixed solvents enhanced the extraction by 10^3- fold over either of the components alone. The extraction procedure provided a clean and efficient separation of radiocerium from other fission products. Ten extractions were made and the average yield was 91.2 ± 0.7% removal.

Astakhov, Mikhaleva, and Teslin (113) studied the possibility of isolating Ru-106 from aqueous solutions by extraction with sodium piperidinedithiocarbamate. Extraction took place from ammonium acetate buffer solutions with pH values from 1.3 to 11 and from an aqueous solution containing only the extractant, using a solution of radioactive $RuCl_3$ with an activity of 15 to 20 x 10^4 cpm/ml. The maximum extraction or removal of Ru-106 was 99.5% which occurred at a pH of 7.08 using two extraction cycles.

9. Evaporation

One of the first evaporators used to concentrate and decontaminate radioactivity was installed in 1949 at the Oak Ridge National Laboratory (114). The evaporator was a steam heated pot still with a capacity of 300 gal/hr. A decontamination factor of 10^5 was obtained with a volume reduction of about 60 to 1.

According to Rodger (115), evaporation has proved to be exceedingly useful in the processing of radiochemical wastes at both production and research sites. A wide variety of wastes can be evaporated and many types of evaporators have been used. Decontamination factors as high as 10^5 have been achieved in a single effect. With a double-effect evaporator overall decontamination factors of 10^8 were reported.

Chemical precipitation followed by filtration and followed by ion exchange, as proposed by Cartwright (72), yields a DF of 10^3 to 10^4. Treatment with an evaporator, followed by a separator packed with wire mesh yields a DF of 10^5.

The evaporator at KAPL (114) is a single-effect, forced-circulation type with a capacity of 300 gal/hr. A decontamination factor to 10^7 has been obtained.

The following table gives the performance data for most of the larger radioactive waste evaporators.

TABLE XXIII

Decontamination Achieved by Radioactive Waste Evaporators

Location	References	Date Installed	Type	Capacity gal/hr	Performance Concentrate	DF
ORNL	(116)(117) (a)	1949	pot with steam coil	300	60:1	10^5
KAPL	(117)(118) (a)	1950	A	300	70% solids	10^7
BNL	(119)(117) (a)	1952	B	300		10^6
Bettis	(117)(120) (a)		Recompression	200		10^3

A = forced circulation with four-bubble tray separator
B = recompression with wire mesh separator
(a)= see reference (121)

Glueckauf (122) reports that evaporation, though expensive, is effective since very few of the dissolved species are volatile and all the dissolved material, both ionic and non-ionic, is removed, while in chemical treatments and ion exchange only ionic solutes are removed.

In the absence of volatile isotopes (i.e. I-131) decontamination factors of over 10^4 can be obtained by evaporation and condensation without removal of entrained liquid. Decontamination factors between 10^5 and 10^7 can be obtained by the use of

entrainment separators. Glass wool was found to be a better separator than either Raschig rings or bubble-cap towers according to Glueckauf (122). Evaporation is currently practiced where there are severe restrictions on the amount of activity that can be discharged. The loss of iodine from the evaporator may be decreased by operating in alkaline solution.

10. Biological Uptake

Fontaine and Aeberhardt (123) conducted an experimental laboratory study on radioactive cerium-144 contamination of a complex fresh-water community which extended over a period of 41 days. The cerium-144 is rapidly extracted from the water by fixation on all solids and living organisms, particularly on green algae and water fleas (Daphnia). Internal contamination of fish and moluscs was very slight, but these animals were exposed to intense irradiation due to the presence of cerium-144 in their digestive tracts. Eighteen days after introduction of the radioelement the concentration of cerium-144 in the above algae, water fleas, molusc viscera and contents of the digestive tracts of the fish varied between 20 and 300 times the initial radioactivity (per g) of the water. The viscera of the moluscs undergo irradiation estimated at 215 rad/day, for an initial contamination of the water of 0.02 μc/g.

11. Coprecipitation and Fusion

Levi (124) in a comprehensive report has investigated the coprecipitation of various radionuclides effected by a coprecipitation mechanism using titanium dioxide hydrate. The results which have been obtained are summarized in Table XXIV.

TABLE XXIV

Maximum Decontamination Factors For Various Radionuclides

Radionuclide	Optimum pH	DF
Sr-89	12	> 1000
Ce-144	10	> 1000
Zr/Nb-95	10	400
Ru-106	8	7
Cs-137	--	1.1
I-131	4	1.2

Krieger, Goldin and Straub (107) also employed coprecipitation in their studies to remove long-lived hazardous fission products and some of the results are shown in Table XXI. Maximum removal efficiencies from coprecipitation were 99.8% for Sr-89, 97.9% for Ru-106, 99.9% for Cs-137 and 99.98% for Ce-144. The authors also reported removals of 99.94% for Y-91 and 99.8% for Zr-Nb-95, although these values were not reproduced in Table XXII.

Watson (125) found that a Raschig-ring-packed tower with counter-current flow of air and nitric acid gave an indicated DF of 10^3 on the gross activity unadsorbed by iron oxide-firebrick treatment. An inefficient caustic scrubber gave a further DF of 2 to 10. Generally over 99% of ruthenium and over 95% of the cesium was removed by the iron oxide coated firebrick granule adsorption treatment. Filtration yielded a DF which averaged 70, according to Watson.

Caulkins (126) reports that coprecipitation of low-level radioactive materials with glass forming solids, followed by filtration, drying, and fusing to a chemically stable block can produce effective decontaminations. The best results were achieved from a lead borosilicate glass precipitated from solution at pH 11. With the addition of small amounts of calcium silicate, a DF of about 10^3 is obtained. However, the major difficulty in obtaining consistently good decontamination factors occurred when waste streams contained detergents or complexing agents.

D. Emergency Methods for the Decontamination of Radioactive Water

A review of the literature reveals that few emergency-type decontamination units are presently available for municipal use, although the U.S. Army has developed several mobile units which could find wide application for public use in an emergency. Efforts by the Department of the Army (Corps of Engineers, Office of the Surgeon General) are continuing and intensifying toward a more efficient and lightweight unit. In addition, several smaller decontamination units are commercially available, most of these employ ion exchange techniques.

Additional treatment following conventional water treatment processes would probably be the most efficient means of supplying potable water to a large segment

of the population following radioactive contamination.

Swanson and Associates have recently made a survey of the "Control of Radioactive Fallout in Water Systems" for the Government of Canada (127). The following sources of drinking water were suggested for consideration: ground water wells; ground water springs; household storage; covered reservoirs, clear wells and elevated tanks; ion exchange beds and demineralizers; domestic water softener; clay slurry water treatment; and evaporators and condensers.

Ion-exchange systems, particularly those of mixed bed design, are very efficient decontaminating agents that will usually remove more than 99% of the soluble and insoluble components of water-borne contamination.

Many areas will experience a considerable delay before fallout arrives after a nuclear attack. A few minutes of this period may be profitably spent in filling bathtubs, basins and buckets with uncontaminated water. Provided that windows and doors are closed and that paper or cloth covers are placed over the filled receptacles, there is little danger of the stored water becoming contaminated.

The foregoing sources of supply are those that are likely to be found already in existence. However, research has pointed to newer methods of removing radioactive contaminants from water. Almost all of them depends on fixing radioactive elements by an ion exchange process. Some use natural ion-exchange or adsorption media; others use artificial zeolites. One of the most promising of these processes uses clinoptilolite, a volcanic glass that has produced excellent results in experimental work carried out by the Atomic Energy of Canada at Chalk River, Ontario, while vermiculite has been used with considerable success at a nuclear energy establishment in England.

1. Municipal Size Decontamination Units

Woodward and Robeck (128) reported on an ion exchange process that may be used to supplement the normal water treatment procedure. An ion exchange column in the form of a cartridge is inserted into the system and is disposed of after breakthrough occurs. The type of resin will vary according to the time after deto-

nation that the water will be put into use. A mixed-bed resin will be necessary for immediate use of the water, whereas a cation resin will suffice for long-term usage, due to the decay of short-lived iodine-131. The life of each ion cartridge will depend upon the total solids present.

Although large, centrally located, decontamination units are more economical, smaller decentralized units would be preferable as the problem of water distribution would be lessened.

2. Field Decontamination Units

The U.S. Army (129)(130) has developed several mobile decontamination units primarily for use by troops in the field, but these could also be used to supply water for small population groups in case of nuclear attack. One such unit is comprised of a flocculator, filters, dual-bed ion exchange column and a chlorinator. The entire unit is mounted on two 2-1/2 ton trucks. A 1,500 gph output is obtainable. Regeneration of the ion exchange resins is effected by hydrochloric acid and soda ash.

(a) Mobile Water Purification Units

Lindsten and Schmitt (131) reported that with the Army's Standard Mobile Water Purification Unit (1,500-GPH) and Prctotype Mobile Ion Exchange Unit (1,500-GPH) the following decontamination results can be obtained as shown in Table XXV.

The Army Corps of Engineers (132) tested three decontamination methods for water: an Erdlator [a], a mobile ion exchange unit, and an electrodialytic demineralizing unit.

The Erdlator followed by ion exchange yielded a decontamination factor of 1.2×10^4 for soluble Sr-Y-90. The same combination resulted in a decontamination factor of 6.4×10^3 for Cs-137. With the electrodialysis process a decontamination factor of 1.1×10^3 was obtained for Cs-137.

(a) Erdlator is standard purification unit consisting of chemical coagulation and diatomite filtration.

TABLE XXV

Removal of Radioactive Materials from Water at A.E.C.'s Nevada Test Site by the Standard Mobile Water Purification Unit (1,500-GPH) and Prototype Mobile Ion Exchange Unit (1,500-GPH)

Contaminant	Process	% Removal
Nuclear bomb debris 1-year old	Coagulation & Filtration	99.2
Strontium-90, Yttrium-90	Coagulation & Filtration	
	Strontium-90	13.3
	Yttrium-90	96.7
	Coagulation, Filtration & Cation exchange (H cycle) Strontium-90, Yttrium-90	> 99.9
Cesium-137, Barium-137	Coagulation & Filtration	2.4
	Coagulation, Filtration & Cation exchange (H cycle)	> 99.9
Strontium-90, Yttrium	Cation Exchange (Na cycle)	
	Strontium-90	95.5
	Yttrium-90	74.6

Swanton and Hyman (133) reported that a liquid radioactive waste disposal facility was designed, developed, and installed at the Nuclear Defense Laboratory. The facility employs a film evaporator to effect gross decontamination of the waste and concentration of the waste by a factor of approximately 100. The condensate is further decontaminated by passage through mixed-bed demineralizers. The facility is self-contained, transportable, semi-automatic assembly of monitoring, feed, and residue tanks. Results of preliminary evaluation tests, using feed spiked with Co-60 to an activity > 8.7×10^{-4} μc/ml in β activity, indicate an overall DF of approximately 10^6 to 10^7. The DF for alpha activity appears to be about 10^3.

(b) Mobile Distillation Unit

Lindsten and Schmitt (131)(134) report that a trailer-mounted, 60-gph, thermocompression distillation unit can remove 99.98 percent of mixed fission products, 99.96 percent of proctactinium-223, and 99.86 percent of I-131 from contaminated water. These figures correspond to decontamination factors of 4.1×10^3, 2.3×10^3, and

7.0×10^2, respectively. The use of an experimental glass-wool, steam filter improved the performance even further.

(c) Miscellaneous Decontamination Units

A unit known as Ray-Di-Pak combines distillation and demineralization for a reported decontamination factor of 10^6 and a distillate solids content of 2 ppm. The waste is evaporated at low temperature and high vacuum (135).

Nease (136) and Lacy (137) describe a method of radioactive water decontamination whereby the water is passed through a column of natural materials, such as clay, leaves, humus, gravel and sand. Removals of over 90% were reported. The problem would be to obtain uncontaminated materials from the environment for use in such a column.

E. Discussion and Conclusions

The six biologically important radionuclides that appear initially in contaminated water are Ba, Cs, I, La, Ru and Sr. Laboratory data indicate that the combination of standard water treatment methods, namely, coagulation, lime-soda ash softening, and sand filtration, is capable of removing 99% strontium. The removal of 95% iodine can be accomplished by the addition of silver ions.

Lower plant scale efficiencies, in comparison to laboratory results, generally result from two major factors: (a) among the various decontamination processes mentioned, only one or two may be employed by the conventional water treatment plant and the operating conditions may not be optimized; and (b) the radionuclides are generally present under controlled laboratory conditions in the form of simple salts. In contrast, the contaminants in water reaching the treatment plant are generally more difficult to remove because the readily removable portion has already been eliminated by natural decontamination mechanisms before reaching the water plant.

Fundamental developments in nuclear methods of analysis from late 1961 to late 1963 have been presented in a general review by Leddicotte (138). A major portion of this review was concerned with applications of radioisotopes as tracers. Sections

on activation analysis, isotope dilution and radiometric methods, separation procedures, and the use of radioisotopes as sources and as tracers in developing analytical methods were presented. In addition, significant information about investigations in age determinations, radiochemistry measurement, and the use of computer-integrated programs to reduce data from such measurements to an accurate and reliable form was given. Leddicotte (138) cited 1767 references of which 22 are of interest as potential decontamination processes.

It should be pointed out that the decontamination data reported in the literature, both on laboratory and plant scale, are based on one of the following three sources of radioactivity:

(1) added radioactive salts
(2) low-level radioactivity waste
(3) long-range (world-wide) fallout from atomic bomb tests

The chemical and physical characteristics of radioactive materials from any of the above sources is different from that present in local fallout. The latter is characterized by a water solubility of 2 or 3% and not to exceed 50% in comparison to the 50% or higher solubility of radioactive materials of the above three categories. Low water solubility generally will increase the removal of local fallout by conventional water treatment methods which are efficient in dealing with particulate or colloid materials.

The maximum decontamination factor for each of six selected elements are listed in Table XXVI. These values are based on the best available data in the literature. It is emphasized that the percentage of removal is greatly dependent on the chemical and physical state of the radioactive element, as well as the concentration of the treatment additives, and other related conditions such as pH and temperature of the water. It is apparent from this table that ion exchange is the only single decontamination process that will remove sizeable amounts of each of the six selected isotopes and that no process will adequately remove the maximum radioc nt minant, namely I-131.

TABLE XXVI Maximum Decontamination Factors Reported for Selected Isotopes and Gross Fission Products

Decontamination Factors (D.F.) and Literature References

Decontamination Method	Ba-140	Cs-137	I-131	La-140	Ru-106	Sr-89,90	Gross Fission Products
1. Chemical Coagulation	6.2 (39)	5×10^2 (45)	25 (39)	6.2 (39)	25 (39)	2.5×10^2 (42)	11 (40)[d]
2. Lime-Soda Softening	10^2 (67)	1.3 (140)		10 (67)		3.3×10^2 (46)	10 (40)[d]
a. Hot Softening						$>10^3$ (50)	17 (50)
3. Rapid Sand Filtration	10^2 (39)	3.3 (39)		10^2 (39)		20 (39)	7.7 (40)
4. Ion Exchange	10^4 (46)	10^4 (46,59)	10^3 (142)	10^3 (46)	2×10^2 (67)	$3\text{-}12\times10^3$; 5×10^4 (64,54) ; (58)	$10^5\text{-}10^6$ (57)
5. Clinoptilolite		10^7 (87)			10^5 (73)	6.4×10^9 (69)	$2\text{-}8\times10^7$ (71)
6. Phosphate Coagulation	8.2 (139)	1.5 (142)		50 (139)	10^2 (98)	45 (102,143)	$>10^2$ (102)
7. Clay	50 (92)	50 (46,94)	2.4 (92)	35 (9C)	2.6 (90)	$0.25\text{-}1\times10^4$ (54)	10.3 (90)
8. Metalic Dusts	19.4 (53)	2.4 (96,53)	2.8 (53)	19.4 (53)	250 (53)	3.3 (96)	
9. Coagulation w/Silver Ions			2.2×10^1 (144)				
10. Coagulation with Clay	33 (145)	33 (145)	1.1 (46)	6.7 (46)	3.8 (145)	2.0 (46,40)	
11. Coprecipitation & Solvent Extraction	10^3 (111)	10^3 (107)	10^2 (111)	10^2 (111)	48 (107)	10^3 (124)	
12. Lime-Soda with Clay		7.1 (145)			4.2 (145)		
13. Foaming (Flotation)	167 (76)	>25; 10^4 (105) (76)		4.5 (103)	11 (103)	$>1.5\times10^4$ (106)	7 (105)
14. Slow Sand Filtration			2 to 9 (47,147)		7 (48)	10^2 (47)	50 (47)
15. Mobile Water Purification Unit		6.4×10^3 (132)				1.2×10^4 (132)	7(134)[a] 14(134)[b] 10^7 10^3(134)[c](133)[e]
16. Mobile Distillation Unit		10^5 (72)	7.0×10^2 (131,134)				4.1×10^3 (131,134)

[a][b] coagulation, filtration, and disinfection procedure.
[c] procedure (a) with clay pretreatment.
[d] procedure (b) with post ion exchange treatment.
[e] trivalent rare earths.
overall D.F. for β activity.

The results of these investigations show the high level of development and sophisticated methodology which has been achieved to obtain the high degree of removal of individual radionuclides. To achieve the necessary degree of decontamination was considered almost unattainable just a few years ago. The development of sorption materials and techniques must be credited with much of this success.

VI. COMPUTER PROGRAMS FOR THE FALLOUT MODEL

Computer programs in various stages of development were presented in previous reports (36)(34)(26)(14)(17), issued in that order. The final programs, if previously incomplete or in error, are reproduced in this section.

A. Idealized Ionization Rate Contours

Although the physical characteristics and the mathematical approximation for the rising stem and the cloud have been discussed in detail, little was said about how the fallout contours are determined.

The method used in this model to construct the ionization rate contours, also called fallout patterns or intensity contours, is mainly by scaling actual test data of the intensity at selected downwind distances as a function of weapon yield and particle size parameter. The fallout pattern is obtained by projection from the intensity profile. This method was discussed in considerable detail in Interim Technical Report No. 1 (26) and a computer program, written in ALGOL, was presented previously as Figure 5, p. 44(28). Because most of the observed properties of the fallout patterns are in terms of intensity, the fallout contours are usually given in units of roentgen/hour (where the time has been corrected to a standard reference time of H + 1 hour). The general shape of the fallout pattern can be obtained by the overlapping of ellipses for both the stem and cloud fallout.

Figure 22 presents the flow diagram for the ionization rate contour computer program, written in FORTRAN II language. As presented in Figure 23, the ionization rate contour program was run for 5, 10 and 20 MT weapon yields. Various scaling functions were read into the computer. The evaluation was performed for a constant wind velocity of 15 mph. The resultant downwind and crosswind distances are in miles and the intensities in r/hr.

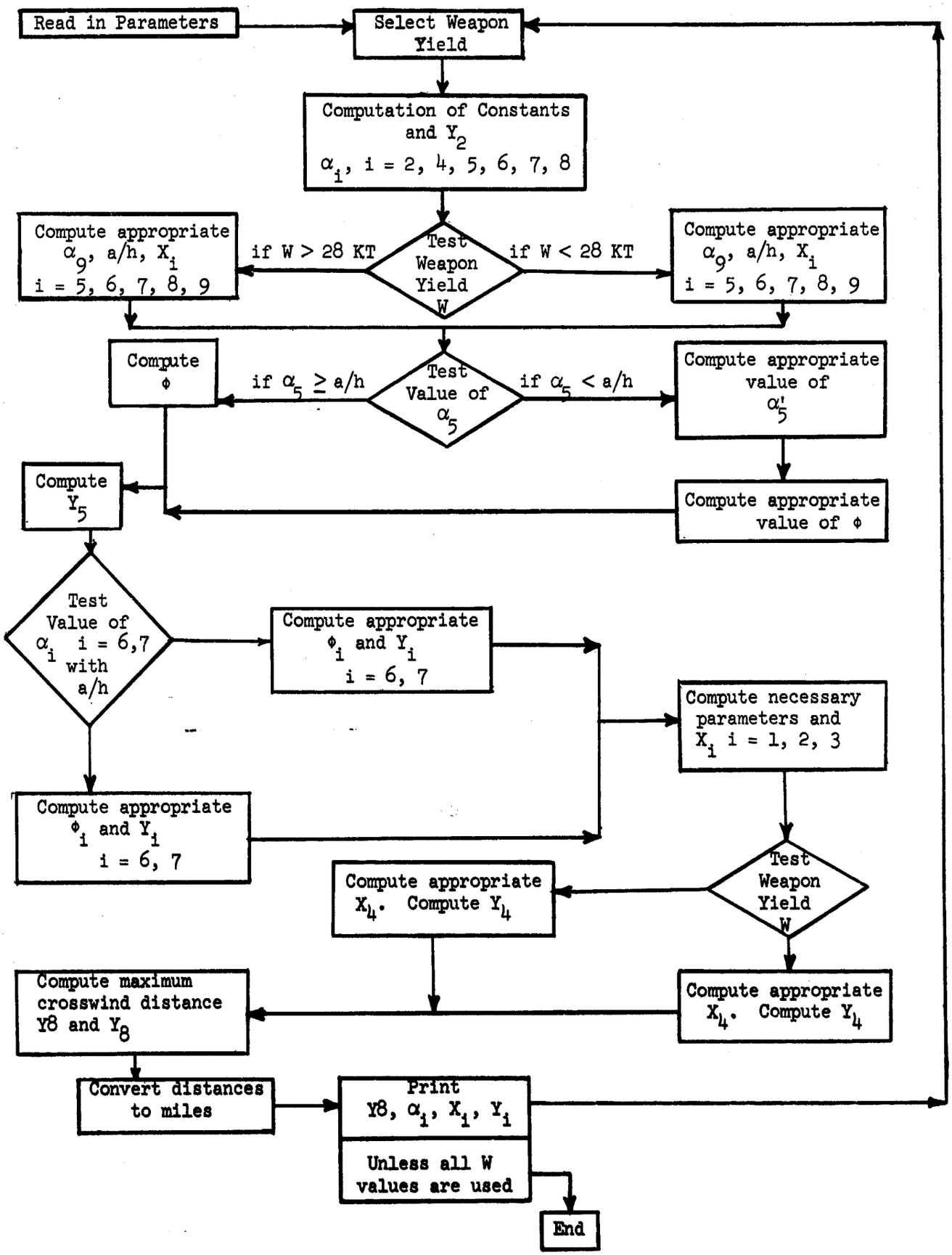

Figure 22. Flow Diagram for Ionization Rate Contour Computer Program

```
*       N1585-1463,FMS,DEBUG,1,5,2000,0    GOLLER  8-24-64
*       XEQ
        INTENSITY CONTOUR AND PROFILE POINTS
        DIMENSION Z(4), VN(4), WW(4)
        READ 101, VN
        READ 102, WW, Z
        DO 1000 I=1,4
        W=WW(I)
        VW=22
        WL=LOGF(W)/LOGF(10.)
        AB2=10.**(.[illegible]2*WL)
        A=10.**(3.3[illegible]*WL)
        ALPHA5=10.**([illegible]+.022*WL)
        ALPHA4=10.**(.27+.089*WL)
        ALPHA2=10.**(-.509+.076*WL)
        ALPHA6=10.**(0.03+.036*WL)
        ALPHA7=10.**(.043+.141*WL)
        ALPHA8=10.**(.185+.151*WL)
        YINT2=10.**(2.088-.452*WL)*Z(I)*(VW*15./22.)**VN(I)
         IF(W-28.)1,1,2
      1 ALPHA9=10.**(1.371-.124*WL)
        CC=6.6E3*W**.445
        X5=CC*ALPHA5
        X6=CC*ALPHA6
        X7=CC*ALPHA7
        X8=CC*ALPHA8
        X9=CC*ALPHA9
        AH=10.**(-.431-.014*WL)
        AK5=10.**(-3.286-.289*WL)
        BK12=10.**(-2.503-.404*WL)
        GO TO 3
      2 ALPHA9=10.**(.98+.146*WL)
        CC=1.68E4*W**.164
        X5=CC*ALPHA5
        X6=CC*ALPHA6
        X7=CC*ALPHA7
        X8=CC*ALPHA8
        X9=CC*ALPHA9
        AH=10.**(-.837+.267*WL)
        AK5=10.**(-2.889-.572*WL)
        BK12=10.**(-2.6-.337*WL)
      3 IF(ALPHA5-AH)4,6,6
      4 ALPHA5=10.**(-.054+.095*WL)
        IF(W-28.)41,41,42
     41 X5=6.6E3*W**.445*ALPHA5-1.4E3*W**.3*SQRTF(3.06*W**.262+ALPHA5**2)
        GO TO 43
     42 X5=1.68E4*W**.164*ALPHA5-1.4E3*W**.3*SQRTF(3.06*W**.262+ALPHA5**2)
     43 IF(ALPHA5-AH)5,6,6
      5 PHI=(ALPHA5+AH+SQRTF(AB2+(ALPHA5+AH)**2))/(ALPHA2+SQRTF(AB2+ALPHA2
       1 **2))
        AK5=10.**(-3.185-.406*WL)
        GO TO 7
      6 PHI=(ALPHA5+AH+SQRTF(AB2+(ALPHA5+AH)**2))/(ALPHA5-AH+SQRTF(AB2+
       1 (ALPHA5-AH)**2))
      7 YINT5=4.606*A*AK5*LOGF(PHI)/LOGF(10.)
```

Figure 23. Computer Program for Ionization Rate Contours

```
      IF(ALPHA6-AH)9,8,8
    8 AK6=10.**(-1.134-.074*WL)
      PHI=(ALPHA6+AH+SQRTF(AB2+(ALPHA6+AH)**2))/(ALPHA6-AH+SQRTF(AB2+
     1 (ALPHA6-AH)**2))
      GO TO 10
    9 AK6=10.**(-1.225-.022*WL)
      PHI=(ALPHA6+AH+SQRTF(AB2+(ALPHA6+AH)**2))/(ALPHA2+SQRTF(AB2+ALPHA2
     1 **2))
   10 YINT6=4.606*A*LOGF(PHI)/LOGF(10.)*AK6
      IF(ALPHA7-AH)12,11,11
   11 AK7=10.**(-.989-.037*WL)
      PHI=(ALPHA7+AH+SQRTF(AB2+(ALPHA7+AH)**2))/(ALPHA7-AH+SQRTF(AB2+
     1 (ALPHA7-AH)**2))
      GO TO 13
   12 AK7=10.**(-1.079-.02*WL)
      PHI=(ALPHA7+AH+SQRTF(AB2+(ALPHA7+AH)**2))/(ALPHA2+SQRTF(AB2+ALPHA2
     1 **2))
   13 YINT7=4.606*A*AK7*LOGF(PHI)/LOGF(10.)
      YINT9=22./VW
      AS=10.**(2.88+.348*WL)
      H=10.**(4.226+.164*WL)
      ARSL=1.07+.098*WL
      RS=10.**(2.319+.333*WL)
      AKS=2.303*ARSL/(H-RS)
      AO=10.**(LOGF(A)/LOGF(10.)-H*ARSL/(H-RS))
      ZS=2.303*(LOGF(AS)/LOGF(10.)-LOGF(AO)/LOGF(10.))/AKS
      X2=ALPHA2*ZS-AS
      X3=ALPHA2*ZS+AS
      X1=X2-2.303*(LOGF(YINT2)/LOGF(10.))/BK12
      IF(W-9.)14,15,15
   14 ZO=H-A/SQRTF(10.**(.486+.262*WL))
      GO TO 18
   15 IF(50000.-ZS)16,17,17
   16 ZO=(1160.+(ALPHA2+.035)*ZS)/ALPHA2
      GO TO 18
   17 ZO=(1900.+(ALPHA2+.02)*ZS)/ALPHA2
   18 X4=VW*(ZO*ALPHA4/VW-86.36)/(1.+9.273E-4*VW/ALPHA4)
      YINT4=22./VW
      Y8=EXPF((((((9.9684814E-4)*LOGF(W)-.027025999)*LOGF(W)+.22433052)
     1 *LOGF(W)-.12350012)*LOGF(W)+8.7992249)
      YINT8=10.**(LOGF(YINT7)/LOGF(10.)*(X9-X8)/(X9-X7))
      X1=X1/5280.
      X2=X2/5280.
      X3=X3/5280.
      X4=X4/5280.
      X5=X5/5280.
      X6=X6/5280.
      X7=X7/5280.
      X8=X8/5280.
      X9=X9/5280.
      Y8=Y8/5280.
      PRINT 103,ALPHA2, ALPHA4,ALPHA5,ALPHA6,ALPHA7,ALPHA8,ALPHA9,Y8,X1,
     1  X2,X3,X4,X5,X6,X7,X8,X9,YINT2,YINT4,YINT5,YINT6,YINT7,YINT8,YINT
```

Figure 23. (cont'd) Computer Program for Ionization Rate Contours

```
    2 9
1000 CONTINUE
 101 FORMAT (4F5.2)
 102 FORMAT (8F5.0;
 103 FORMAT (8E15.5)
     CALL EXIT
     END
*    DATA

          PART OF THE RESULTS
     5 M.T.
  X1          X2          X3          X4          X5          X6          X7          X8          X9
-10.550      .72385      6.2911      26.273      6.0703      18.727      47.191      71.261      425.95
  I1          I2          I3          I4          I5          I6          I7          I8          I9
   1        4787.7      4787.7           1           1      3814.6      6286.8      3606.1           1
  Y8 = 54.422
     10 M.T.
  X1          X2          X3          X4          X5          X6          X7          X8          X9
-13.150      .58521      7.6711      30.801      4.3961      21.512      58.301      88.649      528.05
  I1          I2          I3          I4          I5          I6          I7          I8          I9
   1        3544.6      3544.6           1           1      5248.2      9057.0      5027.4           1
  Y8 = 65.219
     20 M.T.
  X1          X2          X3          X4          X5          X6          X7          X8          X9
-16.389      .35717      9.3761      36.225      1.4010      24.710      72.026      110.28      654.63
  I1          I2          I3          I4          I5          I6          I7          I8          I9
   1        2668.0      2668.0           1           1      7218.3      13047.      7003.1           1
  Y8 = 77.073
                                                                                          136

                                                                          TOTAL           136*
```

Figure 23. (cont'd) Computer Program for Ionization Rate Contours

B. Ionization Rate at Any Location for Multiple Weapons

For multiple weapon yields having the same ground zeros and prevailing wind directions, the computer program for single weapon yield can be easily modified to evaluate their cumulative effects, by a few changes in the program to effect direct summation. However, for multiple weapon yields having different ground zeros and prevailing wind directions, the problem is somewhat more complicated. A method has been devised to evaluate the cumulative effect at a location inside the fallout region from two weapons. This method can be readily generalized for more than two weapons.

The method takes advantage of trigonometric expressions to directly evaluate the relations between (x_1, y_1) and (x_2, y_2). They are:

$$x_2 = (x_1 - r) \cos \theta - y_1 \sin \theta + R$$

$$y_2 = (x_1 - r) \sin \theta + y_1 \cos \theta$$

The physical significance of R, r, θ can be seen from the following sketch:

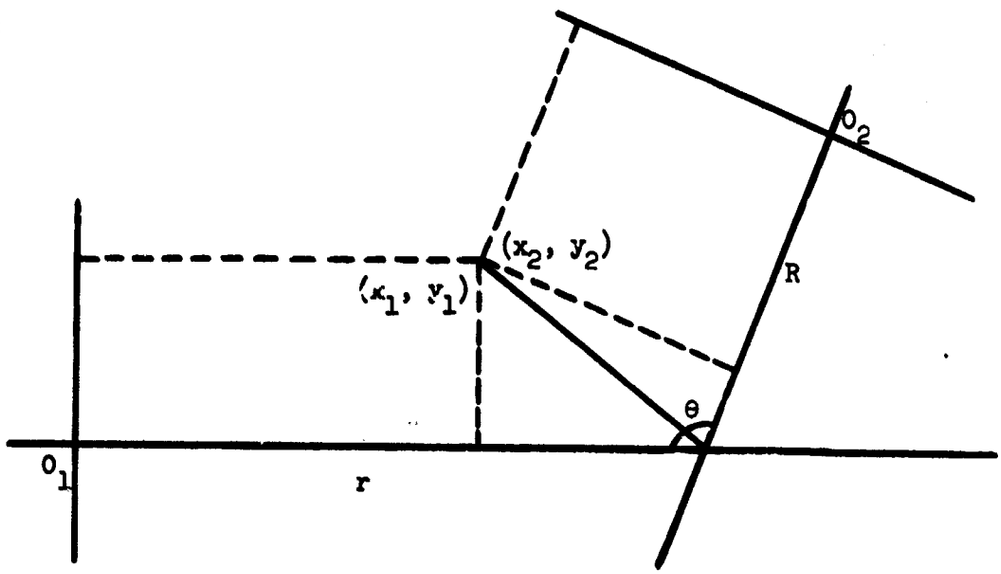

The program which follows was run for a combined five and ten megaton detonation. The input data used was that computed by the program for ionization rate contours for a single weapon. Evaluation of the intensity in r/hr was completed for various downwind and crosswind distances as shown in Figure 24, the flow diagram to evaluate the ionization rate at any location for multiple weapons and Figure 25, the actual computer program for multiple weapons.

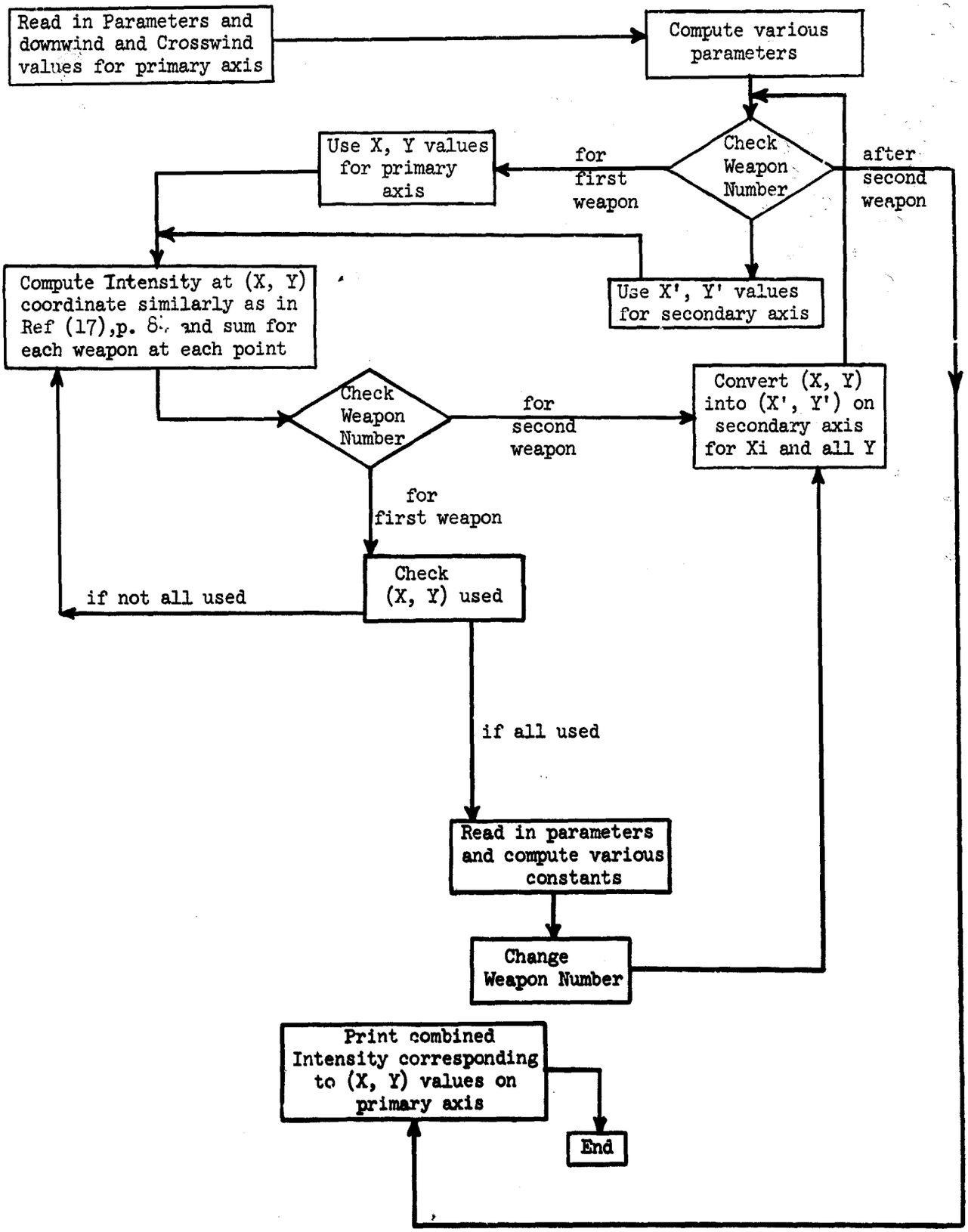

Figure 24. Flow Diagram for Ionization Rate at Any Location for Multiple Weapons Computer Program

```
*       N1585-1463,FMS,DEBUG,1,5,2000,0     GOLLER    8-24-64
*       XEQ
        MULTIPLE WEAPON YIELD
        DIMENSION A(42,13), XX(42), YY(13),XN(13), YN(13)
        READ 100,X1,X2,X3,X4,X5,X6,X7,X8,X9,Y8,A2,A6,A7,R,RR,THE
        READ 101,XX,YY
        LN=1
        I=1
        XP8 = X8 - (LOGF(A6)/LOGF(A7))*(X8 - X7)
        YP8 = ((XP8 -X7)/(X8 - X7))*Y8
        C1 = (X2 - X1)**2
        C2 = (X2 - X1)
        C3 = (X4 - X3)**2
        C4 = X8*Y8**2
        C5 = X7*(X5 - X8)**2
        C6 = (X5 - X8)*Y8
        C7 = (X5 - X8)**2
        C8 = (X8 - X7)**2
        C9 = (X8 - X7)
        C10 = XP8*YP8**2
        C11 = (X6 - XP8)**2
        C12 = (X6 - XP8)*YP8
        C13 = (XP8 - X7)**2
        C14 = (X9 - X8)**2
        C15 = (X9 - X8)*Y8
    22  J=1
    33  IF(LN-2)23,34,99
    34  X=XN(J)
        Y=YN(J)
        GO TO 35
    23  X=XX(I)
        Y=YY(J)
    35  IF(X - X2) 1,1,2
     1  RA= SQRTF((X - X2)**2 + Y**2)
        RI = C2 - RA
          ZZ      = EXPF(RI*LOGF(A2)/C2)
         GO TO 12
     2  IF(X-X3) 3, 3, 4
     3  RA= C2 - Y
        AA=EXPF(RA*LOGF(A2)/C2)
        GO TO 6
     4  IF(X-X7)5,5,8
     5  AA= EXPF(LOGF(A2)*(SQRTF(C3*(X-X3)**2*C1/((X-X3)**2*C1+Y**2*C3))
      1 +X3-X)/SQRTF(C3*(X-X3)**2*C1/((X-X3)**2*C1+Y**2*C3)))
        AO = (X-XP8)**2/C11+Y**2/YP8**2
        IF(AO-1.)7,7,6
     6  XA1 = (((X-X7)**2*C4+C5*Y**2)-(X-X7)*C6*SQRTF((X-X7)**2*Y8**2+C7
      1 *Y**2-C8*Y**2))/((X-X7)**2*Y8**2+C7*Y**2)
        XA6 = (((X-X7)**2*C10+X7*C11*Y**2)-(X-X7)*C12*SQRTF((X-X7)**2
      1 *YP8**2+C11*Y**2-C13*Y**2))/((X-X7)**2*YP8**2+C11*Y**2)
        AB = EXPF((X-XA1)/(XA6-XA1)*LOGF(A6))
         ZZ       = AA + AB
        GO TO 12
     7  XA6 = (((X-X7)**2*C10+X7*C11*Y**2)-(X-X7)*C12*SQRTF((X-X7)**2
      1 *YP8**2+C11*Y**2-C13*Y**2))/((X-X7)**2*YP8**2+C11*Y**2)
```

Figure 25. Computer Program for Ionization Rate at Any Location for Multiple Weapons

```
      AB=EXPF((XA6-X)/(XA6-X7)*(LOGF(A7)-LOGF(A6)))+A6
        ZZ      = AA + AB
      GO TO 12
    8 IF(Y-(X-X7)/C9*Y8)9,9,5
    9 XA1 = (((X-X7)**2*C4+X7*C14*Y**2)+(X-X7)*C15*SQRTF((X-X7)**2
     1 *Y8**2+C14*Y**2-C9**2*Y**2))/((X-X7)**2*Y8**2+C14*Y**2)
        ZZ      = EXPF((XA1-X)/(XA1-X7)*LOGF(A7))
   12 A(I,J)=A(I,J)+ZZ
      J=J+1
      IF(J-13)33,33,44
   44 I=I+1
      IF(I-42)55,55,66
   55 IF(LN-2)22,77,99
   66 READ 100, X1, X2, X3, X4, X5, X6, X7, X8, X9, Y8, A2, A6, A7,
     1 R, RR, THE
      XP8 = X8 - (LOGF(A6)/LOGF(A7))*(X8 - X7)
      YP8 = ((XP8 -X7)/(X8 - X7))*Y8
      C1 = (X2 - X1)**2
      C2 = (X2 - X1)
      C3 = (X4 - X3)**2
      C4 = X8*Y8**2
      C5 = X7*(X5 - X8)**2
      C6 = (X5 - X8)*Y8
      C7 = (X5 - X8)**2
      C8 = (X8 - X7)**2
      C9 = (X8 - X7)
      C10 = XP8*YP8**2
      C11 = (X6 - XP8)**2
      C12 = (X6 - XP8)*YP8
      C13 = (XP8 - X7)**2
      C14 = (X9 - X8)**2
      C15 = (X9 - X8)*Y8
      LN=LN+1
      I=1
   77 X=XX(I)
      J=1
  122 Y=YY(J)
      XN(J)=RR-Y*SINF(THE)+(X-R)*COSF(THE)
      YN(J)=Y*COSF(THE)+(X-R)*SINF(THE)
      J=J+1
      IF(J-13)122,122,22
   99 DO 1000 I=1,42
      DO 1000J=1,13
      PRINT 102, XX(I), YY(J), A(I,J)
 1000 CONTINUE
  100 FORMAT (7F10.4)
  101 FORMAT (6F12.0)
  102 FORMAT(2F5.0,E20.8)
      CALL EXIT
      END
*     DATA

          PART OF THE RESULTS
```

Figure 25. (cont'd) Computer Program for Ionization Rate at any Location for Multiple Weapons

3

A 5 M.T. SUPERIMPOSED ON A 10 M.T.

DOWN WIND DISTANCE	CROSS WIND DISTANCE	INTENSITY IN R/HR
-10 MILES	0 MILES	.79951715E 01
-10 MILES	10 MILES	.68748377E 00
-10 MILES	20 MILES	.52045174E-02
-10 MILES	30 MILES	.21414360E-04
-10 MILES	40 MILES	.71722032E-07
0 MILES	0 MILES	.52329799E 04
0 MILES	10 MILES	.11637860E 02
0 MILES	20 MILES	.25252611E-01
0 MILES	30 MILES	.62974576E-04
0 MILES	40 MILES	.16243138E-06
10 MILES	0 MILES	.25650773E 04
10 MILES	10 MILES	.17887089E 02
10 MILES	20 MILES	.24119284E 01
10 MILES	30 MILES	.70085033E 00
10 MILES	40 MILES	.17642100E 00
20 MILES	20 MILES	.23951590E 02
30 MILES	30 MILES	.26543110E 02
40 MILES	40 MILES	.14196339E 02
50 MILES	50 MILES	.52021906E 01
60 MILES	60 MILES	.15841987E 01
70 MILES	30 MILES	.18689948E 03
80 MILES	40 MILES	.43787947E 02
90 MILES	50 MILES	.10341805E 02
100 MILES	10 MILES	.24146936E 04
140 MILES	30 MILES	.13705508E 03
200 MILES	50 MILES	.65361667E 01
280 MILES	40 MILES	.99201906E 01

137

TOTAL 137*

Figure 25. (cont'd) Computer Program for Ionization Rate at Any Location for Multiple Weapons

C. Evaluation of Fallout Particle Size Distribution at Any Downwind Location

As discussed in previous progress reports (34)(35), provided that the particle fall-rate is known, the particle size groups that fall at any given downwind location can be estimated from scaling functions. The fall-rate for each size particle varies with the altitude from which it falls. Hence, the particle size parameter α represents a group of particles with a range of diameters which is dependent on the thickness of the cloud.

It is necessary to use a different method of evaluation for α values of particles falling from the stem and from the cloud areas. The downwind distance of the point of intersection of the lines connecting (X_5, I_5) to (X_6, I_6) and (X_3, I_3) to (X_4, I_4) on the semi-logarithmic plot of the intensity profile is taken to be the point of division between stem and cloud affected areas. For the purposes of this report, only cloud originating particles are considered.

For particle groups falling inside the cloud range at any downwind location, the maximum and minimum α values can be calculated by:

$$\alpha_m = \frac{hX \pm \sqrt{X^2 b^2 (1-y^2/a^2) + (a^2 - y^2)\left[h^2 - b^2 (1-y^2/a^2)\right]}}{h^2 - b^2 (1-y^2/a^2)}$$

where distances are expressed in feet and where the "plus" sign is used for α_{max} and the "minus" sign for α_{min}. The two extremes for height of fall for cloud fallout are:

$$Z = h \pm \frac{\alpha_m b^2}{\sqrt{a^2 + \alpha_m^2 b^2}}$$

where the "plus" sign is used with α_{min} and the "minus" sign with α_{max}.

These formulae are valid for a constant wind velocity V_w. The fall-rate is:

$$V_f = \frac{V_w}{\alpha_m}$$

A flow diagram and the computer program used to find values for α, Z, and V_f are shown in Figures 26 and 27, respectively. Values were obtained for downwind distances from 15 mi. to 500 mi. and for weapon yields of 5 MT, 10 MT, and 20 MT.

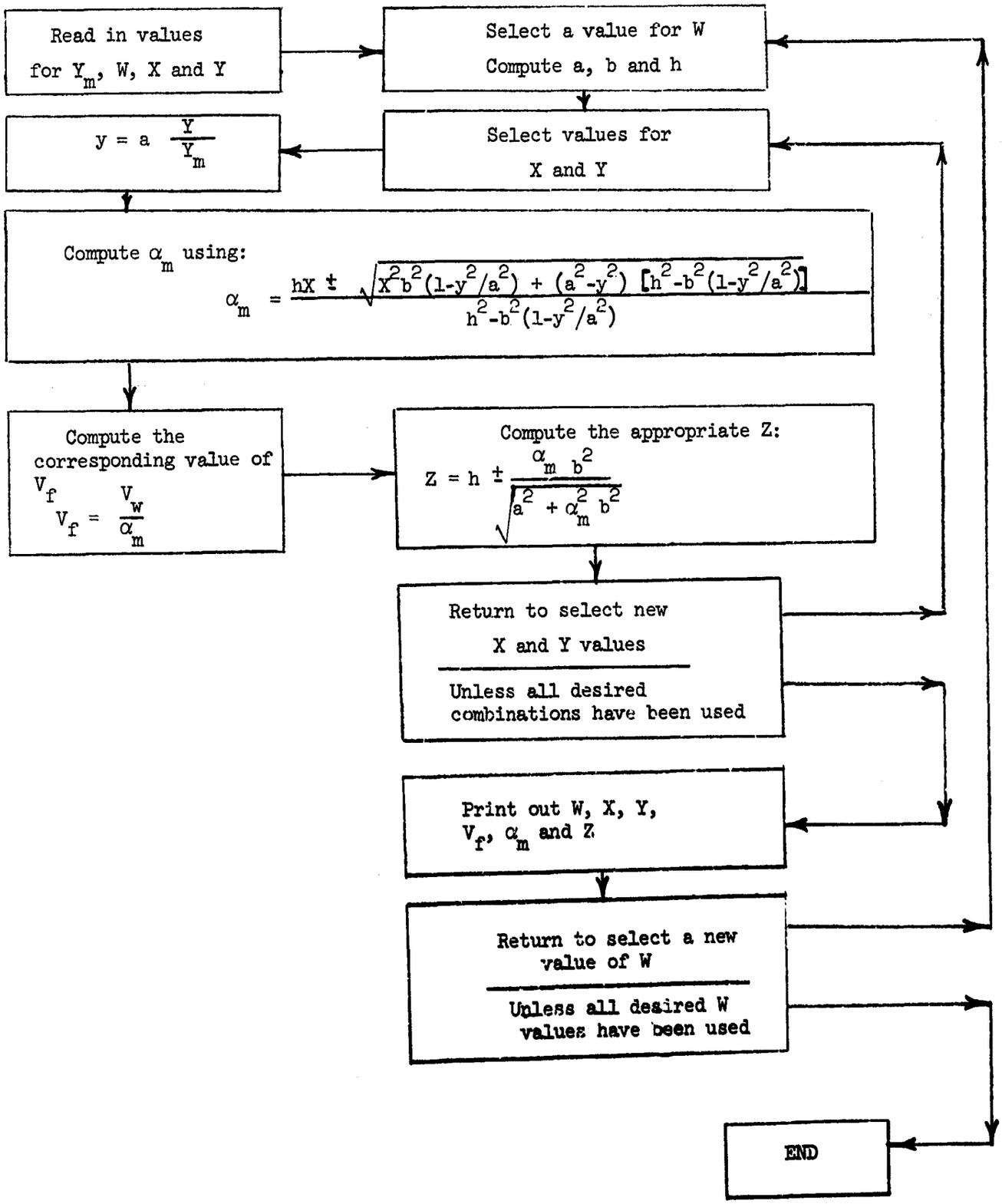

Figure 26. Flow Diagram for Computer Program to Evaluate Fallout Particle Size Distribution for Any Downwind Location

```
*       N1585-1463,FMS,DEBUG,1,5,5000,0     GOLLER   ALPHA VS X
*       XEQ
        PARTICLE SIZE CORRELATION WITH DOWN WIND DISTANCE
        DIMENSION W(4), YM(4), X(18), Y(1), ALPHA(3), VF(3), Z(3)
        READ 100, YM, W
        READ 101, X,Y
        K=1
        DO 3000 I=1,3
        WL=LOGF(W(I))/LOGF(10.)
        A=10.**(3.389+.431*WL)
        B=10.**(LOGF(A)/LOGF(10.)-(.486+.262*WL)/2.)
        H=10.**(4.226+.164*WL)
        PRINT 103, A,B,H,WL
        DO 3000 J=1,18
        DO L=1,3,2
        XL=L-2
        C1=X(J)**2*B**2
        C2 =1.-(Y(K)/A)**2
        C3=A**2-Y(K)**2
        ALPHA(L)=(H*X(J)+XL*SQRTF(C1*C2+C3*(H**2-B**2*C2)))/(H**2-B**2*C2)
        VF(L)=22./ALPHA(L)
        C4=X(J)-ALPHA(L)*H
        C5=ALPHA(L)**2*B**2
        Z(L)=H-XL*ALPHA(L)*B**2/SQRTF(A**2+ALPHA(L)**2*B**2)
 1000 CONTINUE
        DO 2000 L=1,3,2
        PRINT 102, W(I),X(J), Y(K), VF(L), ALPHA(L),Z(L)
 2000 CONTINUE
 3000 CONTINUE
  100 FORMAT(8F9.0)
  101 FORMAT (6E12.3)
  102 FORMAT (3F8.0,5F20.5)
  103 FORMAT (8E12.4)
        CALL EXIT
        END
*       DATA
```

PART OF THE RESULTS

	W MT.	X MI.	ALPHA	FALLING VELOCITY FT/SEC	HEIGHT OF FALL FT.
MIN	5	15	-.251	-87.3833	67170.618
MAX	5	15	2.756	7.98186	59755.644
MIN	5	100	5.694	3.86331	81161.546
MAX	5	100	11.00	1.99964	51810.312
MIN	5	500	30.58	.71924	85767.950
MAX	5	500	52.89	.41592	50092.883
MIN	10	15	-.674	-32.6327	73667.460
MAX	10	15	2.945	7.47005	66230.532
MIN	10	100	4.737	4.64356	90171.336
MAX	10	100	10.40	2.11503	56872.171
MIN	10	500	26.68	.824300	97875.769
MAX	10	500	49.00	.448900	54182.166
MIN	20	15	-1.15	-19.0709	80540.842
MAX	20	15	3.220	6.83190	73113.656
MIN	20	100	3.801	5.78652	99324.063
MAX	20	100	9.975	2.20543	62401.162
MIN	20	500	23.21	.94760	111708.54
MAX	20	500	45.66	.48172	58337.851

Figure 27. Computer Program to Evaluate Fallout Particle Size Distribution for Any Downwind Location

D. Estimation of Nuclide Solubility Contour Ratios

The large volume of computations necessary to estimate the soluble nuclide contour ratios, N'_{α} (1) or N'(A)/I(1), suggested the use of digital electronic computer methods. A flow diagram was presented previously (14) but due to the large volume of input data - about 9,000 - this program had not yet been completely tested. However, the difficulties were overcome and the corrected FORTRAN flow diagram is shown in Figure 27.

The computer program to evaluate soluble nuclide contour ratios has been developed. During the preparation of this program, two major problems were encountered and successfully resolved. The first one was the evaluation of vaporization or sublimation pressures which involves different temperature ranges for different elements. An equal number of temperature ranges is assigned to all elements in order that an iterating process to test them consecutively may be established for all elements.

The second problem lies in the evaluation of the fractionation number which involves various kinds of decay chains of different lengths. If a generalized chain containing all elements(*) is assumed for all mass numbers, the number of input data will increase beyond the capacity of available computer facilities. However, after an extensive exploration of the properties of these chains, this difficulty was overcome by the discovery that a general decay chain of five members can be established. An identification number was assigned to each of these general decay chains. All fission-product elements can then be considered in succession by the following arrangement: Each general decay chain containing five members, is cited four times with consecutive identification numbers to form a group of four chains. Each group of chains is followed by another group of four chains, each composed of five members but which have been elevated by one element from the previous set of five elements. Therefore, the four new chains will have as their first element the second element of the pre-

(*) Note: "all elements" refers to 38 significant fission products

vious four chains, and their second element will be the third element of the previous chains, etc.; and their fifth element will be the element which is not included in the previous chains but follows the last-mentioned element in order. According to this arrangement, the entire set of actual decay chains for all U-238 fission products may be replaced by 130 five-member chains. The relationships between the actual decay chains and their corresponding five-member chains were presented in Table VI (14). Using this type of five-member chain, the total input data are reduced to one-sixth of the data required for the all-element, generalized chain.

The computer program is composed of six sub-programs. These sub-programs were written for: (1) the vaporization or sublimation pressures, (2) the yield at initial time of condensation, (3) the fractionation numbers of the first period of condensation, (4) the fractionation number of the second period of condensation, (5) the gross fractionation numbers, and (6) the nuclide solubility contour ratios. Each of these sub-programs may be executed separately. Due to the limitation of the available computer facility (IBM 7094), which allows only three-dimensional arrays, this program applies only to a single weapon yield. The computer program has been reproduced as Figure 29.

E. Biological Uptake Models

Following an analysis of several biological uptake models in interim report No. 2 (14) and the presentation of five completed computer programs in interim report No. 3 (17), the program for the Miller-Brown Model - modified for periodic ingestion - was completed successfully. The results for absorbed dose for Total Body from periodic ingestion were shown in Table XIII, page 69. Similar values for bone and the GI tract have been computed.

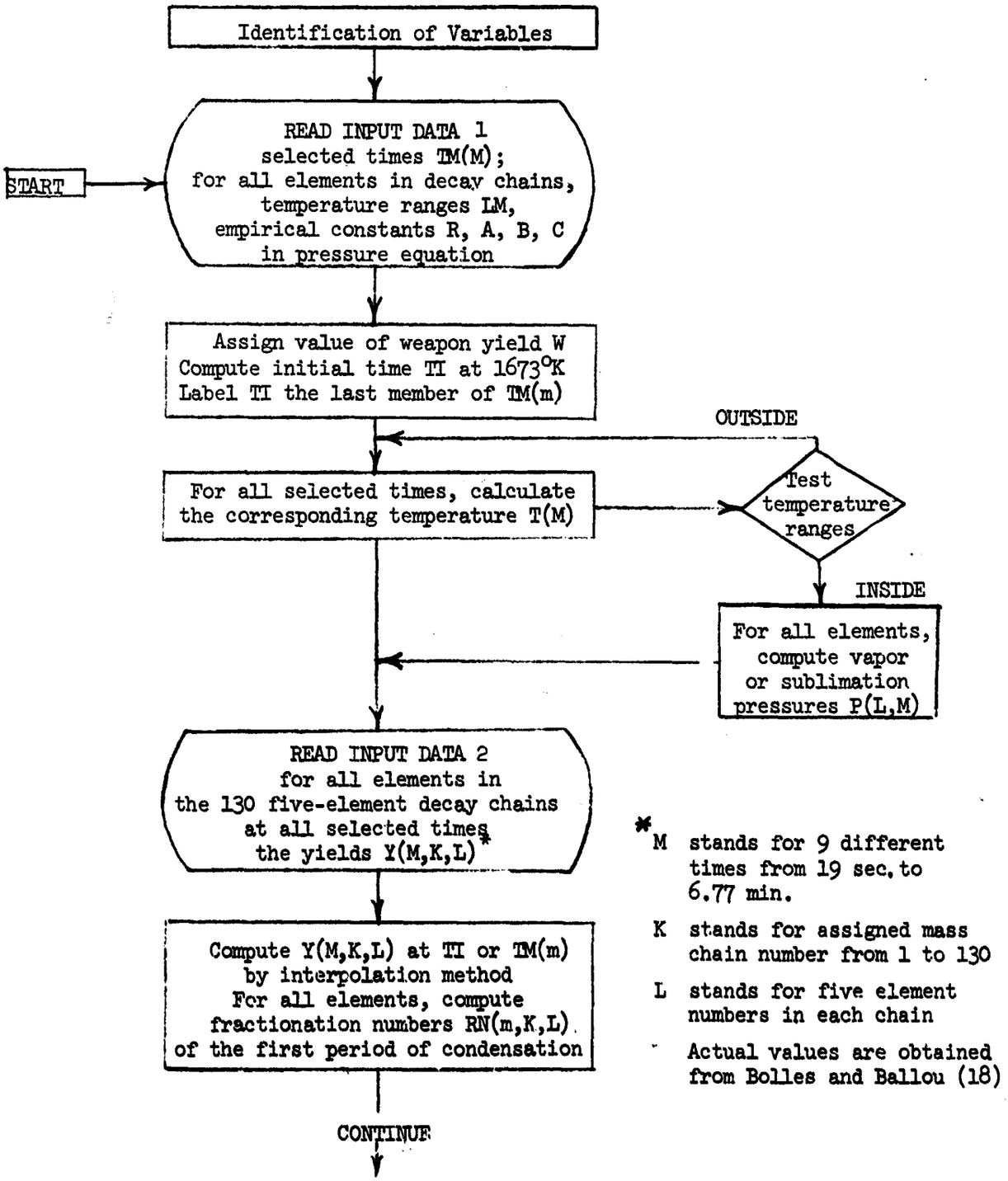

Figure 28. Flow Diagram for Computer Program for Soluble Nuclide Contour Ratios

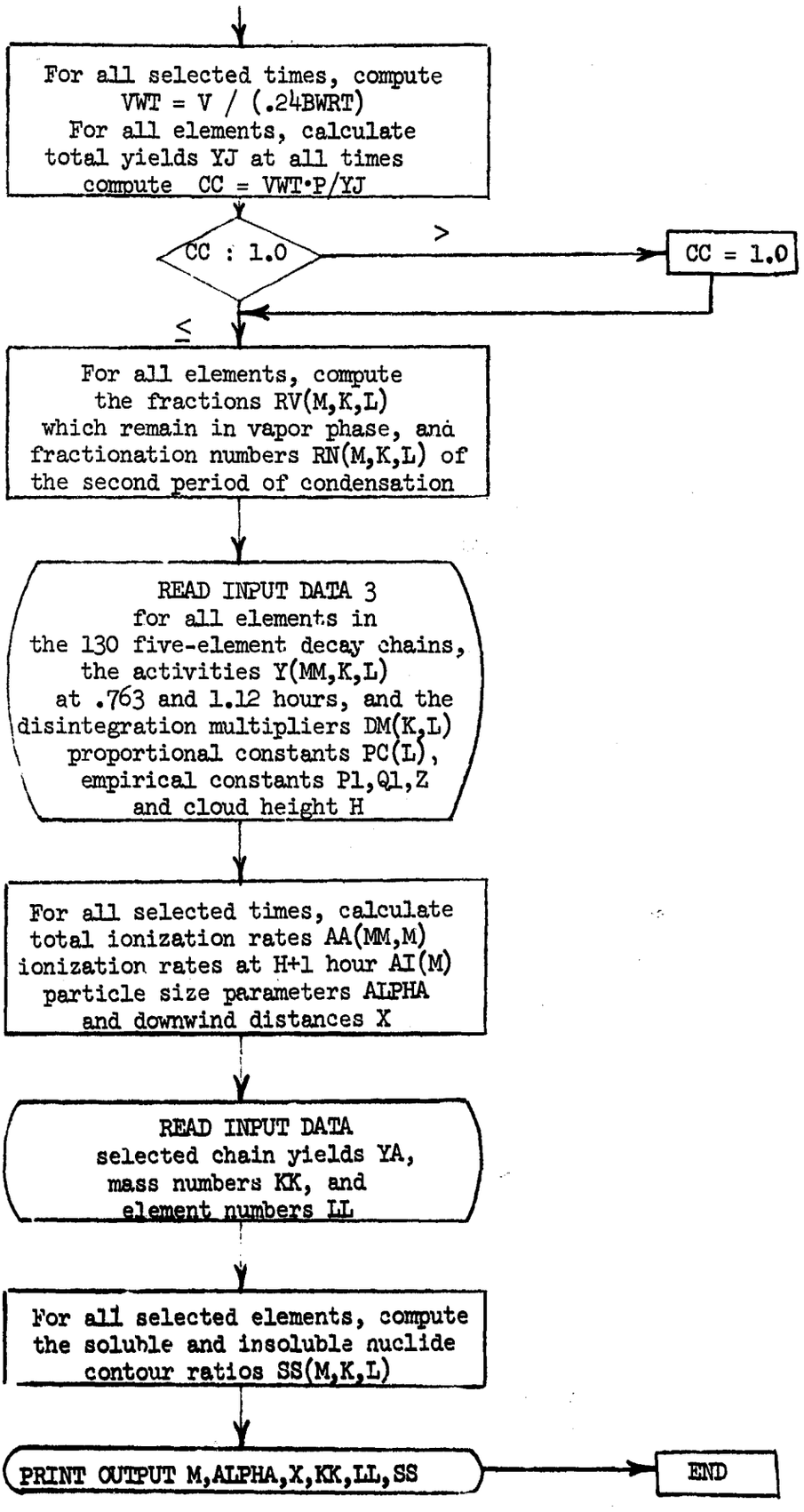

Figure 28. (cont'd) Flow Diagram for Computer Program for Soluble Nuclide Contour Ratios

```
*       N1585-1463,FMS,DEBUG,1,5,9000,0    YU    4-22-64
*       XEQ
*       LIST
        NUCLIDE SOLUBILITY CONTOUR RATIO PARAMETERS
        DIMENSION TM(10),LM(16,34),A(8,34),B(8,34),C(8,34),T(10),
       1   P(37,10),Y( 0,130,5),VWT(9),YN(10,130  ),SN(10,130  ),RN(10,130
       2   ,5),YJ(37,9), CC(37,9),                          PC(130),AA(2,10),
       3   AI(10),R(10),ALPHA(10),X(10),                      RR(8,34)
        READ 101, (TM(M),M=1,9)
        READ 102, LM
        READ 103,RR,A,B,C
        W=5000
        TI=LOGF(1673./4660.*W**( .01))/(-.546*W**(-.373))
        TM(10)=TI
        DO 1001 M=1,10
        T(M)=4660.*W**(-.01)*EXPF(-.546*W**(-.373)*TM(M))
        DO 1001 N=1,34
        DO 1001 I=1,15,2
        IF (XINTF(T(M))-LM(I,N)) 1001,1,1
    1   IF (XINTF(T(M))-LM(I+1,N)) 2,2,1001
    2   J=(I+1)/2
        P(N,M)=P(N,M)+RR(J,N)*EXPF(2.302585*(A(J,N)/T(M)+B(J,N)+C(J,N)))
 1001   CONTINUE
        DO 1011 M=1,10
        P(8,M)=.99999E10
        P(26,M)=.99999E10
 1011   CONTINUE
        PRINT 106, TM
        PRINT 106, T
        PRINT 110, ((P(N,M),M=1,10),N=1,34)
        READ 104, (((Y(M,K,L),M=1,9),K=1,130),L=1,5)
        M=1
    3   IF (TI-TM(M)) 5,5,4
    4   M=M+1
        GO TO 3
    5   CR=(TI-TM(M-1))/(TM(M)-TM(M-1))
        D=5.67E-7*EXPF(-.51*W**(-.373)*TI)
        DO 1003 K=1,130
        DO 1003 L=1,5
        Y(10,K,L)=Y(M-1,K,L)+CR*(Y(M,K,L)-Y(M-1,K,L))
        YN(10,K)=YN(10,K)+Y(10,K,L)
        N=(K-1)/4+L
        SN(10,K)=SN(10,K)+Y(10,K,L)/(1.+P(N,10)/D)
        IF (YN(10,K  )) 52,51,52
   51   RN(10,K,L)=1.
        GO TO 1003
   52   RN(10,K,L)=SN(10,K  )/YN(10,K  )
 1003   CONTINUE
        PRINT 110, (YN(10,K),K=1,130)
        PRINT 110, (SN(10,K),K=1,130)
        PRINT 110, ((RN(10,K,L),K=1,130),L=1,5)
        DO 1004 M=1,9
        VWT(M)=((7.62E8/4.66)*W**(+.01)*EXPF(1.056*W**(-.373)*TM(M)))/
       1        (.24*83.36)
        PRINT 107, VWT(M)
```

Figure 29. Computer Program for Soluble Nuclide Contour Ratios

```
      DO 1035 N=1,37
      J=1+4*(N-5)
      IF(N-5) 6,6,7
    6 J1=J+19
      DO 1005 K=1,J1
      I=N-(K-1)/4
      YJ(N,M)=YJ(N,M) +(1.-RN(10,K,I))*Y(M,K,I)
 1005 CONTINUE
      GO TO 1035
    7 IF(N-32) 8,9,9
    8 J1=J+19
      DO 1015 K=J,J1
      I=N-(K-1)/4
      YJ(N,M)=YJ(N,M) +(1.-RN(10,K,I))*Y(M,K,I)
 1015 CONTINUE
      GO TO 1035
    9 DO 1025 K=J,130
      I=N-(K-1)/4
      YJ(N,M)=YJ(N,M) +(1.-RN(10,K,I))*Y(M,K,I)
 1025 CONTINUE
 1035 CONTINUE
      PRINT 110, (YJ(N,M),N=1,37)
      DO 1004 N=1,37
      IF (YJ(N,M)) 11,11,13
   13 CC(N,M)=P(N,M)*VWT(M)/YJ(N,M)
      IF (CC(N,M)-1.) 12,12,11
   11 CC(N,M)=1.
   12 DO 1004 K=1,130
      DO 1004 L=1,5
      YN(M,K  )=YN(M,K  )+Y(M,K,L)
      N=(K-1)/4+L
      SN(M,K  )=SN(M,K  )+Y(M,K,L)*(1.-RN(10,K,L))*CC(L,M)
      IF (YN(M,K  )) 122,121,122
  121 RN(M,K,L)=1.
      GO TO 1004
  122 RN(M,K,L)=1.-SN(M,K  )/YN(M,K  )
 1004 CONTINUE
      PRINT 109, ((CC(N,M),M=1,9),N=1,37)
      READ 105, (((Y(M,K,L),M=1,2),K=1,130),L=1,5)
      READ 101, ((Y(3,K,L),K=1,130),L=1,5)
      READ 101, PC
      P1=.95
      Q1=1.02E-5
      Z=35566.
      H=68019.
      DO 1006 M=1,10
      DO 1007 MM=1,2
      DO 1007 K=1,130
      DO 1007 L=1,5
      AA(MM,M)=AA(MM,M)+RN(M,K,L)*Y(3,K,L)*PC(K)*Y(MM,K,L)
 1007 CONTINUE
      AI(M)=EXPF(.29526*LOGF(AA(1,M)+.70474*LOGF(AA(2,M))))
      R(M)=AI(M)/6.973
```

Figure 29. (cont'd) Computer Program for Soluble Nuclide Contour Ratios

```
      ALPHA(M)=2000.*((P1/Z+Q1)*EXPF(.011*(TM(M)+180.))-Q1)
      X(M)=H*ALPHA(M)
 1006 CONTINUE
      DO 1009 M=1,10
      DO 1009 L=1,5
      DO 1009 K=1,130
      PRINT 111, RN(M,K,L)
 1009 CONTINUE
      DO 1010 M=1,10
      DO 1020 MM=1,2
      PRINT 107, AA(MM,M)
 1020 CONTINUE
      PRINT 108, AI(M),R(M),ALPHA(M),X(M)
 1010 CONTINUE
  101 FORMAT (13F5.0)
  102 FORMAT (8I5)
  103 FORMAT (8F8.0)
  104 FORMAT (9E8.3)
  105 FORMAT (10E7.3)
  106 FORMAT(10F12.4)
  107 FORMAT (2E20.8)
  108 FORMAT (E20.8,2F10.4,E20.8)
  109 FORMAT(9E14.8)
  110 FORMAT(5E20.8)
  111 FORMAT(10E10.3)
      CALL EXIT
      END
*     DATA

      PART OF THE RESULTS
W = 5 M.T.      TM = 41.237 SEC      T = 1673.0 DEG. KELVIN
      VAPORIZATION AND SUBLIMATION PRESSURES
SR      .4609E-12
RU      .2321E 04
CS      .2249E 01
BA      .9999E 10
      GROSS ACTIVITY
AT 45.8 MIN    .10953E 02
AT 1.12 HRS    .65408E 01
      FRACTIONATION NUMBERS OF FIRST PERIOD OF CONDENSATION
SR-89     .494E-02
SR-90     .806E-01
RU-106    .368E-03
I-131     .189E-06
CS-137    .338E-07
BA-140    .311E-01
      FRACTIONATION NUMBER OF FIRST + SECOND PERIOD OF CONDENSATION
SR-89     .495E-02
SR-90     .807E-01
RU-106    .369E-03
I-131     .190E-06
CS-137    .338E-07
BA-140    .312E-01
      GROSS FRACTIONATION NUMBER
.3007
      NORMAL IONIZATION RATE
.20968E 01
```

Figure 29. (cont'd) Computer Program for Soluble Nuclide Contour Ratios

VII. SUMMARY AND CONCLUSIONS

1. A theoretical study of the extent of potential water contamination from fallout and the biological hazards associated with the ingestion of water following hypothetical nuclear attack has been conducted. The water supply systems of three cities were selected for this evaluation; San Francisco, Calif., with a 155 MT attack, Paterson, N. J. with a 115 MT attack and Springfield, Mass. with a 30 MT attack.

2. Following a thorough analysis of the Miller Fallout Model, a number of important functions derived from this model were utilized in this study. It should be cautioned that the validity of the results can be no greater than the validity of this model, which has been estimated by Miller to yield values that agree with available unclassified data within a factor of two. The choice of the proper chemical reactions for estimating the sublimation pressures has presented a problem in computing fractionation numbers. The pressure data used was selected to agree with Miller's calculations for 1673° K. As the pressure decreases rapidly with temperature, it will not exert a significant effect on the computation of fractionation numbers for the second period of condensation.

3. Maximum levels of six biologically important radionuclides under adverse wind conditions and including watershed runoff were calculated and reported in μc/ml as follows:

	Sr-89	Sr-90	Ru-106	I-131	Cs-137	Ba-140
San Francisco	2.7×10^{-2}	2.1×10^{-4}	2.7×10^{-3}	2.7×10^{-1}	1.7×10^{-4}	1.8×10^{-1}
Paterson	9.6×10^{-1}	8.9×10^{-3}	1.2×10^{-1}	1.2×10	5.9×10^{-3}	7.9
Springfield	1.4×10^{-3}	2.5×10^{-5}	4.3×10^{-4}	3.7×10^{-2}	7.4×10^{-6}	2.2×10^{-2}

While the results show that direct contamination of reservoirs will be of relatively low level, when watershed runoff, due to precipitation following nuclear attack, is considered the potential hazard from water contamination is higher by a factor of 10 to 100. Whereas in many cases the water may be fit for human consumption during

the immediate post-attack period as far as radioactive contamination goes, the more difficult problem may be posed by organic pollution during this critical period. The maximum contamination levels were estimated as 8 μc/ml for Ba-140 and 12 μc/ml for I-131. Therefore, the maximum decontamination required appears to be for the removal of I-131 and Ba-140 from the Paterson, N. J., water supply system. Although these levels of contamination exceed the peacetime MPC values by factors of 10^4 to 10^5, these levels of activity may not be too high for the immediate post-attack period and for a limited period of consumption. As there is an urgent need for culinary water supply during this period, as soon as power can be restored, water decontamination processes should be implemented to reduce the Ba-140 and I-131 activity concentrations in water.

4. The subject of water decontamination was studied in detail and the maximum decontamination factor for each of the six selected elements listed for 16 different treatment processes presented in Table XXIV, p. 164. It must be noted that the degree of decontamination is a function of the chemical form and physical state of the radioactive element, concentration of treatment additives, and many other variables including pH and temperature of the water. However, it is apparent from the table that ion exchange in one form or another, is the only single decontamination process that will remove sizeable amounts of each of the six selected isotopes and that this process will reduce the maximum radiocontaminant, I-131, to a safe drinking water concentration from the initial 12 μc/ml level estimated for Paterson, New Jersey.

5. Various criteria for biological uptake were analyzed. Results from four mathematical models of biological uptake were summarized and found to be in close agreement with each other. Absorbed dose for various organs has been presented in two types of graphs for use by Civil Defense personnel. The internal hazard from ingestion of contaminated water for the populations residing in the three selected cities was estimated. For ingestion starting at 7 days and 30 days of consumption,

a maximum absorbed dose of 22 rems (for Sr-89) for total body was estimated for Paterson, N. J. Of course the total absorbed dose will vary greatly with the time of onset of ingestion and the period of consumption.

6. A total of ten computer programs were established to assist the computations of various phases of this study. Six of these were concerned with different biological uptake models to compute the absorbed dose due to ingestion for total body organs and for the GI tract. The other programs were established to estimate sublimation pressures; to calculate ionization rate contours; to obtain the ionization rate at any location from multiple weapon effects; to evaluate fallout particle size distributions for any downwind location; and to obtain soluble nuclide contour ratios.

7. A study was also made to obtain a first approximation of the relationship between activity distribution and fallout particle size. The relationship is observed to be in close conformance to a log-normal distribution.

8. It has been found that the effect due to watershed runoff on contamination may be significant. Therefore, it is suggested that additional research be performed to study the runoff contribution in greater detail during the blast and thermal period from land areas to streams and from watersheds into reservoirs. It appears that rainfall during the initial 24 to 48 hours following nuclear attack will exert a significant effect on surface water contamination.

VIII. LIST OF REFERENCES

(1) Callahan, E. D., Rosenblum, L. Kaplan, J. D., and Batten, D. R., "The Probable Fallout Threat over the Continental United States" Report No. TO-B 60-13, Technical Operations Inc., Burlington, Massachusetts (December 1, 1960)

(2) Miller, C. F., "Fallout and Radiological Countermeasures", Vols. I and II, Stanford Research Institute Report, Project IMU-4021 (January 1963)

(3) "The Recovery and Restoration of Metropolitan Water Works Following Nuclear War Attack", A Report prepared for the Office of Civil Defense, Dept. of Defense, under Contract No. OCD-OS-64-106 by Engineering - Science, Inc., Arcadia, California (May 1963)

(4) "Biological and Environmental Effects of Nuclear War-Summary-Analysis and Hearings, June 22-26, 1959", Joint Committee on Atomic Energy, 86th Congress of the United States, First Session 1959, United States Government Printing Office (August 1959)

(5) "Nuclear Attack and Industrial Survival", McGraw-Hill Special Report, Nucleonics, 20, 1 (January 1962)

(6) "Definition of the Target System", (Stanford Research Institute) Private Communication with Postattack Research Division, Office of Civil Defense, Department of Defense, Washington 25, D. C.

(7) Turner, J. H., "San Francisoo's Water Supply" Journal, American Water Works Assn., 51, 1061 (September 1959)

(8) Personal communication from Charles G. Bourgin, General Superintendent and Chief Engineer, Passaic Valley Water Commission, Clifton, New Jersey, March 3, 1964

(9) National Committee on Radiation Protection, "Maximum Permissible Body Burdens and Maximum Permissible Concentrations of Radionuclides in Air and Water for Occupational Exposure", Handbook 69, U. S. Department of Commerce, National Bureau of Standards, Washington 25, D. C. (1959)

(10) Bale, W. F., "Levels of Radioactivity in Water and Food that can be permitted under Emergency Conditions in Wartime", Division of Biology and Medicine, U. S. Atomic Energy Commission, Washington, D. C., (1954)

(11) Miller, D. W., Geraghty, J. J. and Collins, R. S., "Water Atlas of the United States", Water Information Center, Inc., Port Washington, L. I., New York (1963)

(12) Lee, H., "Vulnerability of Municipal Water Facilities to Radioactive Contamination from Nuclear Attacks", Stanford Research Institute Report, Project IM-4536 (March 1964)

(13) Miller, C. F., and Brown, S. L., "Models for Estimating the Absorbed Dose from Assimilation of Radionuclides in Body Organs of Adult Humans" OCD-OS-62-135, Stanford Research Institute, Menlo Park, California (May 1963)

(14) Grune, W. N. and Yu, O. S. K., "Evaluation of Fallout Contamination of Water Supplies", Interim Technical Report No. 2 to the Office of Civil Defense, Contract No. OCD-PS-64-62 (April 30, 1964)

VIII. LIST OF REFERENCES (cont'd)

(15) Morgan, K. Z., et al., "Report of Committee II on Permissible Dose for Internal Radiation - 1959", Health Physics, 3, Supplement (1960)

(16) Greitz, U. and Edvarson, K., "Internal Doses from Mixed Fission Products", Health Physics, 9, 721-730 (1963)

(17) Grune, W. N. and Yu, O. S. K., "Evaluation of Fallout Contamination of Water Supplies", Interim Technical Report No. 3 to the Office of Civil Defense, Contract No. OCD-PS-64-62 (August 1, 1964) pp. 41 and 52

(18) Bolles, R. and Ballou, N., "Calculated Activities and Abundances of U-235 Fission Products, USNRDL-456 (1956)

(19) Glendenin, L. E., Technical Report No. 35, Massachusetts Institute of Technology, Cambridge, Mass., 1959

(20) Present, R. D., Phys. Rev., 72, 7 (1957)

(21) Bethe, H. A., et al., "Blast Wave", Los Alamos Scientific Laboratory, Los Alamos, New Mexico, March 27, 1958, LA-2000

(22) Glasstone, S., "Effects of Nuclear Weapons", p.497, 2nd Ed., United States Atomic Energy Commission (April 1962)

(23) Miller, C. F., Analysis of Fallout Data, I. The Jangle "S" and "U" Shot Fallout Patterns, USNRDL-TR-220, Dec. 1958

(24) Kelley, K. K.,"Contributions to the Data on Theoretical Metallurgy, XIII. High Temperature Heat-Content, Heat-Capacity, and Entropy Data for the Elements and Inorganic Compounds," U. S. Bureau of Mines, Bulletin 584, 1960.

(25) Stull, D. R., and Sinke, G. C., The Thermodynamic Properties of the Elements, American Chemical Society, Washington, D. C. 1956

(26) Grune, W. N. and Yu, O. S. K., "Evaluation of Fallout Contamination of Water Supplies", Interim Technical Report No. 1 to the Office of Civil Defense, Contract No. OCD-PS-64-62 (Dec. 31, 1963), p. 21

(27) Anderson, A. D., "Application of 'Theory for Close-In Fallout' to Low-Yield Land Surface and Underground Nuclear Detonations", USNRDL-TR-289 (1959)

(28) Grune, W. N., Craft, T. F., Jr., and Sloan, W. M., "Evaluation of Water Contamination from Fallout", Final Technical Report to the Office of Civil Defense, Contract No. OCD-OS-62-189 (July 31, 1963), pp. 45 & 54

(29) Pugh, G. E. and Galiano, R. G., "An Analytic Model of Close-In Deposition of Fallout for Use in Operational-Type Studies." Research Memorandum No. 10, Weapons Systems Evaluations Group, (1959)

(30) Schuert, E. A., "A Fallout Forecasting Technique With Results Obtained at the Eniwetok Proving Ground", USNRDL-TR-139, (1957)

(31) Anderson, A. D., "A Theory for Close In Fallout", USNRDL-TR-249, (1958)

(32) Katcoff, S., "Fission-Product Yields from U, Th and Pu", Nucleonics, 4, 78-85 (1958)

VIII. LIST OF REFERENCES (cont'd)

(33) Bunney, L. R., Scadden, E. M., Abriam, J. O. and Ballou, N. E., "Radiochemical Studies of the Fast Neutron Fission of U-235 and U-238" Second UN International Conference on the Peaceful Uses of Atomic Energy, A/Conf. 15/P/643, USA (June 1958)

(34) Grune, W. N., Craft, T. F., Jr., and Sloan, W. M., "Evaluation of Water Contamination from Fallout", Final Technical Report to the Office of Civil Defense, Contract No. OCD-OS-62-189 (July 31, 1963)

(35) Miller, C. F. and Loeb, P., "Ionization Rate and Photon Pulse Decay of Fission Products from the Slow-Neutron Fission of U-235", USNRDL-TR-247 (1958)

(36) Grune, W. N., and Gutermuth, J. M., "Evaluation of Water Contamination from Fallout", Quarterly Technical Report No. 2 to the Office of Civil Defense, Contract No. OCD-OS-62-189 (November 9, 1962), p. 21

(37) Saule, R., "Water Supply As Related to Nuclear Attack", Journal of the New England Water Works Association, 77, 1, 10-15, (March 1963)

(38) Lacy, W. J. and Stangler, J. J., "The Postattack Water-Contamination Problem", Health Physics, 8, 423-427, (1962)

(39) Straub, C. P., Lacy, W. J., Morton, R. J., "Methods for the Decontamination of Radioactive Liquid Wastes", Proceedings of the International Conference on the Peaceful Uses of Atomic Energy, Geneva, 9, 24, (1955)

(40) Cowser, K. E., and Morton, R. J., "Treatment Plant for the Removal of Radioactive Contaminants from Process Waste Water. Part II Evaluation of Performance", Statement of the Record, Hearings on Industrial Radioactive Waste Disposal, Joint Committee on Atomic Energy, 86th Congress of the United States, p. 547, (August 1959)

(41) Voznesenskii, S. A. et al., "Use of Flotation in Treating Radioactive Effluents", Atomnaya Energiya, 9, 3, 208, (1960)

(42) Matsumura, J., Ishiyama, T., Mamuro, T., "On the Decontamination of Radioactive Waste Water by Ferric Hydroxide Flocculation (I)", Annual Rep. of Radiation Center of Osaka Pref., (Japan), 4, 32, (1963)

(43) Gardiner, D. A. and Cowser, K. E., "Optimization of Radionuclide Removal from Low-Level Process Wastes by the Use of Response Surface Methods", Health Physics, 5, 1/2, 70-78, (1961)

(44) Graham, R. J., Beard, E. L., and Kvam, D. J., "A Decontamination Process for Low-Level Waste Waters", University of California, Lawrence Radiation Laboratory, Livermore, California, Contract No. W-7405-eng-48 (September 27, 1961)

(45) Fernandez, N., "La section de traitement des effluents, ses problemes, son fonctionnement, ses resultats", Energie Nucleaire, 5, 4, 282-290, (June 1963)

(46) Health Physics Division Oak Ridge National Laboratory and Robert A. Taft Sanitary Engineering Center, Public Health Service. "Report of the Joint Program of Studies on the Decontamination of Radioactive Waters", Oak Ridge National Laboratory, Oak Ridge, Tennessee, ORNL-2557, 65 pps., TID-4500, 14th Ed., (Issued Feb.11, 1959)

(47) Gemmell, L., "Efficiency of Filter Beds for Treating Radioactive Waste", Nucleonics, 10, 10, 40 (1952)

VIII. LIST OF REFERENCES (cont'd)

(48) Eden, G. E., Elkins, G. H., Truesdale, G. A., "Removal of Radioactive Substances from Water by Biological Treatment Process", Atomics, 5, 133, (1954)

(49) Hannah, S. A., and Printz, A. C., Jr., "An Evaluation of the Effectiveness of Polyelectrolyte Coagulant Aids for the Removal of Radioactive Isotopes by Water Treatment Process, "A report to the Office of Civil Defense and Mobilization under provisions of contract CDM-SR-60-56 with the University of Florida," NP11105, (1961)

(50) McCauley, R. F., Lauderdale, R. A., and Eliassen, R., "A Study of the Lime-Soda Softening Process as a Method for Decontaminating Radioactive Waters", NYO-4439, (Sept. 1,1953)

(51) McCauley, R. F. and Eliassen, R., "Radioactive Strontium Removal by Lime-Soda Softening", Journal of American Water Works Association, 47, 494-502, (1955)

(52) Moeller, D. W., Leddicotte, G. W. and Reynolds, S. A., "Behavior of Radionuclides on Ion-Exchange Resins", Journal of American Water Works Association, 53, 862-872, (July 1961)

(53) "Radioactivity in Water Supplies", Public Works, 91, 176, (June 1960)

(54) Burns, R. H. and Glueckauf, E., "Development of a Self-Contained Scheme for Low-Activity Wastes", Proceedings of the Second United Nations International Conference on the Peaceful Uses of Atomic Energy, 18, Waste Treatment and Environmental Aspects of Atomic Energy, Geneva (1 September-13 September 1958)

(55) Thomas, K. T., et al., "Strontium Sorption Studies Using Naturally Occurring Ion Exchange Materials", ORNL Central Files No. 60-10-35, (December 1960)

(56) Klein, G., Harten, P., and Kaufman, W., "Radiological Decontamination of Drinking Water by Ion Exchange", The Office of Civil and Defense Mobilization, Contract No. CDM-SR-60-58, (November 1962)

(57) Ayres, J. A., (Knolls Atomic Power Laboratory, Schenectady, N.Y.) "Treatment of Radioactive Waste by Ion Exchange", Industrial and Engineering Chemistry, 43, 7, 1526-1532, (July 1951)

(58) Sammon, D. D. and Watts, R. E., Unpublished work. Reference 31, p. 239, in "Atomic Energy Waste" by E. Glueckauf. Interscience Publishers Inc., New York (1961)

(59) Hickok, R. L., "Calcination of Zirconium Fluoride Waste and Ion-Exchange Separation of Cesium From Process Wastes Using Ammonium Phosphomolybdate", Report of the Second Working Meeting on Fixation of Radioactivity In Stable, Solid Media at Idaho Falls, Idaho. Sponsored by National Reactor Development, U. S. Atomic Energy Commission, Washington, D. C., TID-7613, Book 1, p. 300 (Sept. 27-29, 1960)

(60) Roberts, J. T. and Holcomb, R. R., "A Phenolic Resin Ion Exchange Process for Decontaminating Low-radioactivity Level Process Water Wastes", Oak Ridge National Laboratory, Oak Ridge, Tennessee, ORNL-3036, (1961) UC-70

(61) Caron, H. L., "A Highly Specific Method of Separating Cesium by Exchange on Thallous Phosphotungstanate", Anal. Chem., 34, 9, 1082-1086,(August 1962)

17

VIII. LIST OF REFERENCES (cont'd)

(62) Culler, F. L., et al., "Low-Activity Waste Treatment", Chemical Technology Division Annual Progress Report for Period Ending June 30, 1962, 78-90 ORNL-3314 TID-4500, UC-10

(63) Skarpelos, J. M., "Low-and Intermediate-Level Waste Treatment", Quarterly Progress Report Research and Development Activities Fixation of Radioactive Residues October-December, 1962, edited by E. R. Irish, 33-34, HW-76262 (January 1963)

(64) Brooksbank, R. E., et al., "Low-Radioactivity-Level Waste Treatment. Pilot Plant Demonstration of the Removal of Activity from Low-Level Process Wastes by a Scavenging-Precipitation Ion-Exchange Process", U. S. Atomic Energy Comm., ORNL-3349, TID-4500 (1963) UC-41

(65) Wolfsberg, K., "Determination of Rare Earths in Fission Products by Ion Exchange at Room Temperature", Anal. Chem., 34, 518, (1962)

(66) Lloyd, M. H., "An Anion Exchange Process for Americium-Curium Recovery from Plutonium Process Waste", Nuclear Science and Engineering, 17, 3, 452-456, (November 1963)

(67) Skarpelos, J. M., (Process Demonstration and Analysis Chemical Effluents Technology. Hanford Laboratories), "Progress in Treatment of a Radioactive Condensate Waste", Performed Under Contract No. AT(45-1)-1350 between the Atomic Energy Commission and General Electric Company. HW-79174, TID-4500, 24th Ed., (October 1963) UC-70

(68) Mathers, W. G., "Some Properties of Hydrogen - Based Clinoptilolite", The Use of Inorganic Exchange Materials for Radioactive Waste Treatment, A Working Meeting Held at Washington, D. C., 13-14 August 1962, Jamison, D. K., et al., editors, 47-65, TID-7644, (January 1963)

(69) "Waste Disposal", Reactor Fuel Processing, 4, 1, 46, (January 1961)

(70) Tuthill, E. J., Weth, G. G. and Abriss, A., "Studies on Ion Exchange and Glass Formation as Applied to Ultimate Waste Disposal", Report of the Second Working Meeting on Fixation of Radioactivity In Stable, Solid Media at Idaho Falls, Idaho, September 27-29, 1960, Book 1, 310-334, TID-7613, (February 1961)

(71) Honstead, J. F. et al., "Waste Fixation on Minerals", Report of the Second Working Meeting on Fixation of Radioactivity In Stable, Solid Media at Idaho Falls, Idaho, September 27-29, 1960, Book 2, 623-640, TID-7613, (February 1961)

(72) Cartwright, A. C., "The Treatment of Low Activity Aqueous Wastes", Nuclear Engineering, 7, 68, 26-28 (January 1962)

(73) Nelson, J. L., "Hanford Mineral Exchange Program" The Use of Inorganic Exchange Materials for Radioactive Waste Treatment, A Working Meeting Held at Washington, D. C., 13-14 August 1962, Jamison, D. K., et al., editors, 83-108, TID-7644, (January 1963)

(74) Coleman, L. F., Mercer, B. W. and Unzicker, W. F., "Low-and Intermediate-Level Waste Treatment", Quarterly Progress Report Research and Development Activities Fixation of Radioactive Residues, edited by E. R.Irish, HW-80526, (January 1964)

VIII. LIST OF REFERENCES (cont'd)

(75) "Procedure and Apparatus For the Treatment of Liquid Radioactive Wastes", Belgian P. 552, 692, Water Pollution Abstracts, 34, 1511, (Aug. 1961)

(76) Pushkarev, V. V., Skrylev, L. D., and Bagretsov, F., "Concentration of Radioactive Cesium Using Gelatine Foam Formation", Radiokhimiya, 1, 6, 709-11, (1959)

(77) Tamura, T., et al., "Fundamental Studies of Sorption by Minerals", Health Physics Division Annual Progress Report for Period Ending July 31, 1961, ORNL-3189, TID-4500 (16th ed.), 27-42, UC-41-Health and Safety

(78) Jacobs, D. G., "Cesium Exchange Properties of Vermiculite", Nuclear Science and Engineering, 12, 285-292, (1962)

(79) Struxness, E. G., Jacobs, D. G. and Mohan, A. L., "Ruthenium Sorption by Minerals", ORNL-TM-329, (August 31, 1962)

(80) Pushkarev, V. V., et al., "Sorption of Same Radioactive Isotopes from Aquaeous Solutions by Active Manganese Dioxide", Radiokhimiya, 4, 1, 49-54 (1962)

(81) Kokotov, Y. A., et al., "Sorption of Long-Lived Fission Products by soils and Argillaceous Minerals", Radiokhimiya, 4, 2, 227-228, (March-April 1962)

(82) Tamura, T. et al., "Mineral Exchange Studies", Health Physics Division Annual Progress Report for Period Ending June 30, 1963, ORNL-3492, TID-4500 (22nd Ed.), 62-70, UC-41-Health and Safety

(83) Mercer, B. W., "High-Level Waste Treatment, Sorption", Quarterly Progress Report Research and Development Activities Fixation of Radioactive Residues October-December, 1962, Irish, E. R., editor, 34-37, HW-76262 (January 1963)

(84) Katy, H. and Rothbart, M., "Decontamination of Savannah River Waste Supernatant by Ion Exchange", BNL 853 (T-339), (February 1964)

(85) Kolarik, Z. and Kritil, J., "Sorption Radioaktiver Isotopen an Niederschlägen. Elution von Spaltprodukten aus der Mangan (IV)-Hydroxidsäule", Collection of Czechoslovak Chemical Communications, 29, 7, 1607-1611, (July 1964)

(86) Rimshaw, S. J. and Winkley, D. C., "Removal of Cs-137, Sr-90 and Ru-106 from ORNL Plant Wastes by Sorption on Various Minerals", CF-60-4-17, (April 1960)

(87) Anon., "Adsorption on Natural Materials", Reactor Fuel Processing, 4, 2, 67-69, (April 1961)

(88) Honstead, J., Ames, L., and Nelson, J., "Mineral Reactions - A New Waste Decontamination Process", Health Physics, 8, 191-196, (1962)

(89) Lacy, Wm. J., "Decontamination of Radioactively Contaminated Water by Slurrying with Clay", Ind. Eng. Chem., 46, 1061, (May 1954)

(90) Glueckauf, E., "Atomic Energy Waste", Interscience Publishers,Inc., New York, N. Y. (1961), p. 210, Table 3

VIII. LIST OF REFERENCES (cont'd)

(91) Tamura, T., "Mineral Exchange Work at Oak Ridge National Laboratory", The Use of Inorganic Exchange Materials for Radioactive Waste Treatment, A Working Meeting Held at Washington, D. C., 13-14 August 1962, Jamison, D. K., et al., editors, TID-7644, (January 1963) 29-36

(92) Brockett, T. W., Jr. and Placak, O. R., "Removal of Radioisotopes From Waste Solutions by Soils-Soil Studies With Conasauga Shale", Proc. Eighth Ind. Waste Conf., Purdue Univ., (1953)

(93) Jacobs, D. G., "Sorption of Cesium by Conasauga Shale", Health Physics, 4, 157-163, (1960)

(94) Jacobs, D. G. and Tamura, T., "The Mechanism of Ion Fixation Using Radio-Isotope Techniques." 7th International Congress of Soil Science, Madison Wisconsin, Vol. II, 206-214, (1960)

(95) Sorathesn, A., et al., "Mineral and Sediment Affinity for Radionuclides", ORNL Central Files No. 60-6-93; (July 1960)

(96) Lauderdale, R. A., and Emmons, A. H., "A Method for Decontaminating Small Volumes of Radioactive Water", Journal American Water Works Association 43, 5, 327-31, (May 1951)

(97) Lacy, W. J., "Removal of Radioactive Material from Water by Slurrying with Powdered Metal", Journal American Water Works Association, 44, 9, 824-28, (September 1952)

(98) Dejonghe, P. and D'Hont, M., "Quelques Etudes en Rapport avec le Traitment Chiminique d'Effluents Radioactifs", Energie Nucleaire, 1, 27 (1957)

(99) Cerrai, E., Scaroni, A., and Triulzi, C., "Some Experiments On The Decontamination of Liquid Radioactive Strontium", Energia Nucleare, 6, 3, 207-217 (1959)

(100) Zlobin, V. S., "Adsorption of Yttrium and Zirconium by Zirconium Phosphates", Radiokhimiya, 4, 1, 54-59, (1962)

(101) Cowser, K. E. and Tamura, T., "Significant Results in Low-Level Waste Treatments at ORNL", Health Physics, 9, 687-96 (1963)

(102) Seedhouse, K. G., Monahan, J., and Wallis, G., "The Removal of Fission Products from Solution with a Precipitator - Column Treatment", Part 1. Laboratory Trials, A.E.R.E. Report No. ES/R 2220 (1958)

(103) Lacy, W. J., "Flotation Method for Treatment of Low or Intermediate Level Wastes", ORNL Central Files No. 57-9-31 (September 3, 1957)

(104) Anon., "Foam Separation", Reactor Fuel Processing, 7, 2, 134 (Spring 1964)

(105) Cardozo, R. L., "The Decontamination of Synthetic Effluent by Flotation", Eur. A. E. Community, EUR-262e (1963)

VIII. LIST OF REFERENCES (cont'd)

(106) Blanco, R. E. and Parker, F. L., (Oak Ridge National Lab., Tenn.) "Waste Treatment and Disposal Quarterly Progress Report, February-April 1963" Contract W-7405-Eng-26, (December 16, 1963) UC-70

(107) Krieger, H. L., Goldin, A.S. and Straub, C. P., "Laboratory Studies of Removal and Segregation of Fission Products from Reactor Wastes", Journal of the Water Pollution Control Federation, 32, 5, 495-504 (May 1960)

(108) Butler, T. A. and Ketchen, E. E., "Solvent Extraction Separation of Cerium and Yttrium from Other Rare Earth Fission Products", Industrial and Engineering Chemistry, 53, 651 (August 1961)

(109) Marsh, S. F. et al., "Solvent Extraction Method for Radiocerium", Anal. Chem., 34, 11 (October 1962)

(110) Bray, L. A. and Roberts, F. P., "Laboratory and Hot-Cell Cesium-Dipicrylamine Solvent Extraction Studies", HW-76222, Hanford Atomic Products Operation, Richland, Washington (January 1963)

(111) Healy, T. V., "Rapid Solvent Extraction Methods for Fission Product Separation and Analysis Part I: Separation and Analysis of Various Constituents of Irradiated Fuels. Part II: Rapid Method for Zr-95 Estimation", Radio Chimica Acta, 2, 2, 52-57 (1963)

(112) Awwal, M. A., "Radiochemical Determination of Cerium by Solvent Extraction Method", Analytical Chemistry, 35, 2048-2050 (Dec. 1963)

(113) Astakhov, K. V., Mikhaleva, S. V., and Teslin, V. I., "Extraction of Radioactive Ruthenium With Sodium Piperidinedithiocarbamate", Radiokhimiya, 4, 5, 540-543 (September-October 1962)

(114) Straub, C. P., "Treatment and Disposal of Liquid Radioactive Water", Chapter 16 in "Industrial Wastes: Their Disposal and Treatment", W. Rudolfs, Ed., A.C.S. Monograph Series 118, Reinhold, New York (1953)

(115) Rodger, W. A., "Radioactive Waste Disposal", ANL-6233 (September 1960)

(116) Chem. & Eng. News, 37, 45, 52 (Nov. 9, 1959)

(117) Lieberman, J. A., "Treatment and Disposal of Fuel-Reprocessing Waste", Nucleonics 16, (2), 82-89 (Feb. 1958)

(118) McCullough, G. E.,"Concentration of Radioactive Liquid Waste by Evaporation," Ind. Eng. Chem., 43, 1505 (1951)

(119) Manowitz, B., et al., "Entrainment in Evaporators", Chem. Eng. Prog., 51, 313-319 (July 1955)

(120) "Industrial Radioactive Waste Disposal", Hearings before the Special Subcommittee on Radiation of the Joint Committee on Atomic Energy, Congress of the U. S. held Jan. 29-30 and Feb. 2 and 3, 1959. In Four Volumes, U. S. Government Printing Office Washington, 1959. "Radioactive Waste Disposal at Bettis Plant", 900-923 in Vol. I (1959)

VIII. LIST OF REFERENCES (cont'd)

(121) Arnold E. D., ed. "Compilation and Analysis of Waste Disposal Information", CF 57-2-20, (Del.) (March 12, 1957)

(122) Glueckauf, E., "Atomic Energy Waste", p. 225, Interscience Publishers, Inc., New York, N. Y. (1961)

(123) Fontaine, Y. A., Aeberhardt, A., "Experimental Laboratory Study of Radioactive contamination by Cerium-144 of a Fresh-Water Supply in a Complex Community", Health Physics, 9, 1047-1056 (November 1963) (in French)

(124) Levi, H. W., "Coprecipitation of Radionuclides with Titanium Dioxide Hydrate", Nukleonik, 4, 319-323 (1962)

(125) Watson, L. C., "Fixation of Fission Products In Glass", Report of the Second Working Meeting on Fixation of Radioactivity In Stable, Solid Media at Idaho Falls, Idaho, September 27-29, 1960, Book 1, 202-214, TID-7613 (February 1961)

(126) Caulkins, K. W., "Radioactive Waste Fixation - Coprecipitation and Fusion", Report of the Second Working Meeting on Fixation of Radioactivity In Stable, Solid Media at Idaho Falls, Idaho, September 27-29, 1960, Book 2, 719-722, TID-7613 (February 1961)

(127) Swanson and Associates, "Control of Radioactive Fallout In Water Systems", A Manual for Water Engineers, prepared for Emergency Health Services, Department of National Health and Welfare, Government of Canada, Ottawa, Canada, p. 69-75 (May 1963)

(128) Woodward, R. L. and Robeck, G. G., "Removal of Radiological, Biological and Chemical Contaminants from Water", R. A. Taft Sanitary Engineering Center, Technical Report W59-2 (1951)

(129) Pressman, M., Lindsten, D. C. and Schmitt, R. P., "Removal of Nuclear Bomb Debris, Strontium-90, Yttrium-90 and Cesium-137-Barium-137 from Water with Corps of Engineers Mobile Water-Treating Equipment", EPDL-1673-RR (May 1961)

(130) Lindsten, D. C., Schmitt, R. P., and Lacy, W. J., "Removal of Radioactive Contaminants From Water", Military Engr., 53, 368-9 (Sept.-Oct. 1961)

(131) Lindsten, D. C., and Schmitt, R. P., "Removal of Chemical, Biological and Radiological Contaminants From Water with Corps of Engineers Field Water Supply Equipment", Sanitary Services Branch Military Department, U. S. Army Engineer Research and Development Laboratories, Corps of Engineers, Fort Belvoir, Virginia (12 December 1961)

(132) Anonymous, "Army Studies Three Ways to Decontaminate Water", Water Works Engineering, 115, 5, 376 (May 1962)

(133) Swanton, W. F. and Hyman, M. L., "Liquid Radioactive Waste Disposal Facility", ASTIA Document No. AD-273977, (March 1962)

(134) "Mobile Army Filter Supplies Safe Water", Water Works Engineering, 114, 824 (1961)

(135) "Radioactive Waste Concentrator", Water and Waste Treatment Journal, 9, 1, 25-26 (May-June 1962)

VIII. LIST OF REFERENCES (cont'd)

(136) Nease, F. R., unpublished material based on data gathered by TVA under AEC sponsorship, ORNL (1951)

(137) Lacy, W. J., Donahew, A. L., Lowe, H. N., and Lindsten, D. C., "Decontamination of Radioactively Contaminated Water with Water Purification Unit Hand Operated 1 1/4-gpm and by a Field Expediant, Salty Dog III", ERDL-1404 (May 1955)

(138) Leddicotte, G. W., (Nuclear Division, Union Carbide Co., Tuxedo, N. Y.),"Nucleonics", Analytical Chemistry, 36, 5, 419R-453R (April 1964)

(139) Matsumura, T., et al., "Treatment of Radioactive Waste Water by Flocculation", Annual Report Radiation Center Osaka Prefect, 2, 33-42, (1961); Chem. Abst., 57, 7047a (1962)

(140) Health Physics Division Quarterly Progress Report for the period ending January 20, 1953, ORNL-1488 (1953)

(141) Amphlett, C. B. and Sammon, D. C., "Survey of Treatments Considered for Low-Activity Wastes", Chapter 4.1 in "Atomic Energy Waste", edited by E. Glueckauf, Interscience Publ., Inc., New York, New York (1961)

(142) Cowser, K.E., et al., "Radioactive Waste Disposal - Low Level Waste Water Treatment", Health Physics Division, Annual Progress Report for period ending July 31, 1960, ORNL-2994 (1960)

(143) Lauderdale, R. A., "Treatment of Radioactive Water by Phosphate Precipitation", Ind. Eng. Chem., 43, 1538 (1951)

(144) Eden, G. E., Downing, A. L., and Wheatland, A. B., "Observations on the Removal of Radioisotopes During Purification of Domestic Water Supplies: 1. Radioiodine", J. Inst. Water Engr., 6, 511 (1952)

(145) Lacy, W. J. and DeLaguna, W., "Decontaminating Radioactive Water", Ind. Eng. Chem., 50, 1193 (1958)

(146) Lacy, W. J., "Flotation Method for Treatment of Low and Intermediate Level Wastes", ORNL CF-9-31 (1957)

(147) Eden, G. E., Elkins, G. H., and Truesday, G. A., "Removal of Radioactive Substances from Water by Biological Treatment Process", Atomics, 5, 3 (May 1954)

IX. LIST OF SYMBOLS

A	nuclide or fission product element
A	atomic mass, mass chain
A	designates chemical species; mass number
A	empirical constant in vapor pressure vs. temperature
A_c	total activity in cloud
A_t	activity per 10^4 fissions at time t
A_x	total activity per unit area on the ground
$A_x(1)$	activity per unit area on the ground at one hour after detonation
$A_x(\alpha)$	activity per unit area on the ground at location (X, y) from particles of size parameter α
$A_Z(\alpha)$	total activity at the altitude Z of the stem carried by particles of size parameter α
A_α	activity per unit volume of cloud, carried by particles of size parameter α
A'_α	the number of fissions per unit cross-sectional area of the stem at an altitude Z corresponding to particle size parameter α
a	final, horizontal semi-axis of the ellipsoidal fireball
a_o	parameter used in describing horizontal semi-axis of fireball as function of altitude
a_s	radius of stem at altitude Z_s
a_Z	horizontal semi-axis of the fireball when it is at altitude Z, stem radius at altitude Z
B	liquid carrier
B	designates chemical species
B	ratio of fission to total yield
B	empirical constant in vapor pressure vs. temperature
b	final vertical semi-axis of the ellipsoidal fireball
b	proportionality constant relating the fission yield of U-238 with 8 MEV broad band neutron spectrum to that of U-235 with thermal neutrons
b_o	parameter used in describing vertical semi-axis of fireball as function of altitude, Z
b_Z	vertical semi-axis of fireball when it is at altitude, Z
C	empirical constant in vapor pressure vs. temperature

IX. LIST OF SYMBOLS (cont'd)

$D_x(1)$	instrument response factor at H + 1 hour
d	particle diameter
d(t,1)	radioactive decay correction factor
F(1)	one-half the number of fission products per unit area, corrected to H + 1 hour
f_α	fraction of total activity that is on particles of size parameter α
g	gas
g_c	fraction of total activity produced that is in the cloud
H	time of detonation
h	final height of center of fireball
I	ionization intensity
I(1)	the air ionization rate (r/hr) 3 feet above an infinite plane uniformly covered with fallout, decay-corrected to one hour after detonation
I_o	ridge peak ionization intensity
$I_x^o(1)$	the true air ionization rate per fission/sq ft
$i_{fp}(1)$	the air ionization rate per fission/sq ft at 3 feet above an infinite plane for a uniform distribution of the normal fission product mixture
$i_i(1)$	the air ionization rate per decay/sq ft at 3 feet above an infinite plane for a uniform distribution of neutron induced activity
J	atomic number of element at the end of mass chain A
j	atomic number; element
(jA)	nuclide of atomic number j in mass chain A (atomic weight)
K	Henry's Law constant
K	yield-independent parameter used in describing temperature history of the fireball
$K_x(1)$	$Dq_x \left[r_x(1)\, i_{fp}(1) + i_i(1)\right]$
k	constant in ionization intensity distribution equation
k_a	parameter used in describing horizontal semi-axis of fireball as function of altitude Z
k_b	parameter used in describing vertical semi-axis of fireball as a function of altitude Z
k_{jA}	Henry's Law proportionality constant for nuclide (j,A)

IX. LIST OF SYMBOLS (cont'd)

k_j^o	$\frac{p_j^o}{(n(\ell)/V)RT}$
k_v	$2k_a k_b$
k_Z	empirical constant describing the rise of the fireball = .011 sec^{-1}
ℓ	liquid
m	disintegration multiplier
m	constant in ionization intensity distribution equation
N(A)	number per unit area of atoms of nuclide J at the end of mass chain A that are in the interior of fallout particles and hence insoluble in water
N'(A)	number per unit area of atoms of nuclide J at the end of mass chain A that are on the exterior of fallout particles and hence soluble in water
N_A	mole fraction of A in mixture = number of moles of A divided by total number of moles in mixture
N_B	mole fraction of component B
N_{jA}	mole fraction of nuclide (j,A)
N_j	mole fraction of element j = number of moles of element j, n_j, divided by total number of moles, n_t
$N'_\alpha(1)$	the soluble nuclide contour ratio = the ratio of the number of soluble atoms of a particular isotope (on particles of size parameter α and therefore at downwind location X = αh) to the standard intensity I(1) at the same location
$N_\alpha(1)$	same for insoluble atoms
n	total number of moles of vapor (gas)
n	yield-independent parameter used in equation describing temperature history of the fireball
n_A	number of moles of A
n_B	number of moles of B
$n_{jA}(t)$	number of moles of nuclide (j,A) dissolved in liquid carrier at time t
$n'_{jA}(t)$	number of moles of nuclide (j,A) adsorbed on the surface of solid particles up to time t($t_Z \geq t_1$)
$n''_{jA}(t)$	number of moles of nuclide (j,A) still in vapor phase at time t
$n^o_{jA}(t)$	number of moles of nuclide (j,A) in the vapor phase at time t for $t < t_1$

IX. LIST OF SYMBOLS (cont'd)

$n_{JA}(t_1)$	number of moles of nuclide (J,A) (at end of mass chain A) that end up in the interior of fallout particles
$n^{o}_{jA}(t_1)$	number of moles of nuclide (j,A) not condensed from vapor phase during first period of condensation
n_{jA}	number of moles of nuclide (j,A)
n_j	number of moles of element j
$n(\ell)$	number of moles of solvent
$n(\ell)$	number of moles of liquid soil in the fireball
n_t	total number of moles
O_2	oxygen
P	total vapor pressure = gas pressure
p	empirical constant in describing falling rate of particles
p_A	partial vapor pressure of A in a mixture containing A
p^{o}_A	vapor pressure of pure A
p_B	partial vapor pressure of B in a mixture containing B
p^{o}_B	vapor pressure of pure B
p_j	partial vapor pressure of element j
p^{s}_j	partial sublimation pressure of element j
p^{o}_j	vapor pressure of element j
p^{os}_j	sublimation pressure of the element j
p_{jA}	partial vapor pressure of nuclide (j,A)
p^{o}_{jA}	vapor pressure of pure nuclide (j,A)
q	empirical constant in describing falling rate of particles
q_x	terrain shielding factor
R	fireball radius
R	gas-law constant = 82.07 $\frac{cm^3 - atmospheres}{mole - {}^{o}K}$
R_m	radius of fireball at time t_m (the time at which it reaches full expansion)
R_s	radius of fireball at time t_s (when it leaves the ground)
R_2	radius of fireball at time t_2, the second-thermal maximum

IX. LIST OF SYMBOLS (cont'd)

$r_\alpha(1)$	gross fractionation number at H + 1 hour (the ratio of the ionization rate of all fractionated fission products to the ionization rate of unfractionated fission products
$r_o(A,t_1)$	fractionation number for the first period of condensation = the ratio of the number of moles of (J,A) that end up in the interior of fallout particles to the total number of moles of mass chain A present
$r'_o(A,t_2)$	fractionation number for the second period of condensation = the fractionation of the yield of mass chain A that ends up on the outside of fallout particles and hence soluble in water
T	temperature
T_1	temperature at time t_1, the end of the first period of condensation = 1673 ^oK
t	time
t_f	time required for particle to fall to ground
t_m	the time the fireball reaches full expansion (ground surface burst)
t_{rise}	time it takes particle to reach altitude Z
t_s	the time at which the fireball in a ground surface burst (originally a hemisphere) first becomes spherical - at this time the fireball leaves the ground
t_1	time of the end of the first period of condensation
t_2	time of the end of the second period of condensation
t_2	time of the second thermal maximum (nuclear weapon detonation)
V	volume of the fireball
V_c	volume of the cloud
V_f	average falling velocity of particle size parameter α
V_o	$\frac{4}{3} \pi a_o^2 b_o$
V_w	prevailing wind velocity
V_Z	instantaneous falling rate of particle at altitude Z
V_Z	volume of the stem
W	weapon yield (total)
X	downwind distance from ground zero
x	downwind a crosswind distance
x	the number of oxygen molecules that combine with each atom of element A

IX. LIST OF SYMBOLS (cont'd)

Y_A^o chain yield of mass A per fission

$Y_A(t_1)$ total fission yield of mass chain A = $\sum_j^J y_{jA}(t_1)$

Y_s half width of stem fallout pattern (to 1 r/hr at 1 hr contour)

Y_8 half width of cloud fallout pattern (to 1 r/hr at 1 hr contour)

y crosswind distance

$y_{jA}(t)$ the number of moles of nuclide (j,A) at time t

Z altitude

Z_s altitude at which stem radius = a_s

Z_o fireball height limit

α particle size parameter = $\frac{V_w}{V_f}$

α_{max} maximum value of α at a given location

α_{min} minimum value of α at a given location

α_o average particle size parameter at downwind distance X

X. STAFF

The following professional personnel have been employed on the project since October 1, 1963:

Werner N. Grune	Professor of Civil Engineering Principal Investigator
Oliver S. K. Yu	Research Associate (October 1, 1963 to August 14, 1964)
Henry S. Atlas	Instructor of Physics Research Associate

Effective July 27, 1964, Mr. Henry Atlas, Instructor, Physics Department, Merrimack College, joined the research staff to take over some of the duties carried out by Mr. Yu who accepted a new assignment at the Stanford Research Institute.

In addition, the following students have assisted these studies on a part-time basis:

Anthony F. Adamczyk	(Civil Engineering)
Eileen E. Bresnahan	(Biology)
Richard F. Casey	(Biology)
Luke A. Gilmore, Jr.	(Civil Engineering)
Richard T. Goller	(Mathematics)
Gerard J. Hamel	(Civil Engineering)
Frances Haniewich	(Biology)
Donald T. Henry	(Chemistry)
Allen C. Herbert	(Civil Engineering)
Thomas E. McDuffie	(Chemistry)
Thomas A. Bonica	(Electrical Engineering)
James E. Thibault, Jr.	(Civil Engineering)

Respectfully submitted,

Werner N. Grune
Professor of Civil Engineering
Project Director

APPENDIX A

Procedure for Determining Activity Concentration in Water Supplies

I. Watershed and Reservoir Contamination

1. Construct a grid system over the surface area of the watersheds and reservoirs of the water supply system with the downwind axis parallel to the prevailing wind direction extending from ground zero.

2. Assign a number to each area that is bounded by the grid lines and/or the outline of the watershed or reservoir under consideration.

3. Determine the x (downwind distance) and y (crosswind distance) coordinates (miles) of the centroid of each grid area.

4. Determine the intensity at these points from the computer programs for Estimating Fallout Intensity at Any Location in the Fallout Region and Total Intensity at Any Value of X, as presented in Figure 18 (17).

5. The average particle size (α_o) for a given downwind distance is found from the relation $\alpha_o = x/h$, where h is given for specific weapon yield. The ratio $\alpha_o = x/h$ is a good estimate only for cloud (i.e. not stem) fallout under the conditions given in the following tabulation:

Weapon	h (miles)	Limits for $\alpha_o = x/h$ (*)
5 MT	12.882	$X \geq 14$ miles
10 MT	14.433	$X \geq 15$ miles
20 MT	16.174	$X \geq 18$ miles

(*) Determined from the intersection of the lines (X_3, I_3), (X_4, I_4) and (X_5, I_5), (X_6, I_6) on the Intensity Profile for each weapon size. This intersection was selected as the division point because the cloud fallout effect predominates beyond this point. Since the stem fallout contributes negligibly to the soluble activity, we believe that the approximation of total fallout by cloud fallout is justified for the evaluation of water contamination. Also, the area predominately covered by the stem is generally subject to severe blast and thermal damages and hence need not be considered in the evaluation of water contamination.

6. For a given isotope the number of atoms that fall on each grid area can be determined from the soluble nuclide contour ratio:

$$N'_\alpha(1) = \frac{N'(A)}{I(1)} = \frac{Y_A r'_o(A,t)}{K_x(1)} \qquad (1)$$

where N'_α (1) is the soluble nuclide contour ratio at (H + 1) hour

N'(A) is the atom concentration of the end number of mass chain A that is condensed on the exterior of the carrier particles

I (1) is the ionization rate at (H + 1) hour

Y_A is the yield in atoms per fission of mass chain A

$r'_o(A,t)$ is the fraction of atoms of the radionuclide that is soluble in water of mass chain A at time t.

$K_x(1)$ is the conversion factor from fissions/sq ft to r/hr, discussed in Chapter IV, Sections (D.4) and (E) of this report.

Substituting known values into Equation (1) yields the following relation:

$$\frac{\text{Atoms}}{\text{Grid Area}} = \frac{N'(A)}{I\,(1)} \left(\frac{\text{atoms/ft}^2}{\text{r/hr}}\right) \times \text{Area (ft}^2\text{)} \times \text{Intensity (r/hr)}$$

$$= \frac{Y_A r'_o\,(A,t)^*}{(3.922 \times 10^{-13})\,(r_\alpha(1) + 0.02)} \times \text{Area} \times \text{Intensity}$$

*Values of Y_A and $r_o(A,t)$

Isotope	Y_A	r_o (A,t) 5 MT	r_o (A,t) 10 MT	r_o (A,t) 20 MT
Sr-89	.0317	.0106	.0192	.0235
Sr-90	.037	.1080	.1380	.1830
Ru-106	.015	.0776	.0522	.0368
I-131	.032	.0153	.01635	.0156
Cs-137	.0585	.00449	.004144	.00393
Ba-140	.056	.3090	.4040	.4560

*Y_A was obtained from Bolles and Ballou (18), (see also Ref. (34) Table I p.27-30) r_o (A,t) was calculated according to the information given on p.94 of this report. r'_o (A,t) is obtained from a curve of α versus the total fractionation number, i.e. (r'_o (A,t) + r_o (A,t)) of soluble (r'_o (A,t)) and insoluble (R_o(A,t)) atoms. The fraction of soluble atoms of a radionuclide is obtained by subtracting the correct value of (r_o(A,t)) as obtained from the above table from the value of (r'_o (A,t) + r_o (A,t)) which is obtained from the curve in Figure 30.

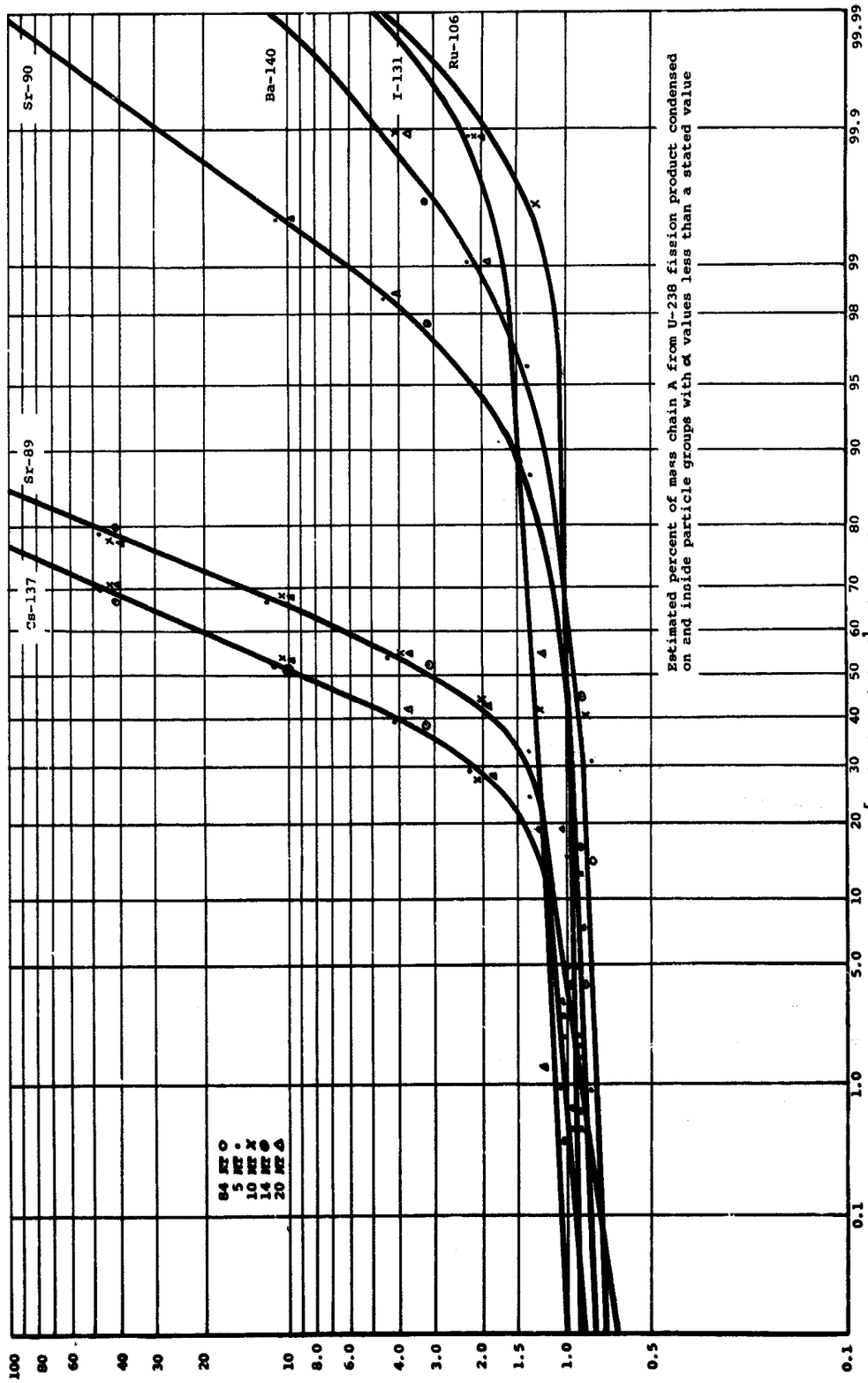

Figure 30. Total Fractionation Number versus α for Various Weapon Yields. (Approximated by a single curve for each radionuclide).

r_α is obtained from the curve of α versus r_α as shown in Figure 31.

7. If it is assumed that initially the water supply is turned off, i.e. prevent the use of contaminated water, homogeneous mixing of the reservoir contents may be achieved. (a) By assuming complete mixing of the atoms in the reservoir we can divide the total number of atoms falling on the reservoir surface by the volume of water in the reservoir to obtain atom concentration in (atoms/liter). Refer to section 8(c) before carrying out this calculation. This value can then be converted to (μc/ml) by multiplication with the conversion factor $\lambda / (3.197 \times 10^{12})$ which was derived as follows:

$$1\ \mu c = 3.7 \times 10^{4}\ \text{dps}$$

$$1\ \mu c = (3.7 \times 10^{4}\ \text{dps})\ (3.6 \times 10^{3}\ \text{sec/hr})\ (24\ \text{hr/day})$$

$$= 3.197 \times 10^{9}\ \text{dpd}$$

then

$$1\ \mu c/ml = 3.197 \times 10^{9}\ \text{dpd/ml} = 3.197 \times 10^{12}\ \text{dpd/liter}$$

and

$$1\ \text{dpd/liter} = (1/3.197 \times 10^{12})\ \mu c/ml$$

but

$$A(\mu c/ml) = \lambda(\text{day}^{-1})\ N\ (\text{atoms/liter})$$

$$= N\ \lambda(\text{dpd/liter})$$

$$= N\lambda/(3.197 \times 10^{12})\ \mu c/ml$$

(b) Reservoir contamination due to watershed is found by first multiplying the total number of atoms falling on the watershed by the given (or assumed) runoff coefficient to determine the number of atoms entering the reservoir from the watershed. (This procedure should be modified to include the volume of runoff water in the concentration estimates)

The activity in μc/ml is then determined as in section 8(a).

(c) If total contamination activity is desired and the individual effects of direct and indirect contamination are not required, a summation of the atoms from direct and indirect watershed contamination divided by the reservoir volume will yield the total contamination in atoms/liter.

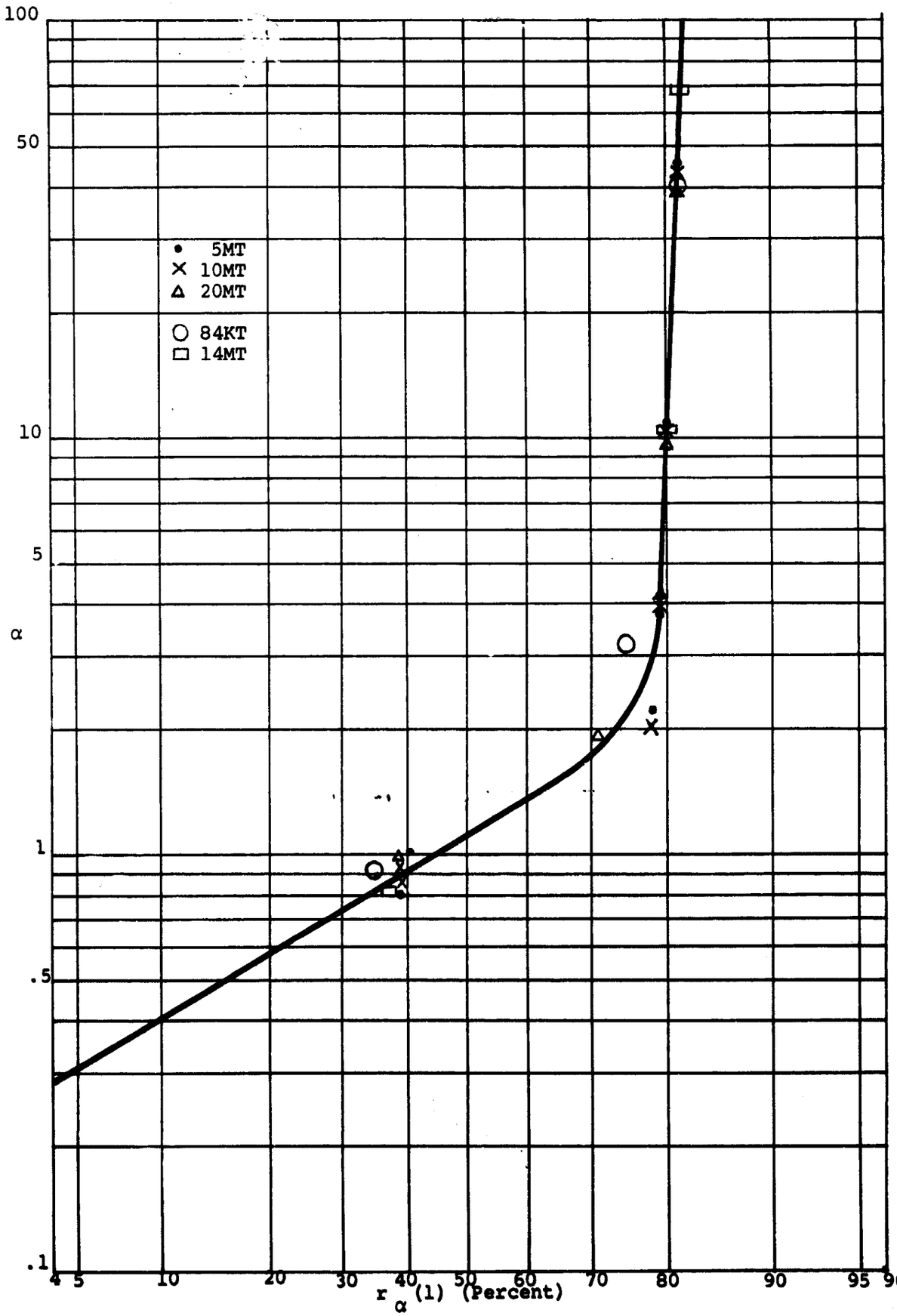

Figure 31. Estimated percent of the fission product activity condensed on particle groups with α values less than a stated value.

The decay constant, λ, days^{-1} is tabulated in Ref. (13), Table I, p. 87, and some pertinent values are shown below:

Isotope	λ
Sr-89	0.013
Sr-90	0.68×10^{-4}
Ru-106	0.19×10^{-2}
I-131	0.0862
Cs-137	0.57×10^{-4}
Ba-140	0.054

9. The concentration in atoms/liter of each isotope is converted to dose for total body (in rems) by multiplication with the appropriate conversion factor, listed under the Miller-Brown Model in Table IX p. 68 of this report. A typical example follows:

Calculation of Internal Hazard of Total Body from Ingestion of Sr-89 in the San Francisco Water Supply System (155 MT):

$(1.70 \times 10^{11}$ atoms/liter) (1 liter/day) = 1.70×10^{11} atoms/day

and

for onset of consumption, t_o = 1 day and for t = 30 days of consumption:

$(1.70 \times 10^{11}$ atoms/day) $(15.5 \times 10^{-14}$ rem/atoms/day) =

Total Body Dose = 2.635×10^{-2} = 0.2635 rems (Compare with value in Table XI p. 71 in this report)

II. River Contamination

1. Only those portions of rivers that are downstream from reservoirs and upstream from water supply intakes are considered in the contamination estimates, unless circumstances call for an evaluation of contamination to reservoir feeder streams. This assumption is based on the large volume of water in a reservoir and that contamination in a river downstream from it would be decreased due to releases from the reservoir. It follows that a maximum degree of contamination for the river is estimated when the contamination effect from reservoirs and their feeder streams is eliminated.

2. The selected portions of rivers are idealized as long rectangular reservoirs with their volume estimated from the rate of stream flow. An outline of the procedure follows:
3. The surface area of the streams is evaluated by using the measured length and an average width.
4. An average intensity value over the stream surface is obtained by taking an arithmetic mean of computer-calculated intensities at selected points along the stream.
5. The average value determined in (4) is assumed to be characteristic of the entire fetch of stream surface area and the total number of soluble atoms, N'(A), is determined by the same procedure as is used for reservoir contamination.
6. The average annual flow in cubic feet per second for each stream is converted to cubic feet per day and then to liters per day, to obtain the approximate volume of water which flows through the stream in one day. With this data, the number of atoms per liter, N, is calculated for each of the isotopes. (The estimated atom concentration in atoms/liter, N, is based on H + 1 hour. It should be emphasized that all intensity contours are corrected to H + 1 hour. This means that after the local fallout stops, essentially 24 hours after detonation, the existing fallout patterns are traced back to a common time basis at H + 1 hour by use of the typical ionization rate decay curve. Therefore, the last calculation can be made since the activity referred to H + 1 hour represents essentially all the 24 hours deposition of fallout. This assumption allows cancellation of the time units in these calculations to obtain atoms per liter.)
7. Stream contamination from watershed runoff is determined in a manner similar to that for watershed contamination of reservoirs. The number of atoms of each isotope, N'(A), which fall on the watershed is determined as before, with the runoff coefficient for the particular watershed in question governing the percentage of those atoms which will be assumed to enter the stream. However, in the case of stream contamination, runoff volume was considered and calculated from the

relation Q = CiA, where C is the runoff coefficient of the watershed, i is the estimated rainfall intensity in inches per hour, and A is the watershed surface area. The volume thus obtained is then converted from cubic feet to liters.

8. The combined effect of stream and runoff contamination is obtained by computing a weighted average of the radioactive concentrations calculated in each case:

$$\frac{(\text{Concentration}_A)\ (\text{Volume}_A) + (\text{Concentration}_B)\ (\text{Volume}_B)}{\text{Volume}_A + \text{Volume}_B}$$

Since the concentrations are determined by dividing the number of soluble atoms, N'(A), by a volume, this averaging process is simply a summation of the atoms falling on the river surface (step 5) and the atoms falling on the watershed surface (step 7) divided by the summation of the river and runoff volumes. If the volumes used are measured in liters, the resulting average concentration in atoms per liter is then converted to μc/ml by the conversion previously discussed. This method of averaging is also used to determine the resulting contamination where two streams join.

9. The conversion of concentration to dose is carried out in the same manner as for reservoir contamination.

APPENDIX B

RECOMMENDATIONS FOR FUTURE INVESTIGATIONS

As an outcome of the studies reported herein, the following recommendations for future investigations are presented:

1. Further analysis and clarification of the Miller Fallout Model is highly desirable. The choice of the proper chemical reactions for estimating sublimation pressures needs further clarification. The analysis of the second period of condensation appears to include some unwarranted assumptions. To compute the fractionation number for the second period of condensation, it has been assumed that each vapor is in equilibrium with its own pure solid phase. It would appear that the sublimation pressure of any particular nuclide would be reduced due to the presence of other nuclides in the solid phase. The present study centered on the evaluation of six specific radionuclides that are considered to be biologically important. The method of calculation finds the amount of a specific nuclide by considering gross fission products and their decay. The current analysis assumes that the specific nuclide has the same half-life as do the gross fission products. This simplifying assumption may lead to considerable error and should be further investigated.

2. From a first approximation of the relationship between activity distribution and fallout particle size it has been observed to be in close conformance to a log-normal distribution. Additional studies to establish a more exact relationship between activity distribution and fallout particle size would be a valuable contribution to the versatility and application of the Miller Fallout Model.

3. The average particle size, α_o, for a given downwind distance can be found from the simple relationship, $\alpha_o = x/h$ for a specific weapon yield. The ratio of x/h is a good estimate only for cloud fallout under the present limitations of the Miller Model. The approximation of total fallout due to cloud fallout in water contamination

APPENDIX B (cont'd)

RECOMMENDATIONS FOR FUTURE INVESTIGATIONS

is probably justified since the stem fallout contributes negligibly soluble activity and the stem area is generally subject to severe blast and thermal damage. Nevertheless, the division between the cloud fallout and that from the stem could benefit from further analysis.

4. The present method to obtain reservoir contamination is by first multiplying the total number of atoms falling on the watershed by the runoff coefficient to determine the number of atoms entering the reservoir from the watershed. This procedure should be changed or modified to include a consideration of the volume of runoff water in estimating the final activity concentrations. A more recent method to obtain total atoms has treated the entire watershed in the same manner as individual grids by assuming that the average activity could be located in the centroid of the watershed. Considering the activity, N (number of atoms), located at the centroid in a like manner as summing up individual grid blocks, multiplying this sum by the total area times the intensity produced total atom concentration values that checked very closely with the more detailed and laborious calculations outlined in Appendix A. For the few cases tested, the simplified procedure gave results of the same magnitude for the entire watershed, the coefficient of the power of 10 was reduced by one-third. In most cases, small sacrifice in accuracy can be justified because the amount of work is reduced significantly. Examinations of several other watersheds by both the long and the short method should be undertaken to predict the level of confidence inherent in the short method of analysis.

5. It seems to be established that the degree of radioactive contamination from surface runoff, depending on such environmental factors as watershed characteristics and meteorological aspects, may be a major factor in the rehabilitation and use of public water supplies during the postattack period. From a limited study of transport of fallout by surface water, the contributions from each mode of contamination, i.e.

APPENDIX B (cont'd)

RECOMMENDATIONS FOR FUTURE INVESTIGATIONS

that from direct contamination of reservoirs and river surfaces and that from watershed runoff have been determined. Therefore, a detailed analysis of the redistribution of fallout and the contribution to contamination from surface runoff during the blast and thermal period from land areas to streams and from watersheds into reservoirs should be conducted. The analysis of the redistribution phenomenon is equally applicable in and around centers of population where the activity concentration may change significantly following precipitation, especially for the soluble nuclides. From the previous studies it appears that surface runoff from rainfall during the first 24 to 48 hours following nuclear attack will be critical as far as water contamination is concerned.

Following initial deposition on watershed or land surfaces, the activity concentration is subject to change from surface runoff which may redistribute the fallout nuclides and contribute to the contamination of water supplies to alter the ingestion hazard. It would be of interest to study the degree of fractionation as only the soluble portion will be exchanged by the soil, retention of activity, etc. Furthermore, the different types of soil cover, vegetation, foliage and trees covering the watershed and their contribution to water contamination, or their retention factor, should be examined in detail. From the results of such a study it will be possible to calculate anticipated amounts of radioactivity intake for selected radionuclides for various periods of time following nuclear attack and provide a valuable asset to the planning and rehabilitation during the postattack period. Estimates of the accumulation of body burden by the individual or the population at large can be made with and without surface runoff contribution, i.e. estimates based on the redistribution phenomenon may be calculated. Modifications of the watershed, especially as these affect future planning, including urban development, could be undertaken with a much higher degree of certainty than is now available.

6. To study the possible long and short term hazards and radiobiological effects from the ingestion of fallout contaminated water it is important to estimate the absorbed dose in the human body over different periods of consumption. Several graphs from which it is possible to make predictions of the absorbed dose by various parts of the human body for various isotopes and time periods of consumption have been prepared. These graphs should be especially useful to water works and civil defense personnel for planning a nuclear attack. However, a similar set of graphs for gross fission products may be of more general interest and should be developed subsequently.

SUPPLEMENTARY

INFORMATION

MERRIMACK COLLEGE
North Andover, Massachusetts
DEPARTMENT OF CIVIL ENGINEERING

December 13, 1965

Defense Documentation Center
Cameron Station
Alexandria, Virginia 22314

Subject: Addendum I to Final Report, Project 3131B, Contract No. OCD-PS-64-62, "Evaluation of Fallout Contamination of Water Supplies"

Dear Sir:

Enclosed is Addendum I to our Final Report, entitled "Estimate of the Absorbed Dose to the Thyroid Calculated by the Simplified Uptake Model." It should be noted that the calculations presented in the Final Report were based on the "total body" case; (see Table VIII page 50 and Table IX on page 68) and that the values for I-131 shown in the attached addendum are for the thyroid, based on the assumed value of 20 gm for the adult-size organ.

It is hoped that you will incorporate this addendum in the Final Report transmitted earlier.

Sincerely yours,

Werner N. Grune

Werner N. Grune
Professor of Civil Engineering
Project Director

WNG/df
Enclosure

Addendum I

to

Final Technical Report

"Evaluation of Fallout Contamination of Water Supplies"
Contract No. OCD-PS-64-62
OCD Subtask 3131B

Estimate of the Absorbed Dose to the Thyroid Calculated by the Simplified Uptake Model

In the Final Technical Report on Contract OCD-PS-64-62 (Ref. 1), a Simplified Uptake Model was presented to calculate absorbed dose to various body organs. In this report calculations by means of this model were presented for six biologically important nuclides for the "total body" case only. These agree quite well with the longer Miller-Brown calculation (Ref. 1 and 2). As an addendum to this report, calculations are herein presented for the dose absorbed from I-131 in the thyroid.

The appropriate equation is Equation (17) of Ref. 1. The parameters to be used are found in Ref. 2, Tables 1, 2 and 3. There it is seen that, of the parameters involved in Equation (17), the only ones that differ from the total body case are:

TABLE I

Parameters for Absorbed Dose Equation in Simplified Model

Parameter	Total Body	Thyroid	Units
m_k	70,000	20	gms
f_{wk}	1	0.3	--
ϵ_k	0.44	0.23	Mev/dis

As these enter into Equation (17) only as multiplicative constants, the results for the thyroid may be immediately derived from those for the total body by a numerical factor, in this case, 548; i.e., multiply the values in Table VIII, p. 50 of Ref. 1 for I-131 by 548 to get the dose absorbed from I-131 in the thyroid. The results are presented in Table II. For comparison, the values given by Miller & Brown, Ref. 2 are also included in the Table on the following page.

TABLE II

Dose Absorbed From I-131 in the Thyroid Per Unit Ingestion Rate, D_k/U_i^o

t_o day ingestion started	t days of consumption	D_k/U_i^o (Simplified Model) (10^{-14} rems/atom per day)	D_k/U_i^o (Miller-Brown Model) (10^{-14} rems/atom per day)
1	30	44,900	75,500
	91	60,300	91,100
	183	60,300	91,100
	365	60,300	91,100
	730	60,300	91,100
7	30	22,600	28,600
	91	35,800	40,000
	183	36,000	40,000
	365	36,000	40,000
	730	36,000	40,000
14	30	8,710	7,800
	91	20,600	15,200
	183	19,700	15,200
	365	19,700	15,200
	730	19,700	15,200

The absorbed dose values from both models compare quite well, although some differences exist. These discrepancies are due to:

(1) daughter elements are neglected in the Simplified Model,

(2) water is taken in periodically (step-function) or once a day vs. Miller-Brown which is continuous ingestion.

However, the results from the Simplified Model are in all cases within a factor of 2, actually within 1.5 of the longer and more intricate Miller-Brown Model method.

REFERENCES

(1) Grune, W. N., Atlas, H. S. and Hamel, G. J., "Evaluation of Fallout Contamination of Water Supplies," Final Technical Report to the Office of Civil Defense, Washington, D.C. 20301, Contract No. OCD-PS-64-62 (15 May 1965).

(2) Miller, C.F. and Brown, S.L., "Models for Estimating the Absorbed Dose from Assimilation of Radionuclides in Body Organs of Adult Humans" OCD-OS-62-135, Stanford Research Institute, Menlo Park, California (May 1963).